E-ISSN 2980-2156

Official Journal of
Erciyes University
Faculty of Medicine

JOURNAL OF CLINICAL PRACTICE & RESEARCH

Formerly Erciyes Medical Journal

KARE MEDYA

Volume 48 Issue 2 Year 2026

jcpres.com

JOURNAL OF
CLINICAL PRACTICE & RESEARCH

Editorial Board

JOURNAL OF
CLINICAL PRACTICE & RESEARCH

Editorial Board

Publishing Coordinator

Emel TORUN / ***E-mail:*** *jclinpr@gmail.com*

Contact

Address: *Erciyes Üniv. Tıp Fakültesi Dekanlığı, Journal of Clinical Practice and Research Bürosu, 38039 Melikgazi, Kayseri, Türkiye*
Phone: *+90 352 207 66 66 (23008)* ***Fax:*** *+90 352 437 52 85* ***E-mail:*** *jclinpr@gmail.com* ***Web address:*** *www.jcpres.com*

Yayın türü / Publication type: Yerel süreli / Bimonthly journal · Basım yeri / Printed at: Filmevi, Yüzyıl Matbaacılar Sitesi, No: 22, Bağcılar, İstanbul, Türkiye (+90 212 429 29 03) · Basım tarihi / Printing Date: Nisan 2026 / April 2026

JOURNAL OF
CLINICAL PRACTICE & RESEARCH

Advisory Board

JOURNAL OF
CLINICAL PRACTICE & RESEARCH

Advisory Board

Abstracting & Indexing

PubMed, PubMed Central, Web of Science-Emerging Sources Citation Index, Web of Science-Current Contents Clinical Medicine, TUBITAK ULAKBIM TR Index, Türk Medline, Embase, DOAJ, HINARI, EBSCO, WorldCat, ProQuest, PharmaPendium, CAS, CABI, CINAHL, GALE, Global Health, Scope Database, MIAR, TurkMedline, Scilit, Open Ukrainian Citation Index (OUCI), Asian Science Citation Index (ASCI), Research4Life.

Owner

On Behalf of Faculty of Medicine, Erciyes University, Dr. İsmail DURSUN

Publisher: *KARE Publishing;* ***Project Assistant:*** *Zeynep PEKŞEN;* ***Graphics, Design:*** *Neslihan ÇAKIR*
Address: *Göztepe Mahallesi, Fahrettin Kerim Gökay Caddesi, No: 200, Daire: 2, Göztepe, Kadıköy, İstanbul, Türkiye;* ***Phone:*** *+90 216 550 61 11;* ***Fax:*** *+90 216 550 61 12;* ***E-mail:*** *kare@karepb.com*

Volume: 48 Issue: 2 Year: 2026

JOURNAL OF
CLINICAL PRACTICE & RESEARCH

Contents

JOURNAL OF
CLINICAL
PRACTICE &
RESEARCH

Volume: 48 Issue: 2 Year: 2026

Brief Report

Case Reports

Official Journal of Erciyes University Faculty of Medicine

DOI: 10.14744/cpr.2026.10880
J Clin Pract Res 2026;48(2):99–109

Pesticides, Environmental Contamination, and Public Health: A One Health Perspective

Filiz Dadaser-Celik,[1] Zafer Sezer,[2] Nuray Ates[1]

[1]Department of Environmental Engineering, Erciyes University Faculty of Engineering, Kayseri, Türkiye
[2]Department of Medical Pharmacology, Erciyes University Faculty of Medicine, Kayseri, Türkiye

ABSTRACT

Pesticides are chemicals used in the agricultural, industrial, and public health sectors to increase crop productivity, prevent plant diseases, and reduce pest-related hazards. They can be classified as herbicides, insecticides, fungicides, and rodenticides based on the pests they target. Their active ingredients include organochlorines, organophosphorus compounds, carbamates, pyrethrins, and pyrethroids. Although the use of pesticides has provided significant benefits to humans, their widespread application has also led to the contamination of air, soil, water, and food systems. After application and distribution among air, water, soil, and biota, several processes control the fate and transport of pesticides in the environment, as well as their transformation through biological, chemical, and physical reactions. Humans and animals are exposed to pesticides through various pathways, including drinking contaminated water, consuming pesticide-contaminated food, and living in areas treated with pesticides. Both acute and chronic exposure to pesticides can cause several adverse health effects on the neurological, endocrine, and reproductive systems and may pose carcinogenic risks. This study provides a comprehensive review of research on the occurrence and fate of pesticides in the environment. It also presents the risks to human health associated with occupational and environmental exposure to pesticides. Available techniques for reducing pesticide-related risks are also discussed. This review showed that human, animal, and ecological health are interconnected and that, therefore, an integrated strategy such as the One Health approach is needed to effectively manage pesticide-related risks.

Keywords: Environmental exposure, environmental health, one health, pesticides, public health.

Cite this article as:
Dadaser-Celik F, Sezer Z, Ates N. Pesticides, Environmental Contamination, and Public Health: A One Health Perspective. J Clin Pract Res 2026;48(2):99–109.

Address for correspondence:
Filiz Dadaser-Celik.
Department of Environmental Engineering, Erciyes University Faculty of Engineering, Kayseri, Türkiye
Phone: +90 352 207 66 66 /32804
E-mail: fdadaser@erciyes.edu.tr

Submitted: 20.02.2026
Revised: 17.04.2026
Accepted: 17.04.2026
Available Online: 07.05.2026

Erciyes University Faculty of Medicine Publications - Available online at www.jcpres.com

INTRODUCTION

An integrated perspective has become crucial for understanding and addressing the significant global challenges we are confronting. In recent years, several examples have demonstrated the necessity of this perspective. For instance, to address the impacts and risks associated with climate change, the need for integrating ecological, economic, and social systems has been emphasized.[1] The challenge of antimicrobial resistance has highlighted the interconnections among human, animal, and environmental health, calling for an interdisciplinary, integrated management approach.[2]

One approach that embodies such an integrated perspective is One Health.[3] One Health acknowledges the interconnectedness of human, animal, and ecosystem health and seeks to create integrated solutions to address complex environmental and health challenges. These challenges are diverse, including antimicrobial resistance, infectious diseases, and diseases related to exposure to toxic chemicals (e.g., pesticides) at the forefront of the list.[4] One Health is an interdisciplinary field encompassing medical sciences, veterinary sciences, ecology, public health, and related disciplines. As such, input from diverse fields and their effective integration are required.[5] However, despite its interdisciplinary nature, the application of One Health often remains conceptual, with limited integration across disciplines in practice. Strengthening its practical integration is essential to address health challenges holistically and achieve overall protection of human, animal, and ecosystem health.

Pesticides are chemicals extensively used in the agricultural, industrial, and public health sectors to increase crop productivity, prevent plant diseases, and repel pests. These are typically complex organic compounds that are relatively resistant to degradation. While this resistance makes them effective for pest control, it also increases their persistence in the environment and potential toxicity to humans. Long-term exposure to pesticides can result in chronic toxic effects, while acute high-dose exposure can lead to severe toxic effects, including death.[6] Conventional pesticide risk assessment approaches are based on human health risk assessment and ecological risk assessment. These methods focus on specific receptors (e.g., humans or aquatic organisms), single substances, and direct exposure pathways. In other words, they often consider separate or primarily single compartments and do not fully account for the interactions among different environmental media, cumulative exposures, or indirect effects.

In contrast, the One Health approach evaluates multiple exposure pathways (e.g., air, soil, water) and their simultaneous and cumulative impacts on multiple receptors. This approach allows for the analysis of feedback mechanisms between environmental processes and human health impacts. By promoting interdisciplinary integration, One Health provides a more comprehensive basis for understanding and managing the complex risks associated with pesticide use.

This review aims to characterize and identify the challenges associated with pesticide contamination from a One Health perspective by discussing the nature of the problem, current approaches, and the lack of integrated frameworks that connect environmental processes to human health outcomes. In the past, many studies have evaluated pesticide occurrence, fate, and toxicity; however, their analyses were often confined to disciplinary boundaries, and the understanding of interactions among these disciplines was limited. This study begins by discussing the occurrence of pesticides in surface waters, groundwater, and soils. It then explains the pathways through which pesticides are introduced into the environment, along with their fate and transport mechanisms. Human and animal exposure pathways, along with the associated health effects of pesticide exposure, are discussed. Finally, the approaches used to manage pesticide-related risks are reviewed, and further research needs are highlighted to emphasize the added value of integrating environmental, ecological, and health-based perspectives for more comprehensive risk evaluation and management.

ENVIRONMENTAL OCCURRENCE OF PESTICIDES

Pesticides are not a uniform group; they comprise a highly heterogeneous class of compounds with distinct target organisms, modes of action, and environmental behaviors. They are classified as herbicides (target weeds), insecticides (target insects), fungicides (target fungi), and rodenticides (target rodents). Their chemical compositions are highly variable, including organochlorines, organophosphorus compounds, carbamates, pyrethrins, and pyrethroids. These differences strongly influence their properties, such as persistence, mobility, bioaccumulation potential, and toxicity. Therefore, the environmental fate, transport pathways, and associated risks of pesticides vary across these classes.

At the global level, total pesticide use has increased significantly in recent decades. According to the FAO's report,[7] the global volume of pesticides used in agricultural production was about 3.73 million tons of active ingredients in 2023. Approximately 51% of global consumption consists of herbicides, while insecticides, fungicides, and bactericides account for 22% each. The remainder consists of rodenticides and other special-purpose pesticides. The consumption of pesticides worldwide varies, with the largest use occurring in Brazil (21.5%), followed by the United States (11.5%), Indonesia (7.9%), Argentina (7.1%), and China (5.8%).[7]

Monitoring studies have shown that pesticide pollution follows a consistent pattern in different countries, both in terms of compound types and concentration levels. Among herbicides, the most frequently reported active substances are atrazine, metolachlor, alachlor, diuron, simazine, and terbuthylazine, while among insecticides, imidacloprid, acetamiprid, thiamethoxam, chlorpyrifos, and dimethoate are most commonly detected, typically in the ng/L–low µg/L range in surface waters.[8,9] In North China, organophosphate pesticides such as dimethoate, dichlorvos, methyl-parathion, and malathion exhibit significant seasonal variability, with

total concentrations ranging from 174-321 ng/L, averages of 3.9-7.1 ng/L, and detection rates of 47-69% during the summer period, and total concentrations of 152-269 ng/L, averages of 3.4-6.0 ng/L, and detection rates of 23-62% during the winter period.[10] In the Llobregat River and its aquifer in Barcelona, significant pesticide pollution was reported, with maximum concentrations of several µg/L for carbendazim, N,N-dietil-m-toluamid, diuron, and propiconazole, and concentrations of 0.1–0.5 µg/L for imidacloprid, simazine, bentazone, metazachlor, and tebuconazole.[11] Long-term monitoring in Germany shows that most substances detected in surface waters are pesticide metabolites, with metazachlor sulfonic acid, metolachlor ethanesulfonic acid, and metazachlor oxanilic acid occurring at higher and more persistent levels than their parent compounds, leading to long-term exposure concerns.[12] Similarly, in the United States, atrazine, metolachlor, glyphosate, and imidacloprid were commonly detected during the 2013-2017 period. Imidacloprid, in particular, was identified as one of the major pesticides posing a chronic ecotoxic risk to aquatic organisms, detected at concentrations of 0.1-1 µg/L in some agriculturally and urban-based impacted areas.[13]

Although pesticides are generally detected at lower concentrations in groundwater than in surface water, levels can be high, especially in areas with intensive agricultural activity. Groundwater samples in France, Denmark, England, and Switzerland commonly contain active substances such as atrazine, metolachlor, bentazone, and simazine, as well as their metabolites. The concentrations of these substances typically range from 0.05 to 0.5 µg/L, and at many sampling points, the European Union (EU) drinking water limit of 0.1 µg/L is exceeded. The greater mobility and persistence of metabolites compared to parent compounds contribute to a dominant, persistent pesticide pollution profile in groundwater.[14]

Among the most common pesticides in agricultural soils are glyphosate and its metabolite aminomethylphosphonic acid (AMPA). Concentrations reaching 100-1900 µg/kg for AMPA and 50-2000 µg/kg for glyphosate have been reported in EU countries. Insecticides such as imidacloprid and chlorpyrifos are measured in the range of 10-120 µg/kg and 5-50 µg/kg, respectively, in intensively farmed areas of Mediterranean countries and China, while herbicides such as terbutylazine, metolachlor, and alachlor are reported to be mostly at levels of 20-1000 µg/kg in the soils of the US, Europe, and South America.

ENVIRONMENTAL FATE AND TRANSPORT OF PESTICIDES

Pesticides are introduced into the environment through multiple pathways. These pathways vary based on the type of application, target use, and physicochemical properties. In agricultural systems, pesticides are applied directly to crops and are distributed in the environment through spray drift, surface runoff, and leaching. In urban and municipal areas, applications for pest control result in surface runoff over impervious surfaces, with final discharge to stormwater collection systems. Localized releases from industrial uses and manufacturing processes occur through effluents or improper handling. These pathways differ substantially among pesticide classes and application practices, influencing their distribution, persistence, and potential exposure routes in environmental systems (Fig. 1).

Crop patterns and application frequency have a significant impact on soil pesticide levels, which can accumulate in agricultural soils over time.[15] For example, fruits and vegetables generally require higher pesticide inputs than cereals, as they are more susceptible to pests and diseases.[16] In urban areas, herbicides and insecticides are widely used in parks, lawns, home gardens, and indoor applications, resulting in more concentrated applications than in agricultural areas. This leads to a condensed application compared to agricultural areas. In the US, lawns and home-and-garden applications are reported to account for 8% of total herbicides, 15% of insecticides, and 10% of fungicides. Urban dust and air have been shown to contain pyrethroid and organochlorine pesticides, and surface waters have been found to contain substances such as atrazine, diuron, metolachlor, and chlorpyrifos, which pose a serious threat to ecosystems and human health.[17]

Pesticide manufacturing facilities create another primary source of pesticides in the environment. These facilities can cause both point and distributed pollution. Pesticides can remain in wastewater even after treatment.[18] Treated or untreated wastewater is eventually discharged into receiving water bodies. Moreover, chemical spills, improper waste disposal, or emissions during production processes in these facilities can provide another route to the environment.[19]

Once pesticides are introduced into the environment, a variety of physical, chemical, and biological processes determine their fate and transport, as well as their distribution among environmental compartments such as the atmosphere, soil, surface water, and groundwater. In the atmosphere, processes such as volatilization and air transport can carry pesticides over long distances. In soils, sorption, degradation, and leaching control their potential transfer to other media or retention. Runoff, erosion, and dilution processes determine surface-water concentrations, along with degradation and sediment interactions. In groundwater, leaching controls transport. In general, the behavior of pesticides in the environment is controlled by transport, transfer, and transformation processes.[20]

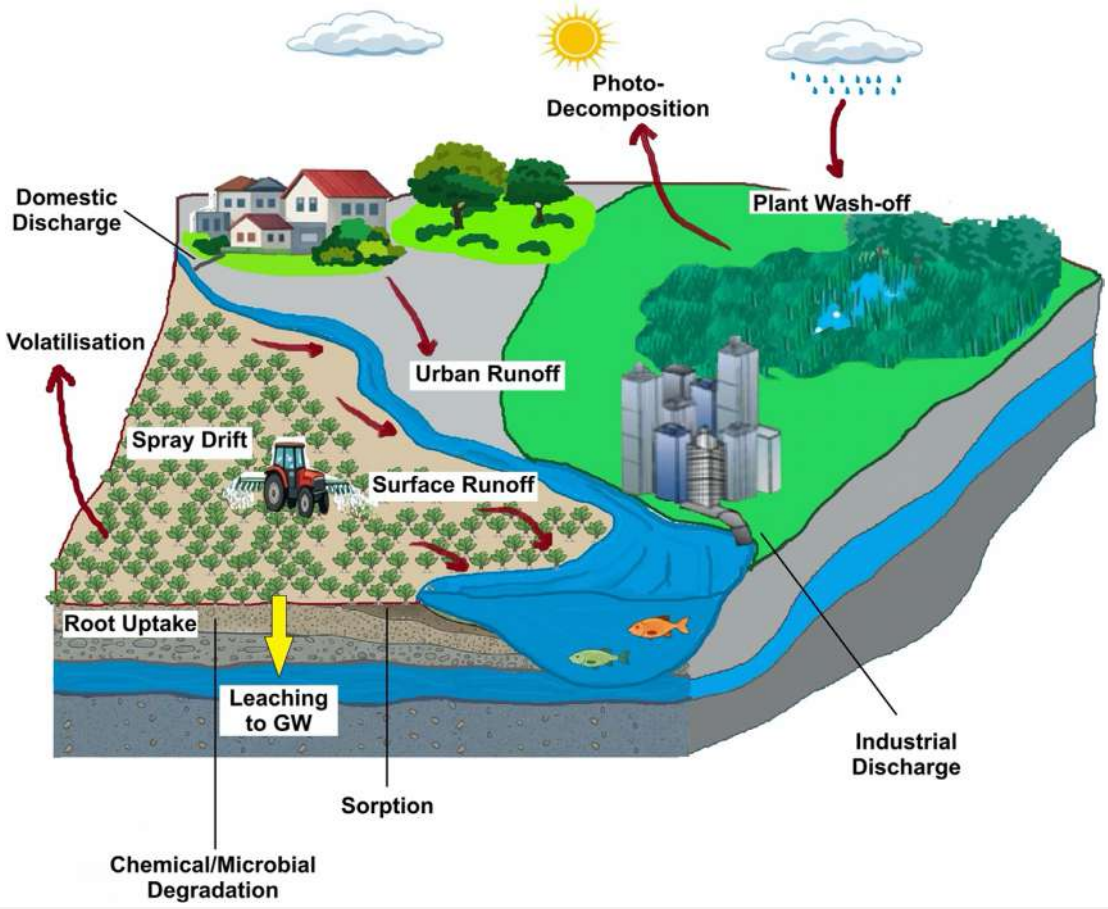

Figure 1. Fate and transport of pesticides in the environment.

Transport processes carry pesticides away from their point of application through air and water, determining the spatial extent of pesticide contamination. During transport, pesticides can be in the form of solid, gas, or liquid. They are first introduced to the air by spray drift during application. However, the transfer to the atmosphere continues after application through evaporation or volatilization from soil and plant surfaces.[21] Air is the major medium for transporting materials over longer distances and is strongly dependent on the method of application and the properties of the compound.[21] The variety of droplet sizes, atmospheric conditions during and after application, and the composition of the spray can all affect spray drift. After application, pesticide passage to air is controlled by pesticide characteristics. Pesticides with higher vapor pressures are more likely to volatilize after application, thus having higher atmospheric concentrations.[21]

Transfer processes affect the distribution of pesticides among water, soil, and biota after application. These processes include volatilization, surface runoff, leaching, adsorption, and plant uptake.[20] Pesticide characteristics (e.g., water solubility, volatility, soil adsorption, and persistence) and soil characteristics (e.g., texture, permeability, depth, pH, organic matter content) affect transfer processes.[20] Meteorological conditions, particularly rainfall timing and intensity following pesticide application, also play a significant role.

Among transfer processes, volatilization is the process through which pesticides are carried from soil or plant surfaces into the atmosphere. Pesticides with higher vapor pressure can easily transition to the gaseous phase after application.[21] The volatilization process is reversible, meaning that pesticides enter the atmosphere but can also redeposit onto soil or plant surfaces. Surface runoff is a process that occurs after rainfall or irrigation events. It is considered one of the primary routes by which pesticides are transported to surface waters, including rivers, lakes, and reservoirs. After a rainfall event or irrigation, excess water flows over the land surface as sheet flow, carrying pesticides from application sites to the nearest surface waters.[22] In surface runoff, pesticides are transported either as dissolved material or particulate matter. The phase of the pesticide is influenced by its solubility and sorption characteristics.

Leaching is the process that controls the downward movement of pesticides in the soil profile through infiltration or percolation processes. This process represents the major route by which pesticides can enter groundwater.[23] Pesticides with higher water solubility and lower sorption affinity to soil particles are generally transported more easily through the soil. Soils with higher permeability also allow greater pesticide movement through leaching. Adsorption refers to the process by which pesticides attach to the surface of soil particles. Adsorption is a reversible process where adsorption and desorption occur continuously, which moves pesticides between the dissolved and particulate phases. The adsorptive capacity of soils is largely influenced by properties such as pH, organic matter content, the presence of clay minerals, and oxide hydroxides.[20] The physicochemical characteristics of pesticides are also important in the adsorption-desorption process. Some pesticides have a higher adsorptive affinity (e.g., hydrophobic pesticides), meaning they are more strongly held on soil particles.

Plant uptake is another important transfer pathway, whereby pesticides are absorbed by plant roots or foliage. After the pesticides are taken up by plants, they may be carried within plant tissues, metabolized, or accumulated.[24]

Transformation processes refer to biological, physical, and chemical reactions that convert pesticides into other substances.[25] The degradation of pesticides involves transformation processes carried out by microorganisms or plants, as well as chemical and photochemical reactions.[25] In microbial degradation, microorganisms consume and transform chemicals into other forms in soil, water, or sediment environments. Chemical and photochemical processes involve hydrolysis, oxidation/reduction, and photolysis, typically occurring at the soil surface and in surface waters. It is possible that the final product can be more toxic than the parent pesticide.[25] Both environmental conditions (e.g., temperature, moisture, redox conditions, and light availability) and pesticide properties (e.g., molecular structure and functional groups) affect the type and rate of transformation.[25]

HUMAN AND ANIMAL EXPOSURE PATHWAYS

Humans are exposed to pesticides through occupational or environmental contact via various mechanisms in work or home environments, such as work-related activities, consuming foods and drinks, using medicines, and during travel and recreational activities. Pesticides can enter the human body through dermal, oral, eye, and respiratory routes.[26] Several factors affect the actual amount of pesticide that enters the human body. These include the physicochemical characteristics of the pesticide (e.g., water solubility, volatility, and persistence), contact duration and frequency, availability of protective equipment, and personal factors such as age.[26]

Occupational exposure refers to direct contact with pesticides, often during work activities. Occupational contact creates the highest-risk type of pesticide exposure because workers (i.e., farm workers, gardeners, workers in pesticide manufacturing plants) involved in the production, transfer, and application of pesticides use them regularly and often in concentrated forms.[6] Protective clothing and equipment can limit exposure; however, these measures are often neglected because they are uncomfortable to use continuously, especially under unsuitable environmental conditions.[26] Even with protective clothing/equipment, skin contact and inhalation can still pose risks for workers.

Environmental exposure occurs through contaminated air, water, soil, and food. Food serves as a significant environmental exposure route. Pesticides applied on farms can remain in smaller concentrations on fruits, vegetables, and grains even after harvesting. Washing and peeling can reduce pesticide residues to some extent, but some pesticides can penetrate the food itself. For instance, it was estimated that by consuming wheat products, humans can ingest 22 mg-2.1 g of pesticide per kilogram applied to wheat.[27] Through the food chain, pesticides can also accumulate in meat, dairy, and fish.[28] Exposure to pesticides can occur by using contaminated water, either as drinking water or during recreational water use. The health risks due to pesticides in drinking water sources have been discussed.[29] Soil exposure occurs when humans come into contact with contaminated agricultural soils. Contact can be in the form of direct handling, inhalation of resuspended soil particles, or incidental ingestion. Air exposure occurs through pesticide volatilization after application and the drift of spray droplets during spraying.[21] Pesticides can be carried over long distances in the atmosphere and may remain in the air or deposit onto soil or water, where human contact may occur.

HEALTH EFFECTS OF PESTICIDE EXPOSURE

Pesticides can cause acute toxicity through inhalation, ingestion, or contact with the skin and eyes. Long-term or repeated exposure to lower doses can lead to chronic toxicity.

Acute Health Effects

An increased incidence of respiratory problems and neurodegenerative diseases has often been reported due to occupational exposure, particularly the exposure of agricultural workers to pesticides.[6] In the US, exposure to chlorpyrifos and other organophosphates is estimated to cause billions of dollars in annual losses due to cognitive decline and abnormalities in brain development. Chlorpyrifos was prohibited in the EU in 2020 and in the US in 2021, while it remains prevalent on other continents.[30] Organophosphate pesticides act as acetylcholinesterase (AChE) inhibitors. By blocking AChE, they prevent the breakdown of acetylcholine (ACh), causing its accumulation at cholinergic nerve endings. This leads to

postsynaptic receptor overstimulation and adverse effects in both the central and peripheral nervous systems.[31]

Some of the anticholinesterase (anti-ChE) agents, such as tabun, sarin, and soman, are extremely toxic and have been used as biological weapons in warfare or in terrorist attacks, such as the one in Tokyo.[32] Acute intoxication by anti-ChE agents produces both muscarinic and nicotinic effects, and except for compounds with very low lipid solubility, also affects the central nervous system. Systemic symptoms usually appear within minutes after inhalation, while onset is slower after gastrointestinal or skin absorption. Ocular and respiratory symptoms occur first. Ocular effects include marked miosis, eye pain, blurred vision, and ciliary spasm, although miosis may be absent during severe systemic poisoning due to sympathetic responses. Respiratory effects include rhinorrhea, chest tightness, wheezing, bronchoconstriction, and increased bronchial secretions. Gastrointestinal symptoms include nausea, vomiting, abdominal cramps, and diarrhea.

With skin exposure, localized sweating and muscle fasciculations are often the first signs. Severe poisoning is characterized by excessive salivation, sweating, lacrimation, involuntary urination and defecation, bradycardia, and hypotension. Nicotinic effects at the neuromuscular junction cause muscle weakness, twitching, and eventually paralysis. The most serious outcome is paralysis of the respiratory muscles, and death usually occurs due to respiratory failure, often with a secondary cardiovascular component.[31,33]

Chronic and Long-Term Health Outcomes

Prolonged pesticide exposure may result in severe impairments in cognitive, somatic movement, visceral, sensory, affective, and neurodevelopmental abilities. A study that included 431 children aged 6-12 from three communities—two in an agricultural region (Community A and B), where mainly organophosphate and pyrethroid pesticides were reported, and one reference population (Community C), located far from agricultural fields in Mexico—showed that dialkylphosphates and 8-hydroxy-2′-deoxyguanosine in urine, as well as malondialdehyde in serum concentrations, significantly increased in communities A and B compared to community C. Proinflammatory cytokine IL-8 also showed a significant increase in community A compared to community C, indicating increased oxidative stress, DNA damage, and inflammation.[34]

A systematic review covering data from 12 countries revealed positive associations between Non-Hodgkin Lymphoma (NHL) and carbamate insecticides, organophosphorus insecticides, lindane (an organochlorine insecticide), and 2-methyl-4-chlorophenoxyacetic acid (a phenoxy herbicide).[35] Glyphosate exposure was also associated with an increased risk of NHL in humans in another meta-analysis.[36]

Pesticides can alter the immune system by disrupting normal immune responses to tumor antigens, allergens, self-antigens, and microbial agents, which may increase the risk of cancers, allergies, autoimmune disorders, and infectious diseases. One of the main mechanisms is the disturbance of cytokine balance, which affects immune regulation.[37] Pesticides have also been linked to an increased risk of obstructive lung diseases such as chronic bronchitis and chronic obstructive pulmonary disease.[38]

Chronic ambient exposure to organophosphates may alter the composition and predicted metabolic functions of the human gut microbiome. In a study of 190 participants from an agricultural region in California, organophosphate exposure was associated with changes in the abundance of several bacterial groups and shifts in microbial metabolic pathways. These changes included disturbances in cellular respiration, increased biosynthesis and degradation of bacterial cell wall components, increased production of RNA and DNA precursors, and reduced synthesis of vitamins B1 and B6.[39] Chronic exposure has also been linked to a higher prevalence of metabolic disorders such as obesity and type 2 diabetes. Dysmetabolism is associated with low-grade inflammation, and the gut microbiota plays a significant role in its development. One key change observed is a decrease in Bacteroidetes and an increase in Firmicutes, a pattern linked to both pesticide exposure and dysmetabolic risk.[40]

In vitro and ex vivo studies showed that acute exposure to the pesticide malathion reduced the viability of pancreatic islet cells and promoted signs of damage in α and β cells at the subcellular level. Moreover, chronic exposure to malathion affected β-cell viability and α-cell voltage-gated K+ currents. Pesticide exposure may increase the prevalence of type 2 diabetes.[41]

A randomized controlled dietary intervention trial evaluated the effects of changing from conventional to organic food consumption. Healthy adults were randomly allocated to either an organic food (n=13) or conventional (n=14) group. The conversion to organic food with a Mediterranean diet reduced exposure to all types of pesticides from different sources by >90%.[42]

To demonstrate how long-term, low-level exposure to glyphosate, metals, and their combination damages kidney structure and function, a study used adult zebrafish as a mechanistic model. Exposure to both glyphosate and metals caused a synergistic effect, leading to more damage to kidney health compared to exposure to individual chemicals. In this study, mitochondria-rich proximal tubules were identified as the main targets of chronic glyphosate-metal combination exposure.[43]

A study in China showed a consistent positive relationship between abnormal blood cell, liver, and peripheral nervous system test results and the intensity of pesticide exposure. Sensory abnormalities were more common than motor problems, and abnormal electrophysiological findings were predominantly observed in sensory nerves in the higher-exposure group, indicating neurotoxicity.[44] Organophosphate, carbamate, pyrethroid, and organochlorine insecticides are known to cause acute neurotoxic effects. Many epidemiological studies have also reported increased risks of long-term behavioral and neurological disorders in populations with chronic exposure. These effects have been linked to mechanisms such as oxidative stress, altered dopamine transporters, mitochondrial dysfunction, α-synuclein aggregation, and neuroinflammation, which are associated with neurodegenerative diseases like Parkinson's and Alzheimer's disease.[45]

Pesticides significantly impact female reproductive health by targeting the ovary. Epidemiological research links these exposures to menstrual cycle disorders, polycystic ovary syndrome, primary ovarian insufficiency, and reduced fertility in women. Toxicological studies demonstrate that pesticides disrupt the estrous cycle, deplete the follicle pool, and impair oocyte maturation. Pesticides influence steroid hormone synthesis due to alterations in the activity of key enzymes and affect ovarian function. Pesticides can also induce oxidative stress, inflammation, and apoptosis, which may cause DNA damage and altered gene expression in ovarian cells.[46] Pesticides also affect male reproductive systems through impaired sperm quality and altered hormone levels. Insecticide exposure significantly impairs fertility in a dose-dependent manner.[47]

Organophosphate chemicals have been found to inhibit the acetylcholinesterase enzyme, as well as a number of other biological targets, including hormones, neurotransmitters, neurotrophic factors, enzymes involved in the breakdown of beta-amyloid protein, and inflammatory alterations.[48] Evidence from animal studies links exposure to the organophosphate chlorpyrifos with neurodegeneration, including elevated beta-amyloid levels and impaired cognition. However, the relationship between these effects is still unclear. Two different pathways may be involved: one in which cognitive deficits result from cholinergic overstimulation, and another that acts directly on the beta-amyloid pathway.[49] On the other hand, the relationship between pesticide exposure and Parkinson's disease is proposed to be related to inhibition of mitochondrial Complex I and oxidative stress. Additionally, organophosphates can cause oxidative stress.[50]

The repetitive or long-term exposure to cholinesterase inhibitors, such as carbamates and organophosphates, is most commonly observed in farm workers. Roldan-Tapia et al.[51] investigated the long-term cognitive effects of pesticide exposure on greenhouse workers in Almería, Spain, to assess whether chronic, low-level exposure to cholinesterase-inhibiting pesticides leads to neuropsychological dysfunction or emotional disturbances. Significant deficiencies in visuo-constructional praxis and integrative perception were observed in workers who had been exposed for more than ten years. Chronic exposure to pesticides for over a decade results in measurable impairments in visual and motor integration as neuropsychological functions.

Even exposure to low doses of pesticides is associated with neurodevelopmental disorders.[30] Organophosphate pesticide exposure during pregnancy may have a detrimental effect on a child's early behavior, motor skills, and mental development. Although the consequences of postnatal exposure are less clear, they may nonetheless affect motor and cognitive abilities and raise the possibility of attention issues.[52]

Another study on 175 pregnant tea garden workers in India evaluated the effects of pesticide exposure on pregnancy outcomes. The results showed significantly reduced AChE activity in both maternal and cord blood among the workers compared to housewives, especially in the low birth weight group. This implies pathological alterations during pregnancy, such as elevated expression of hypoxia-inducible factor (HIF-1α), which could lead to placental insufficiency and fetal growth restriction.[53]

A large study in the Almería region of Spain, an area with one of the world's highest concentrations of greenhouses, examined 4,830 children referred to Early Intervention Centers between 2011 and 2022 from a total population of about 119,897 children. Chromosomal abnormalities were the most common prenatal diagnoses, gestational age under 32 weeks was the main perinatal condition, and brain damage was the most frequent postnatal diagnosis. The findings suggest a possible link between intensive pesticide use in greenhouse areas and neurodevelopmental and learning problems in children.[54]

Selective toxicity of pesticides is extremely desirable; however, all pesticides can elicit toxicological responses in humans.

MANAGEMENT OF RISKS ASSOCIATED WITH PESTICIDES

Studies have shown that only a very limited fraction of the pesticides applied during agricultural practices directly affect the target pest organisms, while the vast majority are transported through soil, surface water, groundwater, and atmospheric systems. Numerous ecotoxicological and epidemiological studies published in recent years have revealed that addressing pesticide management solely from

an agricultural productivity perspective is unsustainable. Therefore, pesticide management is considered not only at the agricultural application scale but also within the framework of human health risk analysis.[55,56]

Integrated Pest Management (IPM) has become a significant approach for pest control in recent years. In the EU, Directive 2009/128/EC makes IPM mandatory for professional users. This approach aims to keep pest populations at a level that does not cause economic damage; in other words, it does not focus on the complete disappearance of pest populations. IPM uses chemical, biological, cultural, and mechanical control methods interactively in a systematic and adaptable way.[56] Barzman et al.[57] defined eight fundamental IPM strategies. These include: (i) designing resistant production systems for pest prevention, (ii) regular monitoring and early warning systems, (iii) threshold-based decision-making processes, (iv) prioritizing non-chemical methods, (v) preferring selective and low-risk pesticides, (vi) reducing pesticide application intensity, (vii) resistance management, and (viii) evaluating the multi-year environmental impacts of applications. This framework transforms pesticide management from a short-term, single-product-focused approach into a dynamic process that needs to be evaluated at the agroecosystem scale.[57]

Biological and "green" control methods, developed as alternatives to chemical pesticides, are fundamental components of IPM systems. In particular, bacterial insecticides (such as Bacillus thuringiensis, B. sphaericus, and Saccharopolyspora spinosa) are safer alternatives to synthetic pesticides due to their high target specificity, rapid degradation in the environment, and low residue risk. These biopesticides play a critical role not only in suppressing pest populations but also in reducing the environmental burden by decreasing the use of chemical pesticides.[58]

Current pesticide management is also significantly transformed by technological innovations. Remote sensing techniques, sensor-based monitoring systems, unmanned aerial vehicles, and digital decision-support platforms enable the monitoring of harmful pest concentrations at high spatial and temporal resolution. These technologies significantly reduce the number of applications and the risk of environmental spread by ensuring that pesticides are applied only in the necessary areas and at the appropriate times. This approach is described in the literature as "precision agriculture-based IPM".[59]

Pesticide management also includes social, economic, and managerial dimensions. The new IPM paradigm proposed by Dara[59] expands the classical ecological IPM approach by incorporating management, business model, and sustainability components. It considers producer-consumer-market interactions to be an integral part of pesticide control. In this model, pesticide management aims to optimize economic feasibility, environmental safety, and social acceptability criteria together.

Overall, the current state of pesticide management and control has evolved from short-term, one-dimensional solutions based on chemical inputs towards an IPM-based, multidisciplinary, and risk-oriented structure. The basic principles of sustainable pesticide management include reducing pesticide use, encouraging biological and cultural approaches, incorporating modern monitoring and decision support technology, and complying with legislation based on scientific findings.[56,57,59]

However, although IPM represents a significant improvement and provides a structured and practical framework for reducing pesticide use and environmental impacts at the agroecosystem scale, its scope still largely focuses on pest control and agricultural sustainability. In practice, IPM applications often evaluate impacts within specific sectors or compartments and may not fully account for cross-media transport, indirect effects, or cumulative exposures affecting human and animal health.[60] In this context, the One Health approach extends the IPM perspective by explicitly addressing the interconnectedness of environmental, human, and animal health systems. Therefore, IPM can be considered an important operational component within a broader One Health framework; however, a more explicit integration across disciplines, environmental compartments, and exposure pathways is needed to capture cumulative risks and support more comprehensive pesticide management strategies.[61]

CONCLUSIONS

In this review, we examined the challenges created by intensive pesticide use in agriculture and other sectors. The review showed that after pesticides are introduced into the environment, they are carried through several pathways and accumulate in surface waters, groundwater, and soils. Pesticide use and occurrence are variable but widespread globally. Both acute and chronic exposure to pesticides create risks for human health. Humans can be exposed to pesticides in different ways, including through drinking water and eating food containing pesticide residues.

For both future research and management, this review addresses the need for a One Health approach. Pesticide pollution is not only an environmental problem but also a public health issue. Starting with pesticide production processes and their application in agricultural fields, households, and urban areas, pesticides contaminate air, water, and soil, affect ecological processes, and enter the food chain, eventually reaching wildlife, livestock, and humans. The One Health approach can provide a holistic perspective for evaluating

pesticide-related risks, recognizing linkages among human, animal, and ecosystem health. By understanding the effects of pest control strategies, the unintended human and ecological health impacts can be minimized. Preventive strategies included in the integrated pest management framework, such as biological control, reducing the use of chemical inputs, and advancing to precision agriculture with technology, can reduce pesticide-related risks not only for humans but also for the entire ecological system.

Conflict of Interest: The authors have no conflicts of interest to declare.

Funding: The authors declared that this study received no financial support.

Use of AI for Writing Assistance: AI Tools (ChatGPT) was used to check grammar and improve clarity of the text. The authors take full responsibility for the content, accuracy, and originality of the manuscript.

Author Contributions: Concept – FDC, ZS, NA; Design – FDC, ZS, NA; Analysis and/or Interpretation - FDC, ZS, NA; Literature Review – FDC, ZS, NA; Writing – FDC, ZS, NA.

Peer-review: Externally peer-reviewed.

REFERENCES

1. Ingwersen WW, Garmestani AS, Gonzalez MA, Templeton JJ. A systems perspective on responses to climate change. Clean Technol Environ Policy 2014;16(4):719-30. [CrossRef]
2. Pham Y, Wozniak TM. Systems thinking to understand the complexity of antimicrobial resistance across One Health: A systematic review of current approaches. One Health 2025;20:101081. [CrossRef]
3. Missoni E. Global health, planetary health, One Health: conceptual and ethical challenges and concerns. Theor Med Bioeth 2024;45(3):241-50. [CrossRef]
4. Briggs DJ. A framework for integrated environmental health impact assessment of systemic risks. Environ Health 2008;7:61. [CrossRef]
5. Lü Y, Lü D, Gao G, Fu B. A holistic framework for facilitating environmental and human health. Geogr Sustain 2021;2(4):298-303. [CrossRef]
6. Ahmad MF, Ahmad FA, Alsayegh AA, Zeyaullah M, AlShahrani AM, Muzammil K, et al. Pesticides impacts on human health and the environment with their mechanisms of action and possible countermeasures. Heliyon 2024;10(7):e29128. [CrossRef]
7. Food and Agriculture Organization of the United Nations. Pesticides use and trade 1990-2023. https://www.fao.org/faostat/en/#data/RP Accessed April 21, 2026.
8. Singh NK, Sanghvi G, Yadav M, Padhiyar H, Christian J, Singh V. Fate of pesticides in agricultural runoff treatment systems: Occurrence, impacts and technological progress. Environ Res 2023;237(Pt 2):117100. [CrossRef]
9. de Souza RM, Seibert D, Quesada HB, Bassetti FD, Fagundes-Klen MR, Bergamasco R. Occurrence, impacts and general aspects of pesticides in surface water: A review. Process Saf Environ Prot 2020;135:22-37. [CrossRef]
10. Wang J, Teng Y, Zhai Y, Yue W, Pan Z. Spatiotemporal distribution and risk assessment of organophosphorus pesticides in surface water and groundwater on the North China Plain, China. Environ Res 2022;204(Pt C):112310. [CrossRef]
11. Quintana J, de la Cal A, Boleda MR. Monitoring the complex occurrence of pesticides in the Llobregat basin, natural and drinking waters in Barcelona metropolitan area (Catalonia, NE Spain) by a validated multi-residue online analytical method. Sci Total Environ 2019;692:952-65. [CrossRef]
12. Wolfram J, Bub S, Petschick LL, Schemmer A, Stehle S, Schulz R. Pesticide occurrence in protected surface waters in nature conservation areas of Germany. Sci Total Environ 2023;858(Pt 3):160074. [CrossRef]
13. Stackpoole SM, Shoda ME, Medalie L, Stone WW. Pesticides in US Rivers: Regional differences in use, occurrence, and environmental toxicity, 2013 to 2017. Sci Total Environ 2021;787:147147. [CrossRef]
14. Baran N, Rosenbom AE, Kozel R, Lapworth D. Pesticides and their metabolites in European groundwater: Comparing regulations and approaches to monitoring in France, Denmark, England and Switzerland. Sci Total Environ 2022;842:156696. [CrossRef]
15. Sabzevari S, Hofman J. A worldwide review of currently used pesticides' monitoring in agricultural soils. Sci Total Environ 2022;812:152344. [CrossRef]
16. Maggi F, Tang FHM, la Cecilia D, McBratney A. PEST-CHEMGRIDS, global gridded maps of the top 20 crop-specific pesticide application rates from 2015 to 2025. Sci Data 2019;6(1):170. [CrossRef]
17. Md Meftaul I, Venkateswarlu K, Dharmarajan R, Annamalai P, Megharaj M. Pesticides in the urban environment: A potential threat that knocks at the door. Sci Total Environ 2020;711:134612. [CrossRef]
18. Ryu HD, Han H, Park JH, Kim YS. New insights into the occurrence and removal of 36 pesticides in pesticide wastewater treatment plants in Korea. Chemosphere 2022;309(Pt 1):136717. [CrossRef]
19. Saw L, Shumway J, Ruckart P. Surveillance data on pesticide and agricultural chemical releases and associated public

health consequences in selected US states, 2003-2007. J Med Toxicol 2011;7(2):164-71. [CrossRef]

20. Gavrilescu M. Fate of Pesticides in the Environment and its Bioremediation. Engineering in Life Sciences 2005;5(6):497-526. [CrossRef]
21. Boonupara T, Udomkun P, Khan E, Kajitvichyanukul P. Airborne Pesticides from Agricultural Practices: A Critical Review of Pathways, Influencing Factors, and Human Health Implications. Toxics 2023;11(10):858. [CrossRef]
22. Neumann M, Schulz R, Schäfer K, Müller W, Mannheller W, Liess M. The significance of entry routes as point and non-point sources of pesticides in small streams. Water Res 2002;36(4):835-42. [CrossRef]
23. Leistra M, Boesten JJTI. Pesticide contamination of groundwater in western Europe. Agric Ecosyst Environ 1989;26(3-4):369-89. [CrossRef]
24. Li Z. Plant Uptake Models of Pesticides: Advancing Integrated Pest Management, Food Safety, and Health Risk Assessment. Rev Environ Contam Toxicol 2025;263(1):3. [CrossRef]
25. Fenner K, Canonica S, Wackett LP, Elsner M. Evaluating pesticide degradation in the environment: blind spots and emerging opportunities. Science 2013;341(6147):752-8. [CrossRef]
26. Karalliedde LD, Edwards P, Marrs TC. Variables influencing the toxic response to organophosphates in humans. Food Chem Toxicol 2003;41(1):1-13. [CrossRef]
27. Fantke P, Charles R, de Alencastro LF, Friedrich R, Jolliet O. Plant uptake of pesticides and human health: dynamic modeling of residues in wheat and ingestion intake. Chemosphere 2011;85(10):1639-47. [CrossRef]
28. Leeman WR, Van Den Berg KJ, Houben GF. Transfer of chemicals from feed to animal products: The use of transfer factors in risk assessment. Food Addit Contam. 2007;24(1):1-13. [CrossRef]
29. Kaplan Bekaroglu SS, Dadaser Celik F, Ates N. Pesticides in Surface Water Resources: Occurrence, Fate, Modeling and Treatment. Bahadir AM, editor. Hydrology and Urban Water Supply. Switzerland, Zürich: Springer Nature;2024.p.239-51. [CrossRef]
30. Sánchez RM, Bermeo Losada JF, Marín Martínez JA. The research landscape concerning environmental factors in neurodevelopmental disorders: Endocrine disrupters and pesticides-A review. Front Neuroendocrinol 2024;73:101132. [CrossRef]
31. Hilal-Dandan R, Brunton LL, editors. Manual of pharmacology and therapeutics. Section VIII: McGraw-Hill Medical: 2008.
32. Moore DH. Health effects of exposure to low doses of nerve agent--a review of present knowledge. Drug Chem Toxicol 1998;21(Suppl 1):123-30. [CrossRef]
33. Eddleston M, Buckley NA, Eyer P, Dawson AH. Management of acute organophosphorus pesticide poisoning. Lancet 2008;371(9612):597-607. [CrossRef]
34. Aguilar-Bañuelos JA, Bernal-Hernández YY, Medina-Díaz IM, Ruiz-Arias MA, Herrera-Moreno JF, Barrón-Vivanco BS, et al. Environmental exposure to pesticides is associated with oxidative stress, oxidative DNA damage, and elevated interleukin-8 in a child population. Environ Toxicol Pharmacol 2025;114:104656. [CrossRef]
35. Schinasi L, Leon ME. Non-Hodgkin lymphoma and occupational exposure to agricultural pesticide chemical groups and active ingredients: a systematic review and meta-analysis. Int J Environ Res Public Health 2014;11(4):4449-527. [CrossRef]
36. Zhang L, Rana I, Shaffer RM, Taioli E, Sheppard L. Exposure to glyphosate-based herbicides and risk for non-Hodgkin lymphoma: A meta-analysis and supporting evidence. Mutat Res Rev Mutat Res 2019;781:186-206. [CrossRef]
37. Gangemi S, Gofita E, Costa C, Teodoro M, Briguglio G, Nikitovic D, et al. Occupational and environmental exposure to pesticides and cytokine pathways in chronic diseases (Review). Int J Mol Med 2016;38(4):1012-20. [CrossRef]
38. Pourhassan B, Meysamie A, Alizadeh S, Habibian A, Beigzadeh Z. Risk of obstructive pulmonary diseases and occupational exposure to pesticides: a systematic review and meta-analysis. Public Health 2019;174:31-41. [CrossRef]
39. Zhang K, Paul K, Jacobs JP, Cockburn MG, Bronstein JM, Del Rosario I, et al. Ambient long-term exposure to organophosphorus pesticides and the human gut microbiome: an observational study. Environ Health 2024;23(1):41. [CrossRef]
40. Djekkoun N, Lalau JD, Bach V, Depeint F, Khorsi-Cauet H. Chronic oral exposure to pesticides and their consequences on metabolic regulation: role of the microbiota. Eur J Nutr 2021;60(8):4131-49. [CrossRef]
41. Martins JRN, Lopes S, Hurtado HN, da Silva FN, Villard DR, Taboga SR, et al. Acute and chronic effects of the organophosphate malathion on the pancreatic α and β cell viability, cell structure, and voltage-gated K+ currents. Environ Toxicol Pharmacol 2023;98:104046. [CrossRef]
42. Rempelos L, Wang J, Barański M, Watson A, Volakakis N, Hoppe HW, et al. Diet and food type affect urinary pesticide residue excretion profiles in healthy individuals: results of a randomized controlled dietary intervention trial. Am J Clin Nutr 2022;115(2):364-77. [CrossRef]

43. Merutka IR, Ettinger KM, Chernick M, Kolli RT, De Silva MCS, Drummond IA, et al. Chronic exposure to low levels of glyphosate and metals induces kidney dysfunction. Toxicol Sci 2026;209(2):kfag007. [CrossRef]
44. Hu R, Huang X, Huang J, Li Y, Zhang C, Yin Y, et al. Long- and short-term health effects of pesticide exposure: a cohort study from China. PLoS One 2015;10(6):e0128766. [CrossRef]
45. Botnaru AA, Lupu A, Morariu PC, Jităreanu A, Nedelcu AH, Morariu BA, et al. Neurotoxic Effects of Pesticides: Implications for Neurodegenerative and Neurobehavioral Disorders. J Xenobiot 2025;15(3):83. [CrossRef]
46. Wang L, Ma X, Liu J. Adverse Effects of Pesticides on the Ovary: Evidence from Epidemiological and Toxicological Studies. Environ Health (Wash) 2025;3(6):575-95. [CrossRef]
47. Selim S, Lona H. Impact of Insecticides on Male and Female Fertility: A Comprehensive Evidence-based Analysis. Bangladesh J Endocrinol Metab 2025;4(3):116-21. [CrossRef]
48. Sánchez-Santed F, Colomina MT, Herrero Hernández E. Organophosphate pesticide exposure and neurodegeneration. Cortex 2016;74:417-26. [CrossRef]
49. Ruiz-Muñoz AM, Nieto-Escamez FA, Aznar S, Colomina MT, Sanchez-Santed F. Cognitive and histological disturbances after chlorpyrifos exposure and chronic Aβ(1-42) infusions in Wistar rats. Neurotoxicology 2011;32(6):836-44. [CrossRef]
50. López-Granero C, Cañadas F, Cardona D, Yu Y, Giménez E, Lozano R, et al. Chlorpyrifos-, diisopropylphosphorofluoridate-, and parathion-induced behavioral and oxidative stress effects: are they mediated by analogous mechanisms of action? Toxicol Sci 2013;131(1):206-16. [CrossRef]
51. Roldan-Tapia L, Nieto-Escamez FA, del Aguila EM, Laynez F, Parron T, Sanchez-Santed F. Neuropsychological sequelae from acute poisoning and long-term exposure to carbamate and organophosphate pesticides. Neurotoxicol Teratol 2006;28(6):694-703. [CrossRef]
52. González-Alzaga B, Lacasaña M, Aguilar-Garduño C, Rodríguez-Barranco M, Ballester F, Rebagliato M, et al. A systematic review of neurodevelopmental effects of prenatal and postnatal organophosphate pesticide exposure. Toxicol Lett 2014;230(2):104-21. [CrossRef]
53. Kumar SN, Vaibhav K, Bastia B, Singh V, Ahluwalia M, Agrawal U, et al. Occupational exposure to pesticides in female tea garden workers and adverse birth outcomes. J Biochem Mol Toxicol 2021;35(3):e22677. [CrossRef]
54. Parrón-Carrillo R, Nievas-Soriano BJ, Parrón-Carreño T, Lozano-Paniagua D, Trigueros R. Environmental Exposure to Pesticides and the Risk of Child Neurodevelopmental Disorders. Medicina (Kaunas) 2024;60(3):475. [CrossRef]
55. Jennings AA, Li Z. Worldwide regulatory guidance values applied to direct contact surface soil pesticide contamination: Part II-noncarcinogenic pesticides. Air Soil Water Res 2017;10(1):1-14. [CrossRef]
56. Ullah F, Guru-Pirasanna-Pandi G, Murtaza G, Sarangi S, Gul H, Li X, et al. Evolving strategies in agroecosystem pest control: Transitioning from chemical to green management. J Pest Sci 2025;98(4):2307-24. [CrossRef]
57. Barzman M, Bàrberi P, Birch ANE, Boonekamp P, Dachbrodt-Saaydeh S, Graf B, et al. Eight principles of integrated pest management. Agron Sustain Dev 2015;35(4):1199-215. [CrossRef]
58. Chattopadhyay P, Banerjee G, Mukherjee S. Recent trends of modern bacterial insecticides for pest control practice in integrated crop management system. 3 Biotech 2017;7(1):60. [CrossRef]
59. Dara SK. The new integrated pest management paradigm for the modern age. J Integr Pest Manag 2019;10(1):12. [CrossRef]
60. Falkenberg T, Ekesi S, Borgemeister C. Integrated Pest Management (IPM) and One Health - a call for action to integrate. Curr Opin Insect Sci 2022;53:100960. [CrossRef]
61. Tonnang HEZ, Tepa-Yotto GT, Sokame BM, Winsou JK, Tamò M, Djouaka RF. Roadmap for mainstreaming integrated pest management (IPM) into a climate smart one-health (CS-OH) framework. One Health 2025;20:101084. [CrossRef]

Official Journal of Erciyes University Faculty of Medicine

DOI: 10.14744/cpr.2026.83356
J Clin Pract Res 2026;48(2):110–119

Glioblastoma Multiforme: Current Developments in Molecular Pathways, Magnetic Field-Based Interventions, and Personalized Therapy

Emel Çolak,[1] Ravza Tosunbayraktar,[1] Sacide Sarıçiçek,[1] Yusuf Emrullahoğlu,[2] Füsun Ferda Erdoğan[3]

[1]Department of Neuroscience, Erciyes University Gevher Nesibe Genome and Stem Cell Institute, Kayseri, Türkiye
[2]Department of Neurosurgery, Erciyes University Faculty of Medicine, Kayseri, Türkiye
[3]Department of Neurology, Erciyes University Faculty of Medicine, Kayseri, Türkiye

ABSTRACT

Glioblastoma multiforme (GBM) is the most common and aggressive brain cancer in adults. It is also one of the most aggressive tumors of the central nervous system and is associated with the worst prognosis. Developing an effective treatment method is complicated by the disease: its resistance to treatment, a high recurrence rate, and genetic and histological heterogeneity. This review provides a detailed assessment of GBM diagnostic methods, molecular pathogenesis, histopathological features, and current treatment approaches. IDH mutations, together with molecular markers such as PTEN, EGFR, TP53, and MGMT promoter methylation, play a significant role in predicting the course of glioblastoma multiforme and determining treatment response. Personalized medicine and immunotherapies, together with routine treatments, represent noteworthy approaches to GBM treatment in the near future. Recent studies report that magnetic field-based interventions are a promising approach and that applications of low-frequency magnetic fields suppress glioma cell proliferation. Studies conducted with the OM-100 device have shown a significant reduction in tumor growth in both in vivo and in vitro models and have demonstrated synergistic effects when the device was combined with anti-PD-1 therapy. Furthermore, static magnetic fields have been reported to increase apoptosis, inhibit proliferation, and may offer a complementary treatment with low toxicity. These findings suggest that magnetic-field-based approaches offer an innovative strategy for GBM treatment.

Keywords: Glioblastoma multiforme, immunotherapy, magnetic fields, mutations, precision medicine, therapeutics.

Cite this article as:
Çolak E, Tosunbayraktar R, Sarıçiçek S, Emrullahoğlu Y, Erdoğan FF. Glioblastoma Multiforme: Current Developments in Molecular Pathways, Magnetic Field-Based Interventions, and Personalized Therapy. J Clin Pract Res 2026;48(2):110–119.

Address for correspondence:
Emel Çolak.
Department of Neuroscience, Erciyes University, Kayseri, Türkiye
Phone: +90 552 215 59 38
E-mail: colakk.emell@gmail.com

Submitted: 11.11.2025
Revised: 27.02.2026
Accepted: 06.03.2026
Available Online: 20.04.2026

Erciyes University Faculty of Medicine Publications - Available online at www.jcpres.com

INTRODUCTION

Glioblastoma multiforme (GBM) is the most common type of aggressive brain cancer in adults. It is also one of the most aggressive and worst-prognosis tumors of the central nervous system. Developing an effective treatment method for the disease is complicated by its resistance to treatment and high recurrence rate, and its genetic and histological heterogeneity. Grade 4 malignant gliomas, as classified by the World Health Organization (WHO), are usually located in the supratentorial area. Histopathologically, it is characterized by both astrocytic and necrotic

Table 1. Epidemiological characteristics of glioblastoma multiforme

Epidemiological characteristics	Information / value	Reference
Frequency of occurrence (Incidence)	Approximately 3.2–4.3 cases per 100,000 people per year	Ostrom et al., 2023[3]
Age group	Most commonly between the ages of 55 and 75	Ostrom et al., 2023[3]
Gender distribution	More common in men than in women (ratio of 1.6:1)	Ostrom et al., 2023[3]
Peak age of onset	around 64 years old	Ostrom et al., 2023[3]
Percentage of all primary brain tumors	Approximately 15–17%	Ostrom et al., 2023[3]
Proportion in high-grade gliomas	Approximately 45–50%	Ostrom et al., 2023[3]
Ethnic distribution	Higher in Caucasians; lower in Blacks and Asians	Ostrom et al., 2023[3]
Risk factors	Ionizing radiation, age, male gender, genetic predisposition	Ostrom et al., 2023[3]
Primary/secondary GBM ratio	Primary GBM ≈ 90%; Secondary GBM ≈ 10%	Nakajima et al., 2018[4]
Survival time (average)	Surgery + Radiotherapy + Chemotherapy for 12–18 months	Stupp et al., 2005[20]
5-year survival rate	Approximately 5–7%	Stupp et al., 2005[20]

GBM: Glioblastoma multiforme.

core-like cells and diffuse neoplastic infiltration of GBM into nerve tissue (e.g., angular nuclei and eukaryotic nuclei).[1] The high heterogeneity of GBM, combined with the blood-brain barrier (BBB) structure, creates an environment conducive to tumor cell survival.[2] In glioblastoma multiforme, difficulty in defining tumor margins during surgical intervention stems from its rapid invasion into surrounding brain tissue. This makes it very difficult to completely remove the tumor and often results in residual tumor tissue. Epidemiological findings indicate that glioblastoma multiforme is more common in men over the age of 50. In these patients, survival time generally ranges from 12 and 18 months despite the addition of radiotherapy and chemotherapy to the surgical intervention. In this context, the basic epidemiological and molecular characteristics of Glioblastoma Multiforme are summarized in Table 1.[1,3]

In recent years, studies, particularly in molecular biology and genetic analyses, have provided a more comprehensive understanding of the disease's pathogenesis. In addition, new treatment options have been developed, and the biological basis of the disease has been established.[3]

CLINICAL AND RESEARCH RESULTS

A literature review was conducted systematically and in detail on glioblastoma multiforme using the PubMed, Web of Science, and Scopus databases between May and August 2025. The search was designed to include studies focusing on human subjects and examining molecular mechanisms, signaling pathways, or treatment strategies in glioblastoma. Appropriate studies were identified through a detailed evaluation of the titles, abstracts, and full texts of the articles.

HISTOPATHOLOGICAL FEATURES

The diagnosis of GBM relies heavily on its histopathological features. Histologically, GBM is characterized by necrotic areas, microvascular proliferation, pleomorphic cells, and high mitotic activity. Glioblastoma multiforme tumor cells exhibit high nuclear atypia (irregularity and enlargement of the nucleus) as well as highly intense mitotic divisions, indicating both uncontrolled cell division and invasive spread to surrounding tissues.[1] Circumscribed gliomas are mostly benign. In contrast, diffuse (spreading) gliomas can infiltrate the surrounding normal brain parenchyma and recur even after complete tumor resection. Diffuse gliomas are the most common type of intrinsic primary brain tumor. Diffuse gliomas are classified into three groups according to malignancy levels: WHO grades 2, 3, and 4. WHO grade 4 diffuse glioma is synonymous with glioblastoma multiforme (GBM). Astrocytoma with GBM is the most common histological subtype of WHO grade 4 diffuse gliomas. In addition, it accounts for almost 50% of all primary malignant brain tumors. Palisade-like necrosis, a commonly observed and distinctive histological finding in GBM, forms as areas of necrosis resulting from depletion of oxygen and nutrients associated with the rapid growth of tumor cells. Microvascular proliferation, known as the abnormal proliferation of small blood vessels, provides the tumor with the blood supply needed to continue its progression. At the same time, this process also paves the way for GBM to become resistant to treatment.[4]

Molecular Markers

In addition to histopathological studies, Both molecular biology techniques and defined genetic and epigenetic parameters play a role in identifying subtypes of GBM. The

Table 2. Clinical significance of prominent molecular markers in glioblastoma multiforme

Molecular marker	Clinical role	Prognostic/predictive value	Relationship to treatment	References
MGMT promoter methylation	DNA repair	Predictive in predicting response to treatment	Temozolomide sensitivity increases	Hegi et al., 2005[6]
EGFR amplification / EGFRvIII	Cell proliferation and invasion	Poor prognosis	EGFR inhibitors (Erlotinib, Gefitinib)	An et al., 2018[11]
PTEN loss	Activation of the PI3K/AKT/mTOR pathway	Associated with tumor progression	Resistance to mTOR inhibitors develops	Bonneau & Longy, 2000[17]
TP53 mutation	Tumor suppressor gene	Poor prognosis, resistant structure	Little effect on standard treatment	Yin et al., 2002[18]
IDH1/2 mutation	Cell metabolism, epigenetic regulation	Good prognosis (especially in secondary GBM)	Targeted therapies potential	Yan et al., 2009[19]

GBM: Glioblastoma multiforme; IDH: Isocitrate dehydrogenase; MGMT: O6-methylguanine-DNA methyltransferase; EGFR: Epidermal growth factor receptor; PTEN: Phosphatase and tensin homolog; TP53: Tumor protein p53; PI3K: Phosphoinositide 3-kinase; AKT: Protein kinase B; mTOR: Mammalian target of rapamycin.

molecular parameters that have contributed most to the clinical application of GBM are IDH1, MGMT, and EGFR.[5] MGMT (O-6-methylguanine-DNA methyltransferase) promoter methylation is directly related to the efficacy of temozolomide treatment. This methylation is removed by an enzyme that repairs methylated bases in DNA and can eliminate DNA damage caused by temozolomide. In short, it has been emphasized that temozolomide causes cancer cell death by increasing the effectiveness of the structural damage it creates in DNA.[6] Among patients receiving temozolomide treatment, those with methylation of this promoter generally have better outcomes, whereas those without methylation may develop resistance to treatment. Therefore, MGMT methylation status plays an important role in personalizing treatment methods and provides clinically meaningful prognostic guidance regarding how patients will respond to treatment.[7] IDH (isocitrate dehydrogenase) mutation has been widely associated with a better prognosis in patients with GBM. These mutations are mostly found in younger patients (secondary GBM) with a high number of mutations in the TP53 gene.[6] In addition, EGFR can serve as a primary therapeutic target. Tyrosine kinase inhibitors, such as erlotinib and gefitinib, are among the treatment methods aimed at inhibiting EGFR activity. This method has been evaluated in clinical trials to block downstream signaling pathways by inhibiting EGFR phosphorylation.[8] The relationship between the most frequently studied molecular markers in GBM and treatment, as well as their clinical significance, are presented in Table 2.[5,7]

Molecular Pathogenesis

The development of GBM stems from numerous genetic and epigenetic alterations. Recent studies have shown that GBM is associated with multiple molecular pathways and that these alterations determine the invasive nature of the tumor. Molecular-level abnormalities encompass multiple processes, such as excessive expression of growth factors, disruption of DNA repair mechanisms, and mutations in genetic factors that regulate the cell cycle. Glioblastoma multiforme (GBM) is a common type of primary brain tumor. Despite ongoing standard treatment, the average survival time is approximately 15 months, and it is a clinically aggressive tumor. Studies have suggested that the molecular pathogenesis of GBM has a highly complex and layered structure.[5] This review provides a detailed assessment of the tumor microenvironment, epigenetic and genetic alterations driving GBM pathogenesis, signaling pathways, and glioma stem cells. These epigenetic and genetic alterations that occur at the molecular level in GBM determine not only the biological behavior of tumor cells, but also the formation of the tumor microenvironment and the shaping of the immune response.

Tumor Microenvironment and Immune Suppression

Mutations in TP53, EGFR, NF1, PTEN, IDH1/2, and the TERT promoter are among the genetic abnormalities that shape the molecular profile of GBM. EGFR amplification, which causes permanent activation of the receptor even without ligand interaction, and especially the EGFRvIII mutation trigger cell proliferation and activate anti-apoptotic mechanisms. Losses in the PTEN gene, which cause disinhibition of the PI3K/AKT/mTOR pathway, promote tumor progression.[9]

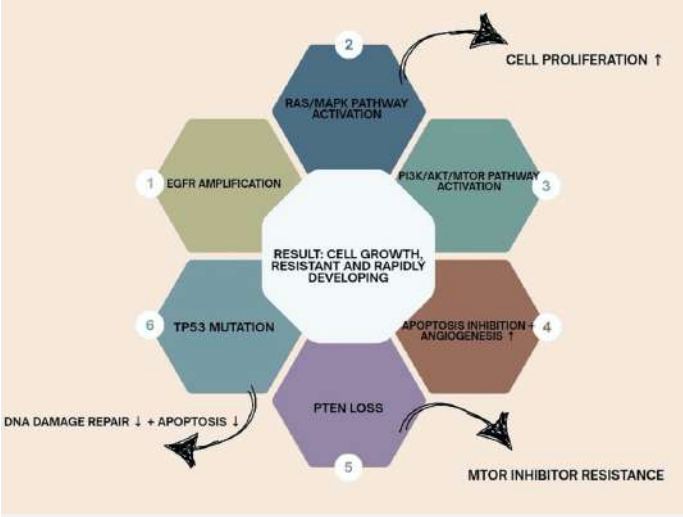

Figure 1. Key signaling pathways involved in the molecular pathogenesis of GBM, including EGFR amplification, RAS/MAPK activation, PI3K/AKT/mTOR signaling, PTEN loss, TP53 mutation, and apoptosis/angiogenesis regulation.

TP53 mutations trigger the disruption of fundamental tumor suppressor mechanisms, such as cell cycle control, DNA repair, and apoptosis. Epigenetic reprogramming occurs as a result of IDH1 mutations, which are frequently seen in secondary GBMs, through the formation of 2-hydroxyglutarate.[5]

Epigenetic Changes

Epigenetic regulation enables control of gene expression without altering the DNA sequence. MGMT promoter methylation is one of the most common epigenetic modifications observed in GBM. Methylation in this gene promoter region reduces DNA repair activity and enhances the drug response of tumor cells to alkylating agents such as temozolomide. Epigenetic mechanisms such as microRNA modulation and histone modifications also play a role in tumor progression. MicroRNAs such as miR-21 and miR-10b have been implicated in the activation of anti-apoptotic signaling pathways and the enhancement of the invasive phenotype.[9]

Genetic Alterations and Mutations

The tumor microenvironment plays a significant role in both the acquisition of invasive properties and the development of resistance to treatment in glioblastoma multiforme. Immune-suppressive cytokines (TGF-β, IL-10), macrophages (TAMs), astrocytes, and microglia associated with the tumor are used to create an immune-suppressive environment.[10] This environment suppresses T cell activation, preventing the elimination of tumor cells by the immune system. In addition, increased PD-L1 expression in GBM prevents effective the therapeutic suppression of immune checkpoints, thereby facilitating protection from the immune system. Consequently, this situation limits both the immune system's ability to recognize tumor cells and its potential to eliminate them.[9]

Signaling Pathways and Intracellular Communication

Various cellular signaling pathways play an important role in both the tumorigenesis and progression of GBM. Figure 1 depicts a pathway diagram summarizing the relationships among the signaling pathways involved in GBM pathogenesis. Among these pathways, the best-characterized are as follows:

The PI3K/AKT/mTOR pathway, activated by PTEN loss, promotes cell proliferation and inhibits apoptosis. PTEN (Phosphatase and Tensin Homolog), a protein-coding gene, is a multifunctional tumor suppressor.[5,7]

EGFR mutations activate proliferation via the RAS/MAPK pathway. The most amplified receptor tyrosine kinase (RTK) in GBM is the epidermal growth factor receptor (EGFR). EGFR gene amplification, which is specific to the basic subtype of glioma, was detected in 57.4% of patients with primary GBM This situation leads to high EGFR protein levels triggering not only tumor formation but also its progression.[11]

The Notch and Wnt/β-catenin pathways promote the regeneration of glioma stem cells. The Notch and Wnt/β-catenin signaling pathways, which are evolutionarily conserved and fundamental, modulate key biological mechanisms such as cell differentiation, proliferation, and stem cell regeneration. In addition to tumor invasiveness, the preservation of tumor stem cells, dysregulation of these pathways, and the development of treatment resistance are also associated with highly malignant gliomas such as glioblastoma multiforme (GBM).[12]

STAT3 (Signal Transducer and Activator of Transcription 3), a transcription factor that plays a key role in the pathogenesis of glioblastoma (GBM), is essential for both the maintenance of neural stem cells and the development of astrocytes. It has also been found to be continuously active in both GBM and GBM-derived cell lines, compared with normal tissues. Consequently, it has been observed to stimulate tumor growth, angiogenesis, and immune effects.[13]

Glioma Stem Cells (GSCs)

Glioma stem cells are a subpopulation with both regenerative and tumor-forming potential. GSCs possess structural features that enable them to resist radiotherapy and chemotherapy. These cells cause the Notch and Hedgehog pathways to remain constantly active, while the hypoxic microenvironment also supports the phenotype of these cells.[14]

Angiogenesis and Hypoxia

Glioblastoma multiforme (GBM) is characterized by both adaptation to hypoxia and a dense vascular structure. VEGF expression supports new blood vessel formation by enhancing the hypoxia-inducible factor-1 alpha (HIF-1α) response. This not only increases tumor size but also hinders the effective delivery of chemotherapy agents to tumor tissue.[15]

Primary Genetic Alterations

EGFR Amplification

EGFR amplification and mutations are key oncogenic drivers in several cancers, including non-small cell lung cancer (NSCLC), breast cancer, and glioblastoma. Approximately two-thirds of primary GBMs exhibit EGFR amplification, and nearly half of these cases harbor concurrent EGFRvIII mutations and single-nucleotide variants. This alteration enhances tumor cell proliferation, invasion, and therapeutic resistance by activating major signaling pathways such as PI3K/AKT, RAS/MAPK and JAK/STAT.[16]

PTEN Loss

PTEN (Phosphatase and Tensin Homolog) is a gene that encodes a protein. In addition to being a multifunctional tumor suppressor, it is very common in human cancers. It is observed to varying degrees in cancers such as glioblastoma, endometrial cancer, prostate cancer, lung cancer, and breast cancer. It has been determined that this gene carries various structural abnormalities, such as mutations or deletions, in a large number of sporadic human tumors.[17]

TP53 Mutations

TP53 encodes the tumor suppressor protein p53, whose stability and activity are negatively regulated by the oncogene product MDM2 through proteasomal degradation. p53 plays a central role in DNA repair, cell cycle control, and inhibition of angiogenesis. TP53 mutations, which are common across multiple cancer types, contribute to glioblastoma development by promoting uncontrolled cellular proliferation.[18]

IDH Mutation

Isocitrate dehydrogenase (IDH) enzymes are key regulators of cellular metabolism, including the Krebs cycle and redox balance. IDH1 is localized in the cytoplasm and peroxisomes, whereas IDH2 and IDH3 are mitochondrial. Mutations in IDH1 and IDH2 define a distinct molecular subtype of glioblastoma by reprogramming cellular metabolism and promoting genomic instability. These alterations are commonly observed in human malignancies and are associated with a more favorable prognosis. According to WHO classification, IDH mutations are present in approximately 80% of grade II/III gliomas.[19]

MGMT Promoter Methylation

MGMT is an important DNA repair enzyme that protects cells against the carcinogenic and cytotoxic effects of alkylating chemotherapy agents. Epigenetic silencing of this gene through methylation of its promoter region reduces DNA repair capacity in glioblastoma cells and weakens the resistance developed against alkylating agents.[20] Furthermore, this promoter methylation is directly related to the efficacy of temozolomide used in treatment.[6]

DIAGNOSTIC METHODS

Accurate diagnosis and classification of GBM play a critical role in both predicting its progression and determining appropriate treatment methods.[21] The diagnosis usually begins with neuroimaging followed by biopsy and histopathological examination.

Neuroimaging

Magnetic resonance imaging (MRI) is the primary diagnostic modality for glioblastoma. Contrast-enhanced T1-weighted sequences are essential for assessing tumor size, margins, and peritumoral edema. Advanced techniques such as magnetic resonance spectroscopy (MRS) further characterize tumor biology and treatment response by analyzing metabolites including choline, creatine, and N-acetylaspartate.[22]

Histopathology and Biopsy

Biopsy is the most reliable method for diagnosing GBM. In the histopathological examination of tissue samples, characteristic findings of glioblastoma such as microvascular proliferation, pleomorphism, and necrosis are examined.[19] These morphological features, characteristic of GBM, both increase diagnostic accuracy and have prognostic significance.

Molecular Analyses

Recently, molecular markers have decisively influenced the identification of GBM subtypes and the development of personalized treatments. Promoter methylation of the MGMT (O6-methylguanine-DNA methyltransferase) gene is a strong predictive biomarker of response to temozolomide chemotherapy. Patients with MGMT methylation tend to respond better to alkylating agents and also exhibit a noticeable increase in overall survival.[6,21] IDH1/IDH2 mutations are commonly found, especially in secondary GBM cases, and correlate with a better prognosis. Both changes in tumor biological behavior and, in most cases, slower-growing tumors are associated with these mutations.[19]

Treatment Methods

Treatment for GBM is highly challenging and usually involves multiple treatment modalities.

Surgical Intervention

In GBM treatment, surgical resection is the initial and most important therapeutic step. The main goal of surgical resection is to relieve mass effect and obtain brain tissue for pathological examination by removing as much of the tumor as possible. Numerous prospective studies have shown that "gross total resection" of glioblastomas provides a better survival advantage than subtotal/partial resection.[23] The combination of techniques, including intraoperative MRI, neuronavigation, ultrasound, and fluorescence-guided surgery, has led to better survival outcomes and postoperative functional improvement by enabling safe and maximal surgical resection.[24] Numerous studies have demonstrated the importance of aggressive surgical resection, when possible, and have reported trends toward better outcomes in patients with greater resection volumes. Various studies have shown statistically significant associations between greater resection extent and longer progression-free survival and overall survival.[25]

Radiotherapy and Chemotherapy

Radiotherapy, which is frequently used in GBM treatment, is typically administered at a dose of 60 Gy, while chemotherapy is administered using chemotherapeutic agents such as temozolomide. Temozolomide, which inhibits DNA repair mechanisms, causes the death of tumor cells.[20] The average survival times of GBM patients by treatment method are shown in Figure 2.

Targeted Therapies

Recent studies indicate that targeted therapies, such as EGFR and VEGF inhibitors (e.g., bevacizumab), have shown positive results. Bevacizumab targets the tumor's blood vessels and also attempts to inhibit its growth.[26]

Immunotherapies

PD-1/PD-L1 immune checkpoint inhibitors, a promising approach in GBM treatment, are being investigated. However, because the GBM tumor microenvironment is immunosuppressive and heterogeneous, the efficacy of these treatments remains limited. A systematic review published by Baskaran and colleagues in 2024 examined clinical trials of PD-1/PD-L1 inhibitors for the treatment of GBM and concluded that these therapies generally provide limited benefit. However, it was emphasized that more positive results could be achieved in patient subgroups with specific biomarkers.[27]

Magnetic Field-Based Approaches and Their Use in GBM Treatment

In recent years, therapies based primarily on magnetic fields have emerged as promising alternatives for the treatment of neurological malignancies, such as glioblastoma multiforme

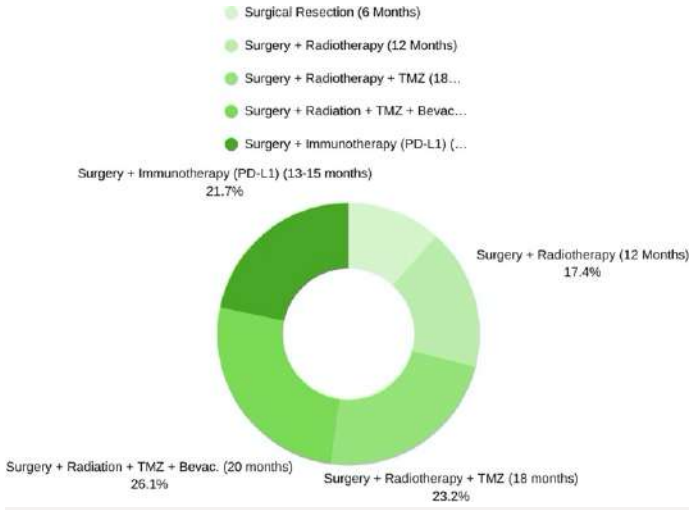

Figure 2. Average survival times observed in glioblastoma multiforme(GBM)patients according to different treatment approaches.

(GBM). These approaches generally include low-frequency magnetic fields (LF-MF), static magnetic fields (SMF), and tumor-treating fields (TTFields).

Low-Frequency Magnetic Fields (LF-MF)

In recent years, it has been demonstrated that low-frequency magnetic fields (LF-MF) have the potential to modulate the tumor microenvironment of glioblastoma multiforme (GBM) cells to favor the immune response, and to inhibit their proliferation. Studies using OM-100, an experimental tumor treatment device evaluated in GBM in both in vivo and in vitro models, report significant suppression of tumor growth. However, current data on the OM-100 device are largely limited to preclinical studies, and studies into clinical applications are still ongoing. In particular, it has been shown that LF-MF applied at a frequency of 100 kHz modulates PD-L1 expression in GBM cells. Furthermore, when combined with anti-PD-1 immunotherapy, it exhibits pronounced synergistic antitumor effects compared with standalone applications. These findings suggest that the integrated use of magnetic field-based approaches with immunotherapy may be a promising strategy in GBM treatment.[28]

Static Magnetic Fields (SMF)

The effects of SMF on GBM are related to mechanisms such as inhibition of cell proliferation, induction of apoptosis, and regulation of the tumor microenvironment. Research shows that SMF reduces the invasion and migration abilities of glioma cells and increases apoptosis, and does so by inhibiting TGF-β1-induced epithelial-mesenchymal transition (EMT).[29]

Tumor Treatment Fields (TTFields)

TTFields target cell division through the application of low-intensity electric fields. In GBM treatment, TTFields have been shown to suppress tumor growth by inhibiting cell division and to prolong patient survival. The NovoTTF-100A device is approved by the FDA and the European Medicines Agency (EMA) and is used in clinical applications.[30]

Glioblastoma multiforme is a significant focus of medical research, but it is also characterized by poor prognosis and resistance to treatment. Years of genetic and molecular research have led to new insights into the development of GBM and to new approaches to treatment. However, the heterogeneous and treatment-resistant nature of GBM complicates the development of effective treatment strategies. In the future, personalized treatment approaches, along with advances in genetic markers and immuno-oncology, will pave the way for significant steps forward in the treatment of GBM.

A meta-analysis evaluated the efficacy and safety of adjuvant temozolomide with radiotherapy for the treatment of glioblastoma. Analysis of randomized controlled trials showed that adding temozolomide to treatment significantly increased overall survival and progression-free survival. Furthermore, the incidence of serious treatment-related side effects was low, and they were tolerable to patients. These findings support the safe use of combined temozolomide therapy with radiotherapy as a standard treatment approach for GBM.[31]

A review examined glioblastoma treatment from a broad perspective, ranging from traditional methods to current multidisciplinary and innovative approaches. Due to the limitations of standard chemoradiotherapy and surgical protocols, novel targeted therapies, nanotherapies, immunotherapies, and non-invasive energy-based approaches are critically important. Furthermore, this study concluded that treatments applied alone are insufficient due to GBM's immune escape mechanisms and adaptive nature; therefore, combination-based treatment strategies may offer more effective solutions in the future.[32]

In a retrospective study, the efficacy and safety of temozolomide treatment, administered during and after radiotherapy, in patients with newly diagnosed glioblastoma were investigated. Based on ten years' experience, this study demonstrates that temozolomide improves tumor control and that treatment-related side effects are acceptable. Consequently, it is demonstrated that radiotherapy supported by temozolomide is appropriate for widespread use in glioblastoma treatment.[33]

A Phase I clinical trial investigated the safety, pharmacokinetics, and tolerability of the WEE1 kinase inhibitor adavosertib in combination with radiotherapy and temozolomide in patients with newly diagnosed glioblastoma. The study examined the drug's penetration into tumor tissue by measuring intratumoral drug levels during the treatment protocol. The results showed that the concurrent treatment had an acceptable toxicity profile and that intratumoral adavosertib concentrations were sufficient to achieve therapeutic efficacy. This study demonstrates the potential for concurrent use of adavosertib with radiotherapy and chemotherapy in glioblastoma treatment.[34]

The OLA-TMZ-RTE-01 Phase I study investigated the feasibility and safety of the combination of temozolomide, olaparib, and concurrent radiotherapy in newly diagnosed glioblastoma (GBM) patients who had undergone biopsy or partial resection. In the study, patients received different dose levels of the treatment protocol, and adverse events, treatment responses, and overall tolerability were examined. The findings indicate that combination therapy has an acceptable safety profile within the specified dose ranges and is clinically feasible.[35]

The study comprehensively examined applications of radiotherapy in patients with WHO Grade 4 adult-type diffuse glioma and evaluated dosing procedures and current clinical protocols. Based on the ASTRO clinical guidelines, the safety and efficacy of radiotherapy were analyzed, and the challenges encountered during the treatment period, as well as methods for optimization, were investigated. The data obtained within the findings contributed to the development of standard radiotherapy protocols for the treatment of high-grade gliomas.[36]

In this study, low-frequency repetitive transcranial magnetic stimulation (rTMS) produced tumor-suppressive effects on glioblastoma (GBM) progression. Experiments conducted in vitro and in vivo revealed that application of low-frequency rTMS limited GBM invasion, reduced cell proliferation, and activated apoptotic mechanisms. On the other hand, rTMS was evaluated for safety and tolerability and was found to have low toxicity and to be well tolerated. The findings suggest that rTMS may be a clinically feasible complementary treatment option that can be included in current standard protocols for GBM treatment.[37]

A study was conducted in China to investigate the efficacy and safety of chemoradiotherapy alone or in combination with Tumor Treating Fields (TTFields) in patients with newly diagnosed glioblastoma (GBM). In this study, patients were divided into two groups: the first group received the standard chemoradiotherapy protocol, while the second group received TTFields therapy in addition to this. Response rates, overall survival (OS), progression-free survival(PFS),and adverse events were evaluated. The findings showed that survival outcomes improved significantly in the group receiving TTFields and that the treatment demonstrated an acceptable safety profile.[38]

Another study evaluated the frequency-dependent effects of magnetic fields on tumor and non-tumor neural cell models. Cellular functions, proliferation, and viability were compared across different exposure frequencies. The results demonstrated that specific frequencies suppressed glioblastoma cell growth while exerting more limited effects on normal neural cells. These findings indicate that frequency-specific magnetic field modulation may represent a selective and complementary therapeutic strategy for glioblastoma.[39]

CONCLUSION

The challenging nature of glioblastoma multiforme stems from its aggressive behavior and resistance to treatment. Findings in the literature suggest that temozolomide-based radiotherapy is the standard approach for glioblastoma treatment. Additionally, innovative strategies such as PARP and WEE1 inhibitors, TTFields, and magnetic field-based methods offer potential for enhancing treatment efficacy. These findings suggest that combination approaches and personalized treatment plans may play a critical role in GBM management. In the future, integrating low-frequency magnetic field-based treatment approaches with personalized medicine strategies could create a significant paradigm shift in glioblastoma treatment. Within the scope of individualized approaches that take into account the characteristics of the tumor immune microenvironment, molecular profile, and patient-specific treatment responses, it may be possible to optimize the frequency, duration, and combination protocols for magnetic field applications, such as OM-100. When used in combination with immune checkpoint inhibitors and targeted agents, magnetic field therapies that are adapted according to patient-specific biomarkers (e.g., PD-L1 expression) may increase treatment efficacy while reducing side effects. In this regard, biomarker-based clinical trials and advanced preclinical studies will provide critical data to support the integration of magnetic field therapies into personalized GBM treatment algorithms.

Ethics Committee Approval: Ethics committee approval was not required since this is a narrative review.

Informed Consent: Written informed consent was not required since this is a narrative review.

Conflict of Interest: The authors have no conflicts of interest to declare.

Funding: The authors declared that this study received no financial support.

Use of AI for Writing Assistance: Artificial intelligence tools (ChatGPT, OpenAI) were used only for formatting suggestions and minor language editing. The authors take full responsibility for the scientific content of the manuscript.

Author Contributions: Concept – EÇ; Design – EÇ; Supervision – FFE; Resource – EÇ, YE; Materials – EÇ, YE; Data Collection and/or Processing – EÇ, YE, RT, SS; Analysis and/or Interpretation – EÇ, YE, RT, SS; Literature Review – EÇ; Writing – EÇ; Critical Review – EÇ, FFE, YE, RT, SS.

Peer-review: Externally peer-reviewed.

REFERENCES

1. Louis DN, Perry A, Wesseling P, Brat DJ, Cree IA, Figarella-Branger D, et al. The 2021 WHO Classification of Tumors of the Central Nervous System: a summary. Neuro Oncol 2021;23(8):1231-51. [CrossRef]
2. Pombo Antunes AR, Scheyltjens I, Duerinck J, Neyns B, Movahedi K, Van Ginderachter JA. Understanding the glioblastoma immune microenvironment as basis for the development of new immunotherapeutic strategies. Elife 2020;9:e52176. [CrossRef]
3. Ostrom QT, Price M, Neff C, Cioffi G, Waite KA, Kruchko C, et al. CBTRUS Statistical Report: Primary Brain and Other Central Nervous System Tumors Diagnosed in the United States in 2016-2020. Neuro Oncol 2023;25(12 Suppl 2):iv1-99. [CrossRef]
4. Nakajima N, Nobusawa S, Nakata S, Nakada M, Yamazaki T, Matsumura N, et al. BRAF V600E, TERT promoter mutations and CDKN2A/B homozygous deletions are frequent in epithelioid glioblastomas: a histological and molecular analysis focusing on intratumoral heterogeneity. Brain Pathol 2018;28(5):663-73. [CrossRef]
5. Lan Z, Li X, Zhang X. Glioblastoma: An Update in Pathology, Molecular Mechanisms and Biomarkers. Int J Mol Sci 2024;25(5):3040. [CrossRef]
6. Hegi ME, Diserens AC, Gorlia T, Hamou MF, de Tribolet N, Weller M, et al. MGMT gene silencing and benefit from temozolomide in glioblastoma. N Engl J Med 2005;352(10):997-1003. [CrossRef]
7. Pouyan A, Ghorbanlo M, Eslami M, Jahanshahi M, Ziaei E, Salami A, et al. Glioblastoma multiforme: insights into pathogenesis, key signaling pathways, and therapeutic strategies. Mol Cancer 2025;24(1):58. [CrossRef]
8. Brar HK, Jose J, Wu Z, Sharma M. Tyrosine Kinase Inhibitors for Glioblastoma Multiforme: Challenges and Opportunities for Drug Delivery. Pharmaceutics 2022;15(1):59. [CrossRef]
9. Shen Y, Thng DKH, Wong ALA, Toh TB. Mechanistic insights and the clinical prospects of targeted therapies for glioblastoma: a comprehensive review. Exp Hematol Oncol 2024;13(1):40. [CrossRef]
10. Kaynar A, Kim W, Ceyhan AB, Zhang C, Uhlén M, Turkez H, et al. Unveiling the Molecular Mechanisms of Glioblastoma through an Integrated Network-Based Approach.

Biomedicines 2024;12(10):2237. [CrossRef]

11. An Z, Aksoy O, Zheng T, Fan QW, Weiss WA. Epidermal growth factor receptor and EGFRvIII in glioblastoma: signaling pathways and targeted therapies. Oncogene 2018;37(12):1561-75. [CrossRef]
12. Kahlert UD, Maciaczyk D, Doostkam S, Orr BA, Simons B, Bogiel T, et al. Activation of canonical WNT/β-catenin signaling enhances in vitro motility of glioblastoma cells by activation of ZEB1 and other activators of epithelial-to-mesenchymal transition. Cancer Lett 2012;325(1):42-53. [CrossRef]
13. Li Y, Jiang F, Zhu S, Jia H, Li C. STAT3 drives the malignant progression of low-grade gliomas through modulating the expression of STAT1, FOXO1, and MYC. Front Mol Biosci 2024;11:1419072. [CrossRef]
14. Lu C, Kang T, Zhang J, Yang K, Liu Y, Song K, et al. Combined targeting of glioblastoma stem cells of different cellular states disrupts malignant progression. Nat Commun 2025;16(1):2974. [CrossRef]
15. Rankin EB, Giaccia AJ. Hypoxic control of metastasis. Science 2016;352(6282):175-80. [CrossRef]
16. Muñoz-Hidalgo L, San-Miguel T, Megías J, Monleón D, Navarro L, Roldán P, et al. Somatic copy number alterations are associated with EGFR amplification and shortened survival in patients with primary glioblastoma. Neoplasia 2020;22(1):10-21. [CrossRef]
17. Bonneau D, Longy M. Mutations of the human PTEN gene. Hum Mutat 2000;16(2):109-22. [CrossRef]
18. Yin Y, Stephen CW, Luciani MG, Fåhraeus R. p53 Stability and activity is regulated by Mdm2-mediated induction of alternative p53 translation products. Nat Cell Biol 2002;4(6):462-7. Erratum in: Nat Cell Biol 2002;4(11):912. [CrossRef]
19. Yan H, Parsons DW, Jin G, McLendon R, Rasheed BA, Yuan W, et al. IDH1 and IDH2 mutations in gliomas. N Engl J Med 2009;360(8):765-73. [CrossRef]
20. Stupp R, Mason WP, van den Bent MJ, Weller M, Fisher B, Taphoorn MJ, et al.; European Organisation for Research and Treatment of Cancer Brain Tumor and Radiotherapy Groups; National Cancer Institute of Canada Clinical Trials Group. Radiotherapy plus concomitant and adjuvant temozolomide for glioblastoma. N Engl J Med 2005;352(10):987-96. [CrossRef]
21. Binabaj MM, Bahrami A, ShahidSales S, Joodi M, Joudi Mashhad M, Hassanian SM, et al. The prognostic value of MGMT promoter methylation in glioblastoma: A meta-analysis of clinical trials. J Cell Physiol 2018;233(1):378-86. [CrossRef]
22. Galijasevic M, Steiger R, Mangesius S, Mangesius J, Kerschbaumer J, Freyschlag CF, et al. Magnetic Resonance Spectroscopy in Diagnosis and Follow-Up of Gliomas: State-of-the-Art. Cancers (Basel) 2022;14(13):3197. [CrossRef]
23. Price SJ, Hughes JG, Jain S, Kelly C, Sederias I, Cozzi FM, et al. Precision surgery for glioblastomas. J Pers Med 2025;15(3):96. [CrossRef]
24. Manrique-Guzmán S, Herrada-Pineda T, Revilla-Pacheco F. Surgical Management of Glioblastoma. De Vleeschouwer S, editor. Glioblastoma. Brisbane (AU): Codon Publications; 2017.
25. Roder C, Bisdas S, Ebner FH, Honegger J, Naegele T, Ernemann U, et al. Maximizing the extent of resection and survival benefit of patients in glioblastoma surgery: high-field iMRI versus conventional and 5-ALA-assisted surgery. Eur J Surg Oncol 2014;40(3):297-304. [CrossRef]
26. Vredenburgh JJ, Desjardins A, Herndon JE 2nd, Marcello J, Reardon DA, Quinn JA, et al. Bevacizumab plus irinotecan in recurrent glioblastoma multiforme. J Clin Oncol 2007;25(30):4722-9. [CrossRef]
27. Baskaran AB, Kozel OA, Venkatesh O, Wainwright DA, Sonabend AM, Heimberger AB, et al. Immune Checkpoint Inhibitors in Glioblastoma IDHwt Treatment: A Systematic Review. Cancers (Basel) 2024;16(24):4148. [CrossRef]
28. Yan Z, Huang L, Zhang X, Yu X, Huang R. Anti-tumor effect of innovative tumor treatment device OM-100 through enhancing anti-PD-1 immunotherapy in glioblastoma growth. Sci Rep 2024;14(1):18444. [CrossRef]
29. Sun Z, Zhu K, Zhao W, Fei XF, Shi L, Zhang Y. Potential mechanisms and clinical applications of static magnetic field therapy in glioma. Front Neurol 2025;16:1594874. [CrossRef]
30. Stupp R, Taillibert S, Kanner A, Read W, Steinberg D, Lhermitte B, et al. Effect of Tumor-Treating Fields Plus Maintenance Temozolomide vs Maintenance Temozolomide Alone on Survival in Patients With Glioblastoma: A Randomized Clinical Trial. JAMA 2017;318(23):2306-16. Erratum in: JAMA 2018;319(17):1824. [CrossRef]
31. Wang Y, Feng Y. The efficacy and safety of radiotherapy with adjuvant temozolomide for glioblastoma: A meta-analysis of randomized controlled studies. Clin Neurol Neurosurg 2020;196:105890. [CrossRef]
32. Obrador E, Moreno-Murciano P, Oriol-Caballo M, López-Blanch R, Pineda B, Gutiérrez-Arroyo JL, et al. Glioblastoma Therapy: Past, Present and Future. Int J Mol Sci 2024;25(5):2529. [CrossRef]
33. Joo JD, Kim H, Kim YH, Han JH, Kim CY. Validation of the

Effectiveness and Safety of Temozolomide during and after Radiotherapy for Newly Diagnosed Glioblastomas: 10-year Experience of a Single Institution. J Korean Med Sci 2015;30(11):1597-603. [CrossRef]

34. Lee EQ, Alexander BM, Romo CG, Supko JG, Agar NYR, Talebi Z, et al. Phase I Study of Adavosertib with Radiotherapy and Temozolomide in Newly Diagnosed Glioblastoma and Intratumoral Drug Levels in Recurrent Glioblastoma. Clin Cancer Res 2025;31(6):983-92. [CrossRef]
35. Stefan D, Lesueur P, Lequesne J, Feuvret L, Bronnimann C, Castéra M, et al. Olaparib, Temozolomide, and Concomitant Radiotherapy for Partially Resected or Biopsy-Only Glioblastoma First-Line Treatment: Results from the OLA-TMZ-RTE-01 Phase I Study. Clin Cancer Res 2025;31(7):1212-22. [CrossRef]
36. Yeboa DN, Braunstein SE, Cabrera A, Crago K, Galanis E, Hattab EM, et al. Radiation Therapy for WHO Grade 4 Adult-Type Diffuse Glioma: An ASTRO Clinical Practice Guideline. Pract Radiat Oncol 2025;15(5):451-71. [CrossRef]
37. Jo S, Im SH, Kim SH, Baek D, Shim JK, Kang SG, et al. Tumor suppressive effect of low-frequency repetitive transcranial magnetic stimulation on glioblastoma progression. Neurotherapeutics 2025;22(4):e00569. [CrossRef]
38. Liang L, Chen L, Ni C, Shi W, Zhou Z, Chen S, et al. Chemoradiation treatment with or without concurrent tumor-treating fields (TTFields) therapy in newly diagnosed glioblastoma (GBM) patients in China. Chin Neurosurg J 2025;11(1):5. [CrossRef]
39. López de Mingo I, Rivera González MX, Ramos Gómez M, Maestú Unturbe C. The Frequency of a Magnetic Field Determines the Behavior of Tumor and Non-Tumor Nerve Cell Models. Int J Mol Sci 2025;26(5):2032. [CrossRef]

Official Journal of Erciyes University Faculty of Medicine

DOI: 10.14744/cpr.2026.49603
J Clin Pract Res 2026;48(2):120–127

The Effect of Myeloid-Derived Suppressor Cells in Graft-versus-Host Disease

Burçin Erdem Kınaş,[1] Fatma Doğruel,[2] Esra Yıldızhan,[3] Nermin Keni Beğendi,[4] Sinan Kütük,[5] Mustafa Yavuz Köker,[6] Mustafa Çetin[7]

[1]Department of Biochemistry, Kayseri Government Hospital, Kayseri, Türkiye
[2]Department of Internal Medicine, Erciyes University, Faculty of Medicine, Kayseri, Türkiye
[3]University of Health Sciences, Kayseri Faculty of Medicine, Kayseri, Türkiye
[4]University of Health Sciences, Konya City Hospital, Konya, Türkiye
[5]Department of Hematology, Erciyes University, Faculty of Medicine, Kayseri, Türkiye
[6]Department of Immunology, Erciyes University, Faculty of Medicine, Kayseri, Türkiye
[7]Department of Hematology, Antalya Medstar Hospital, Antalya, Türkiye

Cite this article as:
Erdem Kınaş B, Doğruel F, Yıldızhan E, Keni Beğendi N, Kütük S, Köker MY, et al. The Effect of Myeloid-Derived Suppressor Cells in Graft-versus-Host Disease. J Clin Pract Res 2026;48(2):120–127.

Address for correspondence:
Esra Yıldızhan.
University of Health Sciences, Kayseri Faculty of Medicine, Kayseri, Türkiye
Phone: +90 505 409 87 26
E-mail:
esra3yildizhan@hotmail.com

Submitted: 17.04.2025
Revised: 12.03.2026
Accepted: 17.03.2026
Available Online: 20.04.2026

Erciyes University Faculty of Medicine Publications - Available online at www.jcpres.com

ABSTRACT

Objective: Myeloid-derived suppressor cells (MDSCs) are immature myeloid progenitors, including monocytic and granulocytic subgroups (M-MDSCs and PMN-MDSCs). They exhibit immunoregulatory and immunosuppressive properties by limiting immune-mediated pathology and protecting the host from destructive inflammatory damage. Graft-versus-host disease (GVHD) comprises a series of immune-mediated inflammatory events in which donor-derived T cells target the tissues and organs of the transplant recipient. This study aims to evaluate the behavior of MDSCs during GVHD in patients undergoing allogeneic hematopoietic stem cell transplantation (HSCT).

Materials and Methods: Fifteen patients who underwent allogeneic HSCT were included in the study. MDSCs and their subsets were identified and characterized by flow cytometry on days 0, 30, 60, and 90 post-engraftment.

Results: The median frequency of monocytic MDSCs (M-MDSCs) on the first day of engraftment was significantly higher in patients without GVHD than in those who developed GVHD. Furthermore, the expansion of M-MDSCs occurred significantly earlier than that of the other MDSC subset.

Conclusion: Monocytic MDSCs play a key regulatory role in limiting GVHD and may serve as potential therapeutic targets for GVHD prevention or treatment.

Keywords: Allogeneic stem cell transplantation, graft-versus-host disease, immunoregulatory cells, monocytic myeloid-derived suppressor cells, myeloid-derived suppressor cells.

INTRODUCTION

Allogeneic hematopoietic stem cell transplantation (HSCT) is a current and promising treatment for hematological malignancies, particularly leukemia. In the post-transplant period, an optimal

immune balance between the recipient and the graft is required to enable donor lymphohematopoietic cells (the graft) to engraft (i.e., settle in the recipient and produce new blood cells) while preventing tumor recurrence. Patients who undergo allogeneic HSCT face a 30% risk of developing acute graft-versus-host disease (GVHD).[1] GVHD comprises a series of immune-mediated inflammatory events and tissue damage driven by donor-derived T cells in the recipient's body. It is a complication of HSCT that can lead to graft failure, cause severe organ damage, or even be fatal.

Myeloid-derived suppressor cells (MDSCs) are immature cells of myeloid origin with predominant regulatory and suppressive properties and incomplete development and differentiation.[2,3] MDSCs are often increased in immunocompromised conditions such as cancer, chronic diseases, and inflammation. These cells may be considered predictors of adverse outcomes because they are associated with increased tumor growth through angiogenesis and metastasis. On the other hand, MDSCs suppress dynamic immune responses through the cytokines they secrete, thereby limiting immune-mediated pathology and protecting the host from destructive inflammatory damage. Based on their phenotypic and morphological characteristics, MDSCs are classified into monocytic (M-MDSC) and polymorphonuclear/granulocytic (PMN-MDSC) subsets. These cells are typically present at very low levels in peripheral blood but can be induced and expanded with granulocyte colony-stimulating factor (G-CSF) stimulation.[4] As their regulatory roles and biology become better understood, *in vitro* production and therapeutic applications may emerge as areas of interest.

This study aims to explore the relationship between GVHD and MDSCs in patients undergoing allogeneic HSCT.

MATERIALS AND METHODS

In this prospective study, 15 patients who underwent allogeneic HSCT at the Hematology and Bone Marrow Transplant Unit of Erciyes University Hospital were included. The following inclusion criteria were applied: age 18–65 years, Eastern Cooperative Oncology Group (ECOG) performance score ≤1, and adequate parenchymal organ function, defined as total bilirubin ≤2× the normal value; AST, ALT, and ALP ≤5× the normal value; creatinine ≤2× the normal value; and creatinine clearance >35 mL/min. Acute GVHD was graded according to the IBMTR/Keystone consensus criteria.[5] Patients with grade II–IV acute GVHD were classified as GVHD-positive. For GVHD prophylaxis, all patients received immunosuppressive therapy consisting of cyclosporine and a short course of methotrexate according to institutional standard protocols.

During post-transplant follow-up, peripheral venous blood samples were collected on days e0, e30, e60, and e90, starting on the first day of neutrophil engraftment (e). Antibody markers used to identify MDSCs were measured by flow cytometry: HLA-DR (PB), CD11b (PE), CD45 (KrO), CD66b (FITC), CD15 (FITC), CD33 (PE), and CD14 (PC5). The analysis was performed using a Beckman Coulter Navios flow cytometer and Kaluza analysis software. After flow cytometric analysis, neutrophils and monocytes were selected, and the mean fluorescence intensity (MFI) values of cells identified as MDSCs were obtained.

KEY MESSAGES

- Myeloid-derived suppressor cells play a major role in limiting inflammation.
- Monocytic MDSC recovery occurs earlier than that of other immunologic cells after allogeneic transplantation.
- The risk of GVHD is inversely proportional to the recovery of monocytic MDSCs.

For PMN-MDSCs, CD14-negative cells were selected from CD45-positive cells. CD11b-positive cells were then isolated from the CD14-negative population. The MFI of CD66b-positive cells among CD11b-positive cells was measured, and these cells were identified as PMN-MDSCs.[6] For M-MDSCs, CD11b-positive and CD15-negative cells were selected from CD45-positive cells. CD14-positive cells were also selected from CD33-positive cells, and HLA-DR-negative cells were defined as M-MDSCs.[6] Figures 1 and 2 present representative flow cytometry images from patient 9.

Chimerism analysis was performed at the Genetics Unit of Erciyes University using a 3500 Genetic Analyzer for fragment analysis following PCR, with subsequent analysis using GeneMapper Generic software. Informed consent was obtained from all patients.

The study was funded by the Scientific Research Projects (BAP) Unit of Erciyes University (Project No: TYL-2017-7831), and ethical approval was granted by the Erciyes University Clinical Research Ethics Committee (Approval Number: 2017/441, Date: 29.09.2017).

For statistical analysis, continuous variables were expressed as mean±standard deviation (SD) or median (minimum–maximum), and categorical variables were presented as counts and percentages (%). Histograms, Q–Q plots, and the Shapiro–Wilk test were used to assess data normality. The Mann–Whitney U test was applied to compare two independent groups of quantitative variables. For comparisons involving more than two repeated measurements, the Friedman test was used, with Bonferroni adjustment applied to control for

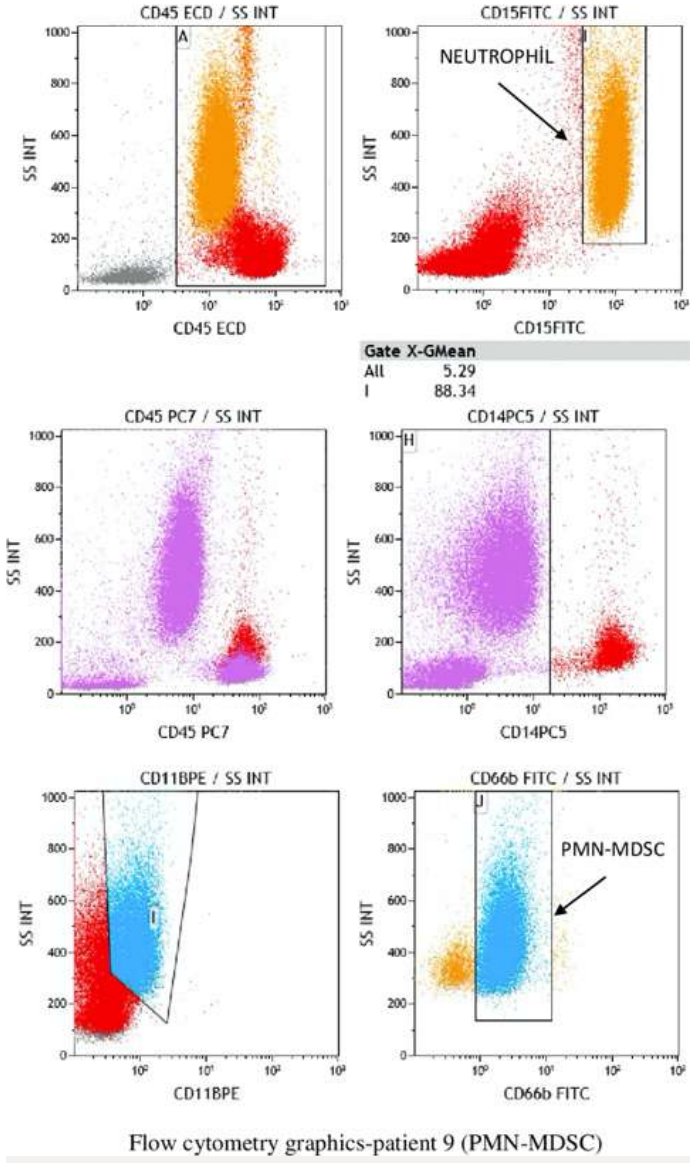

Figure 1. Example of flow cytometry graphics of PMN-MDSC (patient 9). Representative flow cytometry analysis of polymorphonuclear myeloid-derived suppressor cells (PMN-MDSCs) from a representative patient (patient 9). PMN-MDSCs were identified within the neutrophil population based on surface marker expression.

multiple testing. Spearman's correlation test was performed to assess associations between continuous variables. Based on repeated-measures analysis, the overall post hoc observed power was calculated as 63%, using the observed effect size, sample size, and an alpha level of 0.05. Data were analyzed using TURCOSA Cloud (Turcosa Ltd Co, www.turcosa.com.tr) statistical software.[7] A p-value<0.05 was considered statistically significant.

Table 1. Baseline demographic and clinical characteristics of the study population

	Total (n=15) n (%)
Gender (female)	7 (47)
Age, mean (years) ±SD	39.13±16.23
Underlying disease	
AML	6 (40)
AA	3 (20)
MDS	3 (20)
HL	1 (6.7)
MM	1 (6.7)
ALL	1 (6.7)
Donor type	
Full-matched	12 (80)
Haploidentical	3 (20)
Conditioning regimen	
Myeloablative	12 (80)
Nonmyeloablative	3 (20)
Acute GVHD (grade II–IV)	5 (33)
Survival (first 100 days)	12 (80)

Data are presented as number (%) or mean±standard deviation, as appropriate. AML: Acute myeloid leukemia; AA: Aplastic anemia; MDS: Myelodysplastic syndrome; HL: Hodgkin lymphoma; MM: Multiple myeloma; ALL: Acute lymphoblastic leukemia; GVHD: Graft-versus-host disease.

RESULTS

The study included 15 patients who underwent allogeneic transplantation for various hematological diseases. The mean age of the patients was 39 years, and 8 were male. The most common underlying indication for transplantation was acute leukemia, particularly acute myeloid leukemia (AML) (40%). Patients' demographic characteristics and transplantation data are presented in Table 1.

The median engraftment times for neutrophils and platelets were 19 and 17.5 days, respectively. Grade II–IV GVHD developed in 5 (33%) patients (GVHD-positive) (P4, P6, P13, P14, P15) during the 100-day follow-up period. Three of these patients (P13, P14, P15) died of GVHD within the first 100 days. Twelve patients completed the 100-day follow-up. All but one patient had first-month chimerism ranging from 95–100% (complete chimerism). Chimerism in P6 was 61.2; this patient died 7 months after day e90 blood collection due to relapse of the primary disease, diagnosed as MDS. Another patient, P4, who developed GVHD, died from GVHD 6 months after transplantation.

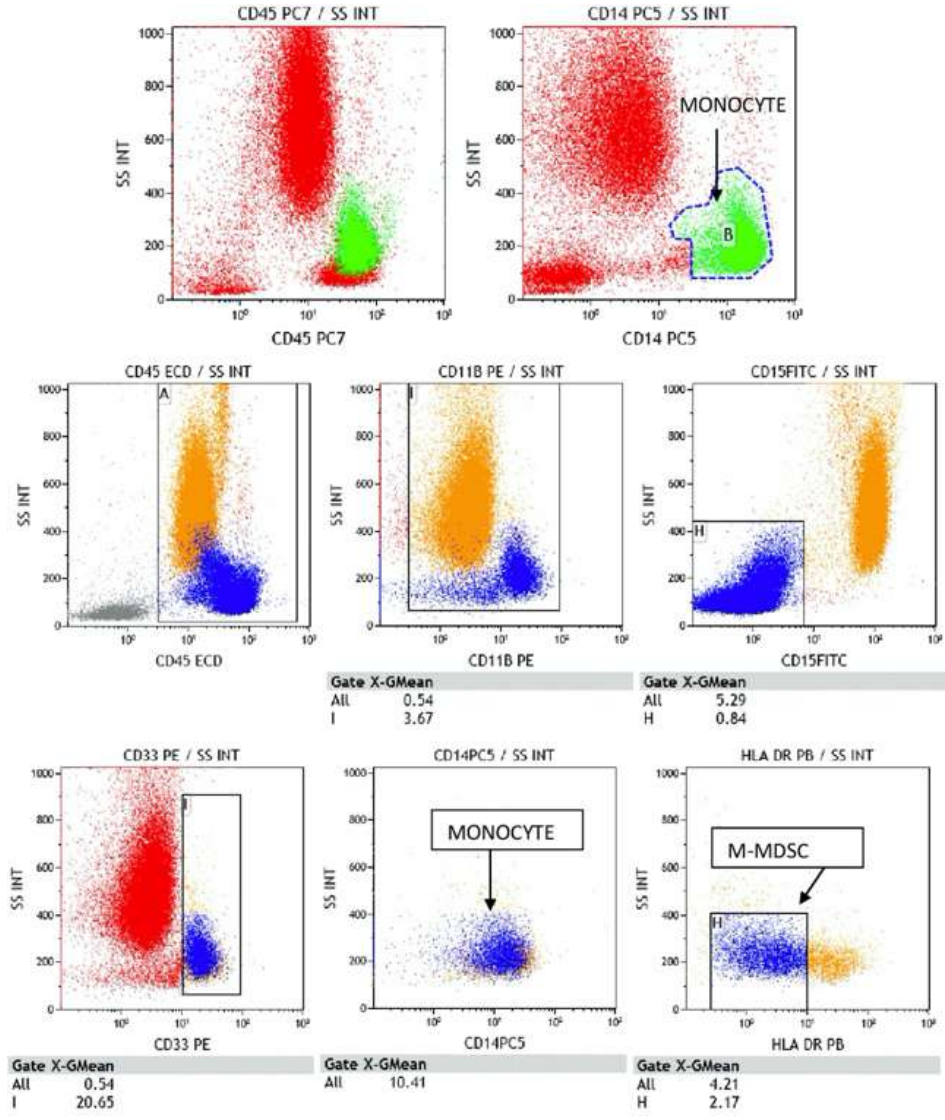

Flow cytometry graphics- patient 9 (M-MDSC)

Figure 2. Example of flow cytometry graphics of M-MDSC (patient 9). Representative flow cytometry analysis of monocytic myeloid-derived suppressor cells (M-MDSCs) from a representative patient (patient 9). M-MDSCs were gated within the monocyte population according to characteristic immunophenotypic features.

Laboratory values, including flow cytometry, blood counts, and chimerism parameters, as well as their changes over time, are presented in Table 2. Changes in M-MDSC and lymphocyte values over time were statistically significant (p=0.039 and p=0.010). Changes in the remaining parameters did not reach statistical significance (CD14/MFI p=0.183, CD15/MFI p=0.896, PMN-MDSC/MFI p=0.071, M-MDSC/MFI p=0.039, WBC p=0.183, neutrophils p=0.281, monocytes p=0.409, lymphocytes p=0.010, thrombocytes p=0.689). Chimerism was preserved in these patients.

In the correlation analysis, a moderate, statistically significant positive correlation was observed between platelet engraftment time (Plt-e) and CD14+ cells (r=0.556, p=0.039). A moderate negative correlation was observed between neutrophil engraftment time (Neu-e) and CD15+ cells (r=-0.472, p=0.076); however, this did not reach statistical significance. No statistically significant correlations were observed between neutrophil or platelet engraftment times and PMN-MDSCs or M-MDSCs (Plt-e and PMN-MDSC r=0.409, p=0.147; Plt-e and M-MDSC r=0.152, p=0.603; Neu-e and PMN-MDSC r=-0.074, p=0.793; Neu-e and M-MDSC r=-0.018, p=0.949).

Table 2. Flow cytometry and blood count parameters across engraftment time points

Parameter	e0 (n=15) Median (IQR)	e30 (n=15) Median (IQR)	e60 (n=13) Median (IQR)	e90 (n=11) Median (IQR)	p
CD14/MFI	14.8 (11.4–90.5)	21.7 (15.7–36.5)	25.0 (18.2–71.3)	104.9 (34.2–143.0)	0.183
CD15/MFI	30.4 (23.4–74.8)	46.9 (28.3–99.9)	61.3 (30.3–86.3)	43.5 (18.9–88.9)	0.896
PMN-MDSC/MFI	147.3 (23.4–250.0)	201.6 (151.6–352.0)	189.2 (145.0–242.0)	191.4 (173.4–293.8)	0.071
M-MDSC/MFI	1.4 (0.9–1.8)[a]	2.0 (1.8–2.6)[b]	2.1 (1.2–2.3)[ab]	1.7 (0.8–2.9)[ab]	0.039
WBC (10^3/μL)	3.3 (1.8–4.9)	3.9 (3.5–4.9)	3.3 (2.8–5.8)	5.3 (3.3–5.7)	0.183
Neutrophils (10^3/μL)	1.8 (1.1–3.2)	3.0 (1.8–3.4)	1.7 (1.3–4.0)	3.5 (1.8–3.7)	0.281
Monocytes (10^3/μL)	0.6 (0.5–1.1)	0.5 (0.4–0.6)	0.4 (0.3–0.6)	0.5 (0.3–0.7)	0.409
Lymphocytes (10^3/μL)	0.5 (0.3–0.7)[a]	0.8 (0.5–1.1)[ab]	1.1 (0.9–1.4)[b]	0.9 (0.7–1.2)[ab]	0.010
Thrombocytes (10^3/μL)	97.0 (42.0–161.0)	126.0 (111.0–159.0)	143.0 (121.0–186.0)	154.0 (115.0–177.0)	0.689

Longitudinal changes in flow cytometry parameters and peripheral blood counts at predefined engraftment time points (e0, e30, e60, and e90). Data are presented as median and interquartile range (IQR). P values indicate overall differences between time points. The same letters within a row indicate similarity between time points, whereas different letters indicate statistically significant differences. e0: Engraftment day; e30: 30th day of engraftment; e60: 60th day of engraftment; e90: 90th day of engraftment; CD: Cluster of differentiation; MFI: Mean fluorescence intensity; PMN-MDSC: Polymorphonuclear myeloid-derived suppressor cell; M-MDSC: Monocytic myeloid-derived suppressor cell; WBC: White blood cell.

The median M-MDSC level measured on day e0 was significantly higher in GVHD-negative patients than in GVHD-positive patients ($p<0.02$). No statistically significant differences were observed for the other parameters with respect to GVHD status and time ($p>0.05$) (Table 3).

The change in lymphocyte levels over time in the GVHD-negative group was statistically significant ($p<0.01$). The median value on day e60 was higher than that on day e0 (Table 3).

DISCUSSION

In normal physiology, when a pathological threat arises—such as infection, tissue damage, or malignant transformation—myelopoiesis is stimulated, leading to myeloid expansion aimed at eliminating the threat. As inflammation and myeloid expansion persist, the morphology of myeloid cells shifts toward a more immature state. These immature cells, defined as MDSCs, possess immunosuppressive capacities and thus prevent excessive tissue damage by suppressing the immune response.[8,9] MDSCs exert immunosuppressive and anti-inflammatory effects through the cytokines they secrete. In the pathogenesis of many solid tumors, an increase in the MDSC population is observed, and elimination of MDSCs enhances the immune response, strengthens anti-tumor activity, and shifts the balance against the tumor. However, in HSCT, suppression of the immune response may represent a therapeutic target.

Notarantonio et al.[10] recently published a study examining the effects of MDSCs on disease relapse in patients who underwent allogeneic stem cell transplantation. In this study, they suggested that MDSCs reduce GVHD development through their immunosuppressive effects and are associated with relapse by impairing the immune system's ability to identify and eliminate blastic cells. Fan et al.[11] demonstrated in a study of allogeneic stem cell recipients with different primary hematological malignancies that bone marrow–derived grafts contained higher numbers of MDSCs than peripherally derived stem cells and that the number of MDSCs in the graft was negatively correlated with the incidence and severity of GVHD. Li et al.[12] conducted a study comparing pegylated G-CSF with conventional G-CSF in relation to GVHD. In this study, severe GVHD was less frequent in patients receiving peg-G-CSF, and the beneficial effects of peg-G-CSF grafts were attributed to increased numbers of M-MDSCs.

In another study investigating the role of MDSCs in immune reconstitution after allogeneic HSCT, 26 patients were followed during the first three months after transplantation.[13] Both MDSC subsets were found to recover within 2–4 weeks, well before the recovery of T and B lymphocytes. MDSCs have been shown to suppress the differentiation of Th1 cells and promote the development of regulatory T (Treg) lymphocytes.[13] Functional MDSCs contribute to the early post-transplant regulatory cell population after HSCT. Monocytes are among the first cells to recover after successful allogeneic transplantation, followed by granulocytes and platelets. In contrast, lymphocyte recovery, along with coordinated immune reconstitution, generally does not occur until approximately 100 days after HSCT.[10,14] The aforementioned study demonstrated that MDSCs begin to recover within the first month after HSCT, with M-MDSCs recovering 1–2 weeks earlier than PMN-MDSCs. This finding is consistent with

Table 3. Comparison of flow cytometry and blood count parameters according to GVHD status

Parameter	Time	GVHD positive (n=5) Median (IQR)	GVHD negative (n=10) Median (IQR)	p*
CD14/MFI	e0	21.7 (11.4–46.9)	16.8 (6.3–159.9)	0.859
	e30	36.8 (21.2–132.5)	21.7 (7.2–80.5)	0.129
	e60	18.1 (15.5–119.9)	24.9 (13.7–200.1)	0.573
	e90	108.2 (74.5–141.9)	104.9 (14.2–257.8)	0.999
	p	0.494	0.392	
CD15/MFI	e0	48.1 (15.3–79.4)	30.1 (14.7–85.1)	0.859
	e30	38.0 (9.8–107.6)	42.2 (9.5–108.6)	0.953
	e60	66.2 (16.1–87.4)	46.3 (13.4–93.3)	0.692
	e90	69.4 (43.5–95.2)	24.7 (12.1–111.4)	0.436
	p	0.896	0.954	
PMN-MDSC/MFI	e0	169.8 (93.0–355.0)	141.0 (5.3–297.0)	0.513
	e30	249.4 (170.0–446.0)	171.6 (101.8–352.0)	0.075
	e60	216.8 (30.2–242.0)	177.0 (82.6–374.0)	0.811
	e90	130.7 (35.4–226.0)	191.4 (101.0–377.2)	0.436
	p	0.308	0.115	
M-MDSC/MFI	e0	0.8 (0.5–1.2)	1.6 (0.1–2.7)	0.028
	e30	1.2 (0.7–2.6)	2.0 (1.1–2.9)	0.440
	e60	1.1 (0.5–2.3)	2.1 (0.7–3.3)	0.287
	e90	1.0 (0.8–1.3)	1.9 (0.7–3.0)	0.327
	p	0.145	0.145	
Neutrophils (10^3/μL)	e0	3.2 (2.3–7.9)	1.6 (0.9–4.8)	0.055
	e30	4.2 (1.7–6.9)	3.0 (1.8–4.3)	0.440
	e60	1.2 (1.2–4.0)	1.7 (1.2–6.8)	0.217
	e90	3.0 (2.5–3.6)	3.5 (1.2–10.8)	0.999
	p	0.896	0.268	
Monocytes (10^3/μL)	e0	1.3 (0.6–2.6)	0.6 (0.2–2.0)	0.075
	e30	0.5 (0.4–0.9)	0.5 (0.2–1.2)	0.513
	e60	0.2 (0.2–0.6)	0.4 (0.1–0.8)	0.371
	e90	0.6 (0.3–0.8)	0.5 (0.3–1.1)	0.582
	p	0.308	0.706	
Lymphocytes (10^3/μL)	e0	0.6 (0.0–0.7)	0.5 (0.2–2.0)[a]	0.953
	e30	0.9 (0.4–1.6)	0.7 (0.2–1.7)[ab]	0.310
	e60	1.1 (0.4–1.2)	1.2 (0.6–1.8)[b]	0.469
	e90	0.7 (0.5–1.0)	0.9 (0.2–2.0)[ab]	0.727
	p	0.112	0.013	

Comparison of flow cytometry parameters and peripheral blood counts between patients with and without acute GVHD at different engraftment time points. Data are expressed as median and interquartile range (IQR). p* indicates the significance of differences between groups, and p indicates the significance of differences over time. The same letters within a column indicate similarity between time points, whereas different letters indicate statistically significant differences. # In the GVHD group, the sample size was n=3 for e60 and n=2 for e90, as three patients died before the respective sampling time points. In the non-GVHD group, the sample size was n=9 for e90, as one patient died before the sampling time point. e0: Engraftment day; e30: 30th day of engraftment; e60: 60th day of engraftment; e90: 90th day of engraftment; CD: Cluster of differentiation; MFI: Mean fluorescence intensity; PMN-MDSC: Polymorphonuclear myeloid-derived suppressor cell; M-MDSC: Monocytic myeloid-derived suppressor cell; WBC: White blood cell.

previous data indicating that monocytes recover earlier than granulocytes following HSCT. The study also emphasized the potentially important role of PMN-MDSCs in HSCT. PMN-MDSCs were noted to be more abundant numerically, to exert stronger suppressive effects on lymphocyte proliferation, to show a positive correlation with other components of the immune system, and to potentially serve as predictors of acute GVHD.[13,14]

In the present study, neither neutrophil nor platelet engraftment times correlated with MDSCs. However, the number of M-MDSCs increased significantly earlier than that of other subsets during the first month after transplantation ($p<0.05$). A significant increase in lymphocyte counts was observed at the end of the second month. Baseline M-MDSC levels were higher in patients who did not develop GVHD than in those who did. This finding is consistent with previous data suggesting that M-MDSCs may serve as predictive biomarkers for acute GVHD.[15] However, unlike the findings of Storek et al.,[14] similar parameters were not found to be significant for PMN-MDSCs.

The recovery of MDSCs during the early post-transplant immune process is thought to depend on growth factors and proinflammatory cytokines.[4] Therefore, changes in clinical practice, such as post-transplant growth factor administration, may influence both the quantity and function of MDSCs in the microenvironment, potentially explaining differences in GVHD outcomes associated with the use of hematopoietic growth factors. A better understanding of the physiological behavior of MDSCs in patients with GVHD will provide valuable insights to guide future studies on the use of these cells to limit the uncontrolled immune response central to GVHD pathophysiology. As cellular therapies continue to advance toward clinical application, MDSCs may represent a promising therapeutic tool.

In addition, age-related immune changes may influence the interpretation of MDSC dynamics in the post-transplant setting. Aging is associated with inflammaging, a chronic low-grade inflammatory state that contributes to immunosenescence-related alterations in hematopoiesis, including myeloid skewing and increased generation of MDSCs in the bone marrow.[16] Consequently, age-related variability in MDSC levels may represent a confounding factor when evaluating immune profiles in transplant recipients. However, the age distribution of our cohort was relatively narrow, as all patients were eligible for allogeneic hematopoietic stem cell transplantation. The mean age of the study population was 39.1±16.2 years, reflecting a relatively young and selected patient population. Therefore, the potential impact of age-related variation in MDSC levels is likely to be limited in this cohort.

The major limitation of this study was the relatively small sample size, including only 15 patients, which inevitably affected the statistical power of some analyses and the generalizability of the findings. In addition, the relapse rate was very low, limiting the ability to assess the potential impact of MDSCs on disease relapse. The overall observed power for the repeated-measures analysis was moderate (63%), reflecting the limited number of cases. Therefore, the findings should be interpreted with caution, considered preliminary, and validated in larger prospective cohorts.

Despite these limitations, the prospective design and serial measurements during the early post-transplant period provide preliminary evidence that M-MDSCs may serve as an early biomarker for acute GVHD.

CONCLUSION

In conclusion, the monocytic subtype of MDSCs plays a predominant role in limiting GVHD and may represent a potential therapeutic target for the prevention or treatment of GVHD.

Ethics Committee Approval: Ethics committee approval was obtained from Erciyes University Clinical Research Ethics Committee (Approval Number: 2017/441, Date: 29.09.2017).

Informed Consent: Informed consent was obtained from all patients.

Conflict of Interest: The authors have no conflicts of interest to declare.

Funding: The study was funded by the Scientific Research Projects (BAP) Unit of Erciyes University (Project No: TYL-2017-7831).

Use of AI for Writing Assistance: No use of AI-assisted technologies was declared by the authors.

Author Contributions: Concept – BEK, FD, EY, NKB, SK, MYK, MÇ; Design – BEK, FD, EY, NKB, SK, MYK, MÇ; Supervision – BEK, FD, EY, NKB, SK, MYK, MÇ; Resource – BEK, NKB, MYK; Materials – BEK, NKB, SK; Data Collection and/or Processing – BEK, FD, SK; Analysis and/or Interpretation – BEK, FD, SK; Literature Review – BEK, FD, EY; Writing – BEK, FD, EY; Critical Review – BEK, EY.

Peer-review: Externally peer-reviewed.

REFERENCES

1. Ferrara JL, Levine JE, Reddy P, Holler E. Graft-versus-host disease. Lancet 2009;373(9674):1550-61. [CrossRef]
2. Fan R, De Beule N, Maes A, De Bruyne E, Menu E, Vanderkerken K, Maes K, et al. The prognostic value and therapeutic targeting of myeloid-derived suppressor cells in hematological cancers. Front Immunol 2022;13:1016059. [CrossRef]

3. Gabrilovich DI. Myeloid-Derived Suppressor Cells. Cancer Immunol Res 2017;5(1):3-8. [CrossRef]
4. Demosthenous C, Sakellari I, Douka V, Papayanni PG, Anagnostopoulos A, Gavriilaki E. The Role of Myeloid-Derived Suppressor Cells (MDSCs) in Graft-versus-Host Disease (GVHD). J Clin Med 2021;10(10):2050. [CrossRef]
5. Przepiorka D, Weisdorf D, Martin P, Klingemann HG, Beatty P, Hows J, et al. 1994 Consensus Conference on Acute GVHD Grading. Bone Marrow Transplant 1995;15(6):825-828.
6. Lv M, Wang K, Huang XJ. Myeloid-derived suppressor cells in hematological malignancies: friends or foes. J Hematol Oncol 2019;12(1):105. [CrossRef]
7. TURCOSA Cloud Statistics Software (Version 2025). Turcosa Analytics, Istanbul, Türkiye. https://www.turcosa.com.tr Accessed March 18, 2026.
8. Yang Y, Li C, Liu T, Dai X, Bazhin AV. Myeloid-Derived Suppressor Cells in Tumors: From Mechanisms to Antigen Specificity and Microenvironmental Regulation. Front Immunol 2020;11:1371. [CrossRef]
9. Vladimirovna IL, Sosunova E, Nikolaev A, Nenasheva T. Mesenchymal Stem Cells and Myeloid Derived Suppressor Cells: Common Traits in Immune Regulation. J Immunol Res 2016;2016:7121580. [CrossRef]
10. Notarantonio AB, Bertrand A, Piucco R, Fievet G, Sartelet H, Boulangé L, et al. Highly immunosuppressive myeloid cells correlate with early relapse after allogeneic stem cell transplantation. Exp Hematol Oncol 2024;13(1):50. [CrossRef]
11. Fan Q, Liu H, Liang X, Yang T, Fan Z, Huang F, et al. Superior GVHD-free, relapse-free survival for G-BM to G-PBSC grafts is associated with higher MDSCs content in allografting for patients with acute leukemia. J Hematol Oncol 2017;10(1):135. [CrossRef]
12. Li L, Yin J, Li Y, Wang C, Mao X, Wei J, et al. Allogeneic Hematopoietic Stem Cell Transplantation Mobilized With Pegylated Granulocyte Colony-Stimulating Factor Ameliorates Severe Acute Graft-Versus-Host Disease Through Enrichment of Monocytic Myeloid-Derived Suppressor Cells in the Graft: A Real World Experience. Front Immunol 2021;12:621935. [CrossRef]
13. Guan Q, Blankstein AR, Anjos K, Synova O, Tulloch M, Giftakis A, et al. Functional Myeloid-Derived Suppressor Cell Subsets Recover Rapidly after Allogeneic Hematopoietic Stem/Progenitor Cell Transplantation. Biol Blood Marrow Transplant 2015;21(7):1205-14. [CrossRef]
14. Storek J, Geddes M, Khan F, Huard B, Helg C, Chalandon Y, et al. Reconstitution of the immune system after hematopoietic stem cell transplantation in humans. Semin Immunopathol 2008;30(4):425-37. [CrossRef]
15. Kim TW, Park SS, Lim JY, Min GJ, Park S, Jeon YW, et al. Predictive Role of Circulating Immune Cell Subtypes Early after Allogeneic Hematopoietic Stem Cell Transplantation in Patients with Acute Leukemia. Int J Stem Cells 2018;12(1):73-83. [CrossRef]
16. Salminen A, Kaarniranta K, Kauppinen A. The role of myeloid-derived suppressor cells (MDSC) in the inflammaging process. Ageing Res Rev 2018;48:1-10. [CrossRef]

Official Journal of Erciyes University Faculty of Medicine

DOI: 10.14744/cpr.2026.93073
J Clin Pract Res 2026;48(2):128–136

Venous Measurements as Predictors of Long-Term Fontan Complications: A Single-Center Echocardiographic Study

Oguzhan Ay,[1] Firat Ergin,[2] Mehmet Baki Beyter,[3] Gulcin Kayan Kasikci,[4] Buket Sura Yardimci,[5] Eser Dogan,[6] Nuri Osman Tuncer,[7] Yuksel Atay,[7] Resit Erturk Levent,[7] Zulal Ulger[7]

[1]Department of Pediatric Cardiology, İzmir Democracy University, Buca Seyfi Demirsoy Training and Research Hospital, İzmir, Türkiye
[2]Department of Pediatric Cardiology, Van Training and Research Hospital, Van, Türkiye
[3]Department of Pediatric Cardiology, İzmir City Hospital, İzmir, Türkiye
[4]Department of Pediatric Cardiology, Kayseri City Hospital, Kayseri, Türkiye
[5]Department of Pediatrics, Ege University Faculty of Medicine, İzmir, Türkiye
[6]Department of Pediatric Cardiology, Faculty of Medicine, Ege University, İzmir, Türkiye
[7]Department of Cardiovascular Surgery, Ege University Faculty of Medicine, İzmir, Türkiye

Cite this article as:
Ay O, Ergin F, Beyter MB, Kayan Kasikci G, Yardimci BS, Dogan E, et al. Venous Measurements as Predictors of Long-Term Fontan Complications: A Single-Center Echocardiographic Study. J Clin Pract Res 2026;48(2):128–136.

Address for correspondence:
Oguzhan Ay.
Department of Pediatric Cardiology, İzmir Democracy University, Buca Seyfi Demirsoy Teaching and Research Hospital, İzmir, Türkiye
Phone: +90 537 490 41 65
E-mail: oguzhanay1@gmail.com

Submitted: 22.10.2025
Revised: 11.03.2026
Accepted: 18.03.2026
Available Online: 27.04.2026

Erciyes University Faculty of Medicine Publications - Available online at www.jcpres.com

ABSTRACT

Objective: This study aims to assess the impact of complications of the Fontan operation, such as protein-losing enteropathy and thrombosis, on patients' quality of life. We hypothesize that alterations in the diameter and flow of the inferior vena cava (IVC) and femoral vein (FV) are associated with these complications. The goal is to evaluate the influence of venous structural modifications on Fontan operation outcomes by analyzing Doppler time measurements of the IVC, FV, aorta (Ao), and femoral artery (FA).

Materials and Methods: We retrospectively analyzed the recorded images of patients who had undergone Fontan palliation at least two years prior to presentation at our outpatient clinic between January 2022 and January 2023. Patients with chest pain but no cardiac pathology served as controls. Demographic and physical examination data were collected retrospectively. In patients with a normal single-ventricular ejection fraction, we measured the widest IVC diameter and Doppler values, the descending aortic diameter in systole, the widest FV diameter and Doppler values, and the femoral artery diameter in systole.

Results: The study included 25 Fontan patients: 7 had an extracardiac Fontan, 4 had a fenestrated extracardiac Fontan, and 14 had an intra-extracardiac fenestrated Fontan. A significant difference (p=0.019) was found in the age at Fontan between patients with NYHA stages 1-2 and those with NYHA stages 3-4. A pathologic microalbumin/creatinine ratio (>15) was correlated with pre-Fontan pulmonary artery pressure >15 mmHg. The IVC/BSA (p=0.031) and FV/BSA ratios differed significantly between groups with and without complications, with lower ratios observed in the group with complications.

Conclusion: Age at Fontan palliation is a risk factor for complications. High pre-Fontan pulmonary pressure is associated with microalbuminuria. IVC/BSA and FV/BSA are inversely associated with mid- to long-term complications following Fontan palliation.

Keywords: Complication, congenital heart disease, echocardiography, femoral vein, Fontan operation, inferior vena cava.

INTRODUCTION

The Fontan operation, first described in 1971 by French physician Dr. Francis Fontan, significantly alters the hemodynamic profile of patients, affecting both the arterial and venous systems. This procedure improves oxygenation in patients with congenital heart disease who are not candidates for biventricular correction, thus enhancing their quality of life. The altered circulatory pattern, known as single-ventricle physiology, warrants further investigation due to its diverse physiological effects and consequences. The profound impact of the Fontan operation on hemodynamics has been well established after over five decades of clinical application in advanced centers.[1] Long-term investigation and monitoring of hemodynamic status in single-ventricle physiology are crucial for understanding patient mortality and morbidity. Complications are common in Fontan patients during long-term follow-up.[2]

Existing literature indicates a strong association between mortality and conditions such as osteoarthritis, protein-losing enteropathy, cirrhosis, and renal failure. Fontan-associated nephropathy, often identified by abnormal microalbumin-to-creatinine ratios, has recently garnered significant attention, although its specific markers remain unclear.[3,4] Studies report a 20% prevalence of nephropathy among young Fontan patients.[4-6] Although MRI and CT modeling have enhanced our understanding of hemodynamics involving surgical connections and energy loss,[7-9] evidence concerning the status of the inferior vena cava (IVC) and femoral vein (FV) in long-term prognosis remains scarce. While the relationship between IVC diameter and nephropathy development has been investigated, its overall prognostic significance remains unclear.[4,10] Therefore, this study aims to examine the potential correlation between inferior vena cava diameter and long-term complications following Fontan palliation.[11,12]

In vitro and computational models, including MRI and CT, have advanced our understanding of Fontan hemodynamics, focusing on surgical connections and energy loss.[7-9] However, research on the relationship between IVC and FV and long-term prognosis remains limited.[4,10] While IVC diameter is linked to nephropathy, its comprehensive prognostic significance is not fully understood. Although echocardiography effectively assesses ventricular function, non-invasive evaluation of venous and pulmonary circulation in single-ventricle patients remains challenging. Monitoring these circulatory changes is crucial due to serious risks such as Fontan-associated nephropathy.[1,2] However, the role of venous measurements in predicting and monitoring post-Fontan complications remains poorly defined, and their long-term clinical utility requires further investigation.[4,10]

KEY MESSAGES

- Unexpectedly, diminished IVC/BSA and FV/BSA ratios suggest that chronic metabolic effects, rather than elevated intravascular pressure, are the primary drivers of long-term Fontan complications.
- Angiography-measured pre-Fontan pulmonary artery pressures greater than 15 mmHg predict an increased risk of subsequent renal complications, as demonstrated by an association with pathological microalbuminuria.
- The study highlights the need for thorough, long-term monitoring of Fontan complications, such as protein-losing enteropathy, arrhythmia, and thrombosis, in patients with reduced IVC/BSA and FV/BSA ratios.

This study aims to investigate the potential correlation between venous measurements (inferior vena cava diameter and femoral vein diameter) and the occurrence of long-term complications, including protein-losing enteropathy, plastic bronchitis, thrombosis, and arrhythmia, in patients undergoing Fontan palliation. Additionally, we examined nephropathy, a chronic Fontan complication, by analyzing spot urine microalbumin/creatinine ratios and correlating these findings with venous diameter measurements (IVC, FV).

MATERIALS AND METHODS

We retrospectively collected data from images of Fontan patients acquired in the previous year. All patients had undergone Fontan palliation within the last 15 years and were seen in the outpatient clinic between January 2022 and January 2023 at the Ege University Faculty of Medicine, Department of Pediatric Cardiology. The study protocol was approved by Ege University Medical Research Ethics Committee (Approval Number: 23-9T/31, Date: 07.09.2023).

Data Collection

Patient data, including age, height, weight, body surface area (BSA), age at the time of operation, exercise capacity (according to the New York Heart Association classification), SpO_2, microalbumin/creatinine ratios, pre-Fontan pulmonary arterial pressure measured during conventional angiography, and complications such as protein-losing enteropathy, plastic bronchitis, thrombosis, and arrhythmia, were obtained from their medical records. Additionally, measurements of the inferior vena cava (IVC), femoral vein (FV), abdominal aorta, femoral artery, and Doppler times for the IVC and FV were retrospectively obtained from recorded echocardiography images.

Study Groups

There is no standard for inferior vena cava measurements, and in pediatric patients, these measurements vary with height and weight. Therefore, a control group was included. The control group consisted of patients presenting with chest pain and no cardiac pathology; their images were evaluated. Initially, measurements from Fontan patients were compared with those from the control group. Subsequently, the patient group was further divided into two subgroups: Fontan patients with complications and those without. Protein-losing enteropathy, plastic bronchitis, thrombosis, and arrhythmia were considered long-term complications arising during patient follow-up.[13] These measurements were then compared between these subgroups.

The exclusion criteria for the patient group were a history of thrombosis both preoperatively and during the first month, femoral vein thrombosis, low single-ventricle ejection fraction, and severe valvular insufficiency.

Additionally, the spot urine microalbumin/creatinine ratio, assessed during polyclinic visits in the Fontan patient group as a marker for chronic nephropathy, was retrospectively evaluated. While no patients presented with renal failure, those with abnormal microalbumin-to-creatinine ratios were classified as having renal dysfunction.[5,6]

Echocardiography

In patients with a normal single-ventricular ejection fraction on echocardiography, the widest inferior vena cava (IVC) diameter in the systolic phase, IVC Doppler measurements, and descending aortic diameter (Ao) measurements were evaluated using subxiphoid short-axis views with a GE Vivid e9 S5 probe (3-7 MHz frequency range). Additionally, the widest femoral vein diameter and Doppler measurements of femoral artery diameter were assessed during the systolic phase using a GE Vivid e9 L11 probe (12 MHz frequency).

Given the lack of standardization for vein measurements relative to age and weight in children, a solution was sought to eliminate the variability described above. This solution involved dividing the IVC and FV diameter measurements by body surface area (BSA). Furthermore, IVC was calculated as a proportion of the descending aorta (IVC/Ao) and as the ratio IVC/FV. The shortest distance at which the FV and IVC Doppler flow exhibited a zero line during the examination was documented. This value was designated as the "Vein Doppler Time." These values were then compared with the incidence of Fontan complications, including thrombosis, arrhythmias, and protein-losing enteropathy. BSA was calculated using the Mosteller formula.[14]

Statistical Analysis

Statistical analyses were performed using IBM SPSS 23.0 software (SPSS Inc., Chicago, IL, USA). The normality of continuous variables was assessed using the Shapiro-Wilk test. Descriptive statistics for normally distributed continuous variables are presented as mean±standard deviation, while non-normally distributed variables are reported as median with their first and third quartiles (median; Q1, Q3). Categorical variables are presented as frequencies. Appropriate analyses were conducted to compare groups. When continuous variables were not normally distributed, the Mann-Whitney U test was applied to compare distributions between groups. Fisher's exact test was used for categorical data. A p-value less than 0.05 was considered statistically significant.

RESULTS

Patient Demographics and Clinical Characteristics

The youngest participant was 5 years old, while the oldest was 19. The median age was 13 years (range 11–17 years), with 6 females and 19 males participating. The median weight and height percentiles were 14% (range: 6.55–26) and 44.83% (range: 14.92–67), respectively. Saturation values ranged from 82% to 95%, with a median of 91% (range: 90–94).

The diagnoses of the patients were as follows: tricuspid atresia, 9 (36%); pulmonary atresia, 6 (24%); large VSD with unbalanced ventricle, 4 (16%); hypoplastic left heart syndrome, 3 (12%); mitral atresia, 2 (8%); and Taussig–Bing anomaly, 1 (4%).

A total of 72% of patients underwent MBT shunt, with the procedure performed at a median of 2 months (IQR: 1.5–6.5 months). Pulmonary banding was performed in 12% (n=5) within a time frame of 0–3 months, with a median duration of 2 months. The Norwood procedure was performed in 8% (n=2) of cases, with a median time to surgery of 1.5 months (IQR: 0–2 months). All cases underwent the Glenn procedure, with a median age at the Glenn procedure of 11.5 months (IQR: 7–25 months). The Fontan procedure was performed at a median age of 54 months (IQR: 48–83 months). The median pulmonary artery pressure measured by angiography from the Glenn shunts before Fontan operations was 14 mmHg (IQR: 12–15 mmHg), with a minimum of 7 mmHg and a maximum of 18 mmHg.

Of the patients included in the study, seven underwent extracardiac Fontan surgery, four underwent fenestrated extracardiac Fontan surgery, and 14 underwent intra-extracardiac fenestrated Fontan surgery. Among patients with uncomplicated cases, 11 underwent a Fontan procedure with an additional fenestration.

Table 1. Comparison of measurements between the patient and control groups

Measurement	Patient group (n=25)	Control group (n=25)	p
IVC/BSA	9.85 (8.63–11.42)	8.49 (7.15–11.4)	0.12
Ao/BSA	7.83 (6.95–8.85)	8.06 (6.55–10.45)	0.33
IVC/Ao	1.28 (1.20–1.50)	1.09 (1.03–1.17)	**0.001**
FV/FA	1.41 (1.05–1.57)	1.16 (1.09–1.25)	**0.009**
IVC/FV	2.05 (1.73–2.44)	1.83 (1.45–2.02)	0.079
FV/BSA	4.96 (3.86–5.58)	4.38 (3.99–6.44)	0.97
FA/BSA	3.78 (3.51–4.12)	3.75 (3.48–5.41)	0.6

IVC: Inferior vena cava diameter; BSA: Body surface area; Ao: Abdominal aorta diameter; FV: Femoral vein diameter; FA: Femoral artery diameter.

Comparisons of Demographic Characteristics Between the Control and Patient Groups

Comparisons between the control and patient groups revealed that the control group included 25 participants (17 males, 8 females), and the patient group had an identical gender distribution. Median values for age were 11 years (range: 8–14) and 13 years (range: 11–17) (p=0.34); for weight, 42 kg (range: 29–49 kg) and 44 kg (range: 33–50 kg) (p=0.497); and for BSA, 1.32 m^2 (range: 1.03–1.44 m^2) and 1.36 m^2 (range: 1.13–1.47 m^2) (p=0.404).

Comparison of Patient and Control Groups

A comparison between the patient and control groups revealed that IVC/Ao and FV/FA ratios were significantly elevated in the patient group (p=0.001, r=0.57 and p=0.009, r=0.29; Table 1). The patient group exhibited higher IVC/Ao and FV/FA ratios. This finding aligns with expectations, as intravascular congestion that develops over time due to passive flow within the Fontan circuit could contribute to the observed differences. The lack of significant differences in other venous-arterial measurements suggests that the Fontan circulation maintains hemodynamics that approximate normal physiology.

Table 2. Comparison of Fontan age and NYHA staging

Measurement	NYHA stage 1-2 (n=21)	NYHA stage 3-4 (n=4)	p
Fontan age (months)	Median (Q1-Q3): 50 (48–57)	Median (Q1-Q3): 143 (121–151)	**0.019**

NYHA: New York Heart Association.

Fontan Operation Age and NYHA Staging

In accordance with the NYHA staging system, 19 patients were classified as stage 1, 2 patients as stage 2, 2 patients as stage 3, and 2 patients as stage 4. A comparison of the age at Fontan operation between NYHA stage 1-2 and stage 3-4 patients revealed that those who underwent the procedure at an older age (median 143 months) were subsequently classified as NYHA stage 3-4 (p=0.019, r=0.88) (Table 2). Furthermore, the age at which the Fontan operation was performed was evaluated for cases in which complications arose during the follow-up period. The Fontan operation was performed at a relatively advanced age (median 108 months) (p=0.018, r=0.30) (Table 3).

Venous Measurements and Complications

A statistically significant difference was found in the ratio of vein measurements to body surface area between the complication group and the non-complication group. The

Table 3. Comparison of measurements between the complicated and uncomplicated Fontan groups

Measurement	Uncomplicated Fontan group (n=17)	Complicated Fontan group (n=8)	p
Fontan age (months)	Median (Q1-Q3): 50 (48–57)	Median (Q1-Q3): 108 (47–148)	**0.018**
IVC/BSA	11.04 (8.91–12.3)	9.09 (8.56–9.91)	**0.031**
Ao/BSA	8.1 (7.0–8.88)	7.2 (5.53–7.68)	0.135
IVC/Ao	1.28 (1.22–1.41)	1.34 (1.14–1.55)	0.75
FV/FA	1.41 (1.07–1.57)	1.31 (1.01–1.53)	0.783
IVC/FV	2.04 (1.64–2.22)	2.27 (1.78–2.49)	0.44
FV/BSA	5.55 (4.59–6.49)	4.29 (3.58–5.06)	**0.021**
FA/BSA	3.93 (3.56–4.39)	3.58 (3.30–3.85)	0.05
IVC Doppler time (ms)	1321 (762–3000)	970 (637–1173)	0.204
Femoral vein Doppler time (ms)	2053 (1242–3000)	2815 (1481–3000)	0.736

IVC: Inferior vena cava diameter; BSA: Body surface area; Ao: Abdominal aorta diameter; FV: Femoral vein diameter; FA: Femoral artery diameter. The complicated Fontan group included patients with protein-losing enteropathy, plastic bronchitis, thrombosis, and arrhythmia.

Table 4. Comparison of measurements between groups stratified by pathological and normal microalbuminuria

Measurement	MCR normal (≤20 µg/ml) (n=18)	MCR high (≥20 µg/ml) (n=6)	p
Pre-Fontan pulmonary artery pressure measurement			**0.047**
<15 mmHg (n=11)	15 (62.5%)	1 (4.2%)	
≥15 mmHg (n=7)	3 (12.5%)	5 (20.8%)	
Fontan operation age (months; median, Q1-Q3)	81 (43–137)	57 (44–127)	0.77
IVC/BSA	10.8 (8.75–11.6)	10.4 (9.01–12)	0.93
Ao/BSA	7.81 (6.79–8.72)	9 (7.95–10.2)	0.36
IVC/Ao	1.42 (1.21–1.49)	1.21 (1.11–1.28)	0.21
FV/FA	1.31 (1.04–1.55)	1.6 (1.45–1.71)	0.8
IVC/FV	2.23 (1.79–2.56)	1.96 (1.68–2.16)	0.34
FV/BSA	5.09 (3.99–6.14)	5.83 (5.36–5.95)	0.5
FA/BSA	3.85 (3.57–4.28)	3.76 (3.14–3.94)	0.86

MCR: Microalbumin/creatinine ratio; IVC: Inferior vena cava diameter; BSA: Body surface area; Ao: Abdominal aorta diameter; FV: Femoral vein diameter; FA: Femoral artery diameter.

p-value for IVC/BSA was 0.031 (r=0.36), and for FV/BSA, it was 0.021 (r=0.54, Table 3). IVC/BSA and FV/BSA ratios were lower in patients with complications. We concluded that the other ratios—IVC/FV, IVC/Ao, FV/FA—and the IVC and FV Doppler time values could not be used to distinguish between complicated and uncomplicated cases.

In the patient cohort under investigation, observed complications included ventricular extrasystoles severe enough to warrant the initiation of antiarrhythmic therapy in one patient during the fourth year after the Fontan operation. A pacemaker was implanted in one patient following the onset of complete AV block. Three patients developed protein-losing enteropathy. Three patients are receiving continuous low-molecular-weight heparin and antiplatelet therapy due to a history of thrombosis.

Pre-Fontan Pulmonary Artery Pressure and Renal Dysfunction

In routine spot urine microalbumin/creatinine (MCR) tests performed at the outpatient clinic, MCR values above 20 mcg/ml were considered pathological. MCR was assessed in 23 of 24 Fontan patients; one patient's results were missing at the time of application. No statistically significant associations were found between pathological and normal MCR values in the patient group and the ratios of IVC/BSA, FV/BSA, IVC/Ao, and IVC/FV, nor with the age at which the Fontan operation was performed (Table 4).

Six patients exhibited a pre-Fontan pulmonary artery pressure of ≥15 mmHg, as determined by catheter angiography. In these cases, the MCR was found to be pathological. A Chi-square analysis revealed a significant difference in the microalbumin/creatinine ratio in spot urine between the group with pre-Fontan Glenn shunt pressure <15 mmHg and the group with pressure ≥15 mmHg (p=0.047) (Table 4).

DISCUSSION

The Fontan procedure, while life-saving for patients with single-ventricle congenital heart disease, is associated with a spectrum of long-term complications that significantly impact morbidity and mortality.[15,16] These Fontan-associated diseases, such as protein-losing enteropathy, plastic bronchitis, liver disease, thrombosis, renal insufficiency, and arrhythmias, can ultimately lead to Fontan failure over time.[15,17] The chronic combination of elevated central venous pressure, non-pulsatile pulmonary blood flow, and a preload-deprived systemic ventricle contributes to this progressive deterioration.[18] This complex pathophysiology leads to chronic systemic venous hypertension and reduced cardiac output, driving peripheral stasis and congestion within the lymphatic system.[13] Persistent venous congestion, particularly affecting the inferior vena cava and its tributaries, often manifests as hepatomegaly, hepatic congestion, and fibrosis, potentially progressing to cirrhosis.[19,20] Indeed, a larger inferior vena cava diameter has been associated with elevated Fontan pressures and increased end-diastolic pressures, further exacerbating the risk of Fontan-associated liver disease.[21] These hemodynamic alterations also predispose Fontan patients to renal dysfunction, evidenced by increased microalbuminuria and decreased estimated glomerular filtration rate (eGFR).[4,5] Furthermore, microalbuminuria, a marker of renal injury, has a high incidence among Fontan patients.[11] The elevated central venous pressure characteristic of Fontan circulation can increase renal venous pressure and reduce renal perfusion pressure, thereby

contributing to the development of nephropathy.[10] Moreover, chronic hypoxemia, an additional factor in Fontan patients, can further impair renal function by promoting tubulointerstitial damage and subsequent proteinuria, a mechanism distinct from hepatorenal syndrome.[6] The persistent elevation of systemic venous pressure, an obligate feature of the Fontan circulation due to the absence of a sub-pulmonary ventricle, demonstrably decreases venous capacitance and compliance, thereby placing patients at increased risk of progressive renal dysfunction.[10,22] This sustained venous congestion also plays a critical role in the pathogenesis of protein-losing enteropathy and plastic bronchitis, conditions arising from lymphatic insufficiency and aberrant lymphatic channel formation, directly attributable to chronically elevated central venous pressures.[16]

It is crucial to monitor and assess the physical activity capacity of patients who have undergone Fontan palliation.[23] NYHA stage 2 or higher in Fontan operation cases is associated with increased mortality and the need for heart transplantation.[24] The findings of our study indicate that a later age at Fontan palliation is associated with an increased incidence of complications and reduced exercise capacity. This further underscores the importance of the age at which Fontan palliation is performed. Our findings show that the daily physical capacity of patients who underwent Fontan surgery aligns with NYHA stage 3-4 at a mean age of 143 months. The mean age at which Fontan palliation was performed in patients with complications was 108 months (9 years). In light of these findings, it is recommended that Fontan patients aged 9 years and older be monitored more closely for the development of complications, including arthritis, thrombosis, protein-losing enteropathy, plastic bronchitis, and microalbuminuria. Early diagnosis and treatment of potential complications will enhance patients' quality of life.

One of the most significant findings of our study is the association between microalbuminuria and a pre-Fontan pulmonary artery pressure of 15 mmHg or more, measured at the Glenn shunt during conventional angiography. Our analysis demonstrated a significant difference in the microalbumin/creatinine ratio between groups with pre-Fontan Glenn shunt pressure <15 mmHg and those with pressure ≥15 mmHg, with pathological microalbuminuria (MCR values above 20 mcg/ml) being significantly more prevalent in the latter group. This association is independent of the time elapsed since the operation. The presence of pathological MCR results serves as a critical indicator of future renal damage, a finding supported by literature that highlights microalbuminuria—highly prevalent in Fontan patients—as a marker of renal injury.[11] In a systematic review, T. Alsaied and colleagues further emphasized the significance of late mortality and renal injury.[25] Given that pre-Fontan pulmonary artery pressures exceeding 15 mmHg are significantly associated with pathological MCR, such elevated pressures are important for predicting the risk of subsequent renal injury and potential mortality.[19,25-27] Therefore, patients with pre-Fontan pulmonary artery pressure exceeding 15 mmHg should undergo periodic assessment of their microalbumin-to-creatinine ratio for early detection and management of renal complications.

Patel et al.[10] demonstrated a significant association between a IVC/BSA ratio exceeding 1 cm/m^2 and the presence of pathological microalbuminuria, underscoring its utility as an indicator for evaluating late nephropathy. In contrast to these findings, our study did not find a significant correlation between the IVC/BSA ratio and the pathological microalbumin/creatinine ratio. This divergence may be attributable to inherent variability in IVC/BSA and femoral vein measurements in the pediatric population, particularly given dynamic growth parameters. The development of robust, standardized venous measurement protocols remains a critical challenge. Establishing clear and reliable reference values will necessitate comprehensive studies involving a substantial number of cases, precise delineation of physiological limits, and mitigation of subjective assessment biases. Further research is needed to refine diagnostic criteria and establish universal thresholds for venous parameters that reliably predict long-term Fontan complications, particularly in the context of renal dysfunction.[4]

Significant differences in the IVC/Ao and FV/FA ratios were observed between the patient and healthy control groups. Subsequent analysis, in which the patient group was further stratified into complication and no-complication subgroups and compared with the healthy control group, revealed that the healthy control group had lower IVC/Ao and FV/FA ratios. This observation not only suggests progressive venous congestion within the passive circulation of the Fontan shunt over time but also underscores a critical pathophysiological mechanism underlying many of the adverse long-term outcomes in these patients. This persistent venous congestion, particularly evident in the inferior vena cava and its tributaries, profoundly influences long-term hemodynamics and the overall prognosis in Fontan patients and contributes to the development of serious complications such as progressive renal dysfunction, protein-losing enteropathy, and plastic bronchitis.[10,16,22]

Our study revealed a statistically significant correlation between the IVC/BSA and FV/BSA ratios and the incidence of complications. In contrast to the existing literature, which often associates an increased indexed inferior vena cava (IVC) diameter with complications such as pathological

microalbuminuria,[10] we observed a paradoxical decrease in IVC/BSA and FV/BSA in complicated cases. This unexpected outcome suggests a unique pathophysiological mechanism within the Fontan circulation, characterized by chronically elevated systemic venous pressures and reduced cardiac output, leading to multifactorial complications.[13,22,28] We postulate that this decrease may serve as an early indicator of reduced intravascular volume in the venous compartment, potentially leading to compensatory redistribution of fluid into extravascular (or "third") spaces. Fluid shifts and issues with fluid balance are recognized challenges in Fontan patients,[29,30] often exacerbated by lymphatic dysfunction and multiorgan sequelae.[13,31] These changes could stem from mechanisms affecting metabolically compromised states, a known aspect of chronic Fontan physiology, which impacts various end organs, including the hepatic and renal systems.[18,19,26] The consistent, parallel alterations observed in both the femoral vein and inferior vena cava measurements strongly suggest that factors beyond isolated hemodynamic pressures, such as systemic metabolic effects and fluid balance dysregulation, significantly influence these venous parameters.

To achieve comprehensive conclusions regarding these venous measurements and ratios, further research is imperative, particularly with larger patient cohorts and the establishment of standardized measurement protocols, considering the complex and multifactorial nature of Fontan circulation.[13,32] We recommend longitudinal follow-up for every Fontan patient, with regular comparative assessments of IVC/BSA and FV/BSA ratios at each visit. This approach is critical for the early identification of these potentially subtle indicators of long-term complications.

Study Limitations

The present study is subject to several limitations. Although the cohort was relatively small, this reflects the rare nature of the disease under investigation. Future multi-center studies with larger sample sizes would strengthen the validity and generalizability of the findings. It was not feasible to measure current pulmonary artery and Fontan shunt pressures due to the absence of clinical indications for angiography, thus precluding their inclusion in this study. Furthermore, reliance on retrospectively collected microalbumin/creatinine ratios from spot urine samples obtained at clinical presentation constitutes an additional limitation

CONCLUSION

Effective long-term management following Fontan palliation is crucial for significantly improving patients' quality of life and reducing mortality rates. We strongly advocate for rigorous monitoring of patients aged nine years or older, with particular attention to complications such as protein-losing enteropathy, arrhythmia, thrombosis, and plastic bronchitis. Furthermore, patients presenting with a pre-Fontan pulmonary artery pressure of 15 mmHg, as measured by angiography, require diligent surveillance for renal complications using the microalbumin-to-creatinine ratio. Our findings underscore the importance of longitudinally tracking IVC/BSA and FV/BSA ratios: a decrease in these ratios—contrary to prior assumptions—emerged as a significant and unexpected indicator of potential future complications. This necessitates a re-evaluation of how these venous parameters are interpreted; a decrease in these ratios in any patient should now be regarded as a critical warning sign, potentially reflecting diminished intravascular volume and fluid accumulation in third spaces. Implementing such comprehensive monitoring strategies is vital for early detection and intervention, ultimately improving long-term outcomes for Fontan patients.

Ethics Committee Approval: Ethics committee approval was obtained from Ege University Medical Research Ethics Committee (Approval Number: 23-9T/31, Date: 07.09.2023).

Informed Consent: Written informed consent was not required due to the retrospective nature of this study.

Conflict of Interest: The authors have no conflicts of interest to declare.

Funding: The authors declared that this study received no financial support.

Use of AI for Writing Assistance: No use of AI-assisted technologies was declared by the authors.

Author Contributions: Concept – YA, REL, ZU; Design – OA; Supervision – ED, YA, REL, ZU; Resource – OA; Materials – NOT, YA; Data Collection and/or Processing – OA, BSY; Analysis and/or Interpretation – FE, MBB; Literature Review – FE, MBB, GKK; Writing – OA; Critical Review – OA, ED, REL.

Peer-review: Externally peer-reviewed.

REFERENCES

1. Fontan F, Baudet E. Surgical repair of tricuspid atresia. Thorax 1971;26(3):240-8. [CrossRef]
2. Ohuchi H, Yasuda K, Miyazaki A, Iwasa T, Sakaguchi H, Shin O, et al. Comparison of prognostic variables in children and adults with Fontan circulation. Int J Cardiol 2014;173(2):277-83. [CrossRef]
3. Alsaied T, Bokma JP, Engel ME, Kuijpers JM, Hanke SP, Zuhlke L, et al. Predicting long-term mortality after Fontan procedures: A risk score based on 6707 patients from 28 studies. Congenit Heart Dis 2017;12(4):393-8. [CrossRef]

4. Van den Eynde J, Westenberg JJM, Hazekamp MG, Lamb HJ, Jongbloed MRM, Wentzel JJ, et al. Noninvasive Advanced Cardiovascular Magnetic Resonance-Derived Fontan Hemodynamics Are Associated With Reduced Kidney Function But Not Albuminuria. J Am Heart Assoc 2024;13(3):e033122. [CrossRef]
5. Khuong JN, Wilson TG, Grigg LE, Bullock A, Celermajer D, Disney P, et al. Fontan-associated nephropathy: Predictors and outcomes. Int J Cardiol 2020;306:73-7. [CrossRef]
6. Muraoka M, Nagata H, Yamamura K, Sakamoto I, Ishikita A, Nishizaki A, et al. Long-Term Renal Involvement in Association with Fontan Circulation. Pediatr Cardiol 2024;45(2):340-50. [CrossRef]
7. Loke YH, Kim B, Mass P, Opfermann JD, Hibino N, Krieger A, et al. Role of surgeon intuition and computer-aided design in Fontan optimization: A computational fluid dynamics simulation study. J Thorac Cardiovasc Surg 2020;160(1):203-12.e2. [CrossRef]
8. Dasi LP, Krishnankuttyrema R, Kitajima HD, Pekkan K, Sundareswaran KS, Fogel M, et al. Fontan hemodynamics: importance of pulmonary artery diameter. J Thorac Cardiovasc Surg 2009;137(3):560-4. [CrossRef]
9. Ryu K, Healy TM, Ensley AE, Sharma S, Lucas C, Yoganathan AP. Importance of accurate geometry in the study of the total cavopulmonary connection: computational simulations and *in vitro* experiments. Ann Biomed Eng 2001;29(10):844-53. [CrossRef]
10. Patel S, Anne P, Somerfield-Ronek J, Du W, Zilberman MV. Inferior Vena Cava Diameter Predicts Nephropathy in Patients Late After Fontan Palliation. Pediatr Cardiol 2020;41(4):789-94. [CrossRef]
11. Anne P, Du W, Mattoo TK, Zilberman MV. Nephropathy in patients after Fontan palliation. Int J Cardiol 2009;132(2):244-7. [CrossRef]
12. Byrne RD, Weingarten AJ, Clark DE, Huang S, Perri RE, Scanga AE, et al. More than the heart: Hepatic, renal, and cardiac dysfunction in adult Fontan patients. Congenit Heart Dis 2019;14(5):765-71. [CrossRef]
13. Mazza GA, Gribaudo E, Agnoletti G. The pathophysiology and complications of Fontan circulation. Acta Biomed 2021;92(5):e2021260.
14. Mosteller RD. Simplified calculation of body-surface area. N Engl J Med 1987;317(17):1098. [CrossRef]
15. Ordonez MV, Biglino G, Bedair R. Routine surveillance of patients post Fontan palliation: lessons learnt from cardiac catheterisation. J Congenit Cardiol 2021;5:3. [CrossRef]
16. de Lange C. Imaging of complications following Fontan circulation in children - diagnosis and surveillance. Pediatr Radiol 2020;50(10):1333-48. Erratum in: Pediatr Radiol 2020;50(10):1478. [CrossRef]
17. Kawasaki Y, Sasaki T, Kobayashi D. Hemodynamic Profiling Using a Cardiac Index-Systemic Vascular Resistance Plot in Patients with Fontan Circulation. Congenital Heart Disease 2023;18(4):431. [CrossRef]
18. van Hassel G, Groothof D, Douwes JM, Hoendermis ES, Liem ET, Willems TP, et al. Deterioration in Renal Function in Patients With a Fontan Circulation and Association With Mortality. JACC Adv 2024;3(12):101399. [CrossRef]
19. Rychik J, Atz AM, Celermajer DS, Deal BJ, Gatzoulis MA, Gewillig MH, et al.; American Heart Association Council on Cardiovascular Disease in the Young and Council on Cardiovascular and Stroke Nursing. Evaluation and Management of the Child and Adult With Fontan Circulation: A Scientific Statement From the American Heart Association. Circulation 2019;140(6):e234-84. [CrossRef]
20. El-Sisi A, Taha AH, Sheba M, Hanna B, Alem SA, Mostafa FAZ, et al. Prevalence of hepatic dysfunction in paediatric patients with Fontan circulation. Pediatria Polska 2024;99(2):105-10. [CrossRef]
21. Gunsaulus M, Wang L, Haack L, Christopher A, Feingold B, Squires J, et al. Cardiac MRI-Derived Inferior Vena Cava Cross-Sectional Area Correlates with Measures of Fontan-Associated Liver Disease. Pediatr Cardiol 2024;45(4):909-20. [CrossRef]
22. Heying R, d'Udekem Y, Gewillig M, Rychik J. Editorial: The Fontan circulation: Problems and solutions. Front Pediatr 2022;10:1087739. [CrossRef]
23. Hedlund ER, Lundell B, Söderström L, Sjöberg G. Can endurance training improve physical capacity and quality of life in young Fontan patients? Cardiol Young 2018;28(3):438-46. [CrossRef]
24. Meyer SL, St Clair N, Powell AJ, Geva T, Rathod RH. Integrated Clinical and Magnetic Resonance Imaging Assessments Late After Fontan Operation. J Am Coll Cardiol 2021;77(20):2480-9. [CrossRef]
25. Alsaied T, Bokma JP, Engel ME, Kuijpers JM, Hanke SP, Zuhlke L, et al. Factors associated with long-term mortality after Fontan procedures: a systematic review. Heart 2017;103(2):104-10. [CrossRef]
26. Rathgeber SL, Lam C, Harris KC, Grewal J. Hepatic and Renal Consequences of Single-Ventricle Physiology Palliated With the Fontan Operation. Can J Cardiol 2022;38(7):1002-11. [CrossRef]
27. Pundi KN, Johnson JN, Dearani JA, Pundi KN, Li Z, Hinck CA, et al. 40-Year Follow-Up After the Fontan Operation: Long-Term Outcomes of 1,052 Patients. J Am Coll Cardiol 2015;66(15):1700-10. [CrossRef]

28. van De Bruaene A, Claessen G, Salaets T, Gewillig M. Late Fontan Circulatory Failure. What Drives Systemic Venous Congestion and Low Cardiac Output in Adult Fontan Patients? Front Cardiovasc Med 2022;9:825472. [CrossRef]
29. Ven JPG van der, Kamphuis VP, Bosch E, Gnanam D, Monteros CTE de L, Bogers AJJC, et al. Cardiac Function and Serum Biomarkers throughout Staged Fontan Palliation: A Prospective Observational Study. J Cardiovasc Dev Dis 2023;10(7):289. [CrossRef]
30. Luppes VAC, Willems A, Hazekamp MG, Blom NA, Ten Harkel ADJ. Fluid Overload in Pediatric Univentricular Patients Undergoing Fontan Completion. J Cardiovasc Dev Dis 2023;10(4):156. [CrossRef]
31. Castellanos DA, Ahmad S, St Clair N, Sleeper LA, Lu M, Schidlow DN, et al. Magnetic resonance three-dimensional steady-state free precession imaging of the thoracic duct in patients with Fontan circulation and its relationship to outcomes. J Cardiovasc Magn Reson 2023;25(1):28. [CrossRef]
32. Baroutidou A, Karagiannidis AG, Dimitroulas T, Kamperidis V, Ziakas A, Dimopoulos K, et al. Pathophysiology of endothelial dysfunction in Fontan circulation: from bench to bedside and back again. Angiogenesis 2025;28(4):45. [CrossRef]

Official Journal of Erciyes University Faculty of Medicine

DOI: 10.14744/cpr.2026.27967
J Clin Pract Res 2026;48(2):137–144

Coronary Artery Origin Anomalies on Coronary CT Angiography: A Single-Center Tertiary-Care Cohort

Nur Betül Karatoprak,[1] Sinan Karatoprak,[1] Ömer Şahin[2]

[1]Department of Radiology, Kayseri City Training and Research Hospital, Kayseri, Türkiye
[2]Department of Cardiology, Kayseri City Training and Research Hospital, Kayseri, Türkiye

ABSTRACT

Objective: In this single-center, tertiary-care coronary CT angiography (CCTA) series, we aimed to report the prevalence of coronary origin anomalies and describe the characteristics of their proximal course.

Materials and Methods: This retrospective study included 3,181 consecutive CCTA examinations performed between January 1, 2020, and June 30, 2025. All scans were acquired using a 64-slice multidetector CT system (SOMATOM Definition AS+, Siemens Healthineers) with retrospective ECG gating. Two radiologists reviewed the studies, and examinations with suspected coronary origin anomalies were re-evaluated by consensus. Anomalies were classified according to the Angelini framework, and the proximal course was categorized as interarterial, retroaortic, transseptal/intraseptal, or prepulmonic.

Results: Coronary artery origin anomalies were identified in 41 of 3,181 patients (1.29%). The largest subgroup was opposite-sinus origin (n=24, 0.76%), which included the right coronary artery (RCA) originating from the left sinus (n=12, 0.38%), the left circumflex artery (LCX) originating from the right coronary sinus (n=8, 0.26%), and the left main coronary artery (LMCA) originating from the right coronary sinus (n=4, 0.13%). An absent LMCA configuration—defined by separate left-sinus ostia for the left anterior descending artery (LAD) and LCX—was identified in 5 patients (0.16%). Single coronary artery anatomy was observed in 3 cases (0.09%), all of which had a common origin from the right coronary sinus. In one case (0.03%), the RCA arose from the noncoronary sinus. High take-off coronary artery origins were observed in 8 patients (0.26%). Regarding the course patterns, interarterial courses were observed in 20 patients, retroaortic courses in 10, and prepulmonic courses in 2. The interarterial LAD and LCX cases also demonstrated a transseptal/intraseptal segment.

Conclusion: CCTA reliably delineates coronary ostial origin and proximal trajectory, supporting a comprehensive anatomic assessment of suspected congenital coronary variants.

Keywords: Computerized tomography, congenital anomalies, coronary angiography, coronary vessel anomalies, coronary vessels.

Cite this article as:
Karatoprak NB, Karatoprak S, Şahin Ö. Coronary Artery Origin Anomalies on Coronary CT Angiography: A Single-Center Tertiary-Care Cohort. J Clin Pract Res 2026;48(2):137–144.

Address for correspondence:
Nur Betül Karatoprak.
Department of Radiology, Kayseri City Training and Research Hospital, Kayseri, Türkiye
Phone: +90 506 993 03 06
E-mail: nebedr@gmail.com

Submitted: 18.01.2026
Revised: 04.03.2026
Accepted: 23.03.2026
Available Online: 20.04.2026

Erciyes University Faculty of Medicine Publications - Available online at www.jcpres.com

INTRODUCTION

Coronary artery anomalies are a diverse group of congenital variants that involve atypical coronary origin, proximal course, or termination. While most of these variants are benign and discovered incidentally, some anomalous patterns—especially those in which the left coronary arteries arise from the contralateral sinus and follow a malignant interarterial course between the aorta and the main pulmonary artery—pose a risk of myocardial ischemia and, in rare cases, sudden cardiac death.[1,2]

The prevalence of coronary artery origin anomalies reported in studies varies significantly depending on participant characteristics and assessment methods. Autopsy series show relatively low incidence rates, ranging from approximately 0.17% to 0.3%. In contrast, angiographic studies of large cohorts evaluated for coronary artery disease generally report higher incidence rates, ranging from approximately 0.6% to 1.2%.[1,3-7]

In studies based on coronary CT angiography (CCTA), reported frequencies are slightly higher, with prevalence rates ranging from approximately 1.04% to 2.33%, depending on the cohort examined.[8,9]

Identifying the origin and course of anomalous coronary arteries with invasive coronary angiography (ICA) can be challenging, particularly when selective catheterization is difficult or the vessel follows an unusual trajectory. In contrast, CCTA, with its inherent three-dimensional data acquisition, is exceptionally well-suited to detect anomalous coronary origins and determine their anatomic course and spatial relationship to adjacent cardiac and non-cardiac structures.[8,10-12] Therefore, CCTA has become the preferred first-step imaging technique for defining coronary origin anomalies when they are known or clinically suspected.

In this study, we examined CCTA studies conducted at our institution to determine the frequency of coronary artery origin anomalies and the types of anomalies observed in our population.

MATERIALS AND METHODS

Study Site and Design

This retrospective, single-center study, conducted at a tertiary-care institution, evaluated the prevalence and anatomic patterns of coronary artery origin anomalies using CCTA.

Ethical Approval

The study protocol was approved by the Non-Interventional Clinical Research Ethics Committee at Kayseri City Training and Research Hospital (Approval Number: 553, Date: 26.08.2025).

KEY MESSAGES

- In 3,181 CCTA examinations from a single-center tertiary-care cohort, coronary artery origin anomalies were identified in 1.29% of patients.
- The clinical significance of origin anomalies is primarily determined by the proximal course; interarterial trajectories were most frequently observed in RCA-related opposite-sinus variants.
- Opposite-sinus anomalies predominated (0.76%); all cases of RCA originating from the left coronary sinus and all cases of LMCA originating from the right coronary sinus showed an interarterial course, whereas all LCX-from-right-sinus cases were retroaortic.

Informed consent was not required, as the study retrospectively analyzed anonymized CCTA datasets. The conduct of the study adhered to the ethical principles outlined in the Declaration of Helsinki.

Patients and Data Collection

All CCTA examinations performed at our institution between January 1, 2020, and June 30, 2025, were reviewed. A total of 3,755 CCTA examinations were identified during the study period. After excluding repeated examinations from the same individuals, 3,388 examinations remained.

Inclusion Criteria

Examinations were included when the image quality allowed reliable assessment of the coronary ostia and proximal coronary segments.

Exclusion Criteria

Examinations were excluded if they showed severe motion artifacts, inadequate contrast opacification, significant flare artifacts due to widespread calcification, or if the patient had prior aortic root or congenital heart surgery that could alter the natural coronary anatomy. After applying these criteria, the final study cohort consisted of 3,181 patients.

Clinical, Surgical, and Laboratory Investigations

Not applicable. This study was based solely on CCTA-derived anatomic evaluation.

CCTA Acquisition Protocol

All CCTA studies were performed using a 64-slice multidetector CT system (SOMATOM Definition AS+, Siemens Healthineers) with retrospective ECG gating. Scan protocol parameters are summarized in Table 1. For contrast enhancement, iodinated contrast material (≥350 mg I/mL) was administered

Table 1. Scan protocol parameters for CCTA

Parameter	Value
Acquisition type	Spiral
ECG gating	Retrospective
Tube voltage	120 kV
Tube current	ECG-based tube current modulation
Nominal single collimation width	0.6 mm
Nominal total collimation width	38.4 mm
Gantry rotation time	0.33 s
Reconstruction increment	0.33 mm

ECG: Electrocardiogram; kV: Kilovolt; mm: Millimeter; s: Second.

intravenously at a flow rate of 5 mL/s, with a total volume ranging from 50 to 70 mL. This was followed by a 20–30 mL saline flush to optimize coronary arterial opacification.

Image Reconstruction and Post-Processing

For image reconstruction, a slice thickness of 0.6 mm and a 0.33-mm overlap were used to create near-isotropic volumes. The coronary tree was then analyzed using workstation-based post-processing.

Diagnostic Criteria and Definitions

Coronary origin anomalies were classified according to the framework proposed by Angelini et al.[1] The absence of the left main coronary artery (LMCA) was defined as the separate ostial origins of the left anterior descending (LAD) and left circumflex (LCX) arteries. A high take-off origin was defined as the location of the coronary ostium above the sinotubular junction. In anomalous cases, the proximal course was classified as retroaortic, interarterial, transseptal/intraseptal, or prepulmonic/precardiac.

Image Evaluation

All eligible CCTA examinations performed between January 1, 2020, and June 30, 2025, were evaluated for coronary artery origin anomalies on a dedicated post-processing workstation (syngo.via, Siemens Healthineers). CCTA examinations were distributed to two radiologists experienced in cardiovascular imaging, who independently reviewed their assigned studies. All cases suspected of coronary artery origin anomalies were subsequently re-evaluated, and consensus classification and proximal course assignments were made. As part of the descriptive dataset, we recorded coronary dominance, the ramus intermedius variant, and a separate origin of the conus artery.

Table 2. Distribution of coronary artery origin anomalies detected on CCTA (n=3,181)

Type of coronary anomaly	n	%
Coronary ostium from non-coronary sinus		
RCA from non-coronary sinus	1	0.03
Anomalous origin from opposite sinus		
RCA from left sinus	12	0.38
LCX from right sinus	8	0.26
LAD from right sinus	0	0
LMCA from right sinus	4	0.13
Absent LMCA (separate LAD & LCX origin from left sinus)	5	0.16
Single coronary artery		
From right coronary sinus	3	0.09
From left coronary sinus	0	0
High take-off coronary artery origins		
High take-off LMCA	1	0.03
High take-off RCA	6	0.18
High take-off LMCA and RCA	1	0.03
Total number of anomalies	41	1.29

CCTA: Coronary computed tomography angiography; RCA: Right coronary artery; LCX: Left circumflex artery; LAD: Left anterior descending artery; LMCA: Left main coronary artery.

Statistical Analysis

Statistical analyses were performed using SPSS (version 24.0; IBM, Armonk, NY, USA). Numerical variables are expressed as mean±standard deviation or median (range), while categorical data are presented as frequencies and percentages. Prevalence estimates were calculated for the entire cohort, and no inferential statistical tests were applied.

RESULTS

A total of 3,181 patients formed the study population: 2,187 (68.7%) were men, and 994 (31.3%) were women. The average age was 45.5±15.9 years, with a median of 46 years (range: 0–96). Among the 3,181 patients, 86.1% (2,738 patients) had right coronary dominance, 10.9% (347 patients) had left coronary dominance, and 3.0% (96 patients) had co-dominance. A separate conus artery was present in approximately 493 patients (15.5%), and a ramus intermedius was identified in approximately 1,001 patients (31.5%).

Coronary origin anomalies were detected in 41 patients, corresponding to 1.29% of the cohort. The distribution of these anomalies is summarized in Table 2.

An RCA origin from the left coronary sinus was observed in 12 patients; all of these cases displayed an interarterial (malignant)

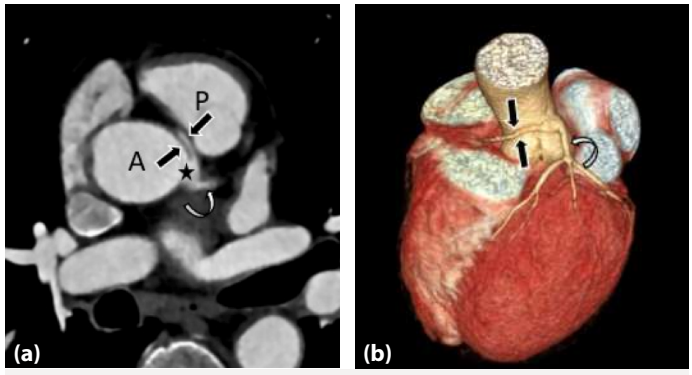

Figure 1. CCTA in a 62-year-old man demonstrates an anomalous origin of the right coronary artery (RCA) (arrows) from the left coronary sinus (asterisk). A) (axial oblique multiplanar reformat) shows the RCA coursing interarterially between the ascending aorta **(a)** and the pulmonary trunk (P). **(b)** (three-dimensional volume-rendered image) demonstrates the same anomalous origin and proximal interarterial trajectory. The left main coronary artery (LMCA) arising from the left coronary sinus is indicated by the curved arrow.

proximal trajectory (Fig. 1). Separately, one patient had an RCA arising from the noncoronary sinus, with a unique course.

The absence of LMCA was observed in 5 patients; in these cases, the LAD and LCX followed a normal proximal course (Fig. 2).

The LMCA ostium was located in the right coronary sinus in four patients, distinct from the RCA ostium in all cases. The proximal LMCA then followed an interarterial course (Fig. 3).

Eight patients had an LCX origin in the right coronary sinus, and all demonstrated a proximal retroaortic course.

Three patients exhibited a single coronary artery configuration, each with a solitary ostium in the right coronary sinus and variable proximal courses. In the first case, the left main coronary artery originated from a right-sided common trunk and reached the left side via a prepulmonic route before dividing into the LAD and LCX. In the other two cases, the common trunk gave rise to the LAD and LCX on the right side of the heart. In the second patient, the LAD demonstrated a proximal interarterial course, followed by a transseptal/intraseptal trajectory, whereas the LCX coursed retroaortically (Fig. 4). In the third patient, the LAD followed a prepulmonic trajectory, while the LCX followed an interarterial proximal course, followed by a transseptal/intraseptal course.

High take-off origins of the coronary arteries were identified in eight patients. One patient demonstrated simultaneous

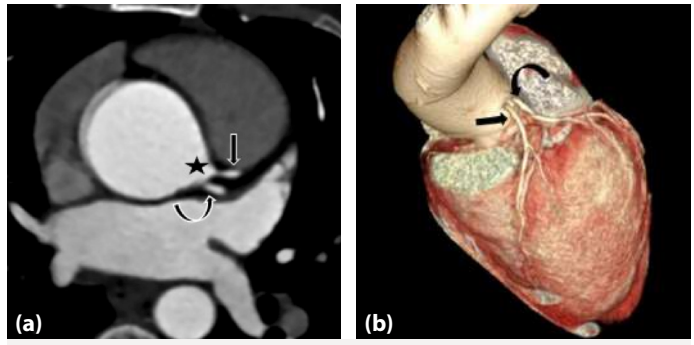

Figure 2. CCTA in a 38-year-old woman demonstrates the absence of the left main coronary artery. **(a)** (axial oblique multiplanar reformat) shows the separate origins of the left anterior descending artery (LAD) (arrow) and the left circumflex artery (LCX) (curved arrow) from the left coronary sinus (asterisk). **(b)** (three-dimensional volume-rendered image) confirms the absence of a common left main trunk and the independent ostial origins of the LAD and LCX.

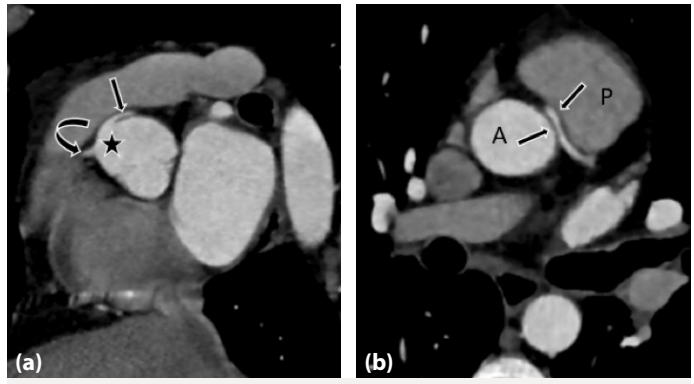

Figure 3. CCTA in a 40-year-old man demonstrates an anomalous origin of the left main coronary artery (LMCA) (arrows) from the right coronary sinus (asterisk) with an interarterial course between the ascending aorta (A) and the pulmonary trunk (P). **(a)** (axial oblique multiplanar reformat) depicts the separate ostial origins, with the LMCA arising from the right coronary sinus and the right coronary artery indicated by the curved arrow. **(b)** (axial oblique multiplanar reformat) highlights the interarterial trajectory of the LMCA between the ascending aorta and the pulmonary trunk.

high take-off origins of both the LMCA and RCA; the RCA originated at the level of the right–left commissural junction, just above the sinotubular junction, and followed a proximal interarterial course, while the LMCA maintained a normal trajectory. Another patient had an isolated high take-off

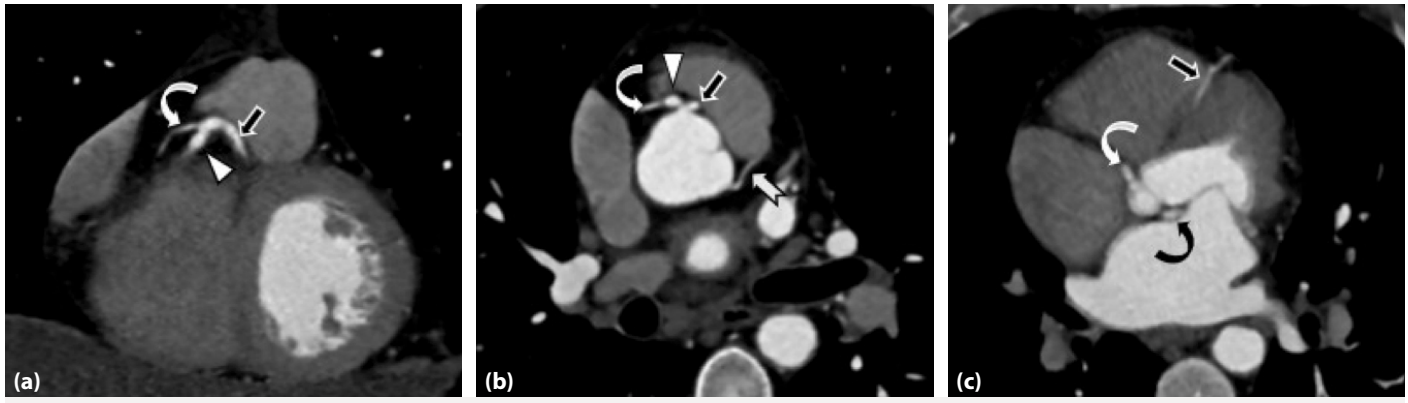

Figure 4. CCTA in a 35-year-old man demonstrates a single coronary artery arising from the right coronary sinus. **(a)** (coronal oblique multiplanar reformat) shows the common right-sided origin (asterisk) with trifurcation: the LAD (arrow), the LCX (curved arrow), and the RCA (arrowhead). **(b)** (axial oblique multiplanar reformat) demonstrates the LAD (arrow) with an interarterial proximal course; a thin accessory diagonal branch arising from the left coronary sinus is also noted (notched arrow), while the RCA (arrowhead) follows a normal course. **(c)** (axial oblique multiplanar reformat) shows the LCX (curved arrow) coursing retroaortically, and the LAD (arrow) continuing with an intraseptal course at the midlevel.

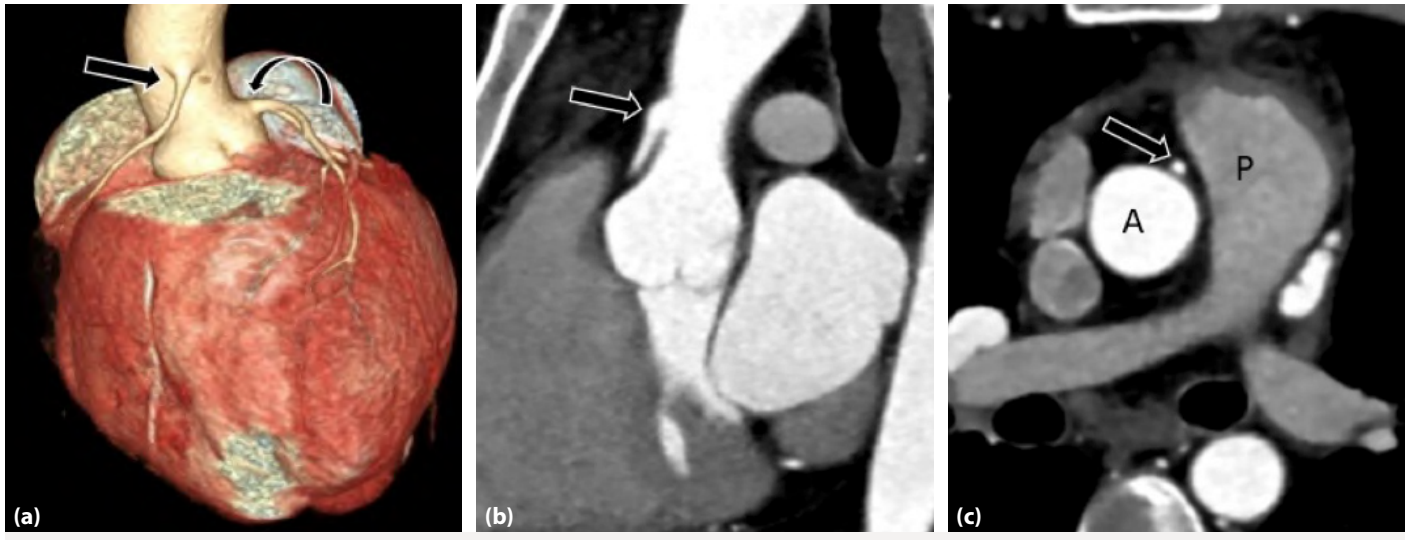

Figure 5. CCTA in a 65-year-old man demonstrates a high take-off origin of the RCA. **(a)** 3D volume-rendered image, **(b)** coronal oblique multiplanar reformat show the RCA (arrows) arising above the sinotubular junction. The LMCA originates normally from the left coronary sinus (curved arrow). **(c)** Axial oblique multiplanar reformat demonstrates the RCA (arrows) with an interarterial proximal course between the ascending aorta (A) and the pulmonary trunk (P).

LMCA arising above the left sinus and following a normal course. The remaining six patients had high take-off RCA origins: five arose above the right sinus and followed a normal proximal course, while one originated superior to the right–left sinus commissure, above the sinotubular junction, and demonstrated an interarterial proximal course (Fig. 5).

When coronary origin anomalies were stratified by proximal course, the interarterial variant was found in 20 patients: RCA (n=14), LMCA (n=4), LAD (n=1), and LCX (n=1). A retroaortic course was observed in 10 patients (LCX n=9, RCA n=1), and a prepulmonic course was seen in 2 patients (LMCA n=1, LAD n=1). In addition, the interarterial courses of the LAD and LCX included a proximal transseptal/intraseptal segment.

DISCUSSION

In this single-center, tertiary-care cohort, CCTA datasets from 3,181 patients were analyzed to define the prevalence

and proximal-course characteristics of coronary artery origin anomalies.

In cohorts evaluated with invasive coronary angiography or CCTA, reported prevalence rates generally range from 0.6% to 1.2%, whereas autopsy-based series typically report markedly lower rates of approximately 0.17% to 0.3%. This difference likely reflects the referral pattern of imaging-based cohorts, which predominantly include patients with chest pain or suspected coronary artery disease, rather than an unselected population.[1-13,14] In our study, the prevalence of coronary artery origin anomalies, including high take-off variants, was 1.29%, consistent with prior imaging-based literature.[3-12]

Origins arising from the contralateral sinus represent a clinically important subset of coronary origin anomalies. Although most courses are benign, interarterial variants are associated with an increased risk of myocardial ischemia and, in rare cases, sudden cardiac death. In contrast, origins from the non-coronary sinus are extremely uncommon and are generally considered incidental imaging findings without hemodynamic consequence.[13] A cardiac MRI study of 5,169 healthy children reported an overall prevalence of contralateral sinus origins of 0.44%, with right coronary arteries arising from the left sinus (0.33%) more frequently than left coronary arteries arising from the right sinus (0.12%).[15] Other studies similarly report that anomalous coronary arteries originating from the opposite sinus and exhibiting an interarterial course occur in less than 0.5% of the population, with the anomaly more often affecting the right coronary artery (0.23%) than the left (0.03%).[16]

In our cohort, the prevalence of contralateral or non-coronary sinus origins was 0.79%. RCA originating from the left sinus and left coronary arteries (LMCA or LCX) originating from the right sinus were each observed in 0.38% of patients. An additional case (0.03%) demonstrated the RCA originating from the non-coronary sinus and coursing retroaortically, consistent with the rarity of this variant in previous literature. In our cohort, every RCA with a left-sinus origin and every LMCA with a right-sinus origin followed a proximal interarterial course, whereas all right-sinus LCX variants followed a retroaortic course.

A single coronary artery is likewise a rare anomaly; in one report, 12 cases (0.27%) were found among 4,445 individuals.[17] We identified three patients (0.09%) with a single coronary artery, each arising from the right coronary sinus. In this subgroup, an interarterial segment with subsequent transseptal/intraseptal extension was seen in the LAD of one patient and the LCX of another (each representing 0.03% of the cohort).

Overall, the pattern of interarterial courses in our series—particularly their greater representation in RCA-related variants—paralleled previously described distributions. Notably, among patients in whom left-sided coronary arteries originated from the contralateral sinus, two patients demonstrated an interarterial proximal segment accompanied by a transseptal (intraseptal) component, a combination that may increase the clinical relevance of the anomalous origin.

Absence of the left main coronary artery, resulting in separate LAD and LCX origins from the left coronary sinus, is a well-described benign anatomical variant, with a reported prevalence ranging from 0.41% to 0.67% in previous studies.[14,18] In our cohort, this configuration was observed in 0.16% of patients, which is at the lower end of the reported range. Although usually regarded as clinically inconsequential, this variant should be recognized—particularly before invasive coronary angiography—because separate LAD and LCX ostia can influence catheter choice, ostial engagement strategy, and interpretation of the coronary origins.

Anomalous coronary origin from the pulmonary artery is exceptionally rare but represents a clinically significant congenital anomaly, most often manifesting in early life with heart failure and, in severe cases, sudden death. While the overall incidence in the general population is estimated to be approximately 0.01%,[3,16] no such cases were identified in our cohort. This absence may be related to the predominantly adult cohort studied, as these anomalies are typically detected in infancy or early childhood and frequently become symptomatic during that time.

In a large cohort of 12,899 patients, the prevalence of high take-off coronary arteries was reported to be approximately 0.20%, with the majority of cases (0.17%) originating from the right coronary artery.[19] In our cohort, high take-off anatomy was detected in 8 patients (0.26%). Of these, one had both the LMCA and the RCA with high take-off, one had an isolated LMCA with high take-off, and six had RCA origins with high take-off. Notably, two high take-off RCA cases exhibited a proximal interarterial course. This finding may increase their potential clinical significance even in the absence of additional anomalies. High take-off variants are important to consider when planning invasive coronary angiography, where catheter placement may be challenging, and in identifying high-risk proximal courses.

This study has several limitations. First, similar to other CCTA- and ICA-based investigations, our cohort does not fully represent the general population, as CCTA is predominantly performed in patients with chest pain or suspected coronary artery disease. For this reason, the frequency reported in our

series should be interpreted as representative of a CCTA-referred population rather than the general community. Furthermore, the single-center nature of the study may limit the broader applicability of the results. Third, due to the large number of examinations included, it was not feasible for both observers to review every CCTA dataset; consequently, interobserver variability could not be assessed.

CONCLUSION

Our analysis of 3,181 CCTA scans demonstrated that both the overall rate and the anatomic distribution of anomalous coronary origins were consistent with those in previously published CT angiography series. In our cohort, proximal course patterns—particularly interarterial trajectories—were common among opposite-sinus anomalies and represent an important anatomic feature to document when reporting coronary origin variants. Although most findings were incidental variants, accurate recognition remains crucial for procedural planning and for identifying anomalies with potentially high-risk proximal courses. CCTA provides noninvasive depiction of coronary ostial origin and proximal trajectory, reinforcing its role as a first-line imaging approach for suspected congenital coronary variants.

Ethics Committee Approval: Ethics committee approval was obtained from Non-Interventional Clinical Research Ethics Committee Kayseri City Training and Research Hospital (Approval Number: 553, Date: 26.08.2025).

Informed Consent: Informed consent was not required, as the study retrospectively analyzed anonymized CCTA datasets.

Conflict of Interest: The authors have no conflicts of interest to declare.

Funding: The authors declared that this study received no financial support.

Use of AI for Writing Assistance: Artificial intelligence–assisted technology was used solely for language editing and stylistic refinement of the manuscript. The authors used ChatGPT (OpenAI) to improve clarity, grammar, and readability of the text. No AI tools were used for study design, data collection, data analysis, interpretation of results, or figure generation. All authors reviewed and edited the manuscript critically and take full responsibility for the accuracy, integrity, and originality of the content.

Author Contributions: Concept – NBK, ÖŞ; Design – NBK, SK; Supervision – NBK, SK, ÖŞ; Resource – NBK; Materials – ÖŞ; Data Collection and/or Processing – NBK, SK; Analysis and/or Interpretation – NBK, SK, ÖŞ; Literature Review – NBK, SK, ÖŞ; Writing – NBK, SK; Critical Review – NBK, SK, ÖŞ.

Peer-review: Externally peer-reviewed.

REFERENCES

1. Angelini P, Velasco JA, Flamm S. Coronary anomalies: incidence, pathophysiology, and clinical relevance. Circulation 2002;105(20):2449-54. [CrossRef]
2. Williams RA. The historical background of sudden death in athletes. Williams RA, editor. The Athlete and Heart Disease: Diagnosis, Evaluation & Management. Philadelphia: Lippincott Williams & Wilkins; 2000.p.1-8.
3. Yamanaka O, Hobbs RE. Coronary artery anomalies in 126,595 patients undergoing coronary arteriography. Cathet Cardiovasc Diagn 1990;21(1):28-40. [CrossRef]
4. Başar E, Eryol NK, Ergin A, Çetin S, Köker AH. Anamolus origin of coronary arteries. Erciyes Tıp Dergisi 1995;17(1):37-42.
5. Figueroa Y, Altieri PI, Banchs H, Escobales N, Crespo M, Defendini E, et al. Coronary artery abnormalities in Puerto Rico. P R Health Sci J 2006;25(3):225-7.
6. Yuksel S, Meric M, Soylu K, Gulel O, Zengin H, Demircan S, et al. The primary anomalies of coronary artery origin and course: A coronary angiographic analysis of 16,573 patients. Exp Clin Cardiol 2013;18(2):121-3.
7. Alexander RW, Griffith GC. Anomalies of the coronary arteries and their clinical significance. Circulation 1956;14(5):800-5. [CrossRef]
8. Yorgun H, Hazırolan T, Kaya EB, Gürses KM, Evranos B, Canpolat U, et al. The prevalence of coronary artery anomalies in patients undergoing multidetector computed tomography for the evaluation of coronary artery disease. Turk Kardiyol Dern Ars 2010;38(5):341-348. Turkish.
9. Graidis C, Dimitriadis D, Karasavvidis V, Dimitriadis G, Argyropoulou E, Economou F, et al. Prevalence and characteristics of coronary artery anomalies in an adult population undergoing multidetector-row computed tomography for the evaluation of coronary artery disease. BMC Cardiovasc Disord 2015;15:112. [CrossRef]
10. Pandey NN, Sinha M, Sharma A, Rajagopal R, Bhambri K, Kumar S. Anomalies of coronary artery origin: Evaluation on multidetector CT angiography. Clin Imaging 2019;57:87-98. [CrossRef]
11. Javadrashid R, Tarzamni MK, Aslanabadi N, Ghaffari M, Salehi A, Sorteji K. Myocardial bridging and coronary artery anomalies detected by ECG-gated 64-row multidetector computed tomography angiography in symptomatic patients. Folia Morphol (Warsz) 2009;68(4):201-6.
12. Kacmaz F, Ozbulbul NI, Alyan O, Maden O, Demir AD, Balbay Y, et al. Imaging of coronary artery anomalies: the role of multidetector computed tomography. Coron Artery Dis 2008;19(3):203-9. [CrossRef]

13. Hoover JA, Catakam K, Wittenberg RE, Bloom JP, Yeh DD, Han QJ, et al. Coronary Artery Anomalies in Review: Anomalous Origin, Aneurysms, and Fistulae. Methodist Debakey Cardiovasc J 2025;21(4):54-64. [CrossRef]
14. Angelini P, Cheong BY, Lenge De Rosen VV, Lopez A, Uribe C, Masso AH, et al. High-Risk Cardiovascular Conditions in Sports-Related Sudden Death: Prevalence in 5,169 Schoolchildren Screened via Cardiac Magnetic Resonance. Tex Heart Inst J 2018;45(4):205-13. [CrossRef]
15. Bigler MR, Kadner A, Räber L, Ashraf A, Windecker S, Siepe M, et al. Therapeutic Management of Anomalous Coronary Arteries Originating From the Opposite Sinus of Valsalva: Current Evidence, Proposed Approach, and the Unknowing. J Am Heart Assoc 2022;11(20):e027098. [CrossRef]
16. Danias PG, Stuber M, McConnell MV, Manning WJ. The diagnosis of congenital coronary anomalies with magnetic resonance imaging. Coron Artery Dis 2001;12(8):621-6. [CrossRef]
17. Al Umairi R, Al-Khouri M. Prevalence, Spectrum, and Outcomes of Single Coronary Artery Detected on Coronary Computed Tomography Angiography (CCTA). Radiol Res Pract 2019;2019:2940148. [CrossRef]
18. Lipsett J, Cohle SD, Berry PJ, Russell G, Byard RW. Anomalous coronary arteries: a multicenter pediatric autopsy study. Pediatr Pathol1994;14(2):287-300. [CrossRef]
19. Loukas M, Andall RG, Khan AZ, Patel K, Muresian H, Spicer DE, et al. The clinical anatomy of high take-off coronary arteries. Clin Anat 2016;29(3):408-19. [CrossRef]

Official Journal of Erciyes University Faculty of Medicine

DOI: 10.14744/cpr.2026.71836
J Clin Pract Res 2026;48(2):145–152

Comparison of Intern Doctors and ChatGPT in Emergency Cases Assessment

Yusuf Kantar,[1] Melih İmamoğlu,[2] Emre Bülbül,[3] Serhat Hayme,[4] Arif Onur Eden,[1] Yasin Bilgin,[1] Fatih Mehmet Sari[1]

[1]Department of Emergency Medicine, Erzincan Binali Yıldırım University, Faculty of Medicine, Erzincan, Türkiye
[2]Department of Emergency Medicine, Karadeniz Technical University, Faculty of Medicine, Trabzon, Türkiye
[3]Department of Emergency Medicine, Erciyes University, Faculty of Medicine, Kayseri, Türkiye
[4]Department of Biostatistics and Medical Informatics Erzincan Binali Yıldırım University, Faculty of Medicine, Erzincan, Türkiye

Cite this article as:
Kantar Y, İmamoğlu M, Bülbül E, Hayme S, Eden AO, Bilgin Y, Sari FM. Comparison of Intern Doctors and ChatGPT in Emergency Cases Assessment. J Clin Pract Res 2026;48(2):145–152.

Address for correspondence:
Yusuf Kantar.
Department of Emergency Medicine, Erzincan Binali Yıldırım University, Faculty of Medicine, Erzincan, Türkiye
Phone: +90 541 927 58 17
E-mail:
dryusufkantar@gmail.com

Submitted: 17.12.2025
Revised: 05.03.2026
Accepted: 26.03.2026
Available Online: 20.04.2026

Erciyes University Faculty of Medicine Publications - Available online at www.jcpres.com

ABSTRACT

Objective: Accurate and timely diagnosis in emergency departments is crucial due to the high patient volume and time-sensitive nature of care. Intern doctors, who are nearing the completion of medical school, frequently work in emergency departments in many countries. However, after graduation, physicians are often expected to assume critical patient care responsibilities despite limited experience. Artificial intelligence models can quickly analyze patient data and generate diagnoses, thus assisting inexperienced physicians in enhancing diagnostic accuracy. This study aims to evaluate the diagnostic performance of ChatGPT-4 in emergency department case scenarios and compare its accuracy with that of intern doctors.

Materials and Methods: This study involved intern doctors participating in the internship program during the 2024–2025 academic year. A total of 36 case-based questions, categorized by difficulty level, were administered to 155 interns and subsequently presented to artificial intelligence. Descriptive statistics were used to summarize the data, and a one-sample t-test was conducted to compare the diagnostic accuracy between intern doctors and ChatGPT. Statistical significance was set at $p<0.05$.

Results: Intern doctors achieved an overall correct response rate of 58.3%, while ChatGPT achieved a rate of 97.2%. A statistically significant, moderate negative correlation was found between question difficulty and interns' performance ($r=-0.684$; $p<0.001$), indicating decreased accuracy as question difficulty increased. ChatGPT consistently demonstrated significantly higher performance across all difficulty levels.

Conclusion: ChatGPT-4 may serve as a valuable diagnostic support tool in emergency departments, particularly for newly graduated physicians with limited clinical experience.

Keywords: Artificial intelligence, ChatGPT, emergency department, intern doctors, medical education.

INTRODUCTION

Medical education is a long and demanding process that requires sustained effort and perseverance. Its final phase is the internship period, during which medical students serve as intern doctors (IDs). In contrast to the predominantly theoretical training received throughout their academic years, the internship provides a structured opportunity for experiential learning, allowing students to apply their knowledge in real clinical settings.[1] Throughout the year, IDs rotate through multiple clinical departments, including emergency medicine. The emergency medicine rotation, however, has several distinguishing features compared with other specialties. Patients typically present to the emergency department (ED) with acute and potentially life-threatening conditions, requiring clinicians to rapidly generate differential diagnoses and initiate timely management. This environment necessitates the development of strong clinical decision-making skills under pressure.[2]

Secondly, and perhaps more importantly, most newly graduated physicians are required to work in EDs for a designated period before selecting a specialty. This requirement stems from the mandatory service obligation implemented by the Ministry of Health in our country. The primary assignments for this compulsory service are EDs and prehospital ambulance services. As a result, newly graduated doctors—often with limited clinical experience—are expected to provide critical patient care immediately after completing medical school. Therefore, it is essential that intern doctors receive comprehensive, high-quality training to adequately prepare them for these responsibilities.[3]

The artificial intelligence (AI) program utilized in our study is ChatGPT, a GPT-based AI model developed by OpenAI, which has made substantial progress in natural language processing.[4] This model is distinguished by its capacity to deliver a human-like experience in text-based communication. Although AI systems have not yet been integrated into routine clinical practice, they have been the focus of experimental research for several years. Their ability to accurately interpret user inputs and generate rapid, coherent outputs indicates strong potential for future applications in the healthcare domain.[5]

In the context of the ED, despite the rising volume of patient visits, several studies have shown that AI can be implemented as early as the triage stage to facilitate the efficient progression of diagnostic and therapeutic processes.[6] Furthermore, when data from patients diagnosed and admitted by ED residents were input into AI programs, the AI generated diagnostic suggestions consistent with those of the physicians.[7] Studies have also indicated that AI can support the diagnostic process, particularly in the interpretation of medical tests. It has shown high efficacy in analyzing radiological images and electrocardiography (ECG) results.[8,9]

KEY MESSAGES

- ChatGPT can serve as a valuable guide for newly graduated doctors who are theoretically well-equipped, helping them apply their knowledge until they gain sufficient practical experience.
- Although artificial intelligence appears successful in case scenarios, presenting these cases to it requires a certain level of medical expertise and knowledge.
- In critical situations, such as patient care, artificial intelligence cannot be given full responsibility. It can only serve as a guide for healthcare professionals.

In this context, it can be confidently asserted that integrating AI-driven technologies into time-sensitive clinical environments such as EDs will enhance patient care and support inexperienced physicians in the near future. By facilitating more accurate and timely diagnoses in critical and complex cases, AI not only promotes public health and the efficient use of healthcare resources but also helps safeguard physicians against malpractice claims.

This study aims to assess ChatGPT's ability to accurately predict diagnoses in ED cases based on provided clinical findings, in comparison with IDs.

MATERIALS AND METHODS

This study is a single-center, cross-sectional observational study. The study population included intern doctors (IDs) who were enrolled in the emergency department (ED) rotation during the 2024–2025 academic year and consented to participate. Ethical approval was obtained from the Erzincan Binali Yıldırım University Non-Interventional Clinical Research Ethics Committee (Approval Number: 2024-13/05, Date: 03.10.2024). This study was conducted in accordance with the principles of the Declaration of Helsinki.

The hospital where the study was conducted is a university hospital, serving as the only public hospital in the city and providing care to a population of approximately 500,000, including patients from surrounding provinces and districts. The ED receives between 1,500 and 2,000 patient visits daily.

The questions were developed by a panel of five faculty members from different medical schools, each with at least five years of professional experience in emergency medicine. This expert panel (EP) designed 36 multiple-choice questions based on scenarios relevant to ED practice. The development

process—including question formulation, arrangement of answer options, and determination of the correct answer—was guided by current literature, clinical guidelines, and the panelists' professional experience. For each question, a single correct answer was established as the gold standard (GS). Participants were subsequently asked to select the "most likely diagnosis" for each case. Their responses were then compared with the GS answers.

Twelve questions were categorized as easy, 12 as moderate, and 12 as difficult. The difficulty level of each scenario was determined by the EP based on consensus, taking into account factors such as presenting complaints, physical examination findings, diagnostic methods used, and the interpretability of test results in relation to the clinical presentation. Participants answered the questions without knowledge of their assigned difficulty levels, ensuring blinding with respect to question difficulty.

To ensure the validity of the difficulty classification, inter-rater reliability among the EPs who categorized the questions was assessed using Fleiss' kappa, an appropriate method for evaluating agreement among multiple raters. Each specialist independently assigned all 36 questions to the easy, moderate, or difficult category. The overall inter-rater agreement was substantial (Fleiss' κ=0.85), indicating a high level of consistency across raters in difficulty classification.

Considering that completing all 36 questions could be time-consuming and to minimize participant fatigue, the questions were distributed evenly according to difficulty level, and two separate evaluation forms were prepared using Google Documents (Fig. 1). To ensure even distribution, six questions from each of the three difficulty levels determined by the expert panel (EP) were selected, resulting in two evaluation forms, each containing 18 questions.

A total of 155 IDs were included in the study. Participants' personal information was not recorded. The IDs completed the ED rotation in groups over two-month periods throughout the one-year academic calendar, with each group comprising 25–30 IDs. The study was conducted during the final two weeks of each group's two-month ED rotation.

The same questions were subsequently posed to ChatGPT. For the AI component of our study, ChatGPT 4.0 (GPT-4-based, 2025 version) developed by OpenAI was used. Prior to presenting the questions, ChatGPT was provided with contextual information, including the fact that the questions were based on cases presenting to the ED. It was instructed to respond concisely using medical terminology, assuming that the questions were asked by a healthcare professional.

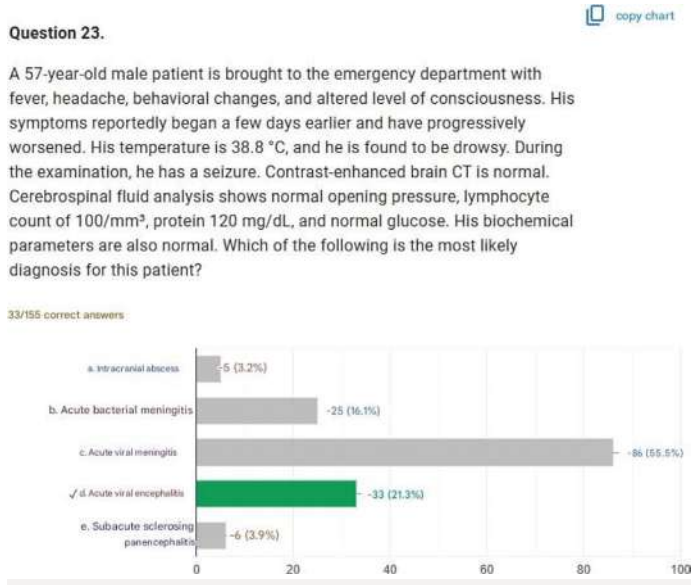

Figure 1. Example of a question completed by intern doctors using Google Documents.

The study was conducted throughout the academic year. Data were collected from IDs during each two-month ED rotation. Initially, a WhatsApp group was created exclusively for IDs on rotation that month, and the link to the Google Documents evaluation form was sent to them. Although the process was conducted online via Google Documents, data collection occurred during the weekly routine ED teaching sessions, with all IDs present and supervised by several proctors, to prevent participants from discussing the questions or consulting written or digital resources. Participants were seated in the classroom in an exam-style arrangement to prevent communication with one another or access to reference materials. Each ID accessed and completed the form using their personal email address, with the form link configured to allow a single view only. Before completing the digitally distributed Google Documents forms, each ID was assigned a unique code, which they entered in the designated field. The same code was used when answering the questions in the second section, ensuring consistency and integrity in data collection. Saving or revisiting the questions was disabled. Subsequently, the questions and correct answers were not shared with any IDs to prevent subsequent groups from becoming aware of the content, thus maintaining optimal blinding.

Responses were evaluated using two different methods. In the first method, all IDs were considered as a single group, and their answers were assessed proportionally. The 50% threshold was used only as a descriptive indicator of how commonly each question was recognized by the intern cohort. This

threshold reflects clinical interpretability rather than statistical classification. In emergency medicine education and Objective Structured Clinical Examination (OSCE)-style.[10,11] competency assessments, a case vignette is typically considered clinically recognizable when at least half of the trainees can identify the correct diagnosis. In the second method, IDs were evaluated individually. Each question was assigned one point (for selecting the correct answer as defined by the gold standard, GS), and scores from each question category were evaluated separately.

Two different approaches were also applied when posing the questions to ChatGPT. Initially, questions were presented in an open-ended format without answer options. The AI was asked to determine the most appropriate diagnosis for each case, and its ability to reach the GS answer was assessed. This section was designated as "GPT-a" (Fig. 2). Subsequently, the questions were presented in a multiple-choice format, similar to how they were posed to IDs, and ChatGPT was asked to select the "most likely diagnosis" from the provided options. Selecting the answer corresponding to the GS was considered a correct response. The results obtained from this phase were designated as "GPT-b" (Fig. 3).

Responses obtained from Google Documents and ChatGPT were collected and compared with the GS answers. The easy, moderate, and difficult question categories were analyzed separately using statistical methods.

Statistical Analysis

Assuming a Type 1 error (α) of 0.05 and a power of 0.95, with an expected joint correct response rate of 0.5 based on expert opinion and a margin of error (d) of 0.2, the sample size required for the study was calculated as 104 intern doctors (IDs) using the confidence interval method. The PASS 11-2025 – Power Analysis and Sample Size Software (v25.0.x) program was used to calculate the sample size. Data analysis was performed using IBM SPSS 25.0 (SPSS Inc., Chicago, IL, USA). Descriptive statistics were presented as mean ± standard deviation and median (min-max) for numerical variables, and as frequency and percentage for categorical variables.

Scores obtained by IDs from easy, moderate, and difficult question categories were compared with scores obtained by ChatGPT in both open-ended and multiple-choice formats using a one-sample t-test. A p-value of <0.05 was considered statistically significant. ChatGPT outputs are deterministic and do not constitute a statistical sample. Since no variance or repeated measurements exist for the AI model, group-to-group comparison tests (e.g., independent-samples t-test) are not statistically appropriate. Thus, intern doctors' mean scores were compared to ChatGPT's fixed score using a one-sample t-test, which evaluates whether a sample mean differs from a fixed, non-random reference value.

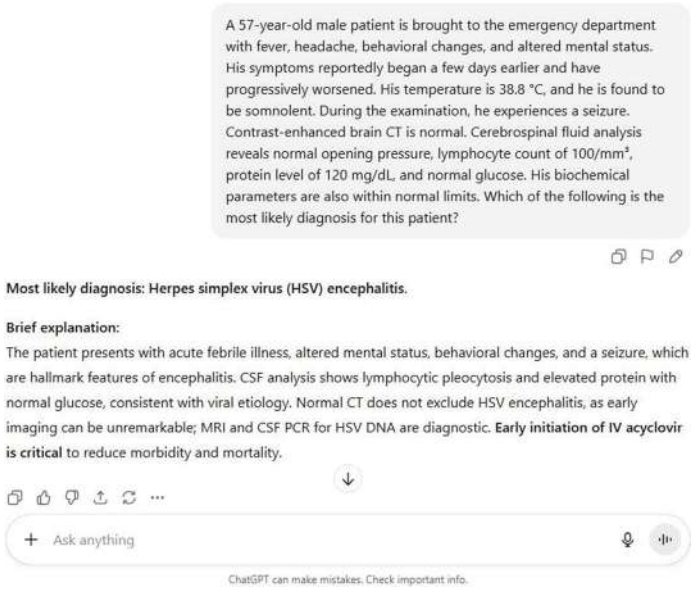

Figure 2. Example of a case presented to Chat-GPT in an open-ended format and its response.

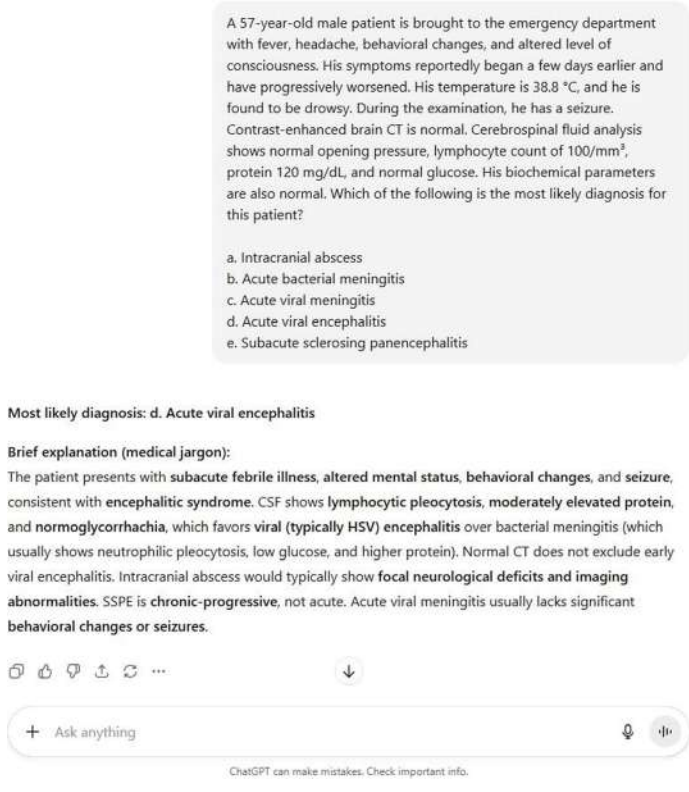

Figure 3. Example of a case presented to Chat-GPT in a multiple-choice format and its response.

Table 1. Comparison of responses given by intern doctors and Chat-GPT based on question difficulty

	Intern doctors n (%)	GPT-a n (%)	GPT-b n (%)
Easy case questions			
True	**11 (30.5)**	8 (22.2)	12 (33.3)
False	1 (2.8)	4 (11.1)	0 (0)
Moderate case questions			
True	**8 (22.2)**	12 (33.3)	12 (33.3)
False	4 (11.1)	0 (0)	0 (0)
Difficult case questions			
True	**2 (5.6)**	8 (22.2)	11 (30.5)
False	10 (27.8)	4 (11.1)	1 (2.8)
Total			
True	**21 (58.3)**	**28 (77.8)**	**35 (97.2)**
False	15 (41.7)	8 (22.2)	1 (2.8)

Table 2. Evaluation of intern doctors' responses based on a percentage system

Easy case questions (%)		Moderate case questions (%)		Difficult case questions (%)	
1	63.9%	13	54.8%	25	**36.8%**
2	93.5%	14	**45.8%**	26	**12.9%**
3	63.9%	15	**45.8%**	27	**26.5%**
4	63.9%	16	51.6%	28	**39.4%**
5	53.5%	17	**43.2%**	29	**36.1%**
6	94.8%	18	60.0%	30	**31.0%**
7	61.9%	19	63.2%	31	**28.4%**
8	58.1%	20	**43.2%**	32	**21.3%**
9	78.7%	21	57.4%	33	**38.1%**
10	93.5%	22	60.0%	34	52.3%
11	78.7%	23	53.5%	35	55.5%
12	**49.0%**	24	70.3%	36	**41.9%**

RESULTS

The responses collected from intern doctors (IDs) via Google Documents were compared with the data obtained from ChatGPT 4.0. It was observed that as question difficulty increased, the accuracy of IDs decreased. In the easy question category, more than 50% of the IDs correctly answered 11 out of 12 questions, whereas this number decreased to 2 out of 12 questions in the difficult category.

When questions were presented to ChatGPT in an open-ended format (GPT-a), it correctly answered all moderate-difficulty questions but provided correct responses for 8 of 12 questions in both the easy and difficult categories. However, in the multiple-choice format (GPT-b), ChatGPT correctly answered all easy and moderate questions, making only one incorrect response in the difficult category.

Overall, the correct response rate for IDs across all questions was 58.3%. In comparison, ChatGPT achieved an accuracy rate of 77.8% in the open-ended format (GPT-a) and 97.2% in the multiple-choice format (GPT-b) (Table 1).

In the easy question category, IDs answered 11 questions correctly, of which ChatGPT correctly answered 8 in the open-ended format and all 11 in the multiple-choice format. The one question answered incorrectly by IDs was correctly identified by ChatGPT when presented in the multiple-choice format. In the moderate category, ChatGPT correctly answered all four questions that IDs had answered incorrectly, in both the open-ended and multiple-choice formats. In the difficult category, ChatGPT correctly answered all 10 questions that IDs failed to answer when presented in the multiple-choice format, and correctly answered 6 of these questions in the open-ended format (Table 1).

The correct response rates for each question among intern doctors (IDs) were analyzed. It was observed that as question difficulty increased, the number of IDs providing correct answers decreased. Correct response rates for difficult questions were significantly lower than those for easy questions. In the easy category, the lowest correct response rate was 49%, while this rate progressively declined with increasing difficulty, with one difficult question being correctly answered by only 12.9% of participants (Table 2).

The data were also analyzed on a question-by-question basis, with one point assigned for each correct answer across the 36 questions. This analysis confirmed that as question difficulty increased, the correct response rate among IDs decreased. A statistically significant, moderate, and negative correlation was observed between IDs' scores and question difficulty ($r=-0.684$; $p<0.001$). Furthermore, the average scores of IDs according to question difficulty were compared with those obtained by ChatGPT in both the open-ended (GPT-a) and multiple-choice (GPT-b) formats, with ChatGPT demonstrating significantly higher performance ($p<0.001$) (Table 3).

DISCUSSION

Our study suggests that ChatGPT-4 could be a valuable tool in the diagnostic process within emergency departments (EDs). It may play a particularly supportive role for newly graduated physicians who lack sufficient clinical experience.

Table 3. Evaluation of intern doctors' responses based on the scoring system and statistical comparison with ChatGPT scores

	Easy case questions	Moderate case questions	Difficult case questions	Total
Intern doctors				
Mean	8.5	6.5	4.2	19.2
(±SD)	1.96	1.81	2.04	4.44
Median	**9**	**6**	**4**	19
Minimum	4	1	0	6
Maximum	12	11	11	30
GPT-a				
Point	8	12	8	28
p value	**0.001**	**<0.001**	**<0.001**	**<0.001**
GPT-b				
Point	12	12	11	35
p value	**<0.001**	**<0.001**	**<0.001**	**<0.001**

SD: Standard deviation.

In a previous study, data from patients admitted from the ED to various departments were retrospectively collected, and both ED residents and ChatGPT-4 were asked, "What could be the diagnosis for these patients?" The results demonstrated that AI provided significantly more accurate responses compared to ED residents ($p<0.05$).[7] In our study, ChatGPT showed statistically significantly higher diagnostic accuracy than intern doctors (IDs) ($p<0.001$). While proportional differences were minimal in easier cases, ChatGPT correctly answered 90% of the questions that IDs had answered incorrectly in more difficult cases.

In another study, ChatGPT-3 was evaluated using 30 case scenarios, presented to both AI and physicians based on limited symptom categories such as abdominal pain, shortness of breath, and vomiting. When ChatGPT-3 was asked to select one diagnosis from ten differential diagnoses in a multiple-choice format, it achieved an accuracy rate of 93.3%. However, when the number of differential diagnoses was reduced to five, its accuracy dropped to 83.3%. When presented with only two answer choices and asked, "What is the most likely diagnosis?", AI correctly answered only 53.3% of the questions.[12]

Our study differs from the aforementioned research. ChatGPT-4 achieved a 97.2% accuracy rate, correctly answering 35 out of 36 multiple-choice questions spanning a wide range of case categories, including varying difficulty levels, traumatic cases, pediatric cases, chronic diseases, and life-threatening clinical conditions. In the previous study, reducing the number of differential diagnoses negatively affected AI's accuracy. In contrast, in our study, ChatGPT-4 achieved a 77.8% accuracy rate even in the open-ended format, without provided answer choices. Considering that IDs achieved a 58.3% success rate in the multiple-choice format, ChatGPT's performance in the open-ended setting can be regarded as highly successful.

The marked improvement of ChatGPT-4 over ChatGPT-3, as observed in our study, underscores the rapid advancements in AI and suggests its potential for even more effective clinical applications in the near future.

In a study by Günay et al.[13] in 2024 on ECG interpretation, ECG findings were converted into text format and presented in a multiple-choice format to experienced ED specialists, cardiologists, and ChatGPT. AI provided more accurate responses than both ED specialists and cardiologists, with statistical significance ($p<0.001$). As the difficulty of the ECG questions increased, the accuracy rates of both physician groups decreased, as did ChatGPT's performance. However, despite this decline, AI remained statistically significantly more successful than both physician groups overall. This study shares similarities with our research in terms of question preparation. In our study, AI was also found to be statistically significantly more successful than intern doctors (IDs) ($p<0.001$). However, whereas no statistically significant difference was observed between cardiologists and ChatGPT in the difficult ECG category in the previous study, we found a statistically significant, moderate, and negative correlation between IDs and ChatGPT as question difficulty increased ($r=-0.684$; $p<0.001$).

Although ChatGPT outperformed IDs overall in our study, it failed to correctly answer 3 questions in the easy category. This may be explained by IDs utilizing their theoretical knowledge to select the correct option from multiple choices, whereas

ChatGPT, applying a more complex reasoning process, sometimes provided multiple possible causes rather than directly stating the correct answer.

As in many areas of life, the potential applications of AI in healthcare have been explored and demonstrated in various experimental studies.[6,14] AI has been shown to be beneficial in clinical settings for tasks such as assigning triage codes, interpreting ECG findings, and analyzing radiological images.[8,9,15] However, studies investigating the use of AI specifically in the diagnostic process of ED cases remain limited.[16] We believe that our study will make a meaningful contribution to the existing literature on this topic.

Although the data on case evaluation in the ED are promising, standardization of ethical considerations, patient consent, and data privacy must be ensured before AI-assisted patient management can be implemented as routine practice.[17]

This study has several important limitations. The most significant limitation is that while one group consisted of scores from 155 intern doctors (IDs), the other group included only a single set of responses obtained from ChatGPT. Since ChatGPT provided a single output per question, its performance does not form a statistical distribution. This required the use of a one-sample comparison approach rather than two-sample methods. Although this is a methodological limitation, it reflects how large language models operate in real clinical use by generating a single diagnostic suggestion.

Another limitation relates to the timing of IDs' ED rotations. Since the study was conducted during the ED rotation, participants joined the study in two-month periods throughout the academic year. Consequently, there was no uniformity regarding the completion of non-ED rotations.

CONCLUSION

It is believed that AI could be a useful tool in the diagnostic phase in EDs. A foundational level of medical knowledge remains essential to correctly input and interpret patient data within AI systems. Therefore, it is essential to recognize that AI should not be considered a standalone diagnostic tool for the general public.

Ethics Committee Approval: Ethics committee approval was obtained from Erzincan Binali Yıldırım University Non-Interventional Clinical Research Ethics Committee (Approval Number: 2024-13/05, Date: 03.10.2024).

Informed Consent: Written informed consent was obtained from the participants.

Conflict of Interest: The authors have no conflicts of interest to declare.

Funding: The authors declared that this study received no financial support.

Use of AI for Writing Assistance: No use of AI-assisted technologies was declared by the authors.

Author Contributions: Concept – YK, MI, EB, SH, AOE, YB, FMS; Design – YK, MI, EB; Supervision – AOE, YB, FMS; Resource – YK, MI, EB, SH, AOE, YB, FMS; Materials – YK, MI; Data Collection and/or Processing – EB, SH, AOE; Analysis and/or Interpretation – SH; Literature Review – YK, YB, FMS; Writing – YK, MI, EB; Critical Review – SH, AOE, YB, FMS.

Acknowledgment: Authors would like to thank the Proofreading & Editing Office of the Dean for Research at Erciyes University for the copyediting and proofreading service for this manuscript.

Peer-review: Externally peer-reviewed.

REFERENCES

1. Güven G, İnceoğlu F, Özdemir F, Bakır OS. Burnout and professional commitment in medical faculty students in Türkiye: a cross-sectional analysis. Res Dev Med Educ 2023;12:14. [CrossRef]
2. Tortum F, Bayramoğlu A, Tasci HK, Kasali K. Evaluation of the development of emergency response skills of intern doctors after emergency medicine internship: A prospective cross-sectional study. J Res Clin Med 2023;11:13. [CrossRef]
3. Turan S, Hayme S. Effect of professional commitment on the career plans of intern doctors. Pak J Med Sci 2025;41(2):525-30. [CrossRef]
4. ChatGPT: Optimizing Language Models for Dialogue. https://openai.com/blog/chatgpt Accessed March 31, 2026.
5. Caldarini G, Jaf S, McGarry K. A Literature Survey of Recent Advances in Chatbots. Information 2022;13(1):41. [CrossRef]
6. Paslı S, Şahin AS, Beşer MF, Topçuoğlu H, Yadigaroğlu M, İmamoğlu M. Assessing the precision of artificial intelligence in ED triage decisions: Insights from a study with ChatGPT. Am J Emerg Med 2024;78:170-5. [CrossRef]
7. Hoppe JM, Auer MK, Strüven A, Massberg S, Stremmel C. ChatGPT With GPT-4 Outperforms Emergency Department Physicians in Diagnostic Accuracy: Retrospective Analysis. J Med Internet Res 2024;26:e56110. [CrossRef]
8. Rao A, Kim J, Kamineni M, Pang M, Lie W, Succi MD. Evaluating ChatGPT as an Adjunct for Radiologic Decision-Making. medRxiv [Preprint] 2023:2023.02.02.23285399. Update in: J Am Coll Radiol 2023;20(10):990-7. [CrossRef]
9. Zaboli A, Brigo F, Ziller M, Massar M, Parodi M, Magnarelli G, et al. Exploring ChatGPT's potential in ECG interpretation and outcome prediction in emergency department. Am J Emerg Med 2025;88:7-11. [CrossRef]

10. Muralidharan J, Lewin S, Nithyanandam S, Stephen J, Joseph M, Ta L, et al. Feasibility and utility of objective structured clinical examination (OSCE) as an end-of-internship assessment of MBBS training in a medical college in Southern India. BMC Med Educ 2025;25(1):1608. [CrossRef]
11. Lee M, Hernandez E, Brook R, Ha E, Harris C, Plesa M, et al. Competency-based Standard Setting for a High-stakes Objective Structured Clinical Examination (OSCE): Validity Evidence. MedEdPublish (2016) 2018;7:200. [CrossRef]
12. Hirosawa T, Harada Y, Yokose M, Sakamoto T, Kawamura R, Shimizu T. Diagnostic Accuracy of Differential-Diagnosis Lists Generated by Generative Pretrained Transformer 3 Chatbot for Clinical Vignettes with Common Chief Complaints: A Pilot Study. Int J Environ Res Public Health 2023;20(4):3378. [CrossRef]
13. Günay S, Öztürk A, Özerol H, Yiğit Y, Erenler AK. Comparison of emergency medicine specialist, cardiologist, and chat-GPT in electrocardiography assessment. Am J Emerg Med 2024;80:51-60. [CrossRef]
14. Sarbay İ, Berikol GB, Özturan İU. Performance of emergency triage prediction of an open access natural language processing based chatbot application (ChatGPT): A preliminary, scenario-based cross-sectional study. Turk J Emerg Med 2023;23(3):156-61. [CrossRef]
15. Zaboli A, Brigo F, Sibilio S, Mian M, Turcato G. Human intelligence versus Chat-GPT: who performs better in correctly classifying patients in triage? Am J Emerg Med 2024;79:44-7. [CrossRef]
16. Farahmand S, Shabestari O, Pakrah M, Hossein-Nejad H, Arbab M, Bagheri-Hariri S. Artificial Intelligence-Based Triage for Patients with Acute Abdominal Pain in Emergency Department; a Diagnostic Accuracy Study. Adv J Emerg Med 2017;1(1):e5.
17. Farangi MR, Nejadghanbar H, Hu G. Use of generative AI in research: ethical considerations and emotional experiences. Ethics & Behavior 2025;35(7):527-43. [CrossRef]

Official Journal of Erciyes University Faculty of Medicine

DOI: 10.14744/cpr.2026.14313
J Clin Pract Res 2026;48(2):153–161

High-Resolution Anterior Segment Optical Coherence Tomography Characteristics of Conjunctival Tumors

Onur Ocaktan,[1] Fatih Horozoglu,[1] Hidayet Sener,[1] Furkan Özer[2]

[1]Department of Ophthalmology, Erciyes University Faculty of Medicine, Kayseri, Türkiye
[2]Department of Ophthalmology, Nevşehir State Hospital, Nevşehir, Türkiye

ABSTRACT

Objective: This study aimed to assess the demographic, clinical, histological classifications, and anterior segment optical coherence tomography (AS-OCT) features of conjunctival malignancies. The goal was to identify factors associated with tumor malignancy.

Materials and Methods: This retrospective analysis included 37 patients with conjunctival tumors. Data collected comprised age, gender, tumor coloration, histological type, location, corneal involvement, subepithelial reflectivity of the lesion on AS-OCT, lesion homogeneity on AS-OCT, and the presence of intralesional cysts on AS-OCT. Statistical analysis was performed using chi-square and t-tests, with a significance level of $\alpha<0.05$. The study protocol was approved by the Erciyes University Health Sciences Research Ethics Committee (Approval Number: 2025/365, Date: 09.07.2025).

Results: Malignant tumors were identified in significantly older patients. No significant gender differences were found regarding malignancy. Amelanotic appearance was significantly more common in malignant tumors. The types of tumors identified included conjunctival nevus, conjunctival ocular surface squamous neoplasia (OSSN), conjunctival lymphoma, conjunctival melanoma, and conjunctival cyst. No significant relationship was found between tumor location and malignancy. Corneal involvement was significantly associated with malignancy. On AS-OCT, malignant tumors exhibited a hyporeflective subepithelial lesion with homogeneous internal reflectivity. Although benign tumors contained more intralesional cysts on AS-OCT, this finding was not statistically significant.

Conclusion: Conjunctival tumors exhibit various characteristics. Advanced age, amelanotic pigmentation, corneal involvement, and a hyporeflective homogeneous lesion on AS-OCT are significant indicators of malignancy, highlighting the importance of detailed examination and increased vigilance.

Keywords: Anterior segment optical coherence tomography, conjunctival melanoma, conjunctival neoplasms, optical coherence tomography imaging, ocular oncology, predictors of tumor malignancy

This study was presented at the 59th National Congress of the Turkish Ophthalmology Association, held on November 19–23, 2025.

Cite this article as:
Ocaktan O, Horozoglu F, Sener H, Özer F. High-Resolution Anterior Segment Optical Coherence Tomography Characteristics of Conjunctival Tumors. J Clin Pract Res 2026;48(2):153–161.

Address for correspondence:
Hidayet Sener.
Department of Ophthalmology, Erciyes University Faculty of Medicine, Kayseri, Türkiye
Phone: +90 555 719 64 03
E-mail:
hidayetsener00@gmail.com

Submitted: 17.10.2025
Revised: 13.03.2026
Accepted: 30.03.2026
Available Online: 22.04.2026

Erciyes University Faculty of Medicine Publications - Available online at www.jcpres.com

INTRODUCTION

Conjunctival tumors span a wide spectrum, ranging from benign lesions that require follow-up to highly malignant invasive neoplasms. If left untreated, these tumors can lead to vision loss, aesthetic concerns, and, in cases of malignancy, potentially fatal complications.[1] Despite the availability of advanced diagnostic and therapeutic methods in tertiary hospitals, early detection and treatment of malignant conjunctival tumors remain challenging.

Malignant conjunctival tumors are predominantly found in older populations and exhibit distinct clinical characteristics, including amelanotic lesions and corneal involvement. Research indicates that the prevalence and severity of these lesions vary across different communities, emphasizing the need for localized investigations to tailor diagnostic and therapeutic strategies.[1,2] Recent studies suggest that 61.2% of conjunctival tumors are premalignant or malignant, with squamous cell carcinoma (SCC) and conjunctival intraepithelial neoplasia (CIN) being the most common types.[3]

Histopathological and anatomical analysis of these tumors offers valuable insights for clinical management and prognostic assessments. For instance, although conjunctival melanomas are rare, they exhibit aggressive behavior with a high recurrence rate and potential for metastasis.[4] Additionally, genetic and immunohistochemical investigations are increasingly recognized as essential tools for the accurate diagnosis and classification of malignant tumors. Recent research has underscored the importance of genetic alterations, immunological checkpoint markers, and ultraviolet light signatures in the etiology of conjunctival cancers.[5]

High-resolution anterior segment optical coherence tomography (AS-OCT) has become an increasingly important adjunct to slit-lamp examination, enabling better characterization of conjunctival lesions and more precise delineation of their extent. Previous reports have described specific imaging patterns that can support clinical impressions in certain entities—such as epithelial thickening with increased epithelial reflectivity and an abrupt transition zone in ocular surface squamous neoplasia, a smooth, homogeneous subepithelial hyporeflective lesion with internal "dot-like" infiltrates in lymphoproliferative disease, and variable posterior shadowing that can limit the assessment of heavily pigmented lesions.[6]

However, clinicians often encounter a broad spectrum of conjunctival lesions in daily practice, and the literature provides relatively limited guidance on applying a standardized set of AS-OCT descriptors across various diagnoses within a single cohort, especially when interpreted alongside routine clinical variables.[7] A pragmatic analysis of these features in a tertiary-care series may help clarify which descriptors are most consistently observed and how they correlate with histopathologic diagnosis and malignancy risk in real-world settings.[6-8]

KEY MESSAGES

- Advanced age and amelanotic appearance are strong predictors of malignancy in conjunctival tumors (mean age 64.1 years; 93.75% amelanotic).
- Tumor invasion into the cornea is significantly associated with malignant behavior and should raise clinical suspicion.
- On AS-OCT, a hyporeflective, homogeneous subepithelial lesion supports malignancy, while intralesional cysts suggest benign lesions.

This study aims to analyze the demographic, clinical, and histological parameters of conjunctival cancers diagnosed at Erciyes University Ophthalmology Clinic, alongside lesion characteristics observed through high-resolution anterior segment OCT imaging. By examining patient age, gender, tumor coloration, location, size, and anterior segment OCT lesion images, the study seeks to identify predictive markers for malignancy and contribute to the existing body of knowledge in ocular oncology. The goal is to improve early detection and management strategies for conjunctival cancers, ultimately enhancing patient outcomes. A pragmatic analysis of these features within a tertiary care setting may help clarify which descriptors are most consistently observed and how they correlate with histopathological diagnosis and malignancy risk in real-world conditions.

MATERIALS AND METHODS

Study Design and Setting

This retrospective cohort study examined the demographics, clinical features, histological classifications, and anterior segment optical coherence tomography (AS-OCT) characteristics of conjunctival malignancies in the Ocular Oncology Division of Erciyes University Ophthalmology Clinic. The study included patients who visited the clinic during a 6-month period from August 2024 – June 2025. Anterior segment OCT imaging was performed using the ANTERION system (Heidelberg Engineering, Heidelberg, Germany), operated on the HEYEX platform. Since the lesions were confined to the conjunctival surface, internal fixation was not used. The imaging area, scan length, and

the number of cross-sectional B-scans were selected based on lesion size to ensure complete coverage of the lesion and its clinically relevant margins. To optimize image clarity while balancing rapid acquisition and minimizing motion-related degradation, B-scan averaging was set to ART=2. Images with inadequate quality due to motion or poor alignment were excluded from the analysis.

On AS-OCT, conjunctival lesions were systematically assessed for epithelial and subepithelial "signature" features to assist with the differential diagnosis of various ocular surface entities, including ocular surface squamous neoplasia (OSSN), conjunctival melanoma, conjunctival lymphoma/benign reactive lymphoid hyperplasia, primary acquired melanosis (PAM), conjunctival nevus, conjunctival papilloma, and other simulating lesions. Specifically, we documented: (i) epithelial thickness and epithelial reflectivity (e.g., thickened hyperreflective epithelium), (ii) the transition pattern between adjacent normal and abnormal epithelium (abrupt vs. gradual), and (iii) the presence of a distinct tissue plane/cleavage plane between the lesion and underlying tissue. Additional descriptors included internal reflectivity and homogeneity, intralesional cystic or hyporeflective spaces (indicative of benign melanocytic or papillomatous lesions), posterior optical shadowing (more prominent in heavily pigmented lesions), and subepithelial patterns such as a smooth, homogeneous hyporeflective mass with "dot-like" infiltrates (suggestive of lymphoproliferative lesions). These parameters were interpreted in conjunction with the slit-lamp examination and clinical context.[6-8]

The study adhered to the STROBE (Strengthening the Reporting of Observational Studies in Epidemiology) guidelines to ensure transparency and scientific rigor in observational research.[9] The study protocol was reviewed and approved by the Erciyes University Health Sciences Research Ethics Committee (Approval Number: 2025/365, Date: 09.07.2025).

Study Population

A retrospective review was conducted on 102 patients diagnosed with ocular oncology-related conditions, including orbital, intraocular, eyelid, and conjunctival cancers. From this group, 37 conjunctival malignancies were selected for examination.

Inclusion Criteria

- Patients diagnosed with conjunctival tumors during the study period.
- Histopathological confirmation of the conjunctival tumor diagnosis.
- Availability of comprehensive medical records.

Exclusion Criteria

- Patients diagnosed with other ocular oncology cancers, such as orbital, intraocular, or eyelid malignancies.
- Individuals with insufficient medical documentation.
- Patients with previously managed recurrent conjunctival neoplasms.
- Patients lost to follow-up before biopsy confirmation.

Data Collection Methods and Sources

Patient data were collected retrospectively from the following sources:

- Medical documentation: including clinical history and examination results.
- Pathology reports: for histopathological confirmation of tumor diagnosis.
- Anterior segment photos: used to characterize tumor attributes, including dimensions, color, and corneal involvement.
- Anterior segment optical coherence tomography (AS-OCT) images: to assess lesion reflectivity, homogeneity, the presence of intralesional cysts, and the abrupt transition zone in the lesion epithelium.

The data covered the period from August 2024, to June 2025. The following variables were documented:

• Demographics: Age, sex.

• Clinical Features:

  o Tumor pigmentation (classified as amelanotic or pigmented).

  o Tumor localization (bulbar, forniceal, palpebral, caruncle).

  o Corneal involvement (present or absent).

• Tumor Size: Measured in millimeters (mm) using slit-lamp biomicroscopy.

• Histopathological Diagnosis: Tumor categorization based on biopsy results.

• AS-OCT Characteristics:

  o Reflectivity of the lesion (hyporeflective or hyperreflective).

  o Homogeneity of the lesion (homogeneous/heterogeneous).

  o Presence of intralesional cysts (present or absent).

  o Abrupt transition zone in the lesion epithelium.

Statistical Analysis

Statistical analysis was performed using NCSS version 21. Descriptive statistics, including mean, standard deviation, frequency, and percentage distributions, were calculated for clinical and demographic data. The Shapiro–Wilk test was used to assess the normal distribution of continuous variables. Variables that exhibited a normal distribution were analyzed using parametric tests (independent t-test), while categorical variables were compared using the chi-square test. Statistical significance was defined as a p-value of less than 0.05.

RESULTS

Of the 37 conjunctival tumors examined in this study, 16 were malignant, and 21 were benign. Patients with malignant tumors were significantly older, with a mean age of 64.1±16.6 years ($p<0.01$), compared to 26.6±16.4 years for patients with benign tumors. The tumor types identified were conjunctival nevus (48.64%, n=18), ocular surface squamous neoplasia (27.02%, n=10), conjunctival lymphoma (10.81%, n=4), conjunctival melanoma (8.10%, n=3), and conjunctival cyst (5.40%, n=2) (Fig. 1).

Analysis of Tumor Size

Benign tumors had an average diameter of 6.4±5.4 mm, while malignant tumors had an average diameter of 12.7±8.4 mm. However, this difference was not statistically significant ($p=0.09$).

Tumor Characteristics

- Pigmentation: A statistically significant difference ($p<0.01$) was observed in the likelihood of malignancy between amelanotic tumors (93.75%, n=15) and pigmented tumors (6.25%, n=1) (Table 1).
- Location: Most tumors were located on the bulbar conjunctiva (78.37%, n=29), but no significant association between tumor location and malignancy was found ($p=0.27$) (Table 1).
- Corneal Involvement: Malignant tumors showed considerably higher rates of corneal involvement (56.25%, n=9) compared to benign tumors (4.76%, n=1) ($p<0.01$) (Table 1).
- AS-OCT Subepithelial Lesion Reflectivity: In malignant tumors, the lesion was significantly more hyporeflective (72.73%, n=8) ($p=0.01$) (Table 1, Fig. 2).
- AS-OCT Lesion Homogeneity: The lesion was significantly more homogeneous in malignant tumors (54.5%, n=6) compared to benign tumors (15.79%, n=3) ($p=0.02$) (Table 1, Fig. 2).

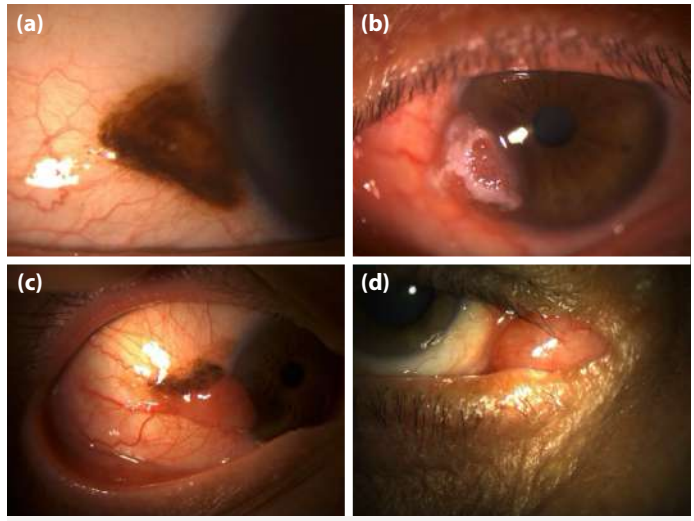

Figure 1. (a) Conjunctival nevus, **(b)** Conjunctival OSSN **(c)** Conjunctival melanoma, **(d)** Conjunctival lymphoma.

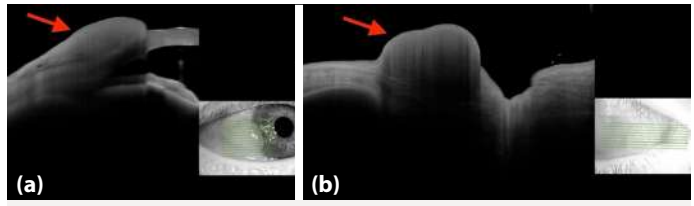

Figure 2. (a) Anterior segment OCT image of a hyperreflective, homogeneous lesion in a case of conjunctival melanoma (arrow), **(b)** Anterior segment OCT image of a hyporeflective, homogeneous lesion seen in conjunctival lymphoma (arrow) (note that the epithelium over the lesion is hyporeflective in both images).

- AS-OCT Intralesional Cyst: Although benign tumors (63.16%, n=12) contained more cysts than malignant tumors (27.27%, n=3), the difference was not statistically significant ($p=0.05$) (Table 1, Fig. 3, 4).
- AS-OCT Abrupt Transition Zone in the Lesion Epithelium: An abrupt transition from normal epithelium to hyperreflective, thickened epithelium was observed in 37.50% (n=3) of patients with ocular surface squamous neoplasia. However, since this finding was absent in other conjunctival tumor patients, statistical evaluation could not be performed (p=n/a) (Table 1).

In the anterior segment OCT examination, the distribution of subepithelial lesion reflectivity, lesion homogeneity, and the presence of intralesional cysts varied according to tumor types (Table 2).

Table 1. Distribution of benign vs. malignant lesion characteristics

Variables	Benign (n=21, 56.75%)	Malignant (n=16, 43.24%)	p
Age (years)	26.6 ± 16.4 (95% CI: 19.4-35.0)	64.1 ± 16.6 (95% CI: 50.9-71.5)	<0.01
Size (mm)	6.4 ± 5.4 (95% CI: 4.0-9.1)	12.7 ± 8.4 (95% CI: 7.7-16.5)	0.09
Gender (male/female)	11 (52.38%) / 10 (47.62%)	10 (62.50%) / 6 (37.50%)	0.53
Pigmentation (amelanotic/pigmented)	8 (38.10%) / 13 (61.90%)	15 (93.75%) / 1 (6.25%)	<0.01
Location			
Exclusively bulbar conj.	17 (80.95%)	12 (75.0%)	0.27
Bulbar conj. and caruncle	2 (9.52%)	1 (6.25%)	
Fornix and tarsus	1 (4.76%)	2 (12.50%)	
Fornix and caruncle	0	1 (6.25%)	
Plica	1 (4.76%)	0	
Corneal involvement (present/absent)	1 (4.76%) / 20 (95.24%)	9 (56.25%) / 7 (43.75%)	<0.01
AS-OCT subepithelial lesion reflectivity	5 (26.32%) / 14 (73.68%)	8 (72.73%) / 3 (27.27%)	0.01
AS-OCT lesion homogeneity (homogeneous/heterogeneous)	3 (15.79%) / 16 (84.2%)	6 (54.5%) / 5 (45.45%)	0.02
AS-OCT intralesional cyst (present / absent)	12 (63.16%) / 7 (36.84%)	3 (27.27%) / 8 (72.73%)	0.05
AS-OCT abrupt transition zone in the lesion epithelium	0 (0%) / 19 (100%)	3 (37.50%) / 8 (62.50%)	n/a

AS-OCT: Anterior segment optical coherence tomography. The first number in each cell indicates the number of patients, while the percentage indicates the proportion of patients.

Table 2. AS-OCT characteristics of conjunctival tumors

Variables	Conj. lymphoma	Conj. MM	Conj. nevus	Conj. OSSN	Conj. Cyst
AS-OCT subepithelial lesion reflectivity (hyporeflective/hyperreflective)	3 (100%) / 0	0 / 1 (100%)	2 (12.5%) / 14 (87.5%)	5 (62.5%) / 3 (37.5%)	2 (100%) / 0
AS-OCT lesion homogeneity (homogeneous/heterogeneous)	3 (100%) / 0	1 (100%) / 0	1 (6.25%) / 15 (93.75%)	3 (37.5%) / 5 (62.5%)	1 (50%) / 1 (50%)
AS-OCT intralesional cyst (present/absent)	0 / 3 (100%)	0 / 1 (100%)	10 (62.5%) / 6 (37.5%)	3 (37.5%) / 5 (62.5%)	2 (100%) / 0
AS-OCT abrupt transition zone in the lesion epithelium (present/absent)	0 / 3 (100%)	0 / 1 (100%)	0 / 16 (100%)	3 (37.5%) / 5 (62.5%)	0 / 2 (100%)

AS-OCT: Anterior segment optical coherence tomography; Conj. lymphoma: Conjunctival lymphoma; Conj. MM: Conjunctival malignant melanoma; Conj. OSSN: Conjunctival ocular surface squamous neoplasia; Conj. Cyst: Conjunctival cyst.

DISCUSSION

A precise clinical and histological assessment is essential for the diagnosis and treatment of conjunctival tumors, which encompass a diverse range of lesions. Malignant conjunctival tumors were significantly associated with corneal involvement, amelanotic pigmentation, and advanced age. In the anterior segment OCT examination, malignant tumors showed a notable association with a hyporeflective, homogeneous lesion appearance and were absent of cysts. Although larger lesion diameters were not statistically significant, they tended to be more common in malignant tumors.

As individuals age, their risk of developing a malignant conjunctival tumor increases. Conjunctival tumors in adolescents and young adults are almost always benign, with malignancies being rare. The average age at which benign tumors are discovered is approximately 11 years, while malignant tumors are typically identified at an average age of 14 years. This suggests that the likelihood of malignancy

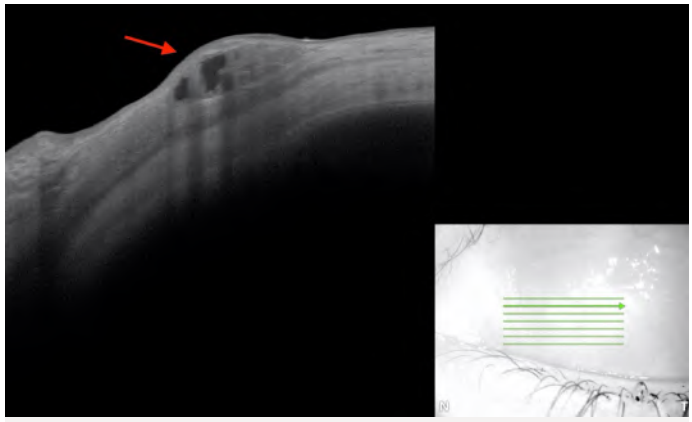

Figure 3. Anterior segment OCT image of a case of conjunctival nevus showing lesion heterogeneity, including cyst formations within the lesion.

increases slightly with age.[10] Although malignant tumors remain uncommon in young adults, benign tumors such as nevi are more frequent.[11]

Malignant conjunctival tumors are far more prevalent in middle-aged and older individuals, with the risk of developing cancer increasing substantially after the age of 40.[10-12] Ocular surface squamous neoplasia, in particular, is common in individuals over 60 years, often presenting with larger and more aggressive lesions compared to benign tumors.[10,13] Conjunctival melanoma is also more frequently diagnosed in older patients,[12,14,15] with a higher risk of recurrence and visual acuity loss.[14,16] Lymphoid lesions, including lymphoma, are more common in older adults and tend to present with larger tumor sizes and diffuse involvement.[11,17] Additionally, malignant conjunctival tumors, particularly ocular surface squamous neoplasia and melanoma, are more frequently observed in males than females.[10,13,18]

Studies have shown that conjunctival melanomas with low pigmentation are associated with a worse prognosis. Specifically, low tumor pigmentation is linked to higher risks of metastasis and death. This association is particularly significant in primary conjunctival melanomas, where low pigmentation correlates with increased metastasis and mortality rates.[19]

Malignant conjunctival tumors, such as melanoma and ocular surface squamous neoplasia, typically exhibit larger basal diameters and thicknesses compared to benign lesions, with a median basal diameter of 8 mm.[1] In conjunctival nevi, a larger basal tumor diameter has been statistically associated with an increased likelihood of surgical excision due to concerns about malignant transformation, although histopathological malignancy was not observed in excised cases.[17]

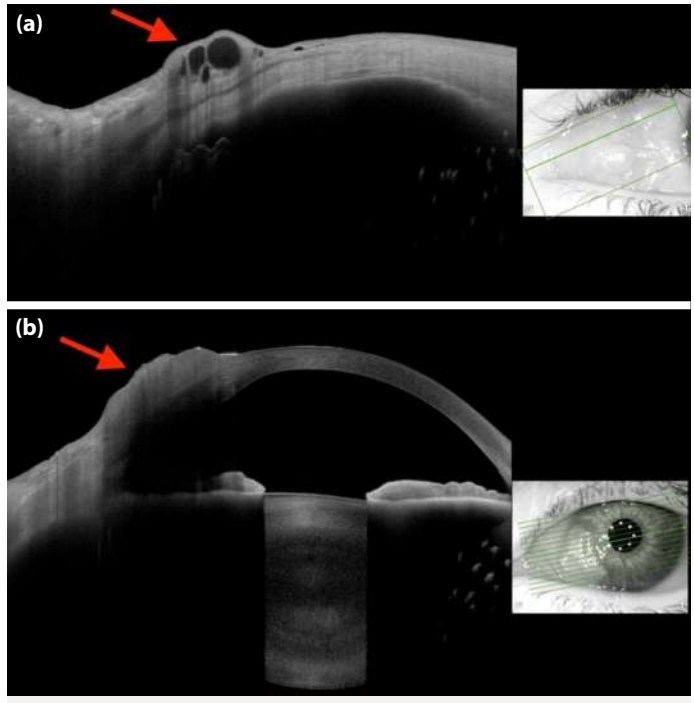

Figure 4. (a) Anterior segment OCT image showing intralesional cysts in a case of conjunctival nevus (arrow), **(b)** Anterior segment OCT image of a case of conjunctival SCC with corneal involvement and hyperreflective epithelium (arrow).

Corneal involvement plays a crucial role in the management of conjunctival tumors. Malignant lesions, including conjunctival squamous intraepithelial neoplasia (CSIN), can exhibit corneal growth, complicating their clinical presentation and necessitating thorough diagnostic evaluation.[1] Similarly, conjunctival melanomas can invade the cornea, sometimes without other conjunctival involvement, emphasizing the need for precise surgical intervention to minimize the risk of recurrence.[20]

Anterior segment optical coherence tomography (AS-OCT) is useful for clearly imaging conjunctival nevi, delineating the lesion's boundaries, and identifying cysts within the lesion. However, a challenge with AS-OCT is the potential for visual ghosting in colored nevi.[22] Shousha et al.[21] demonstrated thicker hyperreflective epithelium and a sudden transition from normal to hyperreflective epithelium in AS-OCT assessments of conjunctival and corneal intraepithelial neoplasia (CCIN) cases. Kieval et al.[22] observed significantly thicker epithelium in cases of epithelial ocular surface squamous neoplasia compared to pterygium when epithelial thickness measured using AS-OCT was compared. Shousha et al.[23] also showed that AS-OCT images offer valuable diagnostic insights when the clinical diagnosis of ocular surface lesions is unclear.

To diagnose corneal and conjunctival disorders, particularly malignant lesions, Nanji et al.[7] investigated the use of high-resolution, spectral-domain optical coherence tomography (HR-OCT). Their study of 82 lesions indicated that HR-OCT can be used to evaluate treatment efficacy, determine the cause of certain ocular surface lesions (such as melanoma, pterygium, nevus, and ocular surface squamous neoplasia), and more. However, pigmented lesions were not as well assessed using this imaging technique. Ocular surface pathology can be identified, and disease resolution can be evaluated with this technology, making it a valuable adjunct to clinical examination and histological diagnosis. A literature review by Janssens et al.[24] demonstrated that AS-OCT and ultrasound biomicroscopy (UBM) are highly effective and complementary modalities for assessing and monitoring corneal and conjunctival tumors, though they cannot replace histological investigation for diagnostic purposes. One drawback of AS-OCT is its limited ability to penetrate pigmented lesions or reach deeper than 1–3 mm. However, AS-OCT offers a more precise technique for small lesions by providing detailed images of the intact cornea, identifying cysts, and aiding in the detection of tumor recurrence. For larger or pigmented lesions, ultrasound biomicroscopy (UBM) provides a more accurate way to assess tumor thickness and define tumor borders.

Venkateswaran et al.[25] demonstrated that high-resolution optical coherence tomography (HR-OCT) can reliably differentiate between epithelial ocular surface tumors, such as ocular surface squamous neoplasia (OSSN), and subepithelial tumors, including conjunctival lymphoma and conjunctival melanoma, in a clinical context. Karp et al.[26] utilized AS-OCT in the surgical treatment of OSSN and showed that the conjunctival tumor margin identified by HR-OCT matched the pathologically confirmed margin in all cases. The high-resolution OCT images of conjunctival lymphoma in Venkateswaran et al.'s[27] research revealed homogeneous, black subepithelial lesions with smooth edges, typically exhibiting monomorphic dot-like infiltrates. These findings provide a foundation for promising areas of future research and potential updates to clinical guidelines.

One of the main barriers to the clinical adoption of AS-OCT as a definitive diagnostic tool is the lack of standardized terminology and reporting protocols.[28] The ongoing development of the Advised Protocol for OCT Study Terminology and Elements for the Anterior Segment (APOSTEL-AS) aims to create a consensus nomenclature. Future studies should use this standardized framework to ensure that findings across different institutions and imaging platforms are comparable. This would facilitate the creation of large, multicenter registries to overcome the sample size limitations of current single-center research.[28]

The application of artificial intelligence (AI) and machine learning (ML) to AS-OCT image analysis represents a frontier with immense potential. Future diagnostic protocols could incorporate AI models trained to automatically segment lesions, measure epithelial thickness with micron-scale precision, and classify internal reflectivity patterns.[29] AS-OCT is increasingly being used intraoperatively to ensure that surgical margins are free of sub-clinical disease. Research has shown that margins identified by high-resolution OCT often coincide with pathologically verified margins, which can reduce the need for repeat surgeries and lower the rate of local recurrence in aggressive malignancies like melanoma and invasive squamous cell carcinoma (SCC). Integrating intraoperative OCT into standardized surgical protocols for ocular surface tumors would represent a significant step toward improving patient outcomes and preserving healthy ocular tissue.[30]

Future protocols may involve a dual-modality approach, using structural AS-OCT to evaluate lesion depth and internal homogeneity, while OCT Angiography (OCTA) assesses metabolic activity and aggressive potential based on vessel density. The transition from a "biopsy-centric" to an "imaging-centric" management model is a key area for development. Future clinical guidelines could leverage AS-OCT for the objective monitoring of treatment response in medically managed OSSN.

This research has several limitations. The retrospective design introduces potential biases associated with incomplete or absent data. The small sample size (37 cases) limits statistical power and generalizability. Additionally, as a single-center study, the findings may not be applicable to broader populations. Another limitation is the absence of conjunctival intraepithelial neoplasia (CIN) cases in our cohort. This likely reflects institutional treatment practices and selection bias rather than a true absence of CIN in the population. At our center, clinically suspected CIN or early ocular surface squamous neoplasia cases are often managed with topical chemotherapeutic agents rather than primary excisional biopsy and histopathological confirmation. As a result, our study population is skewed toward more advanced, invasive, or clinically ambiguous lesions that required surgical intervention, potentially overestimating the prevalence of invasive squamous cell carcinoma (SCC) within the ocular surface squamous neoplasia (OSSN) spectrum. Consequently, such cases may be underrepresented in pathology-based retrospective surgical series. Furthermore, by including only histopathologically confirmed surgical cases, our study does not fully represent the entire spectrum of ocular surface tumors, limiting the generalizability of the results. The single-center design and relatively small sample size also restrict the applicability of our findings regarding tumor distribution

patterns. Only histopathologically confirmed tumors were included, potentially excluding clinically diagnosed cases. The study also lacks long-term follow-up, preventing an assessment of recurrence and metastasis rates. More comprehensive and multicenter studies are needed to establish a consensus on the use of next-generation diagnostic tools in managing conjunctival tumors.

CONCLUSION

This study provides valuable insights into the demographic, clinical, histopathological types, and anterior segment optical coherence tomography (AS-OCT) features of conjunctival tumors in a tertiary care hospital. Our findings indicate that malignant tumors are associated with several factors, including older age, amelanotic pigmentation, larger lesion diameters, and the presence of corneal involvement. Additionally, the presence of homogeneous and hyporeflective lesions on AS-OCT suggests the potential diagnostic value of this technology in the context of ocular malignancies. These findings highlight the importance of early and detailed clinical evaluations to improve the detection and management of conjunctival malignancies.

Key predictors of malignancy, such as amelanotic pigmentation and corneal involvement, should be considered critical red flags during clinical assessments. The observed trend of larger lesion diameters in malignant cases further emphasizes the need for heightened vigilance when encountering large conjunctival tumors. By promptly identifying and addressing these risk factors, clinicians can enhance patient outcomes and potentially reduce the morbidity associated with malignant conjunctival lesions.

For clinicians, the primary takeaway is the importance of a multimodal approach. While AS-OCT serves as an exceptional tool for identifying high-risk structural features, it cannot yet replace histopathology, especially in thick or pigmented lesions where shadowing limits posterior visualization. The future of the field lies in the refinement of these non-invasive "optical biopsies" through standardization, artificial intelligence, and vascular biomarkers. By integrating these advanced tools into clinical practice, the ophthalmological community can move toward a more precise, individualized approach to the diagnosis and management of conjunctival malignancies, ultimately improving both visual outcomes and patient survival.

Ethics Committee Approval: Ethics committee approval was obtained from Erciyes University Health Sciences Research Ethics Committee (Approval Number: 2025/365, Date: 09.07.2025).

Informed Consent: Written informed consent was not required due to the retrospective nature of this study.

Conflict of Interest: The authors have no conflicts of interest to declare.

Funding: The authors declared that this study received no financial support.

Use of AI for Writing Assistance: No use of AI-assisted technologies was declared by the authors.

Author Contributions: Concept – OO, FH, HS, FÖ; Design – OO, FH, HS, FÖ; Supervision – OO, FH, HS, FÖ; Resource – OO, HS; Materials – OO, HS; Data Collection and/or Processing – OO, FH, HS, FÖ; Analysis and/or Interpretation – OO, FH, HS, FÖ; Literature Review – OO, FH, HS, FÖ; Writing – OO, FH, HS, FÖ; Critical Review – OO, FH, HS, FÖ.

Peer-review: Externally peer-reviewed.

REFERENCES

1. Shields CL, Shields JA. Tumors of the conjunctiva and cornea. Surv Ophthalmol 2004;49(1):3-24. [CrossRef]
2. Mirzayev I, Gündüz AK, Gündüz ÖÖ, Özalp Ateş FS, Nalcı Baytaroğlu H. Demographic and clinical features of conjunctival tumours at a tertiary care centre. Clin Exp Optom 2022;105(7):708-14. [CrossRef]
3. Koç İ, Kapucu Y, Kıratlı H. Clinical Features and Treatment Results of Conjunctival Melanoma: Cross-Sectional Study. Acta Medica 2023;54(1):54-8. [CrossRef]
4. Esmaeli B, Gleber-Netto F, Sagiv O, Pickering C, Gross N, Ning J, et al. Abstract 2501: High mutation burden and ultraviolet light signature in conjunctival squamous cell carcinoma. Cancer Res 2024;84(6_Supplement):2501. [CrossRef]
5. Shields CL, Alset AE, Boal NS, Casey MG, Knapp AN, Sugarman JA, et al. Conjunctival Tumors in 5002 Cases. Comparative Analysis of Benign Versus Malignant Counterparts. The 2016 James D. Allen Lecture. Am J Ophthalmol 2017;173:106-33. [CrossRef]
6. Gündüz AK, Mirzayev I, Okcu Heper A, Kuzu I, Gahramanli Z, Cansiz Ersöz C, et al. Anterior segment optical coherence tomography in ocular surface tumours and simulating lesions. Eye (Lond) 2023;37(5):925-37. Erratum in: Eye (Lond) 2023;37(5):1045. Erratum in: Eye (Lond) 2023;37(16):3517-8. [CrossRef]
7. Nanji AA, Sayyad FE, Galor A, Dubovy S, Karp CL. High-Resolution Optical Coherence Tomography as an Adjunctive Tool in the Diagnosis of Corneal and Conjunctival Pathology. Ocul Surf 2015;13(3):226-35. [CrossRef]
8. Gündüz AK, Mirzayev I, Ersöz CC, Heper AO, Gündüz Ö, Ateş FSÖ. Anterior Segment Swept-Source Optical Coherence Tomography in Ocular Surface Tumors and Simulating Lesions and Correlation with Histopathologic Diagnosis. Cornea 2025;44(7):806-18. [CrossRef]

9. Vandenbroucke JP, von Elm E, Altman DG, Gøtzsche PC, Mulrow CD, Pocock SJ, et al.; STROBE Initiative. Strengthening the Reporting of Observational Studies in Epidemiology (STROBE): explanation and elaboration. Epidemiology 2007;18(6):805-35. [CrossRef]
10. Pellerano F, Gil G, Rosario A, Mañon N, Vargas T, Vizcaíno G. Survey of 138 Conjunctival Tumors in the Dominican Republic. Ophthalmic Epidemiol 2020;27(4):278-82. [CrossRef]
11. He LF, Tang SY, Wang YJ, Zhang Y, Huang SM, Huang XJ. Incidence, clinical features, and survival outcomes of primary malignant conjunctival tumor: a US population-based retrospective cohort analysis based on the SEER database (1975-2018). Transl Cancer Res 2025;14(3):1609-25. [CrossRef]
12. Besteiro AVM, de Castro Leao RF, da Trindade Junior CJS, Fernandes ACM, Xavier TC, Lima VHA. Epidemiological Profile of Patients with Conjuntival Tumors in a Reference Ophthalmological Hospital in Eastern Amazonia. BJHR 2023;6(1):4257-79. Portuguese. [CrossRef]
13. Grossniklaus HE, Green WR, Luckenbach M, Chan CC. Conjunctival lesions in adults. A clinical and histopathologic review. Cornea 1987;6(2):78-116. [CrossRef]
14. Dalvin LA, Yaghy A, Vaidya S, Pacheco RR, Perez AL, Lally SE, et al. Conjunctival Melanoma: Outcomes Based on Age at Presentation in 629 Patients at a Single Ocular Oncology Center. Cornea 2021;40(5):554-63. [CrossRef]
15. Paridaens AD, Minassian DC, McCartney AC, Hungerford JL. Prognostic factors in primary malignant melanoma of the conjunctiva: a clinicopathological study of 256 cases. Br J Ophthalmol 1994;78(4):252-9. [CrossRef]
16. García Onrubia L, Pacheco-Callirgos GE, Portero-Benito A, García-Álvarez C, Carreño Salas E, Muñoz-Moreno MF, et al. Spectrum of conjunctival tumours in a Spanish series: A review of 462 cases. Eur J Ophthalmol 2020;30(6):1403-9. [CrossRef]
17. Shields CL, Sioufi K, Alset AE, Boal NS, Casey MG, Knapp AN, et al. Clinical Features Differentiating Benign From Malignant Conjunctival Tumors in Children. JAMA Ophthalmol 2017;135(3):215-24. [CrossRef]
18. Brouwer NJ, Marinkovic M, Luyten GPM, Shields CL, Jager MJ. Lack of tumour pigmentation in conjunctival melanoma is associated with light iris colour and worse prognosis. Br J Ophthalmol 2019;103(3):332-7. [CrossRef]
19. Levecq L, De Potter P, Jamart J. Conjunctival nevi clinical features and therapeutic outcomes. Ophthalmology 2010;117(1):35-40. [CrossRef]
20. Shields CL, Belinsky I, Romanelli-Gobbi M, Guzman JM, Mazzuca D Jr, Green WR, et al. Anterior segment optical coherence tomography of conjunctival nevus. Ophthalmology 2011;118(5):915-9. [CrossRef]
21. Shousha MA, Karp CL, Perez VL, Hoffmann R, Ventura R, Chang V, et al. Diagnosis and management of conjunctival and corneal intraepithelial neoplasia using ultra high-resolution optical coherence tomography. Ophthalmology 2011;118(8):1531-7. [CrossRef]
22. Kieval JZ, Karp CL, Abou Shousha M, Galor A, Hoffman RA, Dubovy SR, et al.Ultra-high resolution optical coherence tomography for differentiation of ocular surface squamous neoplasia and pterygia. Ophthalmology 2012;119(3):481-6. [CrossRef]
23. Shousha MA, Karp CL, Canto AP, Hodson K, Oellers P, Kao AA, et al. Diagnosis of ocular surface lesions using ultra-high-resolution optical coherence tomography. Ophthalmology 2013;120(5):883-91. [CrossRef]
24. Janssens K, Mertens M, Lauwers N, de Keizer RJ, Mathysen DG, De Groot V. To Study and Determine the Role of Anterior Segment Optical Coherence Tomography and Ultrasound Biomicroscopy in Corneal and Conjunctival Tumors. J Ophthalmol 2016;2016:1048760. [CrossRef]
25. Venkateswaran N, Sripawadkul W, Karp CL. The role of imaging technologies for ocular surface tumors. Curr Opin Ophthalmol 2021;32(4):369-78. [CrossRef]
26. Karp CL, Mercado C, Venkateswaran N, Ruggeri M, Galor A, Garcia A, et al. Use of High-Resolution Optical Coherence Tomography in the Surgical Management of Ocular Surface Squamous Neoplasia: A Pilot Study. Am J Ophthalmol 2019;206:17-31. [CrossRef]
27. Venkateswaran N, Mercado C, Tran AQ, Garcia A, Diaz PFM, Dubovy SR, et al. The use of high resolution anterior segment optical coherence tomography for the characterization of conjunctival lymphoma, conjunctival amyloidosis and benign reactive lymphoid hyperplasia. Eye Vis (Lond) 2019;6:17. [CrossRef]
28. Solebo AL, Ang M, Bellchambers A, Chu CJ, Denniston AK, Downie LE, et al. Development of the advised protocol for OCT study terminology and elements anterior segment OCT extension reporting guidelines (APOSTEL-AS): Study protocol. PLoS One 2025;20(11):e0331272. [CrossRef]
29. Enaholo E, Okoye G, Musa M, Suleman A, Ojo O, Foti R, et al. High-resolution optical coherence tomography for screening ocular surface tumors: Historical markers and future directions. World J Clin Cases 2025;13(29):108046. [CrossRef]
30. Rajagopal R, Vijayaraghavan M, Jothi Balaji J, Jayavel K. Anterior segment optical coherence tomography in conjunctival ocular surface disorders - A review. Indian J Ophthalmol 2025;73(4):543-52. [CrossRef]

Official Journal of Erciyes University Faculty of Medicine

DOI: 10.14744/cpr.2026.07992
J Clin Pract Res 2026;48(2):162–168

Do Sexually Transmitted Infections Coexist? Evidence from Human Immunodeficiency Virus and Syphilis Coinfection in a Tertiary Care Center

Kübra Fırtına Topcu,[1] Resul Ekrem Akbulut[1]

[1]Department of Microbiology, Sivas Cumhuriyet University, Faculty of Medicine, Sivas, Türkiye

ABSTRACT

Objective: Syphilis and human immunodeficiency virus (HIV) are sexually transmitted infections that share common risk factors and may facilitate each other's transmission. This study aimed to evaluate the frequency of syphilis coinfection among individuals living with HIV over a five-year period.

Materials and Methods: In this retrospective study, anti-HIV, rapid plasma reagin (RPR), *Treponema pallidum* hemagglutination assay (TPHA), *Treponema pallidum* total immunoglobulin, and HIV confirmatory test results of individuals aged ≥18 years were evaluated between 2020 and 2024. Patients who had both HIV- and syphilis-related tests during the period of HIV positivity were included. Syphilis seropositivity was defined according to the institutional diagnostic algorithm based on the combination of treponemal and non-treponemal tests. Active infection was defined as concurrent positivity of treponemal and RPR tests, whereas isolated treponemal positivity was considered a past infection.

Results: Among 200 individuals living with HIV, 162 underwent syphilis testing. Of these, 85.5% were male. Syphilis seropositivity was detected in 41 patients (25.3%), including 24 (14.8%) with active infection and 17 (10.5%) with past infection. No significant differences were observed based on age, sex, or year ($p>0.05$). During the same period, syphilis seropositivity among HIV-negative individuals was 0.96%. HIV positivity was strongly associated with syphilis seropositivity (OR: 34.8; 95% CI: 23.1–52.6; $p<0.001$).

Conclusion: The high rate of syphilis seropositivity among HIV-positive individuals underscores the importance of routine screening at diagnosis and during follow-up.

Keywords: Coinfection, human immunodeficiency virus, rapid plasma reagin, seropositivity, syphilis.

Cite this article as:
Fırtına Topcu K, Akbulut RE. Do Sexually Transmitted Infections Coexist? Evidence from Human Immunodeficiency Virus and Syphilis Coinfection in a Tertiary Care Center. J Clin Pract Res 2026;48(2):162–168.

Address for correspondence:
Kübra Fırtına Topcu.
Department of Microbiology, Sivas Cumhuriyet University, Faculty of Medicine, Sivas, Türkiye
Phone: +90 505 554 41 12
E-mail: drkubrafirtina@gmail.com

Submitted: 21.01.2026
Revised: 06.03.2026
Accepted: 16.04.2026
Available Online: 30.04.2026

Erciyes University Faculty of Medicine Publications - Available online at www.jcpres.com

INTRODUCTION

Syphilis is a sexually transmitted disease caused by *Treponema pallidum* that can lead to multisystem involvement and serious health problems.[1] Human immunodeficiency virus (HIV) infection is also a sexually transmitted disease and results in a chronic condition characterized by acquired immunodeficiency syndrome (AIDS), which is associated with immunosuppression and the development of opportunistic infections.[2]

Sexually transmitted infections (STIs) are highly prevalent among sexually active individuals and may progress silently, facilitating their spread within the community.[3]

Syphilis and HIV are two systemic sexually transmitted infections that share common risk factors. The World Health Organization (WHO) estimates that there were 7.1 million new syphilis cases worldwide in 2020.[4] According to UNAIDS 2024 data, an estimated 40.8 million people worldwide were living with HIV in 2024, with 1.3 million new infections and approximately 630,000 AIDS-related deaths reported during the same period.[5]

There is a bidirectional epidemiological and biological interaction between these two infections. First, HIV infection may increase the risk of syphilis transmission by weakening the immune system. Conversely, syphilis causes mucosal damage, and syphilitic ulcers provide a portal of entry for HIV, potentially increasing the risk of HIV transmission by approximately twofold. Syphilitic lesions lead to the recruitment of activated immune cells, including macrophages and $CD4^+$ T lymphocytes, to the site of infection, thereby increasing the number of HIV target cells and facilitating HIV acquisition and transmission.[6] All of these interactions make HIV and syphilis coinfection a significant public health concern.[1,7,8]

The aim of this study was to evaluate the frequency of syphilis coinfection among HIV-positive individuals followed at a tertiary care hospital over a five-year period.

KEY MESSAGES

- Syphilis seropositivity was significantly higher among individuals living with HIV compared to HIV-negative individuals, indicating a strong epidemiological association between the two infections.
- Routine and systematic syphilis screening for individuals living with HIV is essential, as coinfection may remain undetected without regular testing at the time of diagnosis and during follow-up.
- Observed differences in HIV/syphilis coinfection rates are influenced by screening practices and population characteristics, emphasizing the need for standardized screening strategies and multicenter data to guide clinical and public health interventions.

MATERIALS AND METHODS

Study Design and Setting

This retrospective, observational, single-center study was conducted in the microbiology laboratory of Sivas Cumhuriyet University Hospital between January 1, 2020, and December 31, 2024. This date range was selected to ensure more complete access to patient data from the hospital system. The study protocol was designed to evaluate syphilis coinfection among HIV-positive individuals aged 18 years and older.

Participants and Data Collection

The study included unique HIV-positive patients who had both HIV-related and syphilis-related serological test results during the period of confirmed HIV positivity. Anti-HIV, rapid plasma reagin (RPR), *Treponema pallidum* hemagglutination assay (TPHA), *Treponema pallidum* total immunoglobulin, and HIV confirmatory test results were retrospectively collected from laboratory records. Cases without documented syphilis testing were excluded from the primary analyses.

Diagnostic Criteria

HIV positivity was defined based on confirmatory testing according to the standard protocols of the General Directorate of Public Health. Syphilis seropositivity was determined by serological testing, including RPR, TPHA, and *T. pallidum* total immunoglobulin results. A TPHA titer of ≥1/80 was considered positive. Syphilis seropositivity was defined as reactivity in at least one treponemal test, and infection status was classified based on the combination of treponemal and non-treponemal results. Cases with reactive treponemal tests (TPHA and/or *T. pallidum* total immunoglobulin) and non-reactive RPR were interpreted as consistent with past or previously treated infection. Concurrent positivity of treponemal and RPR tests was classified as active infection. The term "syphilis seropositivity" encompassed both active and past infections based on the combined interpretation of treponemal and non-treponemal test results.

Inclusion and Exclusion Criteria

Inclusion criteria encompassed all individuals aged ≥18 years with confirmed HIV infection and available syphilis serological test results during the study period. Patients with only a single visit and no subsequent syphilis testing were excluded from the comparative analysis.

Laboratory Methods

Anti-HIV and *T. pallidum* total immunoglobulin tests were performed using enzyme-linked immunosorbent assay (ELISA). The tests were conducted on the Roche cobas 6000 device (Roche Diagnostics, Switzerland) between 2020 and 2022, and on the Architect i2000 device (Abbott Diagnostics, Illinois, USA) between 2023 and 2024. RPR testing was performed using agglutination-based flocculation methods, and TPHA testing was carried out using hemagglutination techniques. The RPR test was performed with Plasmatec test kits from the UK between 2020 and 2022, and with Carbogen and Tulip Diagnostic test kits from India between 2023 and

2024. Omega Diagnostics (UK) and Dialab (Austria) branded kits were used for the TPHA test during the study years. All assays were interpreted according to the manufacturers' instructions.

Syphilis Testing Algorithms

Syphilis serological results were evaluated using both the conventional algorithm (non-treponemal testing followed by treponemal confirmation) and the reverse algorithm (treponemal testing followed by non-treponemal confirmation), depending on the laboratory's available testing strategy. RPR was considered a non-treponemal test, whereas TPHA and *T. pallidum* total immunoglobulin were considered treponemal tests. The use of both algorithms reflected temporal changes in testing strategy and kit availability during the five-year study period. Regardless of the initial screening method, final interpretation was based on the combined assessment of treponemal and non-treponemal test results.

Individuals living with HIV were screened for syphilis as recommended in the HIV-AIDS diagnosis and treatment guidelines of the Ministry of Health of the Republic of Türkiye.[9] When HIV positivity was detected, initial screening for syphilis was performed. If the individual remained at risk, periodic screening (generally once a year) was conducted thereafter. In individuals with multiple partners, a history of unprotected sexual intercourse, those who engage in sex while using drugs, or those with a partner exhibiting these behaviors, screening was performed more frequently (every 3-6 months).

Statistical Analysis

Statistical analyses were conducted using IBM SPSS Statistics for Windows, Version 23.0 (IBM Corp., Armonk, NY, USA). Continuous variables were assessed for normality using the Shapiro–Wilk test. Variables that did not follow a normal distribution were presented as medians with interquartile ranges (IQR), while categorical variables were expressed as counts (n) and percentages (%). Associations between categorical variables were evaluated using the chi-square test or Fisher's Exact Test, as appropriate. Odds ratios (ORs) with 95% confidence intervals (CIs) were calculated to assess the association between HIV status and syphilis seropositivity. A p-value<0.05 was considered statistically significant.

Ethical Approval

Ethics approval for this study was obtained from the Sivas Cumhuriyet University Health Sciences Research Ethics Committee (Approval Number: 2025-11/41, Date: 20.11.2025). The study was conducted in accordance with the principles of the Declaration of Helsinki. Due to the retrospective design of the study, the requirement for informed consent was waived.

Table 1. Distribution of syphilis seropositivity by age group and sex among individuals living with HIV (n=162)

Variable	Syphilis positive n (%)	Syphilis negative n (%)	Total	p
Age group				0.766*
18–24	4 (26.7)	11 (73.3)	15	
25–44	21 (23.1)	70 (76.9)	91	
≥45	16 (28.6)	40 (71.4)	56	
Sex				0.176**
Male	38 (27.1)	102 (72.9)	140	
Female	3 (13.6)	19 (86.4)	22	
Total	41 (25.3)	121 (74.7)	162	

*: Fisher's Exact test; **: Pearson Chi-square test.

RESULTS

During the study period, a total of 226,228 anti-HIV tests were performed in the laboratory, and HIV positivity was confirmed by confirmatory tests in 200 distinct individuals (0.09%). Of these individuals, 171 were male (85.5%) and 29 were female (14.5%). The median age of the study population was 38 years (IQR: 29–48.8).

Of the 200 individuals identified as HIV-positive, 162 (81%) underwent syphilis screening during follow-up in accordance with the HIV-AIDS diagnosis and treatment guidelines after their HIV-positive status was confirmed. The remaining 38 individuals, who were not screened for syphilis, had only a single visit to our hospital during which HIV positivity was detected and did not return thereafter.

Among the 162 individuals who underwent syphilis screening, syphilis seropositivity was detected in 41 patients (25.3%). There was no statistically significant difference in syphilis positivity based on sex (p=0.176) or age group (18–24, 25–44, and ≥45 years) (p=0.766). Among HIV-positive individuals who underwent syphilis serological testing (n=162), no significant difference in syphilis seropositivity was observed across the study years (Fisher's Exact Test, p=0.740). The analysis of a linear trend across years did not demonstrate a significant increase or decrease in syphilis seropositivity (Chi-square test for trend, p=0.764). The relevant data are presented in Tables 1 and 2. The distribution of disease activity status according to the serological results of individuals screened for syphilis is shown in Table 3.

During the same study period, a total of 9,393 non-duplicated patients who underwent both HIV and syphilis testing were

Table 2. Syphilis seropositivity by year (n=162)

Year	Positive, n (%)	Negative, n (%)	Positivity rate (%)
2020	16 (26.2)	45 (73.8)	26.2
2021	8 (25.8)	23 (74.2)	25.8
2022	9 (19.6)	37 (80.4)	19.6
2023	3 (30.0)	7 (70.0)	30.0
2024	5 (35.7)	9 (64.3)	35.7
Total	41 (25.3)	121 (74.7)	25.3

This table includes HIV-positive individuals who underwent serological testing for syphilis (n=162). No statistically significant difference in syphilis seropositivity was detected across years (p>0.05). The p-value was calculated using Fisher's Exact Test. A chi-square test for trend (linear-by-linear association) was performed to evaluate temporal trends.

Table 3. Disease activity according to serological results in individuals living with HIV who underwent syphilis screening

Serological status (n=162)	n (%)
Syphilis positive	41
Active infection	24 (14.8)
Previous infection	17 (10.5)
Syphilis negative	121 (74.7)

HIV: Human immunodeficiency virus.

Table 4. Results of patients tested simultaneously for HIV and syphilis

Group	Syphilis positive n (%)	Syphilis negative n (%)
HIV positive	41 (25.3)	121 (74.7)
HIV negative	89 (0.96)	9,142 (99.04)

Chi-square test: p<0.001; Odds ratio (OR)=34.8 (95% CI: 23.1–52.6); HIV: Human immunodeficiency virus.

evaluated. Of these patients, 162 were HIV-positive, and syphilis seropositivity was detected in 41 of them (25.3%). Among the 9,231 HIV-negative patients, syphilis seropositivity was identified in 89 individuals (0.96%). Syphilis seropositivity was significantly higher in individuals living with HIV compared to HIV-negative individuals (Chi-square test, p<0.001). An approximately 35-fold increased association was observed between HIV positivity and syphilis seropositivity (OR: 34.8; 95% CI: 23.1–52.6). The relevant data are shown in Table 4.

A binary logistic regression analysis was performed to evaluate potential independent predictors of syphilis seropositivity. Age and sex were included as independent variables in the model. Neither age (OR: 0.99; 95% CI: 0.96–1.02; p=0.390) nor sex (OR: 2.48; 95% CI: 0.69–8.91; p=0.165) was independently associated with syphilis seropositivity. The results of the logistic regression analysis are presented in Table 5.

Table 5. Binary logistic regression analysis of factors associated with syphilis seropositivity

Variable	OR	95% CI	p
Age (per year increase)	0.99	0.96–1.02	0.390
Male (vs female)	2.48	0.69–8.91	0.165

OR: Odds ratio; CI: Confidence interval.

Table 6. Studies investigating HIV/syphilis coinfection in Türkiye

Study	Study period	HIV-positive individuals (n)	Syphilis coinfected individuals n (%)
Yağcı Çağlayık et al.[23]	1985–2024	1,042	259 (24.9)
Korkusuz et al. [17]	2015–2019	1,057	194 (18.3)
Sarıgül et al.[21]	2015–2018	384	97 (25)
Arıcı et al.[16]	2015–2023	284	103 (36.2)
Öztürk[18]	2016–2020	201	47 (23.3)
Alıravcı et al.[24]	2018–2024	142	26 (18.3)
Şahin et al.[25]	2019–2022	44	11 (25)
Present study	2020–2024	162	41 (25.3)

HIV: Human immunodeficiency virus.

An evaluation of the syphilis diagnostic algorithms used during the study period revealed that 65 results (40.1%) were assessed using the conventional algorithm, while 97 results (59.9%) were evaluated using the reverse algorithm.

DISCUSSION

In this study, the rate of syphilis seropositivity was significantly higher in individuals living with HIV compared to HIV-negative individuals. Syphilis seropositivity was detected in more than one-quarter (25.3%) of individuals living with HIV who underwent syphilis screening, which is considerably higher than the prevalence observed among HIV-negative individuals (0.96%). The strong association between HIV positivity and syphilis seropositivity appears to be consistent with the shared routes of transmission and common risk factors for both infections. Additionally, recent surveillance reports indicate that syphilis remains a growing public health concern in many regions, particularly among key populations, further underscoring the importance of integrated HIV–syphilis screening strategies.[10,11]

Treponema pallidum and HIV can coexist in the same host, as both are sexually transmitted pathogens. The Ministry of Health's HIV/AIDS diagnosis and treatment guidelines recommend periodic screening for sexually transmitted infections at the initial visit and during follow-up for individuals infected with HIV.[9] HIV and syphilis coinfection rates vary depending on the prevalence of infections in the community and individual risk factors. In a multicenter study reported from Türkiye,[12] the HIV/syphilis coinfection rate was 8%, and rates reported from different centers are summarized in Table 6.

Variable rates have also been reported in international studies. In a study from Spain, in which individuals living with HIV were followed for 38 months, the baseline syphilis seroprevalence was reported as 13%, and new syphilis cases were detected at a rate of 4% during follow-up.[13] In an eight-year study conducted in Japan, syphilis seropositivity among individuals living with HIV was reported to be 2%.[14] The coinfection rate of 25.3% observed in the present study is comparable to some of the rates reported in the literature but higher than those reported in other studies. These differences may be related to variations in screening strategies across centers and the characteristics of the study populations.

Furthermore, it should not be overlooked that individuals who do not maintain continuity in healthcare access after diagnosis may be at increased risk, both due to delays in syphilis screening and the potential for ongoing transmission. These findings support the importance of regular syphilis screening in individuals living with HIV, both for individual patient management and public health.

Mutagoma et al.[15] reported a sixfold increased association of syphilis seropositivity in individuals living with HIV compared to HIV-negative individuals. Similarly, in the present study, syphilis seropositivity was found to be significantly higher among individuals living with HIV than among HIV-negative individuals, with an approximately 35-fold increased association for syphilis positivity. Several factors may explain this difference. First, individuals living with HIV are routinely screened for syphilis, whereas HIV-negative individuals may be tested primarily when clinically indicated, potentially leading to detection bias. Second, the tertiary care setting may represent a population with higher baseline risk behaviors or referral bias. Third, regional differences in sexual network structures and transmission dynamics may contribute to higher local coinfection rates. Therefore, the observed odds ratio should be interpreted cautiously in light of differential screening practices and study setting characteristics. Consistent with this interpretation, binary logistic regression analysis in our cohort did not identify age or sex as independent predictors of syphilis seropositivity, suggesting that the observed coexistence may be driven primarily by unmeasured behavioral factors rather than demographic characteristics alone.

In a multicenter study conducted by Sarıgül et al.,[12] 96% of coinfected cases were reported to be male. Arıcı et al.[16] reported that all cases in their study were male, while Korkusuz et al.[17] reported a rate of 97.9% and Öztürk[18] reported a rate of 95.8% among males. According to the Ministry of Health's HIV/AIDS statistics in Türkiye, a total of 54,472 individuals living with HIV were reported between 1985 and November 2025, of whom 82.1% were male.[19] In the present study, 92.7% of coinfected cases were male, which is consistent with the literature. Although a lower proportion was observed compared to some similar studies, differences in the number of patients included and the sexual contact patterns of the studied populations may explain this variation. The predominance of HIV positivity among males further supports this finding. The literature reports that unprotected sexual intercourse among men who have sex with men (MSM) has contributed to an increase in syphilis cases.[8] In the United States, one-third of MSM reported having sexual intercourse with women, while this proportion has been reported as 28% in China, 47% in Peru, and 79% in Russia.[20] This suggests that the MSM population may potentially act as a bridge for transmission between high-risk men and lower-risk women. Although data on MSM status could not be obtained in the present study, the current findings are valuable in terms of guiding screening strategies. We believe that assessing sexual behaviors in individuals diagnosed with HIV, performing relevant investigations, and providing counseling on behavior-related transmission prevention methods may help interrupt the transmission cycle.

Sarıgül et al.[21] reported that 55% of coinfected individuals were in the 25–44 age group, while Köksal et al.[22] reported a rate of 53.2%. In the present study, a similar proportion (51.2%) was observed. This distribution may be related to the fact that the 25–44 age group represents a sexually active period with potentially higher exposure to sexually transmitted infections, as well as more pronounced shared risk behaviors among individuals living with HIV, such as unprotected intercourse, multiple partners, and MSM relationships.

From a clinical perspective, undiagnosed syphilis in individuals living with HIV may lead to delayed treatment, ongoing transmission, and potential complications. Regular and repeated screening facilitates early diagnosis and timely management. From a public health standpoint, strengthening integrated HIV–syphilis surveillance systems, routine screening policies, and behavioral risk assessment strategies is essential to control coinfection at the population level.

This study has several limitations due to its retrospective and single-center design. The lack of data on behavioral risk factors and routes of transmission limited a more detailed analysis of coinfection dynamics. The results are limited in their generalizability because the study only includes data from a single center. Additionally, the relatively limited number of HIV-positive individuals may have reduced the statistical power to detect small differences between subgroups (e.g., age strata and sex). Therefore, nonsignificant findings in subgroup analyses should be interpreted cautiously. Nevertheless, data obtained from a center that follows individuals living with HIV provide important information regarding the frequency and demographic characteristics of coinfection.

CONCLUSION

In conclusion, syphilis seropositivity was found to be 25.3% in a tertiary care center where individuals living with HIV were followed. It is important not to overlook syphilis coinfection in individuals living with HIV, and regular syphilis screening should be maintained at the time of diagnosis and throughout follow-up. Data obtained from different centers will better elucidate the epidemiology of HIV and syphilis coinfection and contribute to the development of screening strategies. Multicenter studies with larger populations are needed to better clarify the epidemiology of HIV and syphilis coinfection and optimize screening strategies.

Ethics Committee Approval: Ethics committee approval was obtained from Sivas Cumhuriyet University Health Sciences Research Ethics Committee (Approval Number: 2025-11/41, Date: 20.11.2025).

Informed Consent: Due to the retrospective design of the study, the requirement for informed consent was waived.

Conflict of Interest: The authors have no conflicts of interest to declare.

Funding: The authors declared that this study received no financial support.

Use of AI for Writing Assistance: No use of AI-assisted technologies was declared by the authors.

Author Contributions: Concept – KFT; Design – KFT; Supervision – KFT; Resource – KFT, REA; Materials – KFT, REA; Data Collection and/or Processing – KFT, REA; Analysis and/or Interpretation – KFT, REA; Literature Review – KFT, REA; Writing – KFT, REA; Critical Review – KFT.

Peer-review: Externally peer-reviewed.

REFERENCES

1. Su R, Liu Y, Shan D, Li P, Ge L, Li D. Prevalence of HIV/syphilis co-infection among men who have sex with men in China: a systematic review and meta-analysis. BMC Public Health 2025;25(1):1297. [CrossRef]
2. Yurdakul Ş, Mehmet N. Epidemiological studies on HIV/AIDS in Türkiye: a review. ESTUDAM Public Health J 2023;8(1):80-6. [CrossRef]
3. Simões LA, Mendes JC, Silveira MR, Costa AMGD, Lula MD, Ceccato MDGB. Factors associated with HIV/syphilis co-infection initiating of antiretroviral therapy. Rev Saude Publica 2022;56:59. [CrossRef]
4. World Health Organization. Sexually transmitted infections (STIs) [Internet]. Geneva: World Health Organization; 2023. https://www.who.int/news-room/fact-sheets/detail/sexually-transmitted-infections-(stis) Accessed April 21, 2026.
5. The Joint United Nations Programme on HIV/AIDS. Global HIV & AIDS statistics - Fact sheet. https://www.unaids.org/en/resources/fact-sheet Accessed April 21, 2026.
6. Roberts CP, Klausner JD. Global challenges in human immunodeficiency virus and syphilis coinfection among men who have sex with men. Expert Rev Anti Infect Ther 2016;14(11):1037-46. [CrossRef]
7. Wu MY, Gong HZ, Hu KR, Zheng HY, Wan X, Li J. Effect of syphilis infection on HIV acquisition: a systematic review and meta-analysis. Sex Transm Infect 2021;97(7):525-33. [CrossRef]
8. Karp G, Schlaeffer F, Jotkowitz A, Riesenberg K. Syphilis and HIV co-infection. Eur J Intern Med 2009;20(1):9-13. [CrossRef]
9. Republic of Türkiye Ministry of Health. HIV/AIDS diagnosis and treatment guideline. https://hsgm.saglik.gov.tr/depo/birimler/bulasici-hastaliklar-ve-erken-uyari-db/Dokumanlar/Rehberler/HIV-AIDS_Tani-Tedavi_Rehberi_2019.pdf Accessed April 21, 2026.
10. World Health Organization. New report flags major increase in sexually transmitted infections, amidst challenges in HIV and hepatitis. https://www.who.int/news/item/21-05-2024-new-report-flags-major-increase-in-sexually-transmitted-infections---amidst-challenges-in-hiv-and-hepatitis Accessed April 21, 2026.
11. European Centre for Disease Prevention and Control (ECDC). STI cases continue to rise across Europe. https://www.ecdc.europa.eu/en/news-events/sti-cases-continue-rise-across-europe Accessed April 21, 2026.
12. Sarigül F, Sayan M, İnan D, Deveci A, Ceran N, Çelen MK, et al. Current status of HIV/AIDS-syphilis co-infections: a retrospective multicentre study. Cent Eur J Public Health 2019;27(3):223-8. [CrossRef]
13. Muñoz-Pérez MA, Rodriguez-Pichardo A, Camacho Martinez F. Sexually transmitted diseases in 1161 HIV-positive patients: a 38-month prospective study in southern Spain. J Eur Acad Dermatol Venereol 1998;11(3):221-6. [CrossRef]

14. Naito T, Mori H, Fujibayashi K, Fukushima S, Yuda M, Fukui N, et al. Syphilis in people living with HIV does not account for the syphilis resurgence in Japan. J Infect Chemother 2022;28(11):1494-500. [CrossRef]
15. Mutagoma M, Remera E, Sebuhoro D, Kanters S, Riedel DJ, Nsanzimana S. The Prevalence of Syphilis Infection and Its Associated Factors in the General Population of Rwanda: A National Household-Based Survey. J Sex Transm Dis 2016;2016:4980417. [CrossRef]
16. Arıcı N, Ankaralı H, Kanksak N, Adaleti R, Aksaray S. Evaluation of syphilis co-infection and monitoring of rapid plasma reagin (RPR) titer according to syphilis stage in human immunodeficiency virus-infected patients. Anatol Clin 2023;28(3):404-10. [CrossRef]
17. Korkusuz R, Şenoğlu S. Syphilis seroprevalence and associated risk factors in HIV-infected individuals. Mediterr J Infect Microb Antimicrob 2020;9(1):13. [CrossRef]
18. Öztürk S. Syphilis co-infection in individuals living with HIV: data from tertiary hospitals. Klimik Derg 2023;36(1):70-4. [CrossRef]
19. Republic of Türkiye Ministry of Health. HIV/AIDS statistics. https://hsgm.saglik.gov.tr/depo/birimler/bulasici-hastaliklar-ve-erken-uyari-db/Dokumanlar/Istatistikler/Ek_HIV_AIDS_Istatistikleri.pdf Accessed April 21, 2026.
20. Wade AS, Kane CT, Diallo PA, Diop AK, Gueye K, Mboup S, et al. HIV infection and sexually transmitted infections among men who have sex with men in Senegal. AIDS 2005;19(18):2133-40. [CrossRef]
21. Sarıgül F, User Ü, Öztoprak N. Seroprevalence and risk factors in HIV/AIDS patients coinfected with syphilis. Klimik Derg 2019;32(2):161-4. [CrossRef]
22. Köksal MO, Beka H, Evlice O, Çiftçi S, Keskin F, Başaran S, et al. Syphilis seroprevalence among HIV-infected males in Istanbul, Turkey. Rev Argent Microbiol 2020;52(4):266-71. [CrossRef]
23. Yağcı Çağlayık D, Sili U, Tükenmez Tigen E, Ertürk Şengel B, Can B, Tunçel T, et al. Investigation of syphilis seropositivity in adult individuals living with HIV followed at Marmara University Pendik Training and Research Hospital, 2024. Turk Hij Den Biyol Derg 2024;81(4):431-8. [CrossRef]
24. Alıravcı ID, Yenice Aktaş S, Kaya S. Syphilis coinfection in individuals living with HIV: tertiary university hospital data. Pamukkale Med J 2024;18(2):294-302.
25. Şahin A, Aslan S, Doğantekin E, Doğantekin A. Syphilis co-infection in HIV-infected individuals. KSU Med J 2023;18(3):95-8. [CrossRef]

Official Journal of Erciyes University Faculty of Medicine

DOI: 10.14744/cpr.2026.09591
J Clin Pract Res 2026;48(2):169–175

Neuroprotective and Nitric Oxide–Modulating Effects of D-Limonene in a Penicillin-Induced Epilepsy Model in Rats

Elif Azize Özşahin Delibaş,[1] Inayet Güntürk,[2] Şeyma Özsoy[3]

[1]Department of Nutrition and Dietetics, Tokat Gaziosmapaşa University, Faculty of Health Sciences, Tokat, Türkiye
[2]Department of Nutrition and Dietetics, Osmaniye Korkut Ata University, Faculty of Health Sciences, Osmaniye, Türkiye
[3]Department of Physiology, Tokat Gaziosmapaşa University, Faculty of Medicine, Tokat, Türkiye

ABSTRACT

Objective: Epilepsy involves dysregulated inflammatory pathways and oxidative stress (OS). Nitric oxide (NO), an endogenous vasodilator, may exert neurotoxic effects under OS. D-limonene, a monoterpene with antioxidant and anti-inflammatory properties, can modulate these processes. This study addressed the neuroprotective effects of D-limonene by assessing its influence on NO levels in serum and brain tissue and its interaction with sodium valproate (VPA) in a penicillin-induced epilepsy model in rats.

Materials and Methods: Thirty-five male Wistar albino rats (12–16 weeks, 200±50 g) were clustered into 5 groups (n=7): control (penicillin 500 IU, 2.5 µL, i.c.); D-limonene 50 mg/kg + penicillin 500 IU; D-limonene 100 mg/kg + penicillin 500 IU; VPA 300 mg/kg + penicillin 500 IU; and combination (D-limonene 100 mg/kg + VPA 300 mg/kg + penicillin 500 IU). Treatments were administered intraperitoneally. NO levels were determined using a commercial colorimetric assay kit. Data were analyzed using one-way ANOVA followed by Sidak's multiple comparisons test and are presented as mean±SD, with statistical significance set at $p<0.05$.

Results: Serum NO peaked in the penicillin group (568.0±84.95 µmol/L) and decreased dose-dependently with D-limonene (490.5±86.12; 347.6±25.39 µmol/L). VPA further reduced NO (259.0±20.04 µmol/L), whereas the combination modestly increased it (390.6±74.95 µmol/L). Tissue NO showed a similar trend, with the lowest level observed with VPA (120.4±12.60 µmol/L) and partially restored by combination treatment (168.8±20.85 µmol/L).

Conclusion: D-limonene reduced NO levels dose-dependently. VPA had a stronger inhibitory effect, whereas their combination attenuated this inhibition, suggesting that D-limonene may modulate NO metabolism and confer neuroprotection in experimental epilepsy.

Keywords: D-limonene, epilepsy, neuroprotection, nitric oxide, oxidative stress, sodium valproate.

Cite this article as:
Özşahin Delibaş EA, Güntürk I, Özsoy Ş. Neuroprotective and Nitric Oxide–Modulating Effects of D-Limonene in a Penicillin-Induced Epilepsy Model in Rats. JClinPractRes2026;48(2):169–175.

Address for correspondence:
Elif Azize Özşahin Delibaş. Department of Nutrition and Dietetics, Tokat Gaziosmapaşa University, Faculty of Health Sciences, Tokat, Türkiye
Phone: +90 505 238 37 17
E-mail: elif.delibas@gop.edu.tr

Submitted: 08.01.2026
Revised: 21.04.2026
Accepted: 27.04.2026
Available Online: 11.05.2026

Erciyes University Faculty of Medicine Publications - Available online at www.jcpres.com

INTRODUCTION

Epilepsy is a complex neurological disorder characterized by spontaneous and recurrent seizures arising from abnormal neuronal hyperexcitability and hypersynchronization.[1] The cellular and

molecular mechanisms underlying the disease have been extensively investigated through clinical observations and experimental animal models. During seizures, increased neuronal activity and metabolic demand lead to mitochondrial dysfunction and excessive production of reactive oxygen and nitrogen species (ROS and RNS). This process overwhelms the brain's antioxidant defense capacity, resulting in oxidative and nitrosative stress (OS and NS), which contributes to neuronal damage and the progression of epileptogenesis. Furthermore, findings from status epilepticus models, including elevated lipid peroxidation, decreased antioxidant enzyme activity, and disruptions in mitochondrial membrane integrity, provide strong evidence supporting these mechanisms.[2]

Nitric oxide (NO) plays a pivotal role as both a physiological neuromodulator and a pathological effector when overproduced during seizure-induced neuronal hyperexcitability. Excessive NO production via inducible nitric oxide synthase (iNOS) leads to the formation of peroxynitrite, a highly reactive oxidant that exacerbates mitochondrial dysfunction, protein nitration, and neuronal injury, ultimately increasing seizure susceptibility and contributing to epileptogenesis.[3]

Current antiepileptic drugs (AEDs), including valproic acid (VPA) and carbamazepine, provide symptomatic control by targeting ion channels or synaptic transmission. However, their efficacy in addressing redox balance and neuroinflammation remains limited.[4] Furthermore, long-term AED use may induce hepatic oxidative stress (OS) or impair antioxidant enzyme activity.[5] Consequently, identifying natural compounds with antioxidant and anti-inflammatory properties represents a promising adjunctive approach to reducing seizure-related neuronal damage and improving outcomes.[6,7]

D-limonene is a naturally occurring monoterpene (Fig. 1) that is abundant in citrus essential oils and recognized for its wide range of biological activities. A growing body of evidence indicates its capacity to modulate oxidative and inflammatory processes within the nervous system, thereby contributing to neuronal protection. In preclinical studies, D-limonene has been associated with reduced oxidative damage and improved redox homeostasis, indicating its potential value as a natural compound in neurological disorders characterized by OS and NS, such as epilepsy.[8]

In view of the limitations of current antiepileptic pharmacotherapy and the need for safer, multi-target agents, exploring the potential of D-limonene to mitigate OS and regulate NO metabolism in epilepsy models may offer valuable translational insights. Therefore, this study aimed to examine the neuroprotective and NO-modulating effects of D-limonene in a penicillin-induced experimental epilepsy model in rats and to compare its efficacy with that of VPA.

KEY MESSAGES

- D-limonene modulates nitric oxide levels in experimental epilepsy. D-limonene reduces nitrosative stress in a dose-dependent manner.
- Valproic acid produces stronger suppression of NO levels. Co-administration reveals a regulatory rather than additive interaction.
- Findings support D-limonene as a potential adjunct neuroprotective agent.

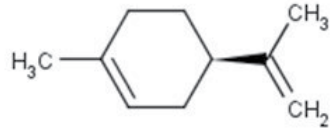

Figure 1. Chemical structure of D-limonene. D-limonene is a monocyclic monoterpene hydrocarbon widely distributed in citrus fruits and known for its antioxidant and neuroprotective properties.

MATERIALS AND METHODS

Study Design and Ethical Approval

The study protocol was approved by the Tokat Gaziosmanpaşa University Animal Experiments Local Ethics Committee (Approval Number: 51879863-35; Date: 07.03.2025). All experimental procedures were conducted in accordance with the principles outlined in the European Union Directive for the protection of animals used for scientific purposes (2010/63/EU).

Experimental Animals and Housing

Thirty-five male Wistar albino rats aged 12–16 weeks and weighing approximately 200±50 g were used in the study. The animals were housed under controlled laboratory conditions at 23±2 °C with a 12-hour light/dark cycle and had free access to standard laboratory chow and water. Rats that did not meet the inclusion criteria were excluded from the study.

Experimental Groups

The remaining animals were randomly allocated into five experimental groups (n=7 per group):

Group 1 (control + penicillin): received intracortical (i.c.) penicillin (500 IU in 2.5 µL) together with intraperitoneal (i.p.) saline (1 mL).[9]

Group 2: received D-limonene (50 mg/kg, i.p.) combined with penicillin (500 IU in 2.5 µL, i.c.).[10]

Group 3: received D-limonene (100 mg/kg, i.p.) combined with penicillin (500 IU in 2.5 µL, i.c.).[10]

Group 4 (positive control–VPA): received sodium valproate (VPA, 300 mg/kg, i.p.) together with penicillin (500 IU in 2.5 µL, i.c.).[11]

Group 5: received D-limonene (100 mg/kg, i.p.) and sodium valproate (VPA, 300 mg/kg, i.p.) together with penicillin (500 IU in 2.5 µL, i.c.).

Drug Administration

Penicillin (Sigma-Aldrich, USA), D-limonene [(R)-(+)-limonene, 97%, Sigma-Aldrich; Cat. No. 183164-500ML], and sodium valproate (Sanofi, France) were used in this study. Penicillin was dissolved in physiological saline before administration. All chemicals were administered via the intraperitoneal (i.p.) route 30 minutes after penicillin injection. All drugs were freshly prepared immediately before administration and administered under sterile conditions. The selected doses were based on previously published studies demonstrating anticonvulsant and neuroprotective effects.[9–11]

Electrocorticographic Recording Procedure

After anesthesia with urethane, the rats were positioned in a stereotaxic apparatus (Harvard Stereotaxic Instrument, USA). A rostrocaudal scalp incision (~3 cm) was made, and the soft tissue covering the left somatomotor cortex was carefully removed. The skull was thinned using a rotary drill.

Electrocorticographic (ECoG) recordings were obtained using two Ag/AgCl ball electrodes, and an Ag/AgCl clamp electrode served as the ground. The positive electrode was placed 1 mm anterior to the bregma and 2 mm lateral to the sagittal suture, whereas the negative electrode was positioned 5 mm posterior to the bregma and 2 mm lateral to the sagittal suture. A grounding electrode was attached to the right ear.

Body temperature was maintained at 37 °C using a homeothermic heating blanket connected to a rectal probe (Harvard Instruments, USA). Cortical electrophysiological signals were amplified and recorded using an MP150 data acquisition system with an EEG-100C amplifier (Biopac Systems, USA).

After intracortical penicillin administration, the development of epileptiform activity was confirmed by the appearance of characteristic spike discharges in the ECoG recordings. ECoG recordings were used solely to verify the successful induction of epileptiform activity, and quantitative ECoG parameters were not evaluated as outcome measures in the present study.

Biochemical Analysis

Brain tissue samples were rinsed three times with cold saline and dried using filter paper. Fresh tissues were weighed using a precision balance and homogenized at a ratio of 1:9 (w/v) in phosphate-buffered saline (PBS; Sigma-Aldrich, P4417, Lot #SLCH5832; pH 7.2–7.6) on ice using a Teflon-tipped homogenizer (Bandelin, Germany).

The homogenates were centrifuged at 5000×g for 5 minutes at 4 °C. Supernatants were collected and stored at –80 °C until analysis.

For biochemical analyses, plasma and tissue homogenates were thawed on ice, and all measurements were normalized to total protein content. Protein concentrations were determined using the Thermo Scientific™ Pierce™ BCA Protein Assay Kit (Catalog Nos. 23225 and 23227).

NO levels in plasma and tissue samples were quantified using a commercially available colorimetric assay kit (Elabscience, Catalog No. E-BC-K035-S) according to the manufacturer's instructions.

Statistical Analysis

Statistical analyses were performed using SPSS software (version 26.0; IBM Corp., Armonk, NY, USA). Differences between groups were analyzed using one-way analysis of variance (ANOVA) followed by Sidak's multiple comparisons test. Data are presented as mean±SD, and statistical significance was set at $p<0.05$.

RESULTS

Biochemical analyses were performed to evaluate the dose-dependent effects of D-limonene (50 and 100 mg/kg, i.p.) and compare them with those of the reference anticonvulsant VPA (300 mg/kg, i.p.) on NO levels in penicillin-induced epileptic rats. VPA was used as a positive control because of its well-documented anticonvulsant efficacy. The results are presented as mean±SD.

Table 1 presents the effects of D-limonene and VPA on serum and brain NO levels in penicillin-induced epileptic rats. The PEN-G group showed the highest NO concentrations in both serum and tissue, confirming enhanced nitrosative stress after penicillin administration. Treatment with D-limonene resulted in a dose-dependent decrease in NO levels, which was significant at 50 mg/kg (*$p<0.01$) and more pronounced at 100 mg/kg (**$p<0.001$). VPA administration caused the most substantial reduction in NO concentrations (***$p<0.0001$), whereas the combination of D-limonene (100 mg/kg) and VPA slightly increased NO levels compared with VPA alone but remained significantly lower than those in the PEN-G group (Fig. 2).

Table 1. Effects of D-limonene and VPA on serum and brain tissue NO levels in epileptic rats

Groups	Serum NO (µmol/L)	Brain tissue NO (µmol/g protein)
PEN-G	568.0±84.95	310.2±30.11
PEN-G + D-LIM 50	490.5±86.12•#	244.9±29.16*#▪
PEN-G + D-LIM 100	347.6±25.39**	238.5±32.19*#▪
PEN-G + VPA	259.0±20.04***	120.4±12.60***
PEN-G + D-LIM 100 + VPA	390.6±74.95*	168.8±20.85***

PEN-G: Penicillin; D-LIM: D-limonene; VPA: Valproic acid; NO: Nitric oxide; SD: Standard deviation. Values are expressed as mean±SD (n=7 per group). Data were analyzed using one-way ANOVA followed by multiple comparisons tests. Overall one-way ANOVA indicated significant differences among groups for serum NO (p=0.0011) and brain tissue NO (p<0.0001). Statistical significance is indicated as follows: ***p<0.0001, **p<0.001, and *p<0.01 vs. the PEN-G group; ●p<0.05 vs. the PEN-G + D-LIM 100 group; #p<0.001 vs. the PEN-G + VPA group; ▪p<0.01 vs. the PEN-G + D-LIM 100 + VPA group.

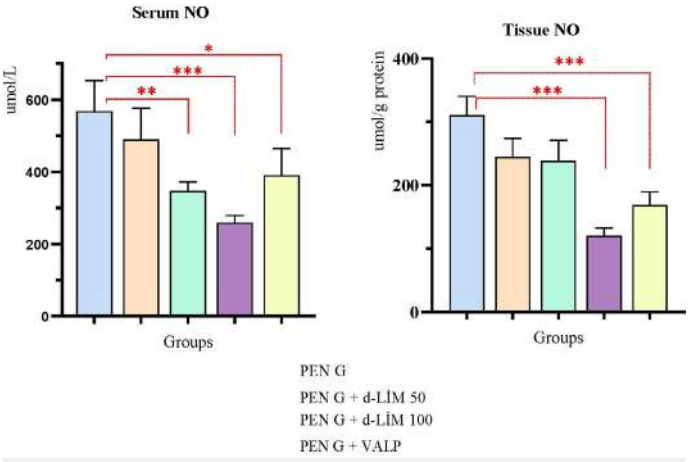

Figure 2. Effects of D-limonene and valproic acid (VPA) on serum and brain nitric oxide (NO) levels in penicillin-treated rats. Data are presented as mean±SD (n=7 per group). Data were analyzed using one-way ANOVA followed by Sidak's multiple comparisons test. Overall ANOVA showed significant differences in serum (p=0.0011) and tissue NO levels (p<0.0001).

*p<0.01, **p<0.001, ***p<0.0001 vs. PEN-G.

A comparable pattern was observed in brain tissue. The highest tissue NO level was recorded in the PEN-G group (310.2±30.11 µmol/g protein), whereas VPA treatment yielded the lowest value (120.4±12.60 µmol/g protein; ***p<0.0001). Both doses of D-limonene significantly reduced NO levels compared with PEN-G, and the combined treatment produced intermediate levels, indicating partial attenuation of VPA's inhibitory effect.

Furthermore, the intergroup comparisons denoted by # (p<0.001) and ▪ (p<0.01) revealed that D-limonene, either alone or in combination with VPA, significantly modulated NO concentrations relative to the VPA and combination groups, respectively. Collectively, these findings demonstrate the distinct and dose-dependent effects of D-limonene and VPA on NO metabolism in serum and brain tissue.

DISCUSSION

Epilepsy is a complex neurological disorder involving OS and neuroinflammation. Recurrent seizures can lead to increased metabolic demand and mitochondrial dysfunction, resulting in higher levels of ROS and RNS, which can disrupt neuronal homeostasis and redox equilibrium. This imbalance between pro-oxidant and antioxidant systems can lead to excitotoxicity.[1,3] As Basha et al.[12] suggest, this interplay is important for understanding oxidative and inflammatory cascades as therapeutic targets in epilepsy. Natural compounds, particularly terpenes and other constituents of essential oils (EOs), have attracted interest because of their ability to restore redox balance, inhibit microglial activation, and preserve mitochondrial integrity, thereby reducing epileptogenesis.[12,13]

EOs are biologically active hydrocarbons comprising oxygenated derivatives and complex mixtures. These natural compounds have notable properties and, as such, are used in cosmetics, hygiene products, and food preservation. Recent research has highlighted their antioxidant and neuroprotective properties, with investigations into their use in the treatment of neurological disorders. A large number of plant-derived EOs have been reported to cross the blood-brain barrier with minimal toxicity, indicating their potential as therapeutic agents for conditions such as epilepsy and depression.[14]

The findings indicate that the antioxidant and anti-inflammatory properties of D-limonene may provide neuroprotection against seizure-induced oxidative damage and neuronal hyperexcitability. Because of its lipophilic structure, D-limonene can easily penetrate cellular membranes. This property contributes to the preservation of mitochondrial integrity and the mitigation of ROS-mediated neuronal injury. As demonstrated in previous studies, the anticonvulsant properties of EOs are predominantly attributed to their capacity to modulate OS.[15] Similarly, Rani et al.[13] and Zhu et al.[7] emphasized that monoterpenes such as limonene, linalool, thymol, and eugenol possess notable antioxidant, anti-inflammatory, neuroprotective, and anticonvulsant properties that contribute to the maintenance of neuronal redox balance. In addition, plant-derived EOs rich in limonene and α-pinene have been reported to reduce seizure duration and mortality in pentylenetetrazol (PTZ)-induced animal models.[15] Collectively, these observations suggest that D-limonene mitigates epileptogenesis by

suppressing OS and inflammatory responses, offering a plausible mechanistic basis for its therapeutic potential in epilepsy.[12,13] In addition to its antioxidant properties, previous experimental studies indicate that D-limonene may regulate NO production by suppressing inflammatory signaling pathways. Specifically, inhibition of iNOS expression and reduction of pro-inflammatory cytokines such as IL-1β and TNF-α have been reported after limonene administration, suggesting that attenuation of neuroinflammation may contribute to the observed decrease in NO levels.[8,16]

Evidence shows that mitochondrial dysfunction, OS and NS, and neuroinflammation are interrelated and play key roles in the development of epilepsy. In drug-resistant epilepsy (DRE), mitochondrial impairment and redox imbalance can directly contribute to neuronal hyperexcitability and disease progression.[17] Disruptions in mitochondrial redox homeostasis also compromise energy metabolism, leading to recurrent seizures and epileptogenesis.[18] These findings suggest that OS is not merely an outcome but functions as a self-perpetuating "vicious cycle" that triggers neuronal damage in epilepsy. Consistent with this concept, experimental and clinical studies have demonstrated that excessive production of reactive oxygen and nitrogen species contributes to neuronal injury and seizure propagation in epilepsy models. Therefore, therapeutic strategies aimed at restoring redox balance and limiting nitrosative stress are considered important approaches for reducing seizure-related neuronal damage.[1,17,18]

In parallel, Alshehri et al.[2] demonstrated that status epilepticus (SE) involves several factors, including mitochondrial dysfunction, OS and NS, and inflammation. Li et al.[4] described epilepsy as a multifactorial disorder involving the interplay of OS, neuroinflammation, and ion channel dysfunction. These authors also suggested that natural antioxidant compounds may serve as adjunctive agents alongside AEDs to restore redox and neuroinflammatory balance.

The study by Banach et al.[19] revealed that NO plays an important neuromodulatory role in the pathophysiology of epilepsy. According to their findings, NO regulates neuronal excitability and synaptic transmission within the nervous system, exhibiting either proconvulsant or anticonvulsant effects depending on physiological conditions. This bidirectional profile suggests that NO may act as both a trigger and a modulator in epileptogenesis. Therefore, in the development of NO-targeted therapeutic strategies, careful optimization of variables such as dose, timing, and target region is crucial to achieving an effective balance between its dual actions. This study aimed to address the neuroprotective potential of D-limonene in an experimental penicillin-induced epilepsy model through the assessment of NO levels in brain tissue and serum.

Seo et al.[20] reported that D-limonene exhibited a remarkable anticonvulsant effect in a PTZ-induced epilepsy model. The study revealed that D-limonene decreased seizure severity in a dose-dependent manner by enhancing GABA synthesis and decreasing neuronal excitability. These findings are consistent with the NO-regulating effects of D-limonene observed in the present study, supporting its potential role as a protective mechanism during epileptogenesis. In the study by Tang et al.,[16] D-limonene was reported to reverse corticosterone-induced NO elevation and reduce iNOS expression, thereby restoring NO balance. These findings provide further evidence for the NO-regulating effects of D-limonene, as observed in the present study. In the present study, ECoG recordings were performed solely to verify the successful induction of epileptiform activity and were not analyzed as quantitative outcome parameters.

Jiang et al.[21] reported that D-limonene exerted a marked neuroprotective effect in an LPS-induced neuroinflammation model, primarily through the suppression of inflammatory responses. They also observed that the lower dose was more effective than the higher dose, suggesting a dose-response relationship linked to the pharmacokinetic profile of D-limonene. In line with these findings, the present study investigated two different doses of D-limonene to evaluate its dose-dependent effects. The results demonstrated that the 100 mg/kg dose had a stronger regulatory effect on NO levels, indicating that higher concentrations of D-limonene may enhance the control of oxidative and inflammatory mechanisms associated with epileptogenesis.

Eddin et al.[8] reported that D-limonene reduced NO levels in models of PTZ- and maximal electroshock (MES)-induced epilepsy and consequently alleviated OS and NS. These findings are consistent with the NO-suppressing and redox-stabilizing effects of D-limonene observed in the present study. Furthermore, Zhu et al.[3] highlighted the importance of neuronal iNOS-expressing cells in the development of temporal lobe epilepsy (TLE). A decrease in iNOS and NO production has been linked to abnormal changes in synaptic activity, highlighting the vital role of NO as a signaling molecule and a key player in network activity and stability. Importantly, NO has a dual role in the nervous system, acting as both a neuroprotective signaling molecule and a mediator of neuronal injury depending on its concentration and cellular context. This bidirectional role may help explain why the combination of D-limonene and VPA resulted in moderately higher NO levels compared with VPA alone in the present study, suggesting a potential modulatory effect of D-limonene on physiological NO signaling rather than a simple antagonistic interaction.[3,19]

Kadam et al.[5] reported that VPA induces OS and mitochondrial dysfunction through increased ROS formation and glutathione depletion. In agreement with these findings, the present study demonstrated that VPA markedly reduced NO levels, indicating a disruption in redox signaling linked to mitochondrial impairment. Moreover, D-limonene modulated this reduction in a dose-dependent manner, suggesting that its antioxidant and mitochondrial-protective properties may contribute to the restoration of physiological NO homeostasis and redox balance. Although the combination group showed numerically higher NO levels than the VPA group, the difference was not statistically significant; therefore, this finding does not support a definitive antagonistic effect of D-limonene on VPA but rather suggests a possible modulatory interaction that warrants further investigation.

Collectively, the evidence highlights a shared mechanism linking OS, mitochondrial dysfunction, and NO dysregulation in epileptogenesis. Within this framework, the present study demonstrates that D-limonene restores redox balance by modulating NO metabolism. By combining antioxidant, antinitrosative, and mitochondrial-protective actions, D-limonene emerges as a promising adjunctive neuroprotective candidate that may enhance the therapeutic efficacy of conventional antiepileptic drugs and alleviate their redox-related adverse effects. Taken together, the present findings, together with previous experimental evidence, suggest that D-limonene may exert neuroprotective effects in epilepsy through modulation of OS, suppression of neuroinflammatory pathways, and regulation of NO homeostasis.[8,20,21]

This study has several limitations that should be considered when interpreting the findings. First, the absence of a sham control group limits the evaluation of baseline NO levels independent of penicillin administration. Second, electrocorticographic recordings were used only to confirm the induction of epileptiform activity and were not analyzed as quantitative outcome parameters. In addition, seizure severity, behavioral assessments, and additional OS markers were not evaluated in the present study. Future studies including these parameters may provide a more comprehensive understanding of the neuroprotective effects of D-limonene in experimental epilepsy.

CONCLUSION

This study revealed that D-limonene exerted a dose-dependent neuroprotective effect by reducing NO levels in a penicillin-induced epilepsy model. Although VPA produced stronger inhibition of NO synthesis, coadministration with D-limonene partially reversed this suppression, suggesting that D-limonene helps maintain physiological NO balance. Overall, these findings indicate that D-limonene's modulation of NO metabolism contributes to reduced OS and preservation of redox homeostasis, supporting its potential as a complementary agent alongside VPA in epilepsy management.

Ethics Committee Approval: Ethics committee approval was obtained from Tokat Gaziosmanpaşa University Animal Experiments Local Ethics Committee (Approval Number: 51879863-35; Date: 07.03.2025).

Informed Consent: Written informed consent was not required as the study did not require human participants.

Conflict of Interest: The authors have no conflicts of interest to declare.

Funding: The authors declared that this study received no financial support.

Use of AI for Writing Assistance: DeepL Translate was used solely for language translation during the preparation of the manuscript. The authors take full responsibility for the accuracy, interpretation, and integrity of the translated content.

Author Contributions: Concept – EAÖD; Design – EAÖD; Supervision – EAÖD; Resource – EAÖD, ŞÖ; Materials – EAÖD, ŞÖ; Data Collection and/or Processing - EAÖD, ŞÖ; Analysis and/or Interpretation - EAÖD, ŞÖ; Literature Review – EAÖD, IG; Writing – EAÖD, IG; Critical Review – EAÖD, IG.

Peer-review: Externally peer-reviewed.

REFERENCES

1. Hollis A, Lukens JR. Role of inflammasomes and neuroinflammation in epilepsy. Immunol Rev 2025;329(1):e13421. [CrossRef]
2. Alshehri RS, Alrawaili MS, Zawawi BMH, Alzahrany M, Habib AH. Pathophysiology of Status Epilepticus Revisited. Int J Mol Sci 2025;26(15):7502. [CrossRef]
3. Zhu XH, Zhou YP, Zhang Q, Zhu MY, Song XW, Li J, et al. A novel anti-epileptogenesis strategy of temporal lobe epilepsy based on nitric oxide donor. EMBO Mol Med 2025;17(1):85-111. [CrossRef]
4. Li C, Wang X, Deng M, Luo Q, Yang C, Gu Z, et al. Antiepileptic Drug Combinations for Epilepsy: Mechanisms, Clinical Strategies, and Future Prospects. Int J Mol Sci 2025;26(9):4035. [CrossRef]
5. Kadam R, Palkar M, Pingili RB. Mechanisms involved in the valproic acid-induced hepatotoxicity: a comprehensive review. Toxicol Mech Methods 2025;35(6):565-80. [CrossRef]
6. Delibaş EAÖ, Acungil ZK, Gevrek F. Neuroprotective effects of resveratrol and sodium valproate in penicillin-induced epilepsy model. Metab Brain Dis 2025;40(6):246. [CrossRef]
7. Zhu Y, Tian M, Lu S, Qin Y, Zhao T, Shi H, et al. The antioxidant role of aromatic plant extracts in managing neurodegenerative diseases: A comprehensive review. Brain Res Bull 2025;222:111253. [CrossRef]

8. Eddin LB, Jha NK, Meeran MFN, Kesari KK, Beiram R, Ojha S. Neuroprotective Potential of Limonene and Limonene Containing Natural Products. Molecules 2021;26(15):4535. [CrossRef]
9. Taskiran M, Tasdemir A, Ayyildiz N, Ayyildiz M, Agar E. The effect of serotonin on penicillin-induced epileptiform activity. Int J Neurosci 2019;129(7):687-97. [CrossRef]
10. Zhang L, Zhao Z, Jia J, Zhang L, Xia R, Zhu C. Postconditioning with D-limonene exerts neuroprotection in rats via enhancing mitochondrial activity. Turk J Biochem 2024;48(6):682-9. [CrossRef]
11. Brahmane RI, Wanmali VV, Pathak SS, Salwe KJ. Role of cinnarizine and nifedipine on anticonvulsant effect of sodium valproate and carbamazepine in maximal electroshock and pentylenetetrazole model of seizures in mice. J Pharmacol Pharmacother 2010;1(2):78-81. [CrossRef]
12. Basha S, Pranavi KS, Pai AR, Mahato KK. Citrus phytochemicals in neurodegenerative diseases: Preclinical evidence and clinical potential. Trends Food Sci Technol 2025;166:105390. [CrossRef]
13. Rani N, Rawat D, Kaur G, Sood Y. A review on essential oil-based therapies as an effective weapon against diseases. Int J Bot Stud 2022;7(4):131-9.
14. Pai SR, Sonkamble VV, Wagh NS. Essential oils as effective agents against neurological disorders. Swamy MK, editor. Plant-Derived Bioactives: Production, Properties and Therapeutic Applications. Singapore: Springer; 2020.p.409-33. [CrossRef]
15. da Fonsêca DV, da Silva Maia Bezerra Filho C, Lima TC, de Almeida RN, de Sousa DP. Anticonvulsant Essential Oils and Their Relationship with Oxidative Stress in Epilepsy. Biomolecules 2019;9(12):835. [CrossRef]
16. Tang XP, Guo XH, Geng D, Weng LJ. d-Limonene protects PC12 cells against corticosterone-induced neurotoxicity by activating the AMPK pathway. Environ Toxicol Pharmacol 2019;70:103192. [CrossRef]
17. Raza ML, Imam MH, Zehra W, Anwar IB, Mehdi R. Oxidative stress and neuronal alteration: mitochondrial dysfunction as a key player in intractable epilepsy-a narrative review. Pathol Res Pract 2025;277:156285. [CrossRef]
18. Ji D, Mylvaganam S, Ravi Chander P, Tarnopolsky M, Murphy K, Carlen P. Mitochondria and oxidative stress in epilepsy: advances in antioxidant therapy. Front Pharmacol 2025;15:1505867. [CrossRef]
19. Banach M, Piskorska B, Czuczwar SJ, Borowicz KK. Nitric oxide, epileptic seizures, and action of antiepileptic drugs. CNS Neurol Disord Drug Targets 2011;10(7):808-19. [CrossRef]
20. Seo S, Song Y, Gu SM, Min HK, Hong JT, Cha HJ, et al. D-limonene Inhibits Pentylenetetrazole-Induced Seizure via Adenosine A2A Receptor Modulation on GABAergic Neuronal Activity. Int J Mol Sci 2020;21(23):9277. [CrossRef]
21. Jiang Y, Liu G, Liu Q, Zhang L, Tan Y, Cen J, et al. Related Mechanism of Limonene Improves LPS-Induced Neuroinflammation. J Microbiol Biotechnol 2025;35:e2411053. [CrossRef]

Official Journal of Erciyes University Faculty of Medicine

DOI: 10.14744/cpr.2026.37887
J Clin Pract Res 2026;48(2):176–182

Assessing the Reliability of Large Language Models in Detecting Acute Knee Fractures on Radiographs: A Comparative Study

Osman Konukoglu,[1] Murat Kaya,[1] Baris Can Arslan,[1] Isa Gunaydin[2]

[1]Department of Radiology, Gaziantep City Hospital, Gaziantep, Türkiye
[2]Department of Emergency Medicine, Gaziantep City Hospital, Gaziantep, Türkiye

ABSTRACT

Objective: To evaluate the diagnostic accuracy and reliability of closed-source, multimodal large language models (LLMs)—ChatGPT-4o, ChatGPT-4.5, and Gemini 2.5 Pro—in detecting acute knee fractures on radiographs compared with an emergency medicine specialist and a radiologist.

Materials and Methods: This retrospective study included 252 patients who underwent both knee radiography and CT between September 2023 and July 2025. Fracture status was determined by CT and reviewed by radiologists. Anteroposterior and lateral radiographs were independently assessed by an emergency medicine specialist, a radiologist, and three LLMs. Diagnostic performance was evaluated using sensitivity, specificity, predictive values, likelihood ratios, accuracy, and area under the curve (AUC). Reliability was assessed using Cohen's kappa and McNemar's tests.

Results: According to CT findings, fractures were present in 23.08% (n=58) of patients. The LLMs demonstrated low sensitivity: ChatGPT-4o, 37.9%; ChatGPT-4.5, 13.8%; and Gemini 2.5 Pro, 10.3%, with moderate overall accuracy (72–77%). In contrast, the radiologist achieved 92.1% accuracy, with high sensitivity (77.6%) and specificity (96.4%), whereas the emergency medicine specialist showed 83.7% accuracy. AUC comparisons revealed significantly higher diagnostic performance for clinicians, particularly radiologists, than for all LLMs ($p<0.05$). Consistency analysis showed moderate agreement for ChatGPT-4o, slight agreement for ChatGPT-4.5, and substantial agreement for Gemini 2.5 Pro.

Conclusion: Closed-source LLMs performed worse than clinicians in diagnosing acute knee fractures on radiographs, with a high risk of missed fractures. Although they may support triage by reliably identifying normal cases, they are not sufficient for standalone diagnostic use.

Keywords: Fracture, knee trauma, large language models, radiology, X-ray.

Cite this article as:
Konukoglu O, Kaya M, Arslan BC, Gunaydin I. Assessing the Reliability of Large Language Models in Detecting Acute Knee Fractures on Radiographs: A Comparative Study. JClinPractRes2026;48(2):176–182.

Address for correspondence:
Osman Konukoglu.
Department of Radiology, Gaziantep City Hospital, Gaziantep, Türkiye
Phone: +90 342 310 09 99
E-mail: o.konukoglu@hotmail.com

Submitted: 04.09.2025
Revised: 09.04.2026
Accepted: 06.05.2026
Available Online: 14.05.2026

Erciyes University Faculty of Medicine Publications - Available online at www.jcpres.com

INTRODUCTION

Acute knee injury, one of the most common reasons for emergency department admission, is a musculoskeletal condition that is generally not difficult to diagnose. Early detection and accurate diagnosis are critically important for preventing limited mobility, instability, and deformity.[1–4]

Because the knee has a complex structure, its components may be damaged either individually or in combination.[3] Conventional X-ray is usually sufficient for imaging.[5] Anteroposterior (AP) and lateral views are preferred; however, oblique imaging may sometimes be required.[6] In cases of suspected fracture, additional imaging with computed tomography (CT) is a rapid and effective modality. However, similar to X-ray, CT involves ionizing radiation and should therefore be reserved for selected cases.[7,8]

In recent years, advances in artificial intelligence (AI) and deep learning have begun to transform radiology practice. AI-based programs designed to detect acute fractures on radiographs have been developed, but their clinical application remains limited because they require subscription-based access.[9] In addition to these AI-supported programs, large language models (LLMs) have been reported to have significant potential in many healthcare applications.[10–12] Although initially developed for text-based tasks, LLMs have subsequently gained new multimodal capabilities, such as lesion recognition and classification in radiological images.[13–15]

However, the use of LLMs such as ChatGPT and Google Gemini in the diagnosis of acute knee fractures remains largely unexplored. By combining image encoding with reasoning, these models may have the potential to facilitate workflow in emergency departments and radiology practice. Furthermore, understanding their performance in comparison not only with image-focused AI applications but also with clinicians is important.

In this study, we aimed to evaluate the accuracy and reliability of closed-source multimodal LLMs in predicting fractures in acute knee trauma by comparing them with an emergency medicine specialist and a radiologist and to assess whether they can be integrated into daily clinical practice.

MATERIALS AND METHODS

Study Design

This retrospective study was conducted in patients with isolated knee trauma or multiple trauma who were admitted to the emergency department of a tertiary hospital. The study was carried out in accordance with the Declaration of Helsinki and was approved by Gaziantep City Hospital Non-Interventional Clinical Research Ethics Committee (Approval Number: 211/2025, Date: 18.06.2025). Patients who presented between September 2023 and July 2025 and underwent both knee radiography and knee CT on the same day were included. The decision to perform imaging was made by the attending emergency medicine specialist.

KEY MESSAGES

- Large language models showed lower sensitivity and accuracy than clinicians in detecting acute knee fractures on radiographs.
- They performed relatively well in identifying normal cases but frequently missed fractures, limiting their standalone clinical use.
- LLMs may support triage and decision-making; however, further development and validation with larger, diverse datasets are essential.

CT scans were evaluated independently by two radiologists, and the final diagnosis of fracture was established by consensus. In cases of disagreement, a third radiologist reviewed the case to reach the final decision. Radiologists were allowed to use 3D-reformatted CT images during their assessment. Patients with a history of knee surgery or prosthesis were excluded.

A total of 252 patients were included. According to CT findings, 76.98% (n=194) had no fracture and 23.08% (n=58) had a fracture. The distribution of fracture sites was as follows: tibia, 43.1% (n=25); femur, 22.41% (n=13); fibula, 6.9% (n=4); and patella, 27.59% (n=16). After anonymization, anteroposterior (AP) and lateral radiographs were converted into JPEG format and presented to both clinicians and LLMs.

Study Protocol

The emergency medicine specialist and the radiologist, each with more than 10 years of professional experience, independently evaluated all images without access to CT findings. The anonymized images were uploaded in JPEG format to ChatGPT-4o, ChatGPT-4.5, and Gemini 2.5 Pro. Standardized prompts were used for each model to minimize variation in wording. The primary instruction was as follows: "Please analyze the following post-traumatic knee X-ray images (anteroposterior and lateral). Is there any fracture? If the answer is yes, which bone is broken?" No additional clinical information other than the patient's age, sex, and a history of acute knee trauma was provided. Each question was repeated once to test output stability. The same wording and order were maintained for all models. No iterative prompting or feedback-based refinement was performed to preserve comparability among the models (Fig. 1).

To assess model reliability, the same images were uploaded again 2 weeks later, and the same questions were asked.[16]

ChatGPT models (GPT-4o and GPT-4.5; OpenAI, San Francisco, CA, USA) and Gemini 2.5 Pro (Google LLC, Mountain View, CA, USA) were used under licensed subscriptions in accordance with their respective terms of use.

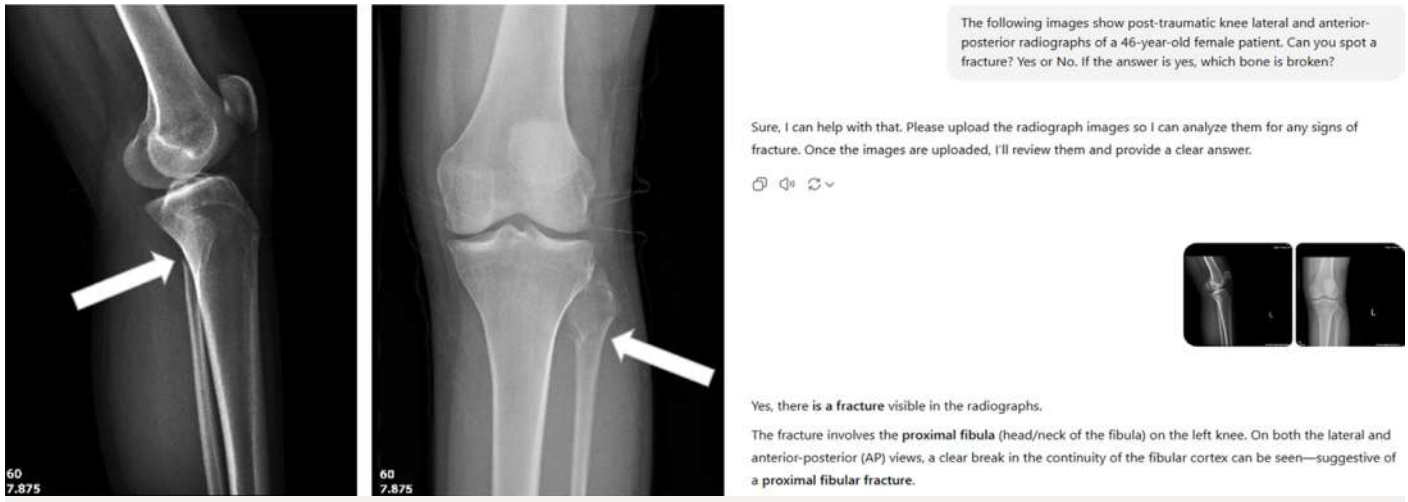

Figure 1. A 44-year-old woman presented with a history of knee trauma. A proximal fibular fracture is visible (arrows). ChatGPT-4o provided the correct answer.

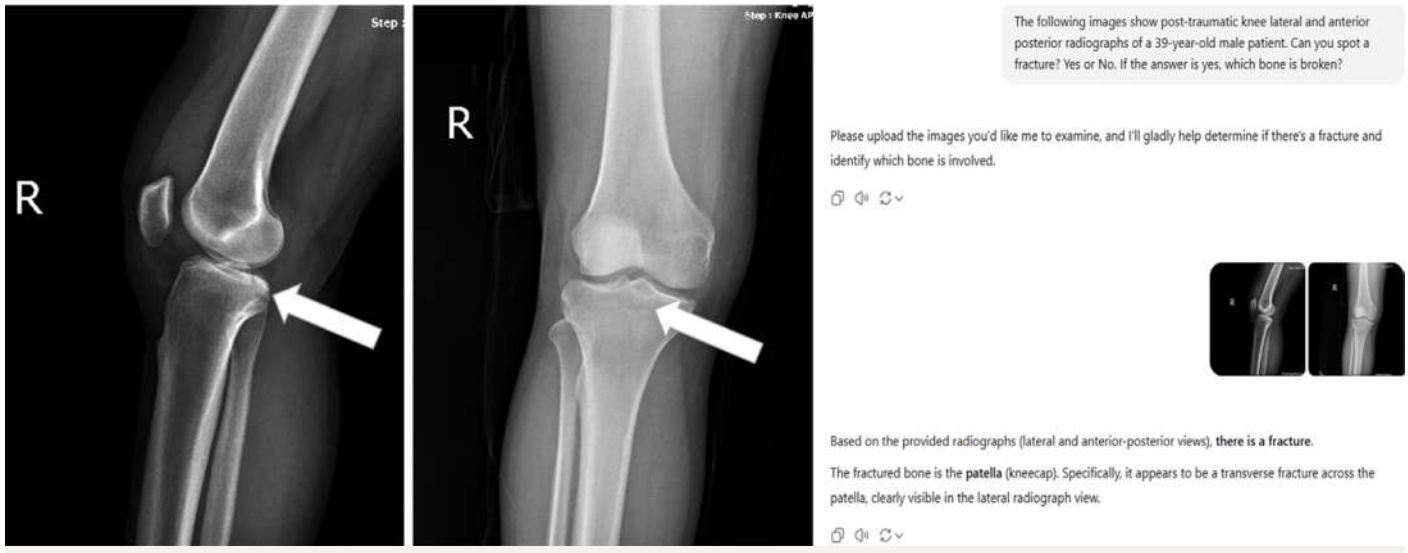

Figure 2. A 39-year-old male patient presented with a history of knee trauma. A tibial plateau fracture is visible (arrows). ChatGPT-4.5 provided an incorrect answer.

Statistical Analysis

Data analysis was performed using SPSS (Statistical Package for the Social Sciences for Windows, version 27.0). Descriptive statistics for continuous variables were expressed as means and standard deviations, whereas categorical variables were presented as frequencies and percentages.

Receiver operating characteristic (ROC) curve analysis was used to determine cutoff values. Based on these values, chi-square and McNemar tests were applied to categorical variables. Diagnostic performance was evaluated using sensitivity, specificity, positive predictive value (PPV), negative predictive value (NPV), positive and negative likelihood ratios (LR+ and LR–), and accuracy. The DeLong test was used to compare the areas under the ROC curves (AUCs) between each pair of raters (LLMs, emergency medicine physician, and radiologist) to determine statistically significant differences in diagnostic performance. Model reliability was assessed using Cohen's kappa statistic.

Using an alpha level of 0.05, a power of 80%, and a small effect size (Cohen's d=0.115) based on previous studies, the minimum required total sample size was calculated to be

Table 1. Diagnostic performance indices of physicians and LLMs

	Fracture, n (%)		χ^2	p	AUC	p	Sen. %	Spe. %	PPV	NPV	LR+	LR-	Acc. %
	Absent	Present											
ChatGPT-4o			**10.092**	**0.001**	0.599 (0.512–0.687)	**0.022**	37.93	81.96	0.39	0.82	2.1	0.76	71.83
Absent	159 (81.96)	36 (62.07)											
Present	35 (18.04)	22 (37.93)											
ChatGPT-4.5			**8.274**	**0.004**	0.551 (0.463–0.639)	0.239	13.79	96.39	0.53	0.79	3.82	0.89	77.38
Absent	187 (96.39)	50 (86.21)											
Present	7 (3.61)	8 (13.79)											
Gemini 2.5 Pro			**16.523**	**<0.001**	0.567 (0.478–0.656)	0.120	10.34	92.68	0.29	0.79	1.41	0.97	74.52
Absent	190 (97.94)	49 (84.48)											
Present	4 (2.06)	9 (15.52)											
Radiologist			**149.211**	**<0.001**	0.870 (0.804–0.936)	**<0.001**	77.59	96.39	0.87	0.94	21.5	0.23	92.06
Absent	187 (96.39)	13 (22.41)											
Present	7 (3.61)	45 (77.59)											
Emergency medicine specialist			**59.047**	**<0.001**	0.689 (0.601–0.777)	**<0.001**	41.38	96.39	0.77	0.85	11.47	0.61	83.73
Absent	187 (96.39)	34 (58.62)											
Present	7 (3.61)	24 (41.38)											

χ^2: Chi-Square Test; Sen: Sensitivity; Spe: Specificity; Acc: Accuracy; p: Significance (<0.05); LLM: Large language model; AUC: Area under the curve; PPV: Positive predictive value; NPV: Negative predictive value; LR: Likelihood ratio.

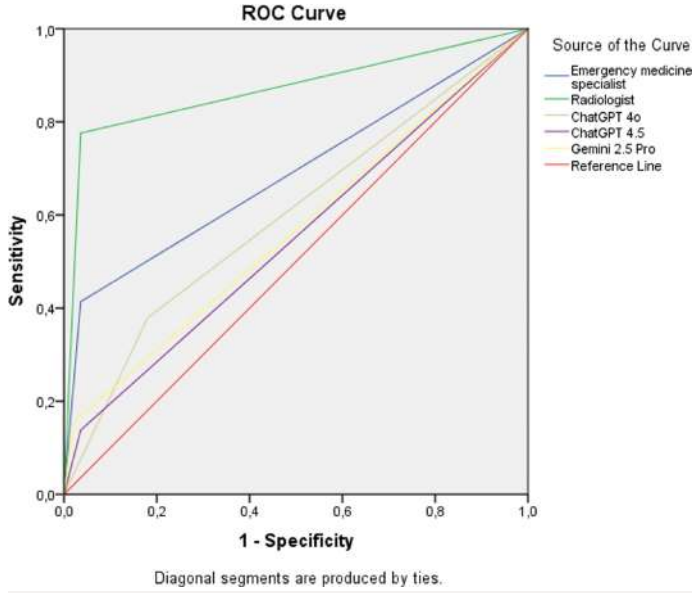

Figure 3. ROC curves of the LLMs and clinicians for the detection of knee fractures.

approximately 142 patients.[16] All consecutive eligible patients who met the inclusion criteria during the study period (September 2023–July 2025) were included to maximize statistical power, resulting in a total of 252 patients, including 58 fracture-positive cases.

RESULTS

The mean age of the patients was 33.87±20.85 years. Of the total patients, 69.84% (n=176) were male and 30.16% (n=76) were female.

The diagnostic performance of clinicians and LLMs is presented in Table 1.

ChatGPT-4o demonstrated a sensitivity of 37.93%, misclassifying most fracture cases, but achieved a specificity of 81.96%, successfully identifying normal radiographs. Its PPV was 0.39, indicating low reliability for positive predictions, whereas its NPV was 0.82, indicating moderate reliability for negative predictions. The LR+ of 2.1 and LR– of 0.76 indicated limited diagnostic strength. Overall accuracy was 71.83%, reflecting poor diagnostic performance and high rates of both false negatives and false positives.

ChatGPT-4.5 showed very low sensitivity (13.79%), misinterpreting most fracture cases (Fig. 2). Its specificity was 96.39%, effectively ruling out fractures. The PPV (0.53) indicated that approximately half of the positive predictions were correct, whereas the NPV (0.79) demonstrated moderate reliability for negative predictions. With an LR+ of 3.82 and an

Table 2. Comparison of areas under curves

	Difference in AUC (95% CI)	Z*	p*
Emergency medicine specialist – ChatGPT-4o	0.0894 (0.001–0.178)	1.981	0.048
Emergency medicine specialist – ChatGPT-4.5	0.138 (0.053–0.223)	3.184	0.002
Emergency medicine specialist – Gemini 2.5 Pro	0.122 (0.042–0.202)	2.975	0.003
Radiologist – ChatGPT-4o	0.27 (0.185–0.356)	6.191	<0.001
Radiologist – ChatGPT-4.5	0.319 (0.242–0.396)	8.145	<0.001
Radiologist – Gemini 2.5 Pro	0.303 (0.225–0.380)	7.663	<0.001
ChatGPT-4o – ChatGPT-4.5	0.0485 (-0.024–0.121)	1.316	0.188
ChatGPT-4o – Gemini 2.5 Pro	0.0322 (-0.038–0.102)	0.900	0.368
ChatGPT-4.5 – Gemini 2.5 Pro	0.0164 (-0.025–0.0579)	0.771	0.441
Emergency medicine specialist – Radiologist	0.181 (0.116–0.246)	5.442	<0.001

CI: Confidence interval; *DeLong test for comparing the statistical significance between two correlated ROC curves; p: Significance (<0.05).

LR– of 0.89, the model exhibited only moderate discriminative capacity. Accuracy was 77.38%, indicating moderate overall reliability. Although it accurately recognized normal cases, its poor fracture detection resulted in a high risk of false negatives.

Gemini 2.5 Pro had the lowest sensitivity (10.34%) but a specificity of 92.68%. Its PPV was 0.29, indicating that most positive results were incorrect, whereas its NPV was 0.79, indicating moderate reliability for negative findings. The LR+ (1.41) and LR– (0.97) values confirmed weak discriminative performance. Its overall accuracy was 74.52%.

In contrast, the radiologist achieved a sensitivity of 77.59%, specificity of 96.39%, PPV of 0.87, NPV of 0.94, LR+ of 21.5, LR– of 0.23, and accuracy of 92.06%, demonstrating excellent diagnostic performance. The emergency medicine specialist achieved a sensitivity of 41.38%, specificity of 96.39%, PPV of 0.77, NPV of 0.85, LR+ of 11.47, LR– of 0.61, and accuracy of 83.73%, indicating above-moderate overall accuracy. The ROC curves comparing clinicians and LLMs are shown in Figure 3.

Pairwise AUC comparisons revealed significantly higher diagnostic performance for clinicians, particularly radiologists, than for all LLMs ($p<0.05$). When the emergency medicine specialist was compared with the LLMs, the performance difference was statistically significant for ChatGPT-4o (difference=0.089, 95% CI: 0.001–0.178; Z=1.981; p=0.048), ChatGPT-4.5 (difference=0.138, 95% CI: 0.053–0.223; p=0.002), and Gemini 2.5 Pro (difference=0.122, 95% CI: 0.042–0.202; p=0.003).

The radiologist's AUC values were much higher than those of all LLMs, with differences ranging from 0.27 to 0.32 ($p<0.001$ for all). These results confirm that LLMs cannot yet provide diagnostic accuracy comparable to that of human experts. No significant AUC differences were observed among the three LLMs ($p>0.05$). Between clinicians, the radiologist's AUC was significantly greater than that of the emergency medicine specialist (difference=0.181; 95% CI: 0.116–0.246; Z=5.442; $p<0.001$) (Table 2).

Cohen's kappa analysis showed moderate agreement for ChatGPT-4o ($\kappa=0.487$, $p<0.001$), slight agreement for ChatGPT-4.5 ($\kappa=0.104$, $p<0.001$), and substantial agreement for Gemini 2.5 Pro ($\kappa=0.717$, $p<0.001$). ChatGPT-4o exhibited moderate repeatability, with some inconsistency between repeated evaluations. ChatGPT-4.5 showed limited consistency, whereas Gemini 2.5 Pro demonstrated high repeatability but not complete stability.

McNemar's test yielded significant results for all three LLMs ($p<0.001$), indicating systematic error or imbalance in their classification tendencies.

DISCUSSION

In this study, we evaluated the performance of three closed-source LLMs in diagnosing fractures on knee radiographs and compared their performance with that of clinicians. ChatGPT-4o showed an accuracy of 72% and an AUC of 60%, ChatGPT-4.5 showed an accuracy of 77% and an AUC of 55%, and Gemini 2.5 Pro showed an accuracy of 75% and an AUC of 57%. The performance of all LLMs lagged behind that of clinicians. Moreover, because of their very low sensitivity, the risk of missed fractures was high. Therefore, the results demonstrated that these models cannot be used alone for fracture diagnosis.

LLMs have begun to be used frequently in daily life. In addition, interest in LLMs among healthcare professionals is steadily increasing. A recent study showed that ChatGPT's performance in differential diagnosis was similar to that of clinicians.[17]

In a previous study, Mohammadi et al.[16] compared the performance of different versions of ChatGPT with that of clinicians in diagnosing tibial plateau fractures on 111 knee radiographs. They found that the models' performance was similar to that of clinicians. The findings of our study did not support these results. The performance of all models lagged behind that of clinicians. Unlike their study, we also included lateral radiographs. Nevertheless, the performance of the models in fracture diagnosis was low. In this study, we also evaluated the performance of Gemini 2.5 Pro. Its performance was largely similar to that of the other models, and the small differences among the models were not clinically decisive.

Öztürk et al.,[18] in their study of 25 traumatic radiographs obtained from radiopaedia.org, found that the sensitivity of ChatGPT-4o in correctly predicting fractures was only 11%, and they argued that its performance in diagnosing fractures on radiographs was inadequate. In our study, ChatGPT-4o's sensitivity was 38%, which was slightly higher. Meanwhile, the sensitivity of ChatGPT-4.5 was 14%, and that of Gemini 2.5 Pro was 10%, both lower than that of ChatGPT-4o. These results, as also noted by Öztürk et al.,[18] demonstrated that these LLMs are inadequate in correctly processing visual information and that their capabilities are not yet reliable for medical use.

Another study, Buyuktoka et al.,[19] evaluated the performance of ChatGPT-4.5, ChatGPT-4o-mini-high, and Gemini 2.5 Pro in pediatric bone age analysis using wrist radiographs. They concluded that Gemini 2.5 Pro demonstrated the highest performance among the models. In our study, however, ChatGPT-4.5 and Gemini 2.5 Pro did not show high performance in traumatic knee radiographs. This result may suggest that the performance of LLMs varies depending on the clinical characteristics of the images.

The poor diagnostic performance of LLMs on traumatic knee radiographs can be explained by several factors. Because these models were primarily developed for text-based data rather than medical imaging, particularly trauma radiographs, their ability to accurately interpret such complex visual data may be limited. Furthermore, considering that the definitive diagnoses in our study were made using CT, another important consideration is potential selection bias. Because our cohort included only patients who underwent both knee radiography and CT, the sample likely represented more complex or ambiguous trauma cases in which initial radiographs were insufficient. Consequently, the dataset may have been skewed toward diagnostically challenging images, possibly underestimating the actual performance of LLMs in an emergency department population. Another factor that may have affected diagnostic fidelity is the conversion of DICOM images into JPEG format for compatibility with LLMs. This process could have introduced compression artifacts and reduced grayscale depth, which are essential for detecting subtle contrast cues and fracture lines. Although the images were converted at the highest possible resolution, even slight loss of pixel detail could have influenced the LLMs' visual interpretation.

Additionally, the McNemar test performed for all LLMs yielded significant results ($p<0.001$). This demonstrated that these models had an imbalance or systematic error in their classification abilities. Therefore, they currently lack sufficient capacity for fracture diagnosis and require further development.

Although not measured, the average response time for each model was up to 20 seconds after image upload, which may be considered rapid for triage settings. However, total processing time also depends on upload latency and user interaction; therefore, a comprehensive evaluation of time efficiency requires a separate analysis.

Our study had several limitations. First, it was conducted solely on radiographs. Even in cases requiring further evaluation, additional tests and physical examination findings were not provided. Therefore, some clinical parameters that might have affected performance were absent. Second, we did not measure the response times of the models. Although the response times were relatively short, we did not evaluate their potential contribution to saving time in emergency clinical practice when considering the image upload, questioning, and response evaluation processes. Third, in our study, using CT as the gold standard for fracture diagnosis may have caused case selection bias and affected the performance of LLMs.

CONCLUSION

In conclusion, our study demonstrated that the current capabilities of both ChatGPT versions and Gemini in diagnosing fractures on traumatic knee radiographs remain inferior to those of experienced clinicians. Therefore, although these LLMs are not sufficient for standalone use in fracture diagnosis, they may be used as supportive tools in the clinical decision-making process. In particular, their relatively better performance in interpreting normal radiographs highlights their potential utility in triage. Future studies with larger patient populations should incorporate diverse, high-quality datasets within the clinical context.

Ethics Committee Approval: Ethics committee approval was obtained from Gaziantep City Hospital Non-Interventional Clinical Research Ethics Committee (Approval Number: 211/2025, Date: 18.06.2025).

Informed Consent: Written informed consent was not required due to the retrospective nature of this study.

Conflict of Interest: The authors have no conflicts of interest to declare.

Funding: The authors declared that this study received no financial support.

Use of AI for Writing Assistance: No use of AI-assisted technologies was declared by the authors.

Author Contributions: Concept – OK; Design – OK, MK, BCA; Supervision – OK, IG; Resource – OK, MK, BCA, IG; Materials – OK, MK, BCA, IG; Data Collection and/or Processing - BCA, IG; Analysis and/or Interpretation - OK; Literature Review – OK, MK, BCA, IG; Writing – OK, MK, BCA, IG; Critical Review – OK, MK, BCA, IG.

Peer-review: Externally peer-reviewed.

REFERENCES

1. Oei EH, Nikken JJ, Ginai AZ, Krestin GP, Verhaar JA, van Vugt AB, et al. Acute knee trauma: value of a short dedicated extremity MR imaging examination for prediction of subsequent treatment. Radiology 2005;234(1):125-33. [CrossRef]
2. Mustonen AO, Koskinen SK, Kiuru MJ. Acute knee trauma: analysis of multidetector computed tomography findings and comparison with conventional radiography. Acta Radiol 2005;46(8):866-74. [CrossRef]
3. Avci M, Kozaci N. Comparison of X-Ray Imaging and Computed Tomography Scan in the Evaluation of Knee Trauma. Medicina (Kaunas) 2019;55(10):623. [CrossRef]
4. Teh J, Kambouroglou G, Newton J. Investigation of acute knee injury. BMJ 2012;344:e3167. [CrossRef]
5. Pinto A, Berritto D, Russo A, Riccitiello F, Caruso M, Belfiore MP, et al. Traumatic fractures in adults: missed diagnosis on plain radiographs in the Emergency Department. Acta Biomed 2018;89(1-S):111-23.
6. Venkatasamy A, Ehlinger M, Bierry G. Acute traumatic knee radiographs: beware of lesions of little expression but of great significance. Diagn Interv Imaging 2014;95(6):551-60. [CrossRef]
7. Chen Y, Zhang K, Qiang M, Li H, Dai H. Comparison of plain radiography and CT in postoperative evaluation of ankle fractures. Clin Radiol 2015;70(8):e74-82. [CrossRef]
8. Caracchini G, Pietragalla M, De Renzis A, Galluzzo M, Carbone M, Zappia M, et al. Talar fractures: radiological and CT evaluation and classification systems. Acta Biomed 2018;89(1-S):151-65.
9. Bousson V, Attané G, Benoist N, Perronne L, Diallo A, Hadid-Beurrier L, et al. Artificial Intelligence for Detecting Acute Fractures in Patients Admitted to an Emergency Department: Real-Life Performance of Three Commercial Algorithms. Acad Radiol 2023;30(10):2118-39. [CrossRef]
10. Akinci D'Antonoli T, Stanzione A, Bluethgen C, Vernuccio F, Ugga L, Klontzas ME, et al. Large language models in radiology: fundamentals, applications, ethical considerations, risks, and future directions. Diagn Interv Radiol 2024;30(2):80-90. [CrossRef]
11. Kim K, Cho K, Jang R, Kyung S, Lee S, Ham S, et al. Updated Primer on Generative Artificial Intelligence and Large Language Models in Medical Imaging for Medical Professionals. Korean J Radiol 2024;25(3):224-42. [CrossRef]
12. Bhayana R. Chatbots and Large Language Models in Radiology: A Practical Primer for Clinical and Research Applications. Radiology 2024;310(1):e232756. [CrossRef]
13. Polis B, Zawadzka-Fabijan A, Fabijan R, Kosińska R, Nowosławska E, Fabijan A. Comparative Evaluation of Large Language and Multimodal Models in Detecting Spinal Stabilization Systems on X-Ray Images. J Clin Med 2025;14(10):3282. [CrossRef]
14. Horiuchi D, Tatekawa H, Oura T, Shimono T, Walston S, Takita H, et al. Comparison of the diagnostic accuracy among GPT-4 based ChatGPT, GPT-4V based ChatGPT, and radiologists in musculoskeletal radiology. medRxiv. 2023 December 09. doi: 10.1101/2023.12.07.23299707 [Epub ahead-of-print]. [CrossRef]
15. Ozenbas C, Engin D, Altinok T, Akcay E, Aktas U, Tabanli A. ChatGPT-4o's Performance in Brain Tumor Diagnosis and MRI Findings: A Comparative Analysis with Radiologists. Acad Radiol 2025;32(6):3608-17. Erratum in: Acad Radiol 2025;32(11):6955. [CrossRef]
16. Mohammadi M, Parviz S, Parvaz P, Pirmoradi MM, Afzalimoghaddam M, Mirfazaelian H. Diagnostic performance of ChatGPT in tibial plateau fracture in knee X-ray. Emerg Radiol 2025;32(1):59-64. [CrossRef]
17. Hirosawa T, Harada Y, Yokose M, Sakamoto T, Kawamura R, Shimizu T. Diagnostic Accuracy of Differential-Diagnosis Lists Generated by Generative Pretrained Transformer 3 Chatbot for Clinical Vignettes with Common Chief Complaints: A Pilot Study. Int J Environ Res Public Health 2023;20(4):3378. [CrossRef]
18. Öztürk A, Günay S, Ateş S, Yiğit Yavuz Yigit Y. Can Gpt-4o Accurately Diagnose Trauma X-Rays? A Comparative Study with Expert Evaluations. J Emerg Med 2025;73:71-9. [CrossRef]
19. Büyüktoka RE, Salbas A. Multimodal Large Language Models for Pediatric Bone-Age Assessment: A Comparative Accuracy Analysis. Acad Radiol 2025;32(11):6905-12. [CrossRef]

Official Journal of Erciyes University Faculty of Medicine

DOI: 10.14744/cpr.2026.44798
J Clin Pract Res 2026;48(2):183–190

Diagnostic Yield and Clinical Utility of Genetic Testing in Turkish Adults with Suspected Inherited Kidney Disease: Insights from a Population with High Parental Consanguinity

Gizem Kumru,[1] Şule Altıner,[2] Ahsen Karakaya,[3] Sadiye Ekinci,[2] Timur Tuncalı,[2] Nüket Yürür Kutlay,[2] Ezgi Gökpınar İli,[2] Halil Gürhan Karabulut,[2] Sim Kutlay,[1] Şule Şengül,[1] Kenan Keven,[1] Gökhan Nergizoğlu,[1] Şehsuvar Ertürk,[1] Hatice Ilgın Ruhi,[2] Kenan Ateş[1]

[1]Department of Nephrology, Ankara University Faculty of Medicine, İbni Sina Hospital, Ankara, Türkiye
[2]Department of Medical Genetics, Ankara University Faculty of Medicine, Ankara, Türkiye
[3]Department of Internal Medicine, Ankara University Faculty of Medicine, Ankara, Türkiye

Cite this article as:
Kumru G, Altıner Ş, Karakaya A, Ekinci S, Tuncalı T, Yürür Kutlay N, et al. Diagnostic Yield and Clinical Utility of Genetic Testing in Turkish Adults with Suspected Inherited Kidney Disease: Insights From a Population With High Parental Consanguinity. J Clin Pract Res 2026;48(2):183–190.

Address for correspondence:
Gizem Kumru.
Department of Nephrology, Ankara University Faculty of Medicine, Ibni Sina Hospital, Ankara, Türkiye
Phone: +90 312 595 81 92
E-mail: gkumru@ankara.edu.tr

Submitted: 21.01.2026
Revised: 05.05.2026
Accepted: 07.05.2026
Available Online: 14.05.2026

Erciyes University Faculty of Medicine Publications - Available online at www.jcpres.com

ABSTRACT

Objective: Inherited kidney diseases (IKDs) significantly contribute to chronic kidney disease (CKD), particularly in regions with high consanguinity rates. Despite the increasing availability of next-generation sequencing, evidence regarding its diagnostic and clinical effectiveness in adult populations remains limited. This study evaluated the diagnostic yield and clinical implications of genetic testing in adults with suspected IKD.

Materials and Methods: A retrospective analysis of 63 adults who underwent genetic evaluation for unexplained or familial CKD was performed. Genetic testing used sequencing-based methods to identify and analyze genes relevant to the clinical phenotype. Clinical and demographic factors, diagnostic yield, genetic etiologies, and clinical utility were documented.

Results: The genetic diagnostic yield in this predominantly female cohort, with a mean age of 37.2±14.9 years, was 54.0%. Autosomal recessive disorders were the most common inheritance pattern (61.8%). Alport spectrum disorders represented the primary etiology (67.6%), followed by ciliopathies/cystic diseases (14.7%). The diagnostic yield varied across clinical diagnostic groups, with Alport spectrum disorders showing the highest yield and other glomerulopathies showing the lowest yield (75.0% vs. 4.5%, $p<0.001$). Extrarenal manifestations were significantly associated with a positive genetic diagnosis (32.4% vs. 0.0%, $p<0.001$). Genetic findings confirmed the clinical diagnosis in 70.6% of positive cases, reclassified the diagnosis in 17.6%, and identified an alternative genetic diagnosis in 11.8%.

Conclusion: Genetic testing demonstrated a high diagnostic yield and considerable clinical utility in Turkish adults with suspected IKD. These findings support the integration of genetic evaluation into routine nephrology practice, particularly for patients with syndromic features and a notable family history.

Keywords: Chronic kidney disease, extrarenal manifestations, genetic testing, inherited kidney diseases, next-generation sequencing.

INTRODUCTION

Chronic kidney disease (CKD) is a global public health concern, affecting approximately 15% of the adult population worldwide and 17% in Türkiye. [1] The causes of CKD are diverse, with diabetes, hypertension, and chronic glomerulonephritis identified as the main contributors; however, a substantial proportion of cases are still categorized as "CKD of unexplained cause" (CKDx) after conventional clinical or histological assessment.[2] The rapid progress of next-generation sequencing (NGS) technologies has significantly improved our understanding of kidney disease pathogenesis. Currently, more than 600 genes have been identified as contributors to monogenic kidney diseases.[3] Research indicates that up to 10–15% of adults with CKD may have an underlying monogenic cause; however, when genetic assessment is performed based on clinical suspicion, such as early onset, family history, and CKDx, the diagnostic yield increases to 50–65%.[4–8] Inherited kidney disease (IKD) and congenital abnormalities of the kidney and urinary tract (CAKUT) have recently been identified as the second most common cause of end-stage kidney disease (ESKD) among patients receiving kidney replacement therapy (KRT) in Europe.[9]

In Türkiye, the burden of IKD is higher than in many Western populations, largely because of the high prevalence of consanguineous marriages and familial clustering.[10] This genetic background increases the likelihood of autosomal recessive kidney disorders and underscores the importance of genetic evaluation in this population. Despite this, the diagnostic yield and clinical utility of genetic testing in the Turkish CKD population remain inadequately described. This study aimed to evaluate the diagnostic yield of NGS-based genetic testing in adults with suspected IKD and to assess its clinical utility, including its impact on diagnosis, patient management, and risk stratification.

MATERIAL AND METHODS

Study Design and Population

This study was a retrospective observational analysis of adult patients who underwent genetic evaluation for suspected hereditary CKD at our tertiary nephrology center. All individuals aged 16 years or older who underwent sequencing-based testing between January 2022 and June 2025 were included. Testing was ordered either because of clinical suspicion arising from factors such as a positive family history, early age at onset, or the presence of extrarenal symptoms, or as part of family screening. Individuals with incomplete clinical data or inadequate sequencing results were excluded. The study was approved by the Ankara University Human Research Ethics Committee in accordance with the Declaration of Helsinki (Approval Number: İ06-566-25, Date: 06.08.2025).

KEY MESSAGES

- Genetic testing provided a diagnosis in 54% of adults with suspected inherited kidney disease, and extrarenal manifestations were the strongest clinical predictor of a positive genetic result.
- Genetic findings confirmed, reclassified, or newly established diagnoses in approximately 30% of patients and directly influenced clinical management, including transplant donor selection.
- Integrating genetic evaluation into routine nephrology practice is essential for managing adult patients with early-onset disease, extrarenal manifestations, or a positive family history.

Sixty-three individuals from 44 families were included. Demographic and clinical data were obtained from electronic medical records, including age, sex, estimated glomerular filtration rate (eGFR; CKD-EPI 2021 [Chronic Kidney Disease Epidemiology Collaboration]), albuminuria levels, CKD duration, family history of kidney disease, parental consanguinity, presence of extrarenal manifestations, and previous kidney biopsy reports.

Variants of uncertain significance (VUS) were categorized as clinically highly concordant when an appropriate genotype–phenotype correlation was established and the variant was consistent with the inheritance pattern and family history. Cases were evaluated through a multidisciplinary review involving nephrologists and medical geneticists and were documented individually as potentially disease-causing variants.[11] Diagnostic yield was defined as the identification of pathogenic (P) or likely pathogenic (LP) variants explaining the phenotype, as well as VUS classified as potentially disease-causing. Cases without these variants were categorized as "negative."

Clinical diagnoses were classified as follows: (1) Alport spectrum disorders, (2) ciliopathy/cystic diseases, (3) CAKUT, (4) tubulopathies, and (5) glomerulopathies. Clinical utility was evaluated in terms of "diagnostic confirmation," indicating genetic findings consistent with the presumed clinical diagnosis; "diagnostic identification," involving the discovery of a new specific genetic diagnosis that was not previously suspected; and "diagnostic reclassification," in which genetic findings changed the original clinical diagnosis. Patients who tested negative and did not receive a diagnosis of IKD were classified as "excluded."

Genetic Testing and Variant Interpretation

Genomic deoxyribonucleic acid (DNA) was isolated from peripheral blood samples from all patients. Patients were

assigned to genetic testing arms based on a standardized clinical stratification protocol to minimize bias. Those presenting with isolated renal involvement or no more than one extrarenal feature were prioritized for targeted gene panel testing. In contrast, patients with multiple extrarenal manifestations were referred for whole-exome sequencing (WES) to evaluate potential syndromic conditions. QIAGEN QIAseq Targeted DNA technology was used in both approaches, and sequencing was performed on the Illumina NextSeq platform. Segregation analysis was systematically performed for all identified VUS variants, as well as for cases with strong family histories or recurrent familial phenotypes, provided that biological samples from relatives were available.

Sequencing data were aligned to the GRCh38 human reference genome and analyzed using QIAGEN bioinformatics software. For WES, more than 98% of the targeted exonic regions reached a minimum coverage depth of 20×. For targeted gene panel sequencing, more than 99% of the targeted regions reached a coverage depth of at least 100×.

Variant analysis focused on genes associated with inherited kidney disorders and was performed genome-wide for WES or within the preestablished kidney gene panel for targeted sequencing (Appendix 1). Variants with a minor allele frequency (MAF)≥1% in population databases were excluded. Rare variants consistent with the patients' clinical phenotypes and the expected mode of inheritance were prioritized. All candidate variants were analyzed and categorized in accordance with the American College of Medical Genetics and Genomics (ACMG) guidelines using population frequency data, computational predictions, and available clinical evidence.[12]

Statistical Analysis

All analyses were performed using IBM Statistical Package for the Social Sciences version 30.0 software (IBM SPSS Corp.; Armonk, NY, USA). The normality of continuous variables was assessed using the Shapiro–Wilk or Kolmogorov–Smirnov tests. Continuous variables are presented as mean±standard deviation (SD), whereas categorical variables are presented as counts and percentages. Comparisons between genetically positive and negative groups were performed using the chi-square test or Fisher's exact test for categorical variables and Student's t-test for normally distributed continuous variables, depending on data distribution. Statistical significance was set at $p<0.05$.

RESULTS

A molecular diagnosis was established in 54.0% of the 63 individuals assessed for suspected IKD (Fig. 1, Appendix 2). Most identified variants were classified as P/LP, whereas potentially disease-causing VUS accounted for a smaller proportion (47.1%, 44.1%, and 8.8%, respectively). Inheritance patterns reflected the underlying disease categories, with autosomal recessive disorders accounting for the largest proportion (61.8%), followed by autosomal dominant disorders (20.6%) and X-linked disease (17.6%). A genetic diagnosis was established in 21 of the 44 families assessed (47.7%). After excluding highly concordant VUS identified as potentially disease-causing (n=3), the individual-level diagnostic yield was 49.2%.

The patient population was predominantly female (58.7%), with a mean age of 37.2±14.9 years. Demographic characteristics, including sex distribution and age at the time of genetic testing, were comparable between the genetically positive and negative groups (Table 1). Similarly, kidney function, assessed by eGFR and albuminuria categories, did not differ significantly at the time of genetic evaluation. A family history of kidney disease was observed in both groups (88.2% vs. 72.4%), whereas parental consanguinity showed no association with diagnostic yield. Notably, the presence of extrarenal manifestations was significantly associated with a positive genetic diagnosis (32.4% vs. 0%, $p<0.001$). Despite comparable kidney biopsy rates between groups, it was noteworthy that 5 of the 11 patients diagnosed with an IKD who had previously undergone kidney biopsy were diagnosed with focal segmental glomerulosclerosis and subsequently received immunosuppressive therapy. Other clinical variables, including CKD duration and the indication for genetic evaluation (clinical suspicion vs. family screening), were not significantly associated with a positive diagnostic outcome. However, 54.2% (n=13) of patients with Alport spectrum disorders and 66.7% (n=3) of patients with CAKUT were identified through familial screening ($p=0.029$).

Before genetic evaluation, the most frequent clinical diagnoses were Alport spectrum disorder (38.1%) and glomerulopathy (34.9%). Genetic testing confirmed the clinical diagnosis in 70.6% of genetically positive individuals, established a new specific diagnosis in an additional 11.8%, and reclassified the presumed diagnosis in 17.6%, thereby demonstrating substantial clinical utility (Fig. 1d). Alport spectrum disorders represented the predominant diagnosis, comprising more than two-thirds of genetically confirmed cases (Fig. 2). Ciliopathies and cystic diseases accounted for 14.7%, whereas CAKUT accounted for 8.8%. Accordingly, *COL4A3*, *COL4A4*, and *COL4A5* were identified as the most prevalent disease-causing genes, including 13 affected heterozygous individuals who were diagnosed through family screening. Disease-causing variants in *PKD1*, *SALL1*, *NPHP3*, *TSC2*, *CTNS*, *CLDN16*, and *COQ6* were less frequent but clinically relevant. After the initial detection of 8 probands, familial screening led to the diagnosis of 14 additional individuals who were previously unaware of the genetic diagnosis.

Table 1. Demographic and clinical data of patients according to genetic diagnosis

Variables	Positive (n=34, 54.0%)	Negative (n=29, 46.0%)	p	Total (n=63, 100.0%)
Female sex	20 (58.8)	17 (58.6)	0.987	37 (58.7)
Age at genetic evaluation (years)	38.2±16.2	35.1±12.7	0.283	37.2±14.9
eGFR at genetic evaluation (CKD-EPI 2021, ml/min/1.73m^2)				0.332
90 or higher	14 (41.2)	8 (27.6)		22 (34.9)
60–89	0 (0.0)	3 (10.3)		3 (4.8)
30–59	6 (17.6)	4 (13.8)		10 (15.9)
15–29	2 (5.9)	3 (10.3)		5 (7.9)
<15	12 (35.3)	11 (37.9)		23 (36.5)
Albuminuria at genetic evaluation (mg/g)			0.989	
<30	12 (35.3)	10 (34.5)		22 (34.9)
30–299	5 (14.7)	4 (13.8)		9 (14.3)
300 or higher	17 (53.1)	15 (51.7)		32 (50.8)
CKD history	22 (64.7)	23 (79.3)	0.201	45 (71.4)
Family history of kidney diseases	30 (88.2)	21 (72.4)	0.111	51 (81.0)
Parental consanguinity	11 (32.4)	8 (27.6)	0.681	19 (30.2)
Extrarenal manifestations	11 (32.4)	0 (0.0)	**<0.001**	11 (17.5)
Time between CKD diagnosis and genetic evaluation (years)	8.4±5.8	7.8±6.9	0.747	8.1±6.3
Kidney biopsy before genetic evaluation	11 (32.4)	11 (37.9)	0.643	22 (34.9)
Genetic evaluation indication			0.259	
Clinical suspicion	20 (58.8)	21 (72.4)		41 (65.1)
Family screening	14 (41.2)	8 (27.6)		22 (34.9)
Clinical diagnosis before genetic evaluation			**0.039**	
Alport spectrum disorders	18 (52.9)	6 (20.7)		24 (38.1)
Ciliopathy/cystic diseases	3 (8.8)	1 (3.4)		4 (6.3)
CAKUT	2 (5.9)	5 (17.2)		7 (11.1)
Tubulopathies	3 (8.8)	3 (10.3)		6 (9.5)
Glomerulopathies	8 (23.5)	14 (48.3)		22 (34.9)

The values are described as the mean ± standard deviation or number (%). Values appears in bold if p-value was significant (below 0.05). CAKUT: Congenital anomalies of the kidney and urinary tract; CKD: Chronic kidney disease; CKD-EPI: Chronic Kidney Disease Epidemiology Collaboration; eGFR: Estimated glomerular filtration rate.

Figure 3a shows that clinical utility differed across diagnostic categories. The categories with the highest utility were Alport spectrum disorders (66.7%) and ciliopathies/cystic diseases (50.0%) (p=0.008). Alport spectrum disorders showed the highest diagnostic rate (75.0%), whereas glomerulopathies (4.5%) and CAKUT (28.6%) had considerably lower yields (p<0.001, Fig. 3b).

DISCUSSION

In this cohort of adults assessed for suspected IKD, the genetic diagnostic yield was 54%, primarily attributed to Alport spectrum disorders. Extrarenal manifestations were identified as the main clinical predictor of positive genetic findings, highlighting the diagnostic importance of syndromic features in adult CKD. In most positive cases, genetic data supported the clinical diagnosis and directly influenced management decisions, including the assessment of potential living kidney donors. These findings indicate that genetic testing provides significant diagnostic and clinical benefits for adults with unexplained CKD, particularly in populations with a high familial disease burden and a greater prevalence of recessive disorders.

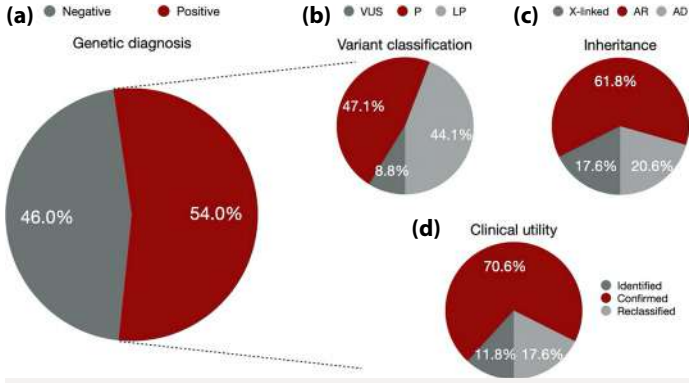

Figure 1. Results of genetic testing and patterns of inheritance. **(a)** Results classified into positive and negative categories. **(b)** Positive results classified as VUS or P/LP variants expected to cause disease. **(c)** Inheritance patterns of positive results, classified as AR, AD, or X-linked. **(d)** Clinical utility of genetic testing.

AD: Autosomal dominant; AR: Autosomal recessive; P/LP: Pathogenic/likely pathogenic; VUS: Variants of uncertain significance.

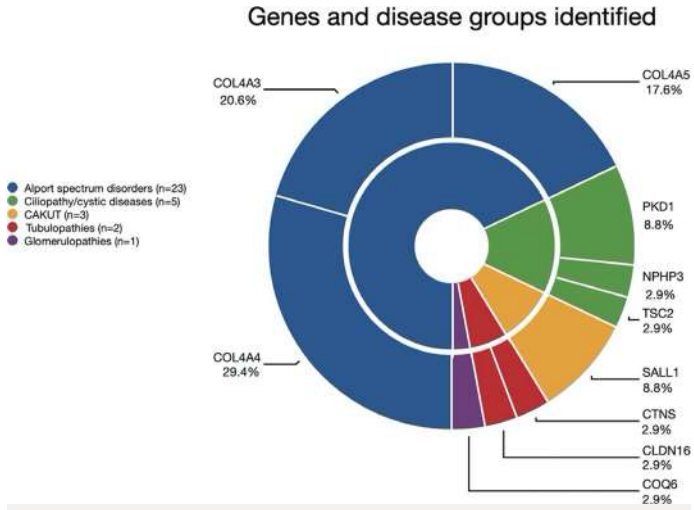

Figure 2. Overview of the study findings. The inner circle illustrates the identified disease groups, whereas the outer circle presents the genes associated with disease-causing variants identified in the study.

CAKUT: Congenital abnormalities of the kidney and urinary tract.

This study demonstrated that the *COL4A4*, *COL4A3*, and *COL4A5* genes accounted for 67.6% of genetic diagnoses, establishing Alport spectrum disorders as the most prevalent category. In large adult cohort studies of patients with early-onset CKD, 8 genes—*COL4A3*, *COL4A4*, *COL4A5*, *HNF1B*, *PKD1*, *PKD2*, *PKHD1*, and *UMOD*—were found to account for approximately two-thirds of disease-causing variants; however, Alport spectrum disorders were identified in only 15–22% of these cases.[6,7] This discrepancy may be explained by the enrichment of individuals undergoing donor screening, who may have had a higher likelihood of harboring pathogenic mutations in the *COL4A3–COL4A5* genes. Indeed, the exclusion of donor-screening cases (n=6) resulted in a reduced yet still substantial proportion of Alport spectrum disease diagnoses (n=17, 50.0%). Referral bias likely influenced this distribution, as individuals with suspected hereditary nephropathies, especially those with hematuria or a family history suggestive of Alport syndrome, may have been preferentially selected for genetic testing. Polycystic kidney diseases significantly contribute to the etiology of ESKD in Türkiye.[13] The lower prevalence of cystic kidney diseases in this study cohort, compared with national and global statistics, may be attributed to diagnoses based on family history and typical clinical presentation, which reduces the need for genetic testing.

Genetic testing provides diagnostic results in 10–20% of adult CKD patients, whereas this percentage increases to 37–65% among individuals with suspected IKD.[5–7,14–16] The young age of the cohort and the high prevalence of CKD history among patients and their families contributed to the 54.0% rate of positive genetic test results observed in our study. A family history of kidney disease is an established factor associated with genetic diagnosis.[17] However, in our cohort, more than 70% of patients and their families reported a history of CKD, and the genetic diagnostic yield remained consistent across groups. The presence of extrarenal features significantly influenced diagnostic yield, with such manifestations observed only in patients with a positive genetic diagnosis. Connaughton et al.[16] demonstrated that a monogenic etiology was identified in 36% of families with a positive family history of CKD, although the rate increased to 69% in families with extrarenal features. The broad spectrum of clinical features also contributes to substantial heterogeneity in the likelihood of obtaining a positive genetic result across different disease groups. Consistent with this, in the Alport group in our study, which had the highest genetic diagnostic yield, 95.8% of patients (n=23) had a family history of CKD, with 13 individuals (54.2%) diagnosed through family screening. These findings support the integration of genetic analysis into nephrology practice, especially for patients with extrarenal manifestations, familial disease patterns, or phenotypes suggestive of monogenic disorders, as it can markedly improve diagnostic precision.[18]

The clinical diagnosis was confirmed in 70.6% of individuals with a positive genetic result in this cohort. The predominance of diagnostic confirmation in the Alport and ciliopathy groups, compared with the lower rate in glomerulopathies,

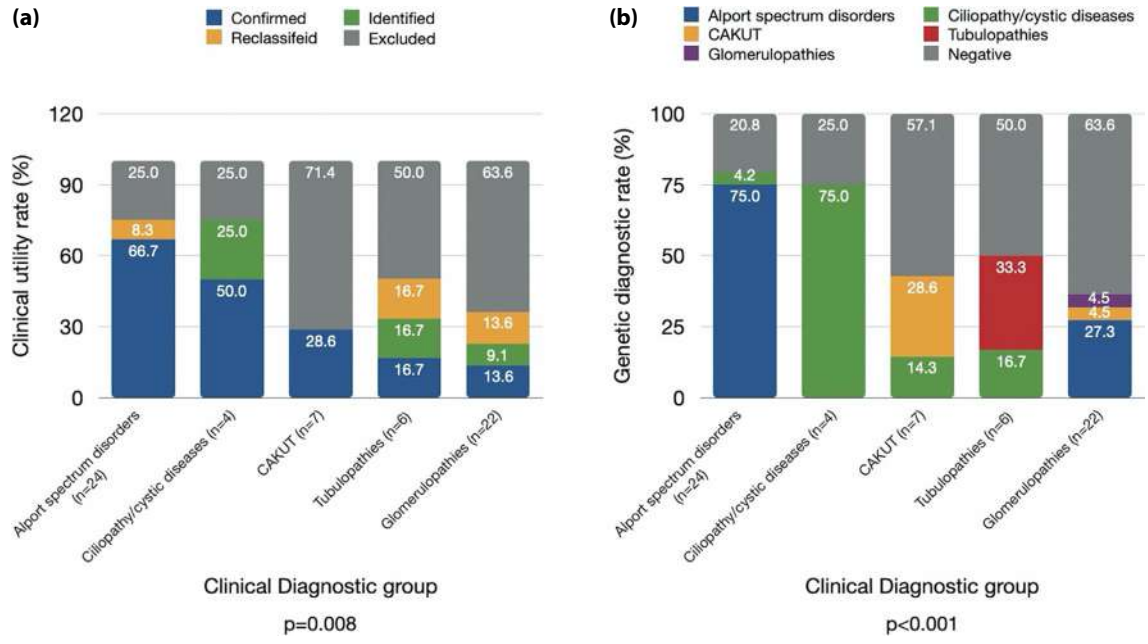

Figure 3. (a) Clinical utility yield across clinical diagnostic groups. **(b)** Genetic diagnostic yield across clinical diagnostic groups. The x-axis represents the distribution of patients across five clinical diagnostic groups before genetic testing. The y-axis illustrates the diagnostic and clinical utility yield resulting from genetic testing.

CAKUT: Congenital abnormalities of the kidney and urinary tract.

underscores the advantages of genetic testing in cases with well-defined genotype–phenotype correlations. Furthermore, a specific diagnosis was established in 11.8% of cases, and the presumptive diagnosis was reclassified in 17.6%. Consequently, a novel etiology of CKD was identified in approximately 30% of patients. The literature indicates that this patient population has high post-diagnosis management change rates, ranging from 20% to 60%.[6,15,16] Physicians have reported that genetic findings influence the medical care of 90.7% of patients with positive results, leading to changes in treatment plans, referrals for genetic counseling, guidance for genetic testing of family members, and discussions about family planning.[15] In our cohort, genetic diagnosis altered clinical interpretation in a subset of patients, particularly in 5 individuals with presumed FSGS in whom immunosuppressive therapy had been initiated but was subsequently considered unnecessary. This highlights the potential of genetic testing to prevent inappropriate treatment and related toxicity. Furthermore, all patients diagnosed with IKD received genetic counseling, and familial screening was advised according to the inheritance pattern. Given these potential advantages, essential precautions should be implemented to address barriers that prevent nephrologists from requesting genetic testing, such as insufficient genetic literacy, challenges in test selection, and time limitations.[19]

Genetic testing also provides several advantages for kidney transplant recipients and donors, including personalized interventions, risk stratification for recurrent disease, and risk assessment for potential donors.[20] Kidney donors are at increased risk of hypertension and ESKD, as well as increased cardiovascular morbidity and mortality.[21] Therefore, potential donors must undergo a thorough evaluation to reduce post-donation risks. Assessing ESKD risk in individuals with VUS and in heterozygous individuals affected by Alport syndrome is crucial for selecting living kidney transplant donors, as well as for those who receive a genetic diagnosis.[22] In this context, 9 potential kidney donors were evaluated in our cohort, leading to the acceptance of 2 candidates with negative results and 5 candidates who were heterozygous for Alport syndrome without clinical manifestations (Table S2, Patient IDs 4, 13, 15, 19, and 23). Two individuals diagnosed with Alport syndrome who presented with urinary abnormalities were disqualified based on genetic findings (Table S2, Patient IDs 1 and 2).

This study provides real-world data from a well-characterized adult cohort in a region with a high prevalence of IKD, offering valuable insights into the diagnostic utility of NGS in routine nephrology practice. The findings provide data that may help prioritize patients for genetic testing, as the inclusion criteria were designed to exclude individuals with

a low likelihood of a monogenic etiology, thereby enhancing the cost-effectiveness of genetic testing. However, certain limitations should be noted. The single-center, retrospective design may limit generalizability, and referral bias may have enriched the cohort with patients with more severe or syndromic presentations. The sample size limited the ability to conduct subgroup analyses for less prevalent disease categories. The high prevalence of familial CKD history and the younger mean age of this cohort relative to the general CKD population should be considered when extrapolating the findings. Intra-family clustering may challenge the assumption of independent observations, as multiple members of the same families were included. However, the 47.7% diagnostic yield at the family level suggests that the clustering effect was not substantial in this study. Participants aged ≥16 years were included, as this threshold is commonly used in clinical nephrology for transitioning patients to adult-oriented care settings. This should be considered when interpreting the findings, as the study population may include a small proportion of late adolescents. The use of a targeted gene panel rather than whole-exome sequencing requires regular updates to the gene list and may limit the identification of novel causal genes. The absence of functional studies for VUS is another limitation, as such analyses are necessary to determine their biological impact and support potential reclassification. A further limitation is that exon-level copy number variant (CNV) analysis was not uniformly applied across all cases, which may have limited the detection of certain structural variants; however, this reflects current real-world diagnostic practice in many clinical settings.

CONCLUSION

In this cohort of adults evaluated for suspected IKD, genetic testing provided a high diagnostic yield and demonstrated substantial clinical value. The presence of extrarenal manifestations was a significant indicator of a positive molecular diagnosis, highlighting the importance of careful clinical assessment in identifying appropriate testing strategies. Importantly, genetic findings not only confirmed or redefined clinical diagnoses but also informed essential management decisions, including the suitability of potential living kidney donors. These epidemiological characteristics underscore the importance of incorporating genetic evaluation into routine nephrology practice, particularly for patients with early-onset disease, extrarenal manifestations, or a positive family history.

Ethics Committee Approval: Ethics committee approval was obtained from Ankara University Human Research Ethics Committee in accordance with the Declaration of Helsinki (Approval Number: İ06-566-25, Date: 06.08.2025).

Informed Consent: Written informed consent was obtained for genetic testing.

Conflict of Interest: The authors have no conflicts of interest to declare.

Funding: The authors declared that this study received no financial support.

Use of AI for Writing Assistance: No use of AI-assisted technologies was declared by the authors.

Author Contributions: Concept – GK, SA; Design – GK, SA; Supervision – SK, SS, KK, GN, SE, KA; Materials – GK, SA, AK; Data Collection and/or Processing – GK, SA, AK; Analysis and/or Interpretation – GK, SA, SE, TT, NYK, EGI, HGK, HIR; Literature Review – GK, SA; Writing – GK, SA; Critical Review – SK, SS, KK, GN, SE, HIR, KA.

Peer-review: Externally peer-reviewed.

REFERENCES

1. GBD 2023 Chronic Kidney Disease Collaborators. Global, regional, and national burden of chronic kidney disease in adults, 1990-2023, and its attributable risk factors: a systematic analysis for the Global Burden of Disease Study 2023. Lancet 2025;406(10518):2461-82.
2. Halbritter J, Figueres L, Van Eerde AM, Capasso G, Hoorn EJ, Nijenhuis T, et al. Chronic Kidney Disease of unexplained cause (CKDx): a consensus statement by the Genes & Kidney Working Group of the ERA. Nephrol Dial Transplant 2025;40(12):2390-400. [CrossRef]
3. Stark Z, Byrne AB, Sampson MG, Lennon R, Mallett AJ. A guide to gene-disease relationships in nephrology. Nat Rev Nephrol 2025;21(2):115-26. [CrossRef]
4. Mallett A, Patel C, Salisbury A, Wang Z, Healy H, Hoy W. The prevalence and epidemiology of genetic renal disease amongst adults with chronic kidney disease in Australia. Orphanet J Rare Dis 2014;9:98. [CrossRef]
5. Groopman EE, Marasa M, Cameron-Christie S, Petrovski S, Aggarwal VS, Milo-Rasouly H, et al. Diagnostic Utility of Exome Sequencing for Kidney Disease. N Engl J Med 2019;380(2):142-51. [CrossRef]
6. Domingo-Gallego A, Pybus M, Bullich G, Furlano M, Ejarque-Vila L, Lorente-Grandoso L, et al. Clinical utility of genetic testing in early-onset kidney disease: seven genes are the main players. Nephrol Dial Transplant 2022;37(4):687-96. [CrossRef]
7. Snoek R, van Jaarsveld RH, Nguyen TQ, Peters EDJ, Elferink MG, Ernst RF, et al. Genetics-first approach improves diagnostics of ESKD patients <50 years old. Nephrol Dial Transplant 2022;37(2):349-57. [CrossRef]
8. Abu Al Rub F, Elsurer Afsar R, Fleetwood VA, Bastani B, Randall H, Nazzal M, et al. The Diagnostic Yield of Genomic

Sequencing-based Genetic Kidney Disease Testing in Kidney Transplant Candidates: Experience at an Urban US Transplant Center. Transplantation 2025;109(7):1201-8. [CrossRef]

9. Ortiz A, Kramer A, Ariceta G, Rodríguez Arévalo OL, Gjerstad AC, Santiuste C, et al. Inherited kidney disease and CAKUT are common causes of kidney failure requiring kidney replacement therapy: an ERA Registry study. Nephrol Dial Transplant 2025;40(5):1020-31. [CrossRef]
10. Demir E, Caliskan Y, Aliyeva N, Yilmaz O, Celik D, Usta Akgul S, et al. Importance of Parental Consanguinity and Family History of Kidney Disease in the Turkish Adult Chronic Kidney Disease Population: An Epidemiologic Study. Turk J Nephrol 2024;33(4):333-41. [CrossRef]
11. Franceschini N, Feldman DL, Berg JS, Besse W, Chang AR, Dahl NK, et al.; NKF Genetic Testing Working Group. Advancing Genetic Testing in Kidney Diseases: Report From a National Kidney Foundation Working Group. Am J Kidney Dis 2024;84(6):751-66. [CrossRef]
12. Richards S, Aziz N, Bale S, Bick D, Das S, Gastier-Foster J, et al.; ACMG Laboratory Quality Assurance Committee. Standards and guidelines for the interpretation of sequence variants: a joint consensus recommendation of the American College of Medical Genetics and Genomics and the Association for Molecular Pathology. Genet Med 2015;17(5):405-24. [CrossRef]
13. Turkish Society of Nephrology Registry Board. National Nephrology, Dialysis and Transplantation Registry Report of Turkey 2024. https://nefroloji.org.tr/uploads/pdf/REGISTRY_2024_web.pdf. Accessed May 12, 2026
14. Blasco M, Quiroga B, García-Aznar JM, Castro-Alonso C, Fernández-Granados SJ, Luna E, et al.; GENSEN Study Investigators. Genetic Characterization of Kidney Failure of Unknown Etiology in Spain: Findings From the GENSEN Study. Am J Kidney Dis 2024;84(6):719-30.e1.
15. Dahl NK, Bloom MS, Chebib FT, Clark D, Westemeyer M, Jandeska S, et al. The Clinical Utility of Genetic Testing in the Diagnosis and Management of Adults with Chronic Kidney Disease. J Am Soc Nephrol 2023;34(12):2039-50. [CrossRef]
16. Connaughton DM, Kennedy C, Shril S, Mann N, Murray SL, Williams PA, et al. Monogenic causes of chronic kidney disease in adults. Kidney Int 2019;95(4):914-28. [CrossRef]
17. Mallawaarachchi AC, Fowles L, Wardrop L, Wood A, O'Shea R, Biros E, et al. Genomic Testing in Patients with Kidney Failure of an Unknown Cause: A National Australian Study. Clin J Am Soc Nephrol 2024;19(7):887-97. [CrossRef]
18. Knoers N, Antignac C, Bergmann C, Dahan K, Giglio S, Heidet L, et al. Genetic testing in the diagnosis of chronic kidney disease: recommendations for clinical practice. Nephrol Dial Transplant 2022;37(2):239-54. [CrossRef]
19. de Haan A, Eijgelsheim M, Vogt L, Hoorn EJ, Rotmans JI, Fortrie G, et al. Genetic testing in a national cohort of adults with chronic kidney disease of unknown origin. Nephrol Dial Transplant 2025;40(6):1225-33. [CrossRef]
20. Gillion V, Devresse A, Olinger E, Dahlqvist G, Demoulin N, Godefroid N, et al. Monogenic Kidney Diseases in Kidney Transplantation. Kidney Int Rep 2023;9(3):549-68. [CrossRef]
21. Kumru G, Lentine KL. Hypertension in living kidney donors: understanding the real risk. Clin Kidney J 2024;17(9):sfae244. [CrossRef]
22. Caliskan Y, Lee B, Whelan A, Abualrub F, Lentine KL, Jittirat A. Evaluation of Genetic Kidney Diseases in Living Donor Kidney Transplantation: Towards Precision Genomic Medicine in Donor Risk Assessment. Curr Transplant Rep 2022;9(2):127-42. [CrossRef]

Appendix 1. List of genes included in the targeted nephropathy panel (97 genes)

Gene symbol	Gene symbol	Gene symbol	Gene symbol	Gene symbol	Gene symbol
ACE	*CLDN16*	*GLA*	*NEK8*	*PKHD1*	*SMARCAL1*
ACTN4	*COL4A3*	*GLIS2*	*NFIA*	*PLCE1*	*SOX17*
AGXT	*COL4A4*	*GRHPR*	*NPHP1*	*PTPRO*	*TCTN2*
APRT	*COL4A5*	*GSN*	*NPHP3*	*RET*	*TMEM216*
ATP6V0A4	*COL4A6*	*HNF1B*	*NPHP4*	*SALL1*	*TMEM231*
AVPR2	*COQ2*	*HPSE2*	*NPHS1*	*SCARB2*	*TMEM237*
B9D1	*COQ6*	*INF2*	*NPHS2*	*SCNN1A*	*TMEM67*
B9D2	*COQ8B*	*INVS*	*NR3C2*	*SCNN1B*	*TRPC6*
BICC1	*CPLANE1*	*IQCB1*	*NUP93*	*SLC12A1*	*TTC21B*
BSND	*CTNS*	*KCNJ1*	*NXF5*	*SLC12A3*	*UMOD*
CA2	*DNASE1L3*	*LAMB2*	*OCRL*	*SLC3A1*	*UPK3A*
CC2D2A	*FAN1*	*LMX1B*	*OSGEP*	*SLC4A4*	*USF2*
CCNQ	*FRAS1*	*LPIN1*	*PAX2*	*SLC5A1*	*WNK1*
CD2AP	*FREM2*	*MAP3K14*	*PDSS2*	*SLC5A2*	*WNK4*
CDC5L	*FXYD2*	*MKS1*	*PKD1*	*SLC7A9*	*WT1*
CEP290	*GATA3*	*MYO1E*	*PKD2*	*SLC9A3R1*	*XDH*
CLCN5					

Appendix 2. Disease-causing variants identified in the cohort (n=34)

Patient ID	Age at Dx	Sex	Kidney manifestation	Extrarenal manifestations	Indication	Family history	Gene and transcript (inheritance)	Variant	Zygosity	Variant classification
Alport spectrum disorders										
1	42	M	Nephrotic range proteinuria	SNHL	Clinical suspicion	Yes	*COL4A4* NM_000092 (AR)	c.1321_1369+3del*	Hom	P
2	51	F	Mild proteinuria	No	Family screening	Yes	*COL4A4* NM_000092 (AR)	c.1321_1369+3del*	Aff. Het	P
3	24	F	Nephrotic range proteinuria, reduced GFR	SNHL	Clinical suspicion	Yes	*COL4A4* NM_000092 (AR)	c.372+1G>A	Hom	LP
4	57	F	Hematuria	No	Family screening	Yes	*COL4A4* NM_000092 (AR)	c.372+1G>A	Aff. Het	LP
5	50	M	No	No	Family screening	Yes	*COL4A4* NM_000092 (AR)	c.372+1G>A	Aff. Het	LP
6	16	F	No	No	Family screening	Yes	*COL4A4* NM_000092 (AR)	c.372+1G>A	Aff. Het	LP
7	25	F	Hematuria	No	Family screening	Yes	*COL4A4* NM_000092 (AR)	c.372+1G>A	Hom	LP
8	38	F	Moderate proteinuria, reduced GFR	No	Clinical suspicion	Yes	*COL4A4* NM_000092 (AR)	c.1321_1369+3del	Aff. Het	P
9	51	F	Moderate proteinuria, reduced GFR	No	Clinical suspicion	Yes	*COL4A4* NM_000092 (AR)	c.5032C>T p.Q1678*	Hom	LP
10	48	M	Nephrotic range proteinuria, reduced GFR	No	Clinical suspicion	Yes	*COL4A4* NM_000092 (AR)	c.3807T>G p.Asp1269Glu	Aff.Het	VUS
11	16	F	Nephrotic range proteinuria,	SNHL	Clinical suspicion	Yes	*COL4A3* NM_000091.5 (AR)	c.2371C>T p.Arg791*	Hom	P
12	64	F	Mild proteinuria	No	Family screening	Yes	*COL4A3* NM_000091.5 (AR)	c.2371C>T p.Arg791*	Aff. Het	P
13	45	M	Mild proteinuria	No	Family screening	Yes	*COL4A3* NM_000091.5 (AR)	c.2371C>T p.Arg791*	Aff. Het	P
14	18	M	Moderate proteinuria, hematuria	SNHL	Clinical suspicion	Yes	*COL4A3* NM_000091.5 (AR)	c.2371C>T p.Arg791*	Hom	P
15	48	M	No	No	Family screening	Yes	*COL4A3* NM_000091.5 (AR)	c.2371C>T p.Arg791*	Aff. Het	P
16	46	F	Moderate proteinuria, hematuria	No	Clinical suspicion	Yes	*COL4A3* NM_000091.5 (AR)	c.898G>A p.Gly300Arg	Aff. Het	LP
17	48	F	Moderate proteinuria	No	Family screening	Yes	*COL4A3* NM_000091.5 (AR)	c.898G>A p.Gly300Arg	Hom	LP
18	43	M	Nephrotic range proteinuria, reduced GFR	No	Clinical suspicion	Yes	*COL4A5* NM_000495.5 (XL)	c.3052G>T p.Gly1018Cys	Hemi	LP
19	63	F	Hematuria	No	Family screening	Yes	*COL4A5* NM_000495.5 (XL)	c.3052G>T p.Gly1018Cys	Aff. Het	LP
20	40	F	Hematuria	No	Family screening	No	*COL4A5* NM_000495.5 (XL)	c.3052G>T p.Gly1018Cys	Aff. Het	LP
21	16	M	Moderate proteinuria, hematuria	SNHL	Clinical suspicion	Yes	*COL4A5* NM_000495.5 (XL)	c.3170G>T p.Gly1057Val	Hemi	P
22	16	M	Nephrotic range proteinuria, reduced GFR	SNHL	Clinical suspicion	Yes	*COL4A5* NM_000495.5 (XL)	c.3170G>T p.Gly1057Val	Hemi	P
23	46	F	No	No	Family screening	Yes	*COL4A5* NM_000495.5 (XL)	c.3170G>T p.Gly1057Val	Aff.Het	P
Ciliopathy/cystic disorders										
24	42	F	Nephrotic range proteinuria, reduced GFR	*Bronchiectasis*	Clinical suspicion	No	*PKD1* NM_001009944.3 (AD)	c.1522T>C p.Cys508Arg	Het	LP
25	16	M	Medullary nephrocalcinosis	No	Clinical suspicion	Yes	*PKD1* NM_001009944.3 (AD)	c.12607C>T p.Arg4203Trp	Het	VUS
26	63	M	Polycystic kidney	No	Clinical suspicion	Yes	*TSC2* NM_000548.5 (AD)	c.5238_5255del p.His1746_Arg1751del	Het	P
27	54	F	Angiomyolipomas	Epilepsy, LAM, angiofibromas	Clinical Suspicion	Yes	*NPHP3* NM_153240.5 (AR)	c.3287T>C p.Leu1096Pro	Hom	LP
28	58	M	Polycystic kidney	No	Clinical Suspicion	Yes				
CAKUT										
29	20	F	Reduced GFR	Hallux anomaly, mild intellectual disability	Clinical suspicion	Yes	*SALL1* NM_002968.3 (AD)	c.2287dupA p.Arg763Lysfs*42	Het	P
30	21	M	Reduced GFR	No	Family screening	Yes	*SALL1* NM_002968.3 (AD)	c.2287dupA p.Arg763Lysfs*42	Het	P
31	45	F	Reduced GFR	No	Family screening	Yes	*SALL1* NM_002968.3 (AD)	c.2287dupA p.Arg763Lysfs*42	Het	P
Tubulopathies										
32	26	F	Fanconi syndrome	Neurologic dysfunction, ocular involvement, diabetes	Clinical suspicion	No	*CTNS* NM_004937.3 (AR)	c.681G>A p.Glu227Glu	Hom	P
33	24	M	Bilateral atrophic kidneys	*Pure* red cell *aplasia*	Clinical suspicion	Yes	*CLDN16* NM_006580.4 (AR)	c.130C>T p.R44*	Hom	LP
Glomerulopathies										
34	16	F	Nephrotic range proteinuria	No	Clinical suspicion	No	*COQ6* NM_182476.3 (AR)	c.1383del p.Ilr462LeufsTer18	Hom	VUS

A: adenine; AD: autosomal dominant; Aff: Affected; AR: Autosomal recessive; CAKUT: Congenital anomalies of the kidney and urinary tract; Dx: Diagnosis; F: Female; GFR: Glomerular filtration rate; Hemi: Hemizygous; Het: Heterozygous; Hom: Homozygous; LAM: Lymphangioleiomyomatosis; LP: Likely pathogenic; M: Male; P: Pathogenic; SNHL: Sensorineural hearing loss; VUS: Variant of uncertain significance; XL: X-linked.

Official Journal of Erciyes University Faculty of Medicine

DOI: 10.14744/cpr.2026.23949
J Clin Pract Res 2026;48(2):191–201

Effect of Continuous Non-Invasive Hemoglobin Monitoring on Blood Transfusion and Mortality in Hip Surgeries: A Randomized Controlled Study

Merve Ezgi Dinçer Yeşilnacar,[1] Özcan Pişkin,[1] Bengü Gülhan Köksal İncegül,[1] Çağdaş Baytar,[1] Rahşan Dilek Okyay,[1] Şule Altuncu,[1] Keziban Bollucuoğlu,[1] Gamze Küçükosman,[2] Hilal Ayoğlu[1]

[1]Department of Anesthesiology and Reanimation, Zonguldak Bülent Ecevit University Faculty of Medicine, Zonguldak, Türkiye
[2]Department of Anesthesiology and Reanimation, Trabzon Health Sciences University, Faculty of Medicine, Trabzon, Türkiye

This study was presented orally at the 4th Zonguldak Spring Symposium, held in Zonguldak, Türkiye on April 20, 2024.

Cite this article as:
Dinçer Yeşilnacar ME, Pişkin Ö, Köksal İncegül BG, Baytar Ç, Okyay RD, Altuncu Ş, et al. Effect of Continuous Non-Invasive Hemoglobin Monitoring on Blood Transfusion and Mortality in Hip Surgeries: A Randomized Controlled Study. J Clin Pract Res 2026;48(2):191–201.

Address for correspondence:
Özcan Pişkin.
Department of Anesthesiology and Reanimation, Zonguldak Bülent Ecevit University Faculty of Medicine, Zonguldak, Türkiye
Phone: +90 505 456 24 49
E-mail: drozcanp@gmail.com

Submitted: 20.01.2026
Revised: 06.05.2026
Accepted: 07.05.2026
Available Online: 14.05.2026

Erciyes University Faculty of Medicine Publications - Available online at www.jcpres.com

ABSTRACT

Objective: This study aimed to determine the effect of non-invasive hemoglobin (SpHb) measurement on blood transfusion decisions in patients undergoing hip surgery and to analyze the effect of these decisions on mortality.

Materials and Methods: Fifty-two patients (ASA I–III, ≥60 years) undergoing hip surgery were randomized into the SpHb or conventional (CONV) group for transfusion management. Hemoglobin (Hb) levels were recorded before induction, at transfusion decision points, immediately after transfusion, and after recovery. Postoperative survival was monitored at 1 and 3 months.

Results: The SpHb group maintained significantly higher Hb levels at the first transfusion decision point, after transfusion, and during recovery (p=0.001, p=0.012, p=0.001). Partial oxygen pressure (PaO_2) was also higher in the SpHb group at the corresponding time points. The CONV group required significantly more blood transfusions (p=0.025) and had longer hospital stays (p=0.043). Although 3-month mortality was numerically lower in the SpHb group than in the CONV group (11.53% vs. 19.23%), no statistically significant difference was detected in this pilot-sized cohort (p>0.05).

Conclusion: According to our findings, SpHb monitoring during hip surgery may be a useful tool for enabling earlier transfusion decisions, which could help prevent significant Hb declines. In our study cohort, this strategy was associated with a trend toward fewer transfusion requirements, shorter hospital stays, and better perioperative oxygenation.

Keywords: Hemoglobins, hemorrhage, hip fractures, intraoperative, monitoring, mortality.

INTRODUCTION

Blood loss is a major cause of morbidity and mortality. In cases of excessive bleeding, the amount of bleeding should be calculated immediately, tests should be completed within a short time, and treatment

should be started.[1] Hip and revision hip arthroplasty surgeries are performed frequently worldwide, and studies have reported that 18–65% of these operations require blood transfusion.[2]

Blood replacement has several complications in addition to its benefits, including providing oxygen supply to tissues and preventing deterioration of organ perfusion.[3] Complications include allergic reactions, transfusion-related circulatory overload, infections, transfusion-related acute lung injury, and thromboembolism. It is also associated with several adverse conditions, including delayed wound healing, acute kidney injury, sepsis, prolonged hospitalization, and mortality.[2–4]

Laboratory-measured complete blood count (CBC) hemoglobin (Hb) level is the primary parameter used to guide transfusion decisions in bleeding operations. However, continuous and non-invasive technologies, such as fingertip probe monitoring, have gained prominence. Bedside non-invasive hemoglobin (SpHb) monitoring offers rapid data collection and allows continuous assessment without additional invasive interventions.[5]

In this study, we examined the differences between blood transfusion decisions made using standard methods and those based on SpHb monitoring in patients undergoing hip surgery. We predicted that SpHb-monitored patients would have lower mortality rates and improved clinical outcomes.

The primary aim of this study was to compare blood transfusion decisions based on SpHb monitoring with those based on conventional methods in patients undergoing hip surgery. Secondarily, it aimed to investigate the effects of these decisions on perioperative oxygenation, length of hospital stay, and mortality. We hypothesized that SpHb-monitored patients would have decreased mortality rates and improved clinical outcomes.

KEY MESSAGES

- Continuous non-invasive hemoglobin (SpHb) monitoring enables earlier transfusion decisions by identifying critical hemoglobin thresholds more accurately than conventional methods in surgeries associated with high bleeding risk.
- The use of SpHb monitoring in hip surgery significantly reduces the total number of red blood cell units transfused and shortens the length of hospital stay.
- Although SpHb monitoring improves perioperative oxygenation and transfusion management, 30-day and 90-day mortality rates remain similar to those associated with conventional transfusion decision-making methods

MATERIALS AND METHODS

Study Place and Design

Following ethical approval from the Zonguldak Bülent Ecevit University, this prospective randomized controlled study was conducted in accordance with the Declaration of Helsinki and registered at ClinicalTrials.gov (NCT04785274). Patient recruitment and the clinical phase took place between April and December 2021.

Randomization was performed using the closed-envelope method by an independent anesthesiologist. Both the patients and the statistician were blinded to group allocation.

Ethics Approval

Following ethical approval from the Zonguldak Bülent Ecevit University Non-Interventional Clinical Research Ethics Committee (Approval Number: 2020/24, Date: 16.12.2020), this prospective randomized controlled study was initiated.

Patients and Data Collection

Written informed consent was obtained from all patients before surgery. Sixty patients aged ≥60 years in the American Society of Anesthesiology Physical Status (ASA PS) I–III risk group, who were expected to have blood loss of more than 10%–20% of the total blood volume and were scheduled for hip surgery in the operating room of Zonguldak Bülent Ecevit University Medical Faculty Hospital, were included in the study.

Hemodynamic data, including mean arterial pressure (MAP), heart rate (HR), and peripheral oxygen saturation (SpO_2), as well as pleth variability index (PVI), partial oxygen pressure (PaO_2), and body temperature, were recorded at intervals. Hospital stay length was recorded at discharge, and 1-month and 3-month survival data were collected via telephone interviews.

Diagnostic Criteria

In the SpHb group, bedside non-invasive hemoglobin (SpHb) measurements were performed using the Radical-7 Pulse CO-Oximeter™ fingertip sensor probe (Masimo Corp., USA).

In Group CONV, the permissible amount of blood loss was calculated for a hemoglobin (Hb) value ≤9 g/dL (hematocrit [Hct]: 27%).

Definitions

In Group CONV, the permissible amount of blood loss was calculated for an Hb value ≤9 g/dL (Hct: 27%). In this calculation, the loss of red blood cell volume (RBCV)=RBCVpreop–RBCV27% formula was used. Permissible blood loss was calculated as loss of RBCV×3.[6]

During the operation, the bloody sponges and compresses were weighed again, and the amount of bleeding was calculated. In this calculation, 1 g of blood was considered equivalent to 1 mL.

Measurements available at common predefined time points for the full cohort were defined as primary longitudinal outcomes and analyzed using a linear mixed-effects model with fixed effects for group, time, and group×time interaction, and a random intercept for patient. Measurements observed only in subsets of patients during additional transfusion-related stages were defined as event-based secondary outcomes and analyzed separately as exploratory analyses. These event-based observations were not included in the main longitudinal model because they were not available for all participants and depended on the occurrence of a clinical event.

Inclusion Criteria

Written informed consent was obtained from all patients before surgery. Sixty patients aged ≥60 years in the American Society of Anesthesiology Physical Status (ASA PS) I–III risk group, who were expected to have blood loss of more than 10%–20% of the total blood volume and were scheduled for hip surgery in the operating room of Zonguldak Bülent Ecevit University Medical Faculty Hospital, were included in the study.

Exclusion Criteria

The exclusion criteria were the presence of arrhythmia, severe heart failure, uncontrolled diabetes mellitus, hypothermia, hyperbilirubinemia, jaundice, sepsis, need for inotropic support, lung resection, existing blood disease, allergy to the study drugs, and rejection.

Clinical, Surgical, and Laboratory Investigations

Routine monitoring was performed and recorded as baseline values. Intra-arterial cannulation of the radial artery was established in all patients for continuous blood pressure monitoring and blood gas analysis, alongside baseline hemogram monitoring. Baseline complete blood count hemoglobin (CBC-Hb) was recorded before induction.

Standardized anesthetic depth was maintained by delivering sevoflurane (1 minimum alveolar concentration [MAC] in 50% O_2/air) and continuous remifentanil infusion (0.1–0.3 µg/kg/min), targeting a bispectral index (BIS) value within the range of 40%–60%. Volume-controlled ventilation was initiated (tidal volume [TV]: 8 mL/kg; respiratory frequency was increased if end-tidal carbon dioxide [$EtCO_2$] was >45 mmHg).

Pleth variability index (PVI) was utilized for intraoperative dynamic fluid monitoring, with a threshold of >15% indicating fluid responsiveness and requiring 100–250 mL of saline loading, aiming to maintain PVI <15%.[7]

In the non-invasive hemoglobin (SpHb) group, bedside non-invasive SpHb measurements were performed using the Radical-7 Pulse CO-Oximeter™ fingertip sensor probe (Masimo Corp., USA). The fingers were wrapped to prevent the sensor from being exposed to light. Blood transfusion was not performed until the SpHb value was measured and was ≤9. Throughout the operation, when the SpHb value was ≤9, 1 unit of red blood cells (RBCs) was administered intravenously and recorded.

SpHb, PVI, and blood gas measurements were performed and recorded before anesthesia induction, after induction, at the first transfusion decision time, immediately after the first transfusion, at the second and third transfusion decision times according to the bleeding condition, and immediately after transfusion. Measurements obtained at later transfusion-related stages were event-dependent and were available only in patients who required additional transfusion.

Dry sponges and compresses were weighed preoperatively and reweighed intraoperatively after blood exposure to calculate blood loss. Blood on the drapes and floor was estimated, and total blood loss was determined by combining aspirator volume with sponge and compress weights. Patients received 1 unit of RBCs when the allowable blood loss threshold was reached.

Statistical Analysis

Sample size was calculated a priori using G*Power based on pilot data (12 patients/group; conventional [CONV] hemoglobin [Hb]: 9.62±0.47; SpHb: 9.04±0.51). With 99% confidence and 95% power, ≥26 patients per group were required; 60 patients were enrolled to account for potential data loss.

Outcomes were classified as primary longitudinal outcomes, measured at predefined time points in all patients, and event-based secondary outcomes, observed only in subsets during transfusion-related stages. Longitudinal data were analyzed using a linear mixed-effects model with fixed effects for group, time, and group×time interaction, and a random patient intercept. Event-based outcomes were analyzed separately as exploratory analyses on an available-case basis.

Continuous variables were expressed as mean±standard deviation (SD) or median (min–max), and categorical variables were expressed as frequency (%). Comparisons were performed using Student's t-test or the Mann–Whitney U test for continuous variables and the Pearson chi-square test or Fisher-Freeman-Halton test for categorical variables. A p-value of <0.05 was considered significant.

RESULTS

A total of 52 patients were randomized into the study following the exclusion of 8 individuals, 3 who did not fulfill the inclusion criteria and 5 who opted out, from an initial pool of 60 candidates (Fig. 1). The demographic distribution comprised 69.2% females and 30.8% males, with a mean age of 75.48±10.63 years (range: 60–93 years). Hemodynamic parameters, including heart rate (HR), peripheral oxygen saturation (SpO_2), mean arterial pressure (MAP), and pleth variability index (PVI), showed no statistically significant differences between the groups at any of the assessed time points (p>0.05). This stability was observed consistently from baseline (pre-surgery) through the induction phase, at all intraoperative intervals (from 10 to 180 minutes), and during the post-anesthesia recovery period.

In terms of perioperative fluid management, no statistically significant differences were observed between the cohorts regarding total fluid administration or urine output (p>0.05). However, Group CONV exhibited a markedly higher volume of estimated intraoperative blood loss compared with the other group, a finding that reached statistical significance (p<0.001; Table 1).

Following the baseline and perioperative descriptive analyses, outcome results were structured according to measurement type. Measurements available at common time points for the full cohort were evaluated as primary longitudinal outcomes, whereas later transfusion-related measurements observed only in smaller patient subsets were presented separately as event-based exploratory outcomes. Accordingly, primary longitudinal analyses were based on linear mixed-effects models, and event-based subgroup findings were interpreted cautiously.

For the primary longitudinal partial oxygen pressure (PaO_2) outcomes, there were no statistically significant differences between the groups at baseline or at the first red blood cell (RBC) transfusion decision time (p>0.05). PaO_2 values measured after completion of the first transfusion were significantly higher in the SpHb group (p=0.015). Linear mixed-effects model analysis demonstrated a significant overall time effect (F=116.692, df=2, 94.663; p<0.001) and group effect (F=9.085, df=1, 123.703; p=0.003), whereas the group×time interaction was not statistically significant (F=0.877, df=2, 94.663; p=0.419) (Table 2a). Event-based transfusion-related PaO_2 measurements are presented separately in Table 2b.

For the primary longitudinal complete blood count hemoglobin (CBC-Hb) outcomes, baseline hemoglobin levels were similar between the groups (p>0.05). CBC-Hb values measured at the first RBC transfusion decision, after completion of the first transfusion, and after extubation were significantly higher in the SpHb group than in the conventional group (p=0.001, p=0.012, and p=0.001, respectively). Linear mixed-effects model analysis showed a significant overall time effect (F=76.536, df=3, 89.403; p<0.001) and group effect (F=27.337, df=1, 120.214; p<0.001), whereas the group×time interaction was not statistically significant (F=0.661, df=3, 89.403; p=0.519), indicating that the overall trajectory of hemoglobin change over time did not differ significantly between the groups (Table 3a). Event-based transfusion-related CBC-Hb measurements are presented separately in Table 3b and should be interpreted as exploratory.

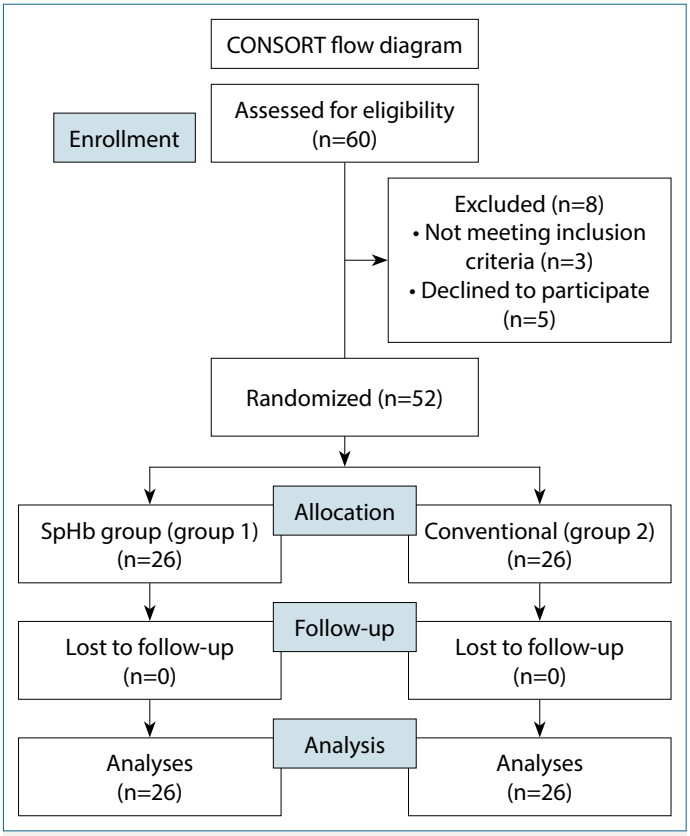

Figure 1. Consolidated standards of reporting trials (CONSORT) flow diagram.

When SpHb and CBC-Hb measurements were compared in the SpHb group, there were no statistically significant differences between the first RBC transfusion decision time and after the first RBC transfusion, the second RBC transfusion decision time and after the first RBC transfusion, or the recovery time of CBC-Hb and SpHb measurements (Fig. 2) (p>0.05).

The 40th-minute temperature values in the CONV group were significantly higher than those in the first group (p=0.042).

Table 1. Demographic and procedural data

Variables	Group SpHb	Group CONV	p
Sex			0.548[a]
Female, n (%)	17 (65.4)	19 (73.1)	
Male, n (%)	9 (34.6)	7 (26.9)	
Age, years	71.5 (60–93)	80.5 (61–92)	0.521[b]
Baseline Hb, g/dL	11.2 (8.4–13.2)	10.2 (9.2–12.7)	0.072[c]
Intraoperative input and output			
Crystalloid, mL	2000 (1000–3000)	2000 (1000–4000)	0.069[b]
Urine output, mL	307 (43–572)	295 (57–532)	0.993[b]
Estimated blood loss, mL	490 (200–850)	750 (475–1200)	<0.001[b]
Duration of surgery, h	2.72±0.86	3.14±1.50	0.237[c]
Duration of anesthesia, h	3.08±0.89	3.63±1.56	0.149[c]

Values are presented as mean±SD, median (min–max), or number (%). [a]p-values were calculated using the Pearson chi-square test. [b]p-values were calculated using the Mann–Whitney U test. [c]p-values were calculated using Student's t-test.

The temperature at the 40th minute was 36.45±0.26°C in Group SpHb and 36.59±0.22°C in Group CONV. The other measurements showed no significant differences between the groups (p>0.05).

The total RBC transfusion count in the CONV group was significantly higher than that in the SpHb group (p=0.025). The average blood transfusion volume was 1.65±0.89 units in Group SpHb and 2.42±1.36 units in Group CONV (Table 4).

The length of hospital stay for patients in the CONV group was significantly longer than that for patients in the SpHb group (p=0.043). The length of hospital stay was 5 (2–19) days in Group SpHb and 9 (2–60) days in Group CONV (Table 4).

In terms of mortality, 38.5% (n=5) of the deceased patients died in the first month, and 61.5% (n=8) died in the third month. Although the 3-month mortality rate in the CONV group (19.23%) was nearly double that in the SpHb group (11.53%), no statistically significant difference was detected in this pilot-sized cohort (p>0.05). No differences were observed between the groups in terms of surgical duration or duration of anesthesia (p>0.05) (Table 4).

DISCUSSION

Our results demonstrated that bleeding management using non-invasive hemoglobin (SpHb) data significantly contributed to a decrease in the need for blood transfusions, increased perioperative oxygenation, and reduced hospital stay duration in patients undergoing hip surgery. Consistent with our hypothesis, SpHb monitoring allowed more precise transfusion decisions compared with conventional methods.

In our study, the primary longitudinal analysis showed that partial oxygen pressure (PaO_2) values were higher in the SpHb group after completion of the first transfusion. Although later transfusion-related PaO_2 measurements also tended to be higher in the SpHb group, these observations were event-based and derived from smaller patient subsets; therefore, they should be interpreted cautiously. We believe that the higher perioperative oxygenation observed in the SpHb group may be related to earlier transfusion decisions enabled by continuous hemoglobin monitoring.

Hart et al.[2] reported that high bleeding occurred during total hip prosthesis surgeries and that 75% of these patients received blood transfusions. For these reasons, in our study, we selected hip surgery cases in which we anticipated a loss of 10%–20% of the patients' total blood volume to make a decision on blood transfusion using non-invasive hemoglobin (Hb) measurement values.

The gold standard method for measuring Hb is a complete blood count performed in the laboratory.[8] However, the most significant disadvantages of this method are its invasiveness, the time required to obtain results, including collecting the blood sample, delivering it to the laboratory, and processing it, and the risk of infection associated with repeated procedures.[9] On the other hand, intravenous fluid replacement is also administered to patients during the operation. Excessive or insufficient fluid replacement can lead to hemoconcentration, thereby leading to incorrect Hb measurement results.[10] We standardized fluid replacement to prevent potential hemodilution or hemoconcentration, and pleth variability index (PVI) monitoring was consequently performed in all patients.[7] In our study, no significant difference was found

Table 2a. Comparison of PaO_2 measurements at primary longitudinal time points: Linear mixed-effects model analysis

Measurement, mmHg	n	Group SpHb Mean±SD	Group SpHb EMM (95% CI)	n	Group CONV Mean±SD	Group CONV EMM (95% CI)	Between group p
Baseline	26	105.31±24.32	105.3 (57.4–153.2)	26	97.64±23.67	97.6 (49.8–145.5)	0.264[b]
First RBC transfusion decision	26	172.51±41.01	172.5 (122.8–222.2)	26	153.27±43.09	153.3 (103.6–202.9)	0.105[b]
After completion of the first transfusion	26	191.36±29.55	191.4 (143.0–239.7)	26	170.51±30.32	170.5 (122.2–218.8)	0.015[b]
Linear mixed-effects model: Fixed effects (Type III Tests, Kenward–Roger df)							
Effect		**F**	**Numerator df**		**Denominator df**	**p**	
Time		116.692	2		94.663	<0.001	
Group (SpHb vs. CONV)		9.085	1		123.703	0.003	
Group×time interaction		0.877	2		94.663	0.419	
Overall between-group comparison (LMM estimated marginal means, averaged over time)							
Group		**Overall EMM mmHg**	**95% CI**		**Mean difference (SpHb–CONV)**	**p**	
SpHb		156.4	108.9–203.9		+15.9 mmHg	0.003	
CONV		140.5	93.0–188.0				

Observed values are presented as mean±SD, and model-based values are presented as estimated marginal means (EMM) with 95% confidence intervals (CIs). RBC: red blood cell; CONV: conventional monitoring; SpHb: non-invasive hemoglobin monitoring. Between-group p-values shown for each primary time point were obtained using independent-samples Student's t-tests and are provided as descriptive time point-specific comparisons of observed values. In addition, the primary longitudinal time points were analyzed using a linear mixed-effects model with fixed effects for group, time, and group×time interaction, and a random intercept for each patient. The corresponding Type III tests and overall between-group comparison are presented in the lower panels of the table. [b]Student's t-test.

Table 2b. PaO_2 measurements at event-based secondary time points: Exploratory analyses

Measurement, mmHg	n (SpHb)	Group SpHb, mean±SD or median (min–max)	n (CONV)	Group CONV, mean±SD or median (min–max)	Between group p
Second transfusion: Event-based exploratory analysis (SpHb n=8; CONV n=16)					
Second RBC transfusion decision	8	199.5 (168–222)	16	159.5 (98–208)	0.027[a]
After completion of the second transfusion	8	204.63±27.42	16	168.06±33.95	0.015[b]
Third transfusion: Descriptive analysis only (SpHb n=1; CONV n=4)					
Third RBC transfusion decision	1	191.0	4	182.5±38.49	–
After completion of the third transfusion	1	201.0	4	182.5±37.78	–

Values are presented as mean±SD or median (min–max), as appropriate; single observations are shown as observed values only. RBC: red blood cell; CONV: conventional monitoring; SpHb: non-invasive hemoglobin monitoring. Event-based secondary time points were analyzed separately and should be interpreted as exploratory because of the small and unbalanced subgroup sizes. [a]Mann–Whitney U test; [b]Student's t-test.

between the PVI scores and the amount of fluid administered to the patients in either group during the perioperative period.

Non-invasive approaches and monitoring strategies have gained considerable popularity worldwide.[11] SpHb monitoring is the most widely used technique among these methods.[12] The primary objectives of our research were to observe the Hb trend during the blood replacement procedure to prevent excessive blood transfusions and to identify dramatic decreases in Hb levels early, allowing immediate choices regarding transfusions.

Non-invasive SpHb monitoring may produce inaccurate results in patients with nail polish, motion artifacts, hypotension, arrhythmias, vasoconstrictor medication use, and hyperbilirubinemia.[13] We eliminated the risk of incorrect SpHb probe measurements by excluding these patients from the study. Another disadvantage of these methods is that they are affected by hypothermia. In our study, no difference in temperature was detected between the two groups except for the scores at the 40th minute. At the 40th minute, it was determined to be 36.45±0.26°C in Group SpHb and 36.59±0.22°C in Group CONV (p=0.042). Although a difference was observed in the scores at the 40th minute, we believe that this did not clinically cause hypothermia; therefore, the SpHb measurements were not negatively affected.

Table 3a. Comparison of CBC-Hb measurements at primary longitudinal time points: Linear mixed-effects model analysis

Measurement, g/dL	n	Group SpHb mean±SD	Group SpHb EMM (95% CI)	n	Group CONV mean±SD	Group CONV EMM (95% CI)	Between group p
Baseline	26	11.06±1.26	11.05 (9.73–12.37)	26	10.51±0.85	10.06 (8.74–11.38)	0.072[a]
First RBC transfusion decision	26	8.73±0.55	8.72 (7.45–9.99)	26	8.13±0.59	8.13 (6.86–9.40)	0.001[a]
After completion of the first transfusion	26	9.58±0.90	9.58 (8.28–10.88)	26	8.94±0.85	8.94 (7.64–10.23)	0.012[a]
After extubation	26	9.34±0.69	9.34 (9.06–9.62)	26	8.56±0.67	8.56 (8.29–8.83)	0.001[a]
Linear Mixed-Effects Model: Fixed Effects (Type III Tests, Kenward–Roger df)							
Effect		**F**	**Numerator df**		**Denominator df**	**p**	
Time		76.536	3		89.403	<0.001	
Group (SpHb vs. CONV)		27.337	1		120.214	<0.001	
Group×time interaction		0.661	3		89.403	0.519	
Overall between-group comparison (LMM estimated marginal means, averaged over time)							
Group		**Overall EMM g/dL**	**95% CI**		**Mean difference (SpHb–CONV)**	**p**	
SpHb		9.790	8.524–11.056		+0.745 g/dL	<0.001	
CONV		9.045	7.779–10.311				

Values are presented as mean±SD. EMM: estimated marginal mean; CI: confidence interval; RBC: red blood cell; CBC-Hb: complete blood count hemoglobin; CONV: conventional monitoring group; SpHb: non-invasive hemoglobin monitoring group. Primary longitudinal time points were analyzed using a linear mixed-effects model with fixed effects for group, time, and group×time interaction. [a]p-values were calculated using the independent-samples Student's t-test. Statistical significance was set at p<0.05.

Table 3b. CBC-Hb measurements at event-based secondary time points: Exploratory analyses

Measurement, g/dL	n (SpHb)	Group SpHb, mean±SD or median (min–max)	n (CONV)	Group CONV, mean±SD or median (min–max)	Between group p
Second transfusion: Event-based exploratory analysis (SpHb n=8; CONV n=16)					
Second RBC transfusion decision	8	8.50 (8.10–9.20)	16	8.40 (7.70–9.00)	0.341[b]
After completion of the second transfusion	8	9.77±1.06	16	9.22±0.78	0.174[a]
Third transfusion: Descriptive analysis only (SpHb n=1; CONV n=4)					
Third RBC transfusion decision	1	8.95	4	8.15±0.31	–
After completion of the third transfusion	1	9.85	4	9.62±0.48	–

Values are presented as mean±SD or median (min–max), as appropriate; single observations are presented descriptively. RBC: red blood cell; CONV: conventional monitoring group; SpHb: non-invasive hemoglobin monitoring group. Event-based secondary time points were analyzed separately and should be interpreted as exploratory. [a]Student's t-test; [b]Mann–Whitney U test. Statistical significance was set at p<0.05.

Awada et al.[14] investigated the effect of SpHb monitoring on blood transfusion in neurosurgical surgeries with bleeding. In this study, the group that underwent SpHb monitoring received fewer blood transfusions. The results of the study showed that SpHb monitoring makes it easier to recognize transfusions that need to be applied on time and causes a decrease in the amount of blood replaced in neurosurgical operations with high blood loss. Similarly, in our study, patients monitored with SpHb required fewer transfusions than those managed with conventional methods. The number of transfused red blood cell (RBC) units per patient was significantly lower in the SpHb group than in the CONV group (p=0.025). This finding suggests that continuous SpHb monitoring may have facilitated earlier recognition of downward hemoglobin (Hb) trends and allowed transfusion decisions to be made before hemoglobin levels declined further. The distribution of second- and third-unit transfusions should be interpreted cautiously, as these analyses were based on smaller event-driven subgroups. Although SpHb monitoring has shown promise in transfusion management, laboratory-measured Hb remains the reference standard because the current evidence is limited by methodological constraints and insufficient statistical power.[8,9] Based on our findings, SpHb monitoring may serve as an adjunct tool to detect downward Hb trends

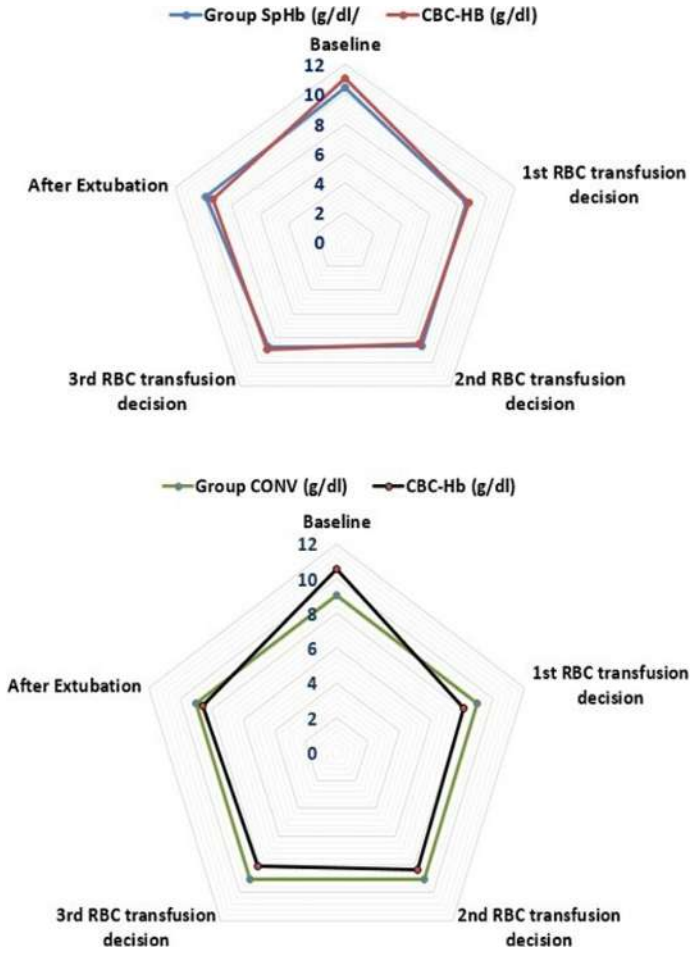

Figure 2. Radar chart design of the groups.

and support earlier transfusion decisions, particularly when Hb approaches the 9 g/dL threshold. Larger randomized controlled trials are needed to better define its clinical utility.

In our study, the length of hospital stay was longer in the conventional group than in the SpHb group (p=0.043). Although hospital stay can be influenced by various factors, such as comorbidities, surgical technique, and postoperative complications, we aimed to control for these variables through our prospective randomized study design. Both groups were comparable in terms of demographic data, American Society of Anesthesiology Physical Status (ASA PS) risk groups, and duration of surgery. Additionally, anesthesia management and fluid therapy were standardized across both cohorts. Therefore, we suggest that the reduction in hospital stay in the SpHb group is likely associated with more accurate transfusion triggers and a subsequent decrease in the total amount of blood transfused. Numerous studies in the literature support that avoiding unnecessary blood transfusions can shorten hospital stay by reducing transfusion-related risks.[10,12]

More than 90% of hip fractures occur in people over the age of 65 years, and the risk of hip fracture doubles every decade after the age of 50 years.[15] The mortality rate in the first year after hip surgery varies between 10% and 40%.[16] The mortality rates observed in our study are consistent with the existing literature. A 10-year retrospective study previously conducted at our clinic reported a 1-year mortality rate of 16.98% for hip surgery patients.[17] In our current cohort, although the numerical values varied slightly between the SpHb and conventional groups at the 1-month and 3-month intervals, no statistically significant differences were observed. This suggests that while SpHb monitoring optimizes perioperative management and reduces transfusion requirements, its direct impact on short-term mortality may be limited, or a larger sample size may be required to detect such a difference.

Several independent risk factors may affect mortality in patients undergoing hip surgery, including advanced age, male sex, anemia, clinical comorbidities, surgical scheduling, and surgical

Table 4. Comparison of secondary outcome measurements between groups

Variables	Group SpHb	Group CONV	p
RBC units transfused per patient	1 (1–4)	2 (1–5)	0.025[a]
Number of RBC units transfused			0.007[b]
1 unit, n (%)	17 (65.38)	6 (23.07)	
2 units, n (%)	8 (30.76)	16 (61.53)	
3 units, n (%)	1 (3.84)	4 (15.38)	
Length of stay, days	5 (2–19)	9 (2–60)	0.043[a]
Mortality, n (%)			
30-day mortality	3 (11.53)	2 (7.69)	0.266[b]
90-day mortality	3 (11.53)	5 (19.23)	0.184[b]

Values are presented as median (min–max) or number (%). [a]p-values were calculated using the Mann–Whitney U test. [b]p-values were calculated using the Fisher-Freeman-Halton test.

technique.[18] When we examined studies on the relationship between low hemoglobin (Hb) levels and mortality rates, we found some inconsistencies. For example, there is currently no global consensus regarding the Hb threshold for transfusion during hip surgery. The National Institute for Clinical Excellence (NICE) recommends blood transfusions for patients with Hb levels <7 g/dL or <8 g/dL in those with cardiac problems; however, the American Association of Blood Banks (AABB) recommends a transfusion threshold of 8 g/dL for surgical patients.[19,20] Therefore, the lack of a standard guideline makes the issue of whether the Hb value used for blood transfusion has a positive or negative impact on mortality debatable. In the present study, a hemoglobin threshold of 9 g/dL was selected as the trigger for blood transfusion. While some guidelines suggest more restrictive thresholds, our choice was informed by the specific clinical profile of our study population, which consisted of patients aged 60 years and older, with a mean age of approximately 75 years. Geriatric patients undergoing major orthopedic procedures often have a high prevalence of cardiovascular and pulmonary comorbidities that may limit their physiological compensatory mechanisms for anemia. Furthermore, hip surgeries are associated with significant perioperative blood loss and fluid shifts. By selecting a 9 g/dL threshold, we aimed to provide a safer margin for oxygen delivery and to prevent potential myocardial or cerebral ischemia in this vulnerable age group, consistent with clinical practices that prioritize perioperative stability in high-risk elderly patients. Second, the results of studies conducted on this subject are contradictory. For example, Engoren et al.[21] reported in a study involving 229 hip fractures that perioperative blood transfusion did not affect postoperative mortality on the 30th or 90th day; however, they showed that transfusion is a risk factor for death at least 90 days or more after hip surgery. Arshi et al.[22] found that the 30-day mortality rate in patients who underwent hip surgery and received blood transfusions was significantly higher than that in patients who did not receive transfusions. Smeets et al.[23] investigated the effect of blood transfusion on survival after hip surgery and found no significant differences in mortality at 30 days, 1 year, or 2 years. Consistent with these findings, we observed no statistically significant difference in 3-month mortality between our groups ($p>0.05$). However, it is important to note that the mortality rate in the conventional group (19.23%) was numerically nearly double that of the non-invasive hemoglobin (SpHb) group (11.53%). Because our sample size was calculated specifically to evaluate transfusion triggers rather than survival outcomes, this pilot-sized cohort is likely underpowered to detect a true statistical difference in mortality. Therefore, while SpHb monitoring shows a promising clinical trend toward reducing short-term mortality, these results should be interpreted cautiously and validated in larger, adequately powered multicenter studies.

Strengths and Limitations

The most significant aspect of this study is that, to our knowledge, no randomized controlled studies investigating the relationship between non-invasive hemoglobin (SpHb) monitoring and mortality have been reported. However, we found that mortality studies are typically conducted retrospectively with large sample sizes. In our study, we chose the sample size based on our main objective and included 52 patients with 95% power in the power analysis. The sample size calculation was based on the primary transfusion-related outcome structure and was not designed to ensure sufficient power for smaller event-based subgroup analyses or secondary outcomes, such as mortality. As a result, we consider the number of patients in our study insufficient for mortality analysis, which is a major limitation.

Another limitation in terms of mortality is related to the study methodology. Patients' families were contacted by phone to collect mortality data. Therefore, information such as survival status may be obscured, which may make the results debatable.

CONCLUSION

Our findings show that SpHb monitoring provides a reliable measure of critical bleeding thresholds during hip operations, which could assist with early transfusion treatments and reduce the total volume of blood required. This condition improved perioperative oxygenation and reduced hospital stay by increasing healing time. Therefore, it may be possible to improve postoperative clinical outcomes by monitoring SpHb levels during surgical procedures that represent a significant risk of blood loss.

Ethics Committee Approval: Ethics committee approval was obtained from Zonguldak Bülent Ecevit University Non-Interventional Clinical Research Ethics Committee (Approval Number: 2020/24, Date: 16.12.2020).

Informed Consent: Written informed consent was obtained from all patients before surgery.

Conflict of Interest: The authors have no conflicts of interest to declare.

Funding: The authors declared that this study received no financial support.

Use of AI for Writing Assistance: During the preparation of this manuscript, the authors used artificial intelligence (AI)-assisted technology to improve the linguistic flow and for copyediting purposes. The scientific content was developed entirely by the authors, and all human authors take full responsibility for the accuracy and integrity of the work.

Author Contributions: Concept – Ö.P, MEDY; Design – ÖP, MEDY; Supervision – BGKİ, RDO; Resource – HA, RDO, ŞA; Materials – HA, ŞA, ÇB; Data Collection and/or Processing – MEDY, ÇB, KB; Analysis and/or Interpretation – BGKİ, GK, KB; Literature Review – RDO, ÇB, GK; Writing – ŞA, GK, KB; Critical Review – ÖP, BGKİ, HA.

Acknowledgment: We would like to thank Editage (www.editage.com) for English language editing.

Peer-review: Externally peer-reviewed.

Clinical Trial Registration: NCT04785274.

REFERENCES

1. McEvoy MT, Shander A. Anemia, bleeding, and blood transfusion in the intensive care unit: causes, risks, costs, and new strategies. Am J Crit Care 2013;22(6 Suppl):eS1-13; quiz eS14. [CrossRef]
2. Hart A, Khalil JA, Carli A, Huk O, Zukor D, Antoniou J. Blood transfusion in primary total hip and knee arthroplasty. Incidence, risk factors, and thirty-day complication rates. J Bone Joint Surg Am 2014;96(23):1945-51. [CrossRef]
3. Glance LG, Dick AW, Mukamel DB, Fleming FJ, Zollo RA, Wissler R, et al. Association between intraoperative blood transfusion and mortality and morbidity in patients undergoing noncardiac surgery. Anesthesiology 2011;114(2):283-92. [CrossRef]
4. Chang WH, Lee NR, Wang PH. The mortality and blood transfusion. J Chin Med Assoc 2020;83(1):102. [CrossRef]
5. Berkow L, Rotolo S, Mirski E. Continuous noninvasive hemoglobin monitoring during complex spine surgery. Anesth Analg 2011;113(6):1396-402. [CrossRef]
6. Butterworth JF, Mackey DC, Wasnick JD. Chapter 51: Fluid Management & Blood Component Therapy. Butterworth JF, Mackey DC, Wasnick JD. Morgan and Mikhail's Clinical Anesthesiology. 6th ed. New York: McGraw-Hill Education; 2018.p.1189-213.
7. Cros J, Dalmay F, Yonnet S, Charpentier M, Tran-Van-Ho J, Renaudeau F, et al. Continuous hemoglobin and plethysmography variability index monitoring can modify blood transfusion practice and is associated with lower mortality. J Clin Monit Comput 2020;34(4):683-91. [CrossRef]
8. Tang B, Yu X, Xu L, Zhu A, Zhang Y, Huang Y. Continuous noninvasive hemoglobin monitoring estimates timing for detecting anemia better than clinicians: a randomized controlled trial. BMC Anesthesiol 2019;19(1):80. [CrossRef]
9. Barker SJ, Shander A, Ramsay MA. Continuous Noninvasive Hemoglobin Monitoring: A Measured Response to a Critical Review. Anesth Analg 2016;122(2):565-72. [CrossRef]
10. Macknet MR, Allard M, Applegate RL 2nd, Rook J. The accuracy of noninvasive and continuous total hemoglobin measurement by pulse CO-Oximetry in human subjects undergoing hemodilution. Anesth Analg 2010;111(6):1424-6. [CrossRef]
11. Johnson M, Marwick PC, Coetzee JF. Comparison of Hemoglobin Measurements by 3 Point-of-Care Devices with Standard Laboratory Values and Reliability Regarding Decisions for Blood Transfusion. Anesth Analg 2020;131(2):640-9. [CrossRef]
12. Adel A, Awada W, Abdelhamid B, Omar H, Abd El Dayem O, Hasanin A, et al. Accuracy and trending of non-invasive hemoglobin measurement during different volume and perfusion statuses. J Clin Monit Comput 2018;32(6):1025-31. [CrossRef]
13. Park J, Yang S, Lee JH, Kim JT, Kim HS, Kim HC. The importance of sensor contacting force for predicting fluid responsiveness in children using respiratory variations in pulse oximetry plethysmographic waveform. J Clin Monit Comput 2019;33(3):393-401. [CrossRef]
14. Awada WN, Mohmoued MF, Radwan TM, Hussien GZ, Elkady HW. Continuous and noninvasive hemoglobin monitoring reduces red blood cell transfusion during neurosurgery: a prospective cohort study. J Clin Monit Comput 2015;29(6):733-40. [CrossRef]
15. Yoo J, Lee JS, Kim S, Kim BS, Choi H, Song DY, et al. Length of hospital stay after hip fracture surgery and 1-year mortality. Osteoporos Int 2019;30(1):145-53. [CrossRef]
16. Chen X, Ma Y, Deng Z, Li Q, Liao J, Zheng Q. Prediction of Early Postoperative Major Cardiac Events and In-Hospital Mortality in Elderly Hip Fracture Patients: The Role of Different Types of Preoperative Cardiac Abnormalities on Echocardiography Report. Clin Interv Aging 2020;15:755-62. [CrossRef]
17. Elmas U, Yurtlu BS, Küçükosman G, Pişkin Ö, Okyay RD, Hancı V, et al. Factors İnfluencing The Mortality And Morbidity Rates At Hip Fracture Operations: A Retrospective Evaluation. Haydarpaşa Numune Med J 2015;55(3):181-95.
18. Beal EW, Bagante F, Paredes A, Akgul O, Merath K, Cua S, et al. Perioperative use of blood products is associated with risk of morbidity and mortality after surgery. Am J Surg 2019;218(1):62-70. [CrossRef]
19. Carson JL, Stanworth SJ, Guyatt G, Valentine S, Dennis J, Bakhtary S, et al. Red Blood Cell Transfusion: 2023 AABB International Guidelines. JAMA 2023;330(19):1892-902. [CrossRef]
20. National Institute for Health and Care Excellence. Blood transfusion, NG24, 2015. https://www.nice.org.uk/guidance/ng24 Accessed May 11, 2025.
21. Engoren M, Mitchell E, Perring P, Sferra J. The effect of erythrocyte blood transfusions on survival after surgery

for hip fracture. J Trauma 2008;65(6):1411-5. [CrossRef]

22. Arshi A, Lai WC, Iglesias BC, McPherson EJ, Zeegen EN, Stavrakis AI, et al. Blood transfusion rates and predictors following geriatric hip fracture surgery. Hip Int 2021;31(2):272-9. [CrossRef]
23. Smeets SJM, Verbruggen JPAM, Poeze M. Effect of blood transfusion on survival after hip fracture surgery. Eur J Orthop Surg Traumatol 2018;28(7):1297-303. [CrossRef]

Official Journal of Erciyes University Faculty of Medicine

DOI: 10.14744/cpr.2026.62805
J Clin Pract Res 2026;48(2):202–205

The Injection of Tranexamic Acid Alone is Not Effective in Reducing Transfusion Requirements Following Total Joint Arthroplasty

Claudio Legnani,[1] Alberto Ventura,[1] Giorgio Oriani[2]

[1]IRCCS Istituto Ortopedico Galeazzi, Sport Traumatology and Minimally Invasive Surgery Center, Milan, Italy
[2]IRCCS Istituto Ortopedico Galeazzi, Department of Anesthesiology, Milan, Italy

ABSTRACT

A retrospective study was conducted to evaluate the need for perioperative autotransfusions and the amount of blood loss by comparing patients receiving different tranexamic acid (TXA) regimens following total joint replacement (TJR). A total of 1675 patients undergoing TJR were included: 76 did not receive TXA administration (group A); 77 received IV TXA (group B); 1510 received IV followed by IA administration of TXA (group C); and 12 received IA TXA administration alone (group D). Significant between-group differences were observed in intraoperative and postoperative blood loss ($p<0.05$). Blood autotransfusion and allogeneic transfusion rates were significantly higher in group D compared with the other treatment strategies ($p<0.001$) and with the control group of patients who did not receive TXA ($p<0.05$). IV combined with IA TXA administration represents the most effective way to prevent blood loss following TJA surgery. Conversely, isolated IA administration of TXA did not reduce the need for postoperative transfusions.

Keywords: Anesthesiology, blood management, injections, surgery, tranexamic acid.

Cite this article as:
Legnani C, Ventura A, Oriani G. The Injection of Tranexamic Acid Alone is not Effective in Reducing Transfusion Requirements Following Total Joint Arthroplasty. J Clin Pract Res 2026;48(2):202–205.

Address for correspondence:
Claudio Legnani.
IRCCS Istituto Ortopedico Galeazzi, Sport Traumatology and Minimally Invasive Surgery Center, Milan, Italy
Phone: +3902487852
E-mail:
claudio.legnani@grupposandonato.it

Submitted: 10.09.2025
Revised: 07.04.2026
Accepted: 24.04.2026
Available Online: 30.04.2026

Erciyes University Faculty of Medicine Publications - Available online at www.jcpres.com

INTRODUCTION

For individuals with end-stage osteoarthritis, total joint arthroplasty (TJA) represents the elective surgical treatment. TJA procedures are becoming more common because they can help elderly patients live better lives by reducing joint pain and improving their quality of life.[1] However, TJA is often associated with a significant risk of blood loss, which can lead to anemia and increased rates of autologous and allogeneic blood transfusions, which may be related to perioperative complications such as transfusion reactions and surgical wound infections, thus prolonging hospital stays and increasing costs for health care systems.[2] Consequently, perioperative blood management techniques aim to reduce blood loss and the requirement for blood transfusions. Reducing bleeding around the knee improves functional results following surgery by lowering hemarthrosis, limb edema, and postoperative discomfort.[3]

Tranexamic acid (TXA) is an antifibrinolytic agent that helps minimize blood loss in patients undergoing TJA.[4] It has shown an excellent safety profile without increasing the risk of side effects, such as thromboembolism during the perioperative period.[5] Moreover, numerous studies have

Table 1. Blood loss and transfusion rates in patients undergoing total joint replacement

	Group A (No TXA administration) (n=76)	Group B (Double intravenous TXA administration) (n=77)	Group C (Double intravenous TXA administration+ intraarticular TXA administration) (n=1510)	Group D (Intraarticular TXA administration) (n=12)
Intraoperative blood loss, mean (SD), mL	250.4 (101.3)	225.3 (84.8)	150.5 (90.8)	260.8 (119.4)
Postoperative blood loss, mean (SD), mL	275.5 (144.4)	264.3 (134.8)	239.1 (125.1)	270.4 (137.4)
Autotransfusion, No. (%)	9 (11.8%)	3 (3.9%)	24 (1.6%)	2 (16.7%)
Allogeneic transfusion, No. (%)	17 (22.4%)	8 (10.4%)	73 (4.8%)	3 (25.0%)

TXA: Tranexamic acid; SD: Standard deviation.

demonstrated that TXA use can significantly lower the need for transfusions after joint replacement surgery.[6–9] Nevertheless, no consensus exists on administration regimens for TXA in joint replacement surgery. Significant differences in TXA administration have been reported, with protocols varying from single- to multiple-dose regimens, with or without IA administration, which is sometimes used alone.

A retrospective study was conducted to evaluate the need for perioperative auto- and allotransfusions by comparing patients with different TXA regimens following joint replacement.

The study hypothesis was that IV administration of TXA combined with IA administration reduces the need for perioperative transfusions following TJA more effectively compared with other treatment regimens.

METHODS

A total of 1702 patients who had undergone primary TJA at the Minimally Invasive Articular Surgery Center of our institute between January 2023 and December 2023 were retrospectively reviewed. Of the original study group, 1675 patients (98.4%) whose medical records could be retrieved were included in the present research. Seventy-six did not receive TXA administration (group A); 77 received a preoperative IV dose of 15 mg/kg TXA followed by a second postoperative IV dose of 15 mg/kg TXA (group B); 1510 received a preoperative IV dose of 15 mg/kg TXA followed by a second postoperative IV dose of 15 mg/kg TXA and IA administration of TXA (group C); and 12 received IA administration of TXA alone (group D). Primary outcomes were the percentage of transfusions (autologous or allogeneic) within the perioperative period and the amount of intraoperative and postoperative blood loss (within 24 hours). Secondary outcomes included major complications occurring during the hospital stay, such as thrombotic events, infections, and adverse events. Blood reinfusion was administered at a hemoglobin threshold of 8 g/dL in patients without comorbidities and a threshold of 10 g/dL in patients with preexisting cardiac pathology, according to international guidelines.[10,11]

Ethical approval was not required for the present study, an observational analytic study with a retrospective design on a well-established surgical procedure, as the patient-reported outcomes used are part of routine follow-up at the authors' institution.

Continuous data are presented as mean±standard deviation (SD). The Shapiro-Wilk test was used to assess data distribution. Differences between the groups were tested using Friedman's test and Dunn's post hoc test for pairwise comparisons in cases of non-normal data distribution or repeated-measures one-way ANOVA with Tukey's post hoc test for multiple comparisons of Gaussian-distributed data. SPSS software (IBM SPSS Statistics version 21, IBM Corp., Armonk, NY, USA) was used. Statistical significance was established at $p<0.05$.

RESULTS

None of the patients who completed TXA therapy reported adverse events during the perioperative period. A detailed overview of blood loss and transfusion rates is reported in Table 1.

Blood autotransfusion and allogeneic transfusion rates were 11.8% (9/76) and 22.4% (17/77) in group A, respectively. Autotransfusion was administered to 3 patients (3.9%), and allogeneic transfusion was administered to 8 patients (10.4%) in group B. In group C, 24/1510 patients (1.6%) and 73/1510 patients received autologous or allogeneic transfusion, respectively, while autotransfusion and allogeneic transfusion rates were 16.7% (2/12) and 25.0% (3/12) in group D. Significant differences between the groups were observed ($p<0.001$).

Similarly, mean intraoperative blood loss in group A (250.4 mL, SD: 101.3) and group D (260.8 mL, SD: 119.4) was significantly higher compared with group B (225.3 mL, SD: 84.8, $p<0.001$) and group C (150.5 mL, SD: 90.8, $p<0.001$). Similarly, regarding

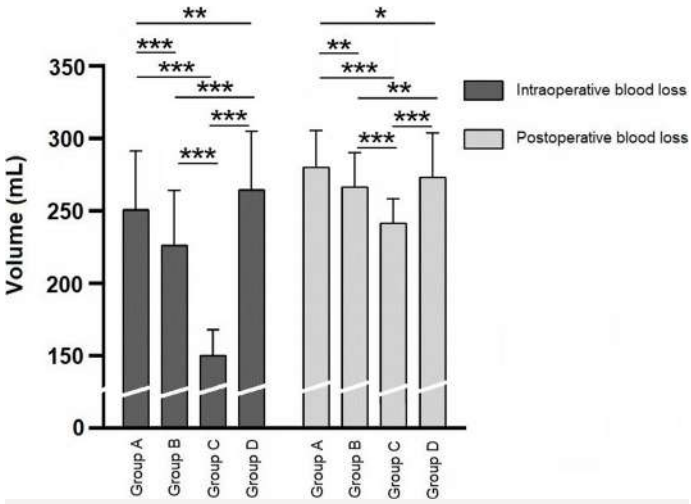

Figure 1. Box plots showing differences in blood loss between groups. The bottom and top of the boxes represent the interquartile range (25th and 75th percentiles), and the top whisker represents the maximum value.

*: P<0.05; **: P<0.01; ***: P<0.001.

postoperative blood loss, higher average values were reported in group A (275.5 mL, SD: 144.4) and group D (270.4 mL, SD: 137.4) compared with group B (264.3 mL, SD: 134.8) and group C (239.1 mL, SD: 125.1) (Fig. 1).

DISCUSSION

According to our findings, IV combined with IA TXA administration represents the most effective way to prevent blood loss following TJA surgery. The use of IV TXA infusion also reduces the need for postoperative transfusions. On the other hand, isolated IA administration of TXA did not reduce the need for postoperative transfusions compared with the control group, in which no TXA was administered. Similar results were reported for intraoperative and postoperative blood loss. The secondary outcomes, including complication rates, were comparable between groups.

Numerous studies have reported that TXA can be safely and effectively used to decrease blood loss and reduce transfusion requirements.[4,5] In our case series, no venous or arterial thromboembolic events occurred, and consistent with previous experience reported in the literature, among patients undergoing joint arthroplasty, treatment-related reductions in transfusion requirements were associated with IV administration of TXA.[6–9]

The administration of TXA after joint replacement surgery varies greatly, with dosage regimens ranging from 10 to 135 mg/kg and treatment durations ranging from one injection to several injections or continuous infusion for up to 3 days.[12]

Because of this, the ideal dosage of TXA for joint replacement surgery is still unknown, and opinions about the best time to begin using TXA, its administration techniques, and its volume of use remain divided.[13]

Different TXA administration dosing regimens—one intravenous, one intravenous combined with intraarticular, and one intraarticular alone—were examined in this study and compared with a control group in which no TXA was administered.

According to a recent meta-analysis, after total knee replacement, the combined treatment of IV and IA TXA was comparatively more successful in lowering postoperative hemoglobin decline, transfusion rate, total blood loss, and drain output.[14] Similarly, Fakharian et al.[15] reported reduced intraoperative blood loss in patients undergoing total knee arthroplasty treated with combined intraarticular and intravenous TXA compared with the intraarticular and intravenous alone groups.

According to our findings, using an intravenous double-dose regimen appreciably reduces the overall volume of blood lost after surgery, with or without the addition of intraarticular administration. On the other hand, group A had a lower transfusion rate than group D, showing that isolated intraarticular administration of TXA did not reduce the need for postoperative transfusions compared with the control group. However, caution must be used when interpreting these results because of the limited sample size.

Major study limitations include its retrospective nature, nonrandomized design, and absence of a power analysis. The imbalance in group sizes may affect the reliability of these findings. The smaller sample size in group D, due to blood management strategies adopted at our institution, could reduce the statistical power to detect true differences among groups.

Further prospective randomized studies with more balanced group sizes are needed to substantiate these findings.

Ethics Committee Approval: Ethical approval was not required, an observational analytic study with a retrospective design on a well-established surgical procedure, as the patient-reported outcomes used are part of routine follow-up at the authors' institution.

Informed Consent: Written informed consent was obtained from the patients.

Conflict of Interest: The authors have no conflicts of interest to declare.

Funding: The authors declared that this study received no financial support.

Use of AI for Writing Assistance: No use of AI-assisted technologies was declared by the authors.

Author Contributions: Concept – CL, GO; Design – CL, AV; Supervision – CL, GO; Resource – CL; Materials – CL; Data Collection and/or Processing – CL; Analysis and/or Interpretation – CL, AV; Literature Review – GO; Writing – CL; Critical Review – AV, GO.

Peer-review: Externally peer-reviewed.

REFERENCES

1. Pacheco-Brousseau L, Stacey D, Desmeules F, Ben Amor S, Dervin G, et al. Determining Appropriateness of Total Joint Arthroplasty for Hip and Knee Osteoarthritis: A Patient-Centred Conceptual Model. Musculoskeletal Care 2024;22(3):e1927. [CrossRef]
2. Sehat KR, Evans R, Newman JH. How much blood is really lost in total knee arthroplasty?. Correct blood loss management should take hidden loss into account. Knee 2000;7(3):151-5. [CrossRef]
3. Moráis S, Ortega-Andreu M, Rodríguez-Merchán EC, Padilla-Eguiluz NG, Pérez-Chrzanowska H, Figueredo-Zalve R, et al. Blood transfusion after primary total knee arthroplasty can be significantly minimised through a multimodal blood-loss prevention approach. Int Orthop 2014;38(2):347-54. [CrossRef]
4. Mannucci PM. Hemostatic drugs. N Engl J Med 1998;339(4):245-53. [CrossRef]
5. Gillette BP, DeSimone LJ, Trousdale RT, Pagnano MW, Sierra RJ. Low risk of thromboembolic complications with tranexamic acid after primary total hip and knee arthroplasty. Clin Orthop Relat Res 2013;471(1):150-4. [CrossRef]
6. Jovanovic G, Lukic-Sarkanovic M, Lazetic F, Tubic T, Lendak D, Uvelin A. The Effect of Intravenous Tranexamic Acid on Perioperative Blood Loss, Transfusion Requirements, Verticalization, and Ambulation in Total Knee Arthroplasty: A Randomized Double-Blind Study. Medicina (Kaunas) 2024;60(7):1183. [CrossRef]
7. Feng P, Feng L, Xiong Z, Zhang C, Wang G. A comparison of efficacy and safety of oral versus intravenous applications of tranexamic acid in total hip and knee arthroplasty: an updated systematic review meta-analysis of randomized controlled trials. BMC Musculoskelet Disord 2025;26(1):914. [CrossRef]
8. Devereaux PJ, Marcucci M, Painter TW, Conen D, Lomivorotov V, Sessler DI, et al.; POISE-3 Investigators. Tranexamic Acid in Patients Undergoing Noncardiac Surgery. N Engl J Med 2022;386(21):1986-97. [CrossRef]
9. Legnani C, Oriani G, Parente F, Ventura A. Reducing transfusion requirements following total knee arthroplasty: effectiveness of a double infusion of tranexamic acid. Eur Rev Med Pharmacol Sci 2019;23(5):2253-2256.
10. So-Osman C, Nelissen R, Brand R, Faber F, Slaa RT, Stiggelbout A, et al. The impact of a restrictive transfusion trigger on post-operative complication rate and well-being following elective orthopaedic surgery: a post-hoc analysis of a randomised study. Blood Transfus 2013;11(2):289-95.
11. Nuttall, GA, Minnesota R, Brost BC, Minnesota R, Connis RT, Washington W et al.; American Society of Anesthesiologists Task Force on Perioperative Blood Transfusion and Adjuvant Therapies. Practice guidelines for perioperative blood transfusion and adjuvant therapies: an updated report by the American Society of Anesthesiologists Task Force on Perioperative Blood Transfusion and Adjuvant Therapies. Anesthesiology 2006;105(1):198-208. [CrossRef]
12. Bi C, Wu D, Xie F, Song X, Yang D. Comparison of Intravenous, Topical, or Combined Routes of Tranexamic Acid in Primary Total Knee Arthroplasty. Geriatr Orthop Surg Rehabil 2023;14:21514593231152377. [CrossRef]
13. Yang YZ, Cheng QH, Zhang AR, Yang X, Zhang ZZ, Guo HZ. Efficacy and safety of single- and double-dose intravenous tranexamic acid in hip and knee arthroplasty: a systematic review and meta-analysis. J Orthop Surg Res 2023;18(1):593. [CrossRef]
14. Ling T, Zhang L, Huang L. The efficacy and safety of combined administration of intravenous and intra-articular tranexamic acid in total knee arthroplasty: An update meta-analysis. J Clin Pharm Ther 2022;47(9):1312-21. [CrossRef]
15. Fakharian M, Fakharian A, Keshmiri Z, Khorrami AM. Comparison of the effect of combined administration of intravenous and intra-articular tranexamic acid versus their administration alone in the management of blood loss in total knee arthroplasty: a prospective, multicenter study in Iran. BMC Musculoskelet Disord 2023;24(1):974. [CrossRef]

Official Journal of Erciyes University Faculty of Medicine

DOI: 10.14744/cpr.2026.29727
J Clin Pract Res 2026;48(2):206–210

Limbic System Glioblastoma Extending to the Papez Circuit: A Case Report

Sena Kıcıklar,[1] Zeynep Fırat,[2] Gazanfer Ekinci[2]

[1]Department of Psychology, Faculty of Science and Letters, İstanbul Kültür University, İstanbul, Türkiye
[2]Department of Radiology, Yeditepe University Hospitals, İstanbul, Türkiye

ABSTRACT

Background: Glioblastoma is the most common malignancy of the central nervous system. Symptoms vary significantly depending on tumor location and size.

Case Report: A 55-year-old man presented with mild memory deficits, occasional eye twitching, and throat irritation for two months. Magnetic resonance imaging revealed a glioma centered in the piriform cortex, infiltrating the amygdala, hippocampus, bilateral fornices, mammillary bodies, anterior cingulate gyrus, and anterior commissure.

Conclusion: Despite extensive involvement of the limbic system and the Papez circuit, the patient exhibited a remarkable paucity of symptoms and maintained his daily functioning. This discrepancy was elucidated by diffusion tensor imaging tractography, which demonstrated that the tumor primarily displaced, rather than destroyed, the adjacent white matter tracts.

Keywords: Diffusion tensor imaging, glioblastoma, limbic system, tractography.

The abstract of this case was presented as a poster presentation at the 1st National Neuroimaging Congress in Ankara (September 2023).

Cite this article as:
Kıcıklar S, Fırat Z, Ekinci G. Limbic System Glioblastoma Extending to the Papez Circuit: A Case Report. J Clin Pract Res 2026;48(2):206–210.

Address for correspondence:
Sena Kıcıklar.
Department of Psychology, Faculty of Science and Letters, İstanbul Kültür University, İstanbul, Türkiye
Phone: +90 536 911 53 11
E-mail: sena.kiciklar@gmail.com

Submitted: 17.12.2025
Revised: 03.02.2026
Accepted: 09.02.2026
Available Online: 26.02.2026

Erciyes University Faculty of Medicine Publications - Available online at www.jcpres.com

INTRODUCTION

Glioblastoma (GBM) is the most aggressive malignant brain tumor of astrocytic origin, and its etiology is currently poorly understood.[1] Although GBM can occur at any age, including childhood, its incidence increases sharply after the age of 54 and peaks between 75 and 84 years of age.[2] The preliminary diagnosis is typically based on characteristic tumor-related radiological findings, initially identified by computed tomography and confirmed by magnetic resonance imaging (MRI). A definitive histopathological diagnosis is obtained through tumor resection or biopsy. Functional MRI and diffusion tensor imaging (DTI) enable the integration of patient-specific anatomical and functional data into preoperative planning. Moreover, data obtained from DTI can be used for tractography, a three-dimensional (3D) reconstruction technique that allows assessment of neural tracts. Tractography provides valuable information not only for surgical planning but also for postoperative evaluation.[3] Therefore, imaging modalities play a crucial role in guiding tissue sampling for surgical resection, establishing histological diagnosis, and performing postoperative assessment.

CASE REPORT

A 55-year-old male patient with an unremarkable medical history was diagnosed with GBM following a biopsy. Neurological examination revealed no cognitive or behavioral deficits, and

the patient reported no functional impairment in daily life other than mild memory problems. Despite the absence of focal neurological findings, the patient was admitted to the hospital with complaints of progressive forgetfulness regarding recent events over the preceding two months, occasional twitching of the right eye, and a tickling sensation in the throat.

The MRI scan was performed using a 48-channel head coil on a 3 Tesla scanner. A T2-weighted fat-saturated turbo spin-echo (TSE) sequence (TR=3000 ms, TE=75 ms, slice thickness=3 mm, and gap=0.5 mm) and DTI using a single-shot spin-echo echo-planar imaging sequence (TR=3443 ms, TE=93.3 ms, slice thickness=2.5 × 2.5 × 2.5 mm, and gap=0 mm) were acquired in the axial plane. DTI data were obtained using 32 different diffusion directions with b-values of 0 s/mm^2 and 800 s/mm^2.

MRI revealed a glioma centered in the piriform cortex, infiltrating the perirhinal cortex, amygdala, and hippocampus. The lesion demonstrated significant midline extension, involving the bilateral fornices, mammillary bodies, anterior cingulate gyrus, and anterior commissure. Furthermore, it invaded the subcallosal area and multiple regions of the corpus callosum, including the genu, rostrum, isthmus, and splenium, ultimately crossing into the contralateral hemisphere (Fig. 1).

Alterations in white matter tracts affect diffusion tensor anisotropy and orientation, resulting in distinct patterns on directional DTI color maps.[4] By differentiating intact, edematous, and disrupted fibers on these maps, we observed evidence of both fiber destruction and fiber displacement, with some tracts displaced by the glioma without complete structural disruption. In this case, intact, edematous, and disrupted fibers were individually identified on the DTI color map shown in Figure 2.

Orientation and integrity of the white matter tracts were also demonstrated by DTI. Several fiber bundles, including the fronto-

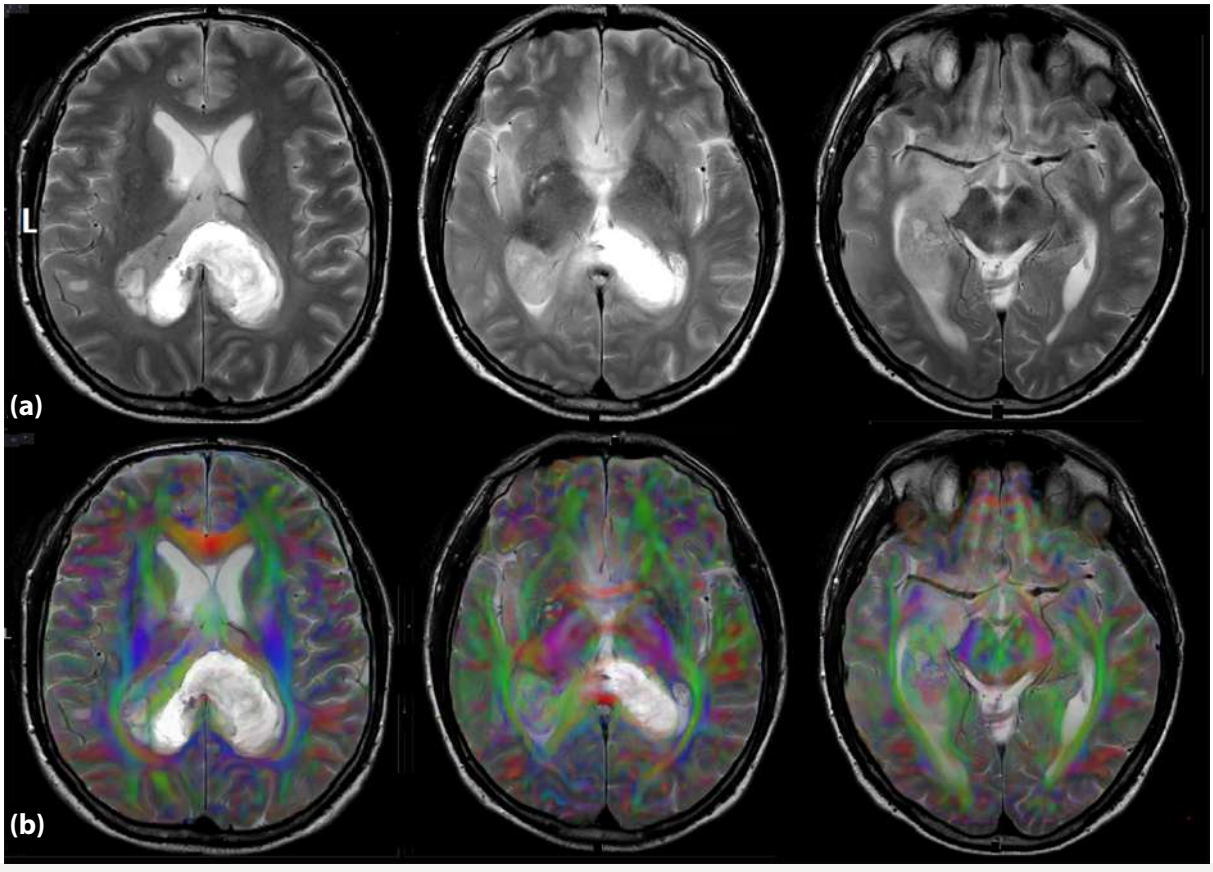

Figure 1. Consecutive axial T2-weighted images reveal an extensive lesion centered in the left anteromedial temporal lobe, involving the mesial temporal structures, limbic pathways, and the splenium of the corpus callosum, with extension into the contralateral hemisphere. Additional cortico-subcortical involvement is observed in the left insular, parietal, and posterior temporal regions **(a)**. Corresponding color-coded fractional anisotropy (FA) maps demonstrate displacement, deviation, and disruption of adjacent white matter tracts caused by the lesion **(b)**.

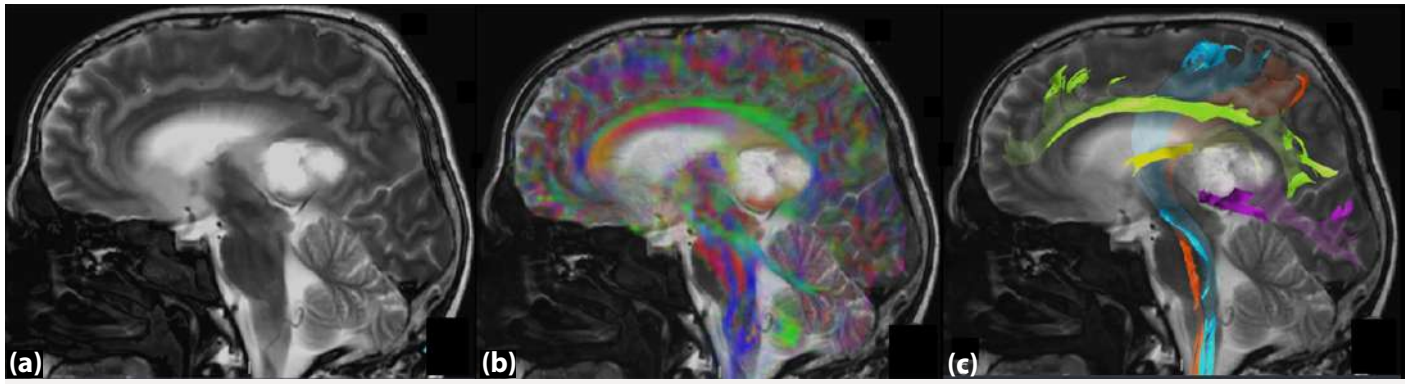

Figure 2. A sagittal T2-weighted image **(a)**, color-coded fractional anisotropy (FA) map **(b)**, and tractography reconstruction **(c)** demonstrate lesion-induced displacement of the corticospinal tract (CST, red), medial lemniscus (ML, blue), fornix (FX, yellow), and cingulum (CI, green). The forceps major (FM, pink) exhibits both displacement and disruption secondary to the lesion.

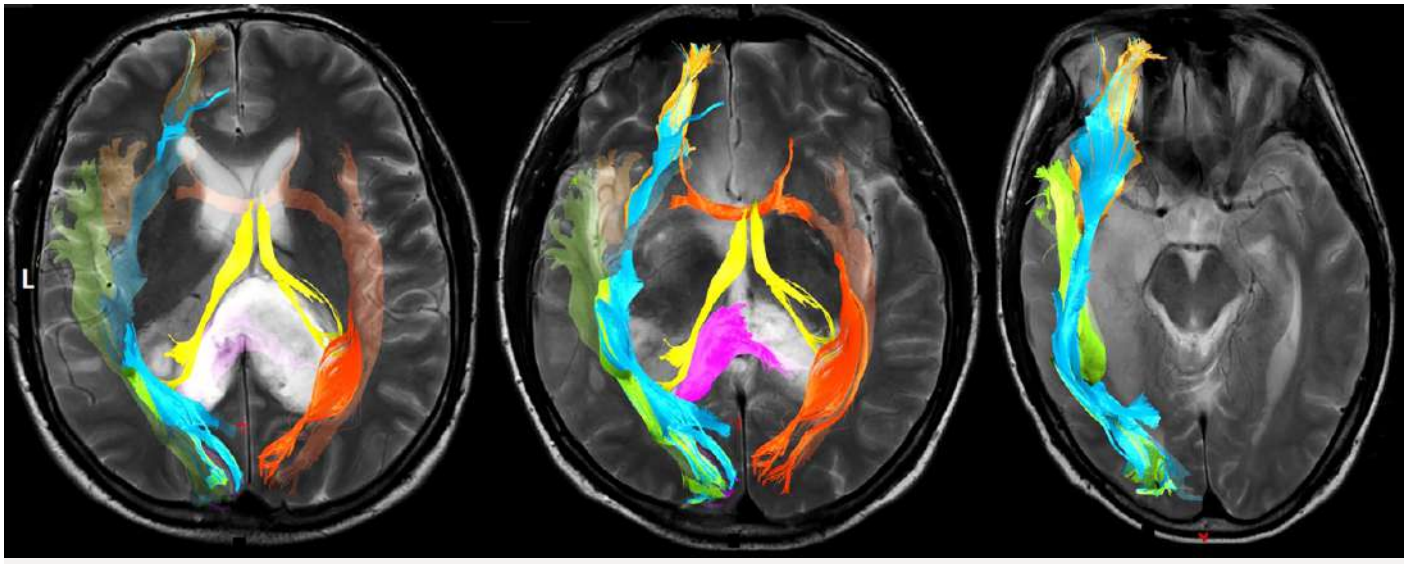

Figure 3. Tractography images demonstrate lesion-related disruption of the left temporal extension of the anterior commissure (AC, red) and the right occipital extension of the forceps major (FM, pink). The fornix (FX, yellow), inferior longitudinal fasciculus (ILF, green), and fronto-occipital fasciculus (FOF, blue) show displacement and deviation due to the lesion. The uncinate fasciculus (UNC, orange) remains intact and follows its normal anatomical course.

occipital fasciculus, inferior longitudinal fasciculus, and fornix, were displaced by the tumor, whereas the left temporal extension of the anterior commissure and the right occipital extension of the forceps major were disrupted (Fig. 3). In addition, the patient's optic radiation was affected by tumor infiltration, which may explain ocular complaints such as twitching.

DISCUSSION

While GBM typically involves the cerebral lobes,[5] this rare case demonstrates extensive involvement of the limbic system and its associated white matter. As noted by Capizzano et al.,[6] central nervous system (CNS) tumor classification prioritizes histology over anatomical origin, often overlooking so-called "limbic" tumors. Given the biological significance of anatomical origin, greater consideration should be given to tumors arising within the limbic system.

Classically, Papez[7] proposed a model linking specific brain structures to emotional processing and memory consolidation. This network, termed the Papez circuit, connects the hypothalamus, anterior thalamic nuclei, cingulate gyrus, and hippocampus. Subsequently, these cortical and subcortical structures, along with their associated fiber tracts, were

collectively described as the limbic system. This system has been implicated in various neurological and psychiatric disorders.[8]

In this rare case, there was widespread involvement of the Papez circuit, including the hippocampus, amygdala, bilateral fornices, mammillary bodies, and anterior cingulate. The tumor's expansion also involved the anterior commissure and multiple subregions of the corpus callosum, extending from the rostrum and genu to the isthmus and splenium, ultimately crossing the midline into the contralateral hemisphere. Most of the brain structures and fibers affected by the tumor correspond to components of the extended version of the Papez circuit. In this respect, the present case supports the concept of an expanded Papez circuit. Owing to the resolution limitations of current neuroimaging modalities, comprehensive *in vivo* visualization of the entire Papez circuit is challenging. Consequently, very few studies have successfully delineated the full pathway in living subjects.[9]

A striking feature of this case is the relative preservation of emotional and cognitive functions despite the extensive involvement of the Papez circuit, with the patient exhibiting only mild memory deficits. As demonstrated on the DTI color maps, the tumor did not completely destroy all white matter tracts, rather, some fibers displaced without structural disruption. Therefore, the displaced white matter fibers may have remained functional.

Given this potential for functional preservation, surgical management of GBM cases involving the limbic system should emphasize not only anatomical resection but also preservation of functional networks. While standard imaging techniques may delineate tumor margins, they may be inadequate for visualizing white matter displaced or infiltrated by the tumor. In this context, tractography plays a critical role in surgical planning and assists in the preoperative mapping of vital subcortical connections, such as the Papez circuit. Thus, while aiming for maximal safe tumor resection, the patient's cognitive and emotional integrity may also be preserved.

CONCLUSION

The temporal lobe is unique in that it contains both predominant isocortex and allocortex.[6] Tumors originating from the limbic lobe may exhibit distinctive characteristics compared to those arising from extralimbic temporal regions. Since Yaşargil et al.[10] described the characteristics of limbic tumors more than three decades ago, primarily focusing on surgical aspects, the concept has received relatively little attention in the pathological and radiological literature. Further discussion and clearer characterization of limbic tumors are needed.

Moreover, this case is rare because of its extensive spread along the Papez circuit. It also supports prior imaging studies that have successfully visualized the entire circuit, as the tumor spread followed the anatomical course of the Papez circuit. In this case, the fact that a tumor affecting the limbic system to this extent did not result in behavioral or emotional disturbances, other than mild memory impairment, can be explained by the DTI color maps, thereby underlining their importance in understanding the symptoms.

Ethics Committee Approval: This is a single case report, and therefore ethics committee approval was not required in accordance with institutional policies.

Informed Consent: Written informed consent was obtained from patients who participated in this study.

Conflict of Interest: The authors have no conflicts of interest to declare.

Funding: The authors declared that this study received no financial support.

Use of AI for Writing Assistance: No use of AI-assisted technologies was declared by the authors.

Author Contributions: Concept – SK, ZF; Design – SK, ZF; Supervision – ZF, GE; Resource – ZF, GE; Materials – SK, ZF; Data Collection and/or Processing - ZF, GE; Analysis and/or Interpretation - SK, ZF; Literature Review – SK; Writing – SK; Critical Review – SK, ZF, GE.

Peer-review: Externally peer-reviewed.

REFERENCES

1. Wirsching HG, Weller M. Glioblastoma. Moliterno Gunel J, Piepmeier JM, Baehring JM, editors. Malignant Brain Tumors: State-of-the-Art Treatment. Cham: Springer; 2017.p.265-88. [CrossRef]
2. Alexander BM, Cloughesy TF. Adult Glioblastoma. J Clin Oncol 2017;35(21):2402-9. [CrossRef]
3. Yu CS, Li KC, Xuan Y, Ji XM, Qin W. Diffusion tensor tractography in patients with cerebral tumors: a helpful technique for neurosurgical planning and postoperative assessment. Eur J Radiol 2005;56(2):197-204. [CrossRef]
4. Jellison BJ, Field AS, Medow J, Lazar M, Salamat MS, Alexander AL. Diffusion tensor imaging of cerebral white matter: a pictorial review of physics, fiber tract anatomy, and tumor imaging patterns. AJNR Am J Neuroradiol 2004;25(3):356-69.
5. Grochans S, Cybulska AM, Simińska D, Korbecki J, Kojder K, Chlubek D, et al. Epidemiology of Glioblastoma Multiforme-Literature Review. Cancers (Basel) 2022;14(10):2412. [CrossRef]

6. Capizzano AA, Kirby P, Moritani T. Limbic Tumors of the Temporal Lobe: Radiologic-Pathologic Correlation. Clin Neuroradiol 2015;25(2):127-35. [CrossRef]
7. Papez JW. A proposed mechanism of emotion. Arch NeurPsych 1937;38;(4):725-43. [CrossRef]
8. Bhattacharyya KB. James Wenceslaus Papez, His Circuit, and Emotion. Ann Indian Acad Neurol 2017;20(3):207-10. [CrossRef]
9. Choi SH, Kim YB, Paek SH, Cho ZH. Papez Circuit Observed by *in vivo* Human Brain With 7.0T MRI Super-Resolution Track Density Imaging and Track Tracing. Front Neuroanat 2019;13:17. [CrossRef]
10. Yaşargil MG, von Ammon K, Cavazos E, Doczi T, Reeves JD, Roth P. Tumours of the limbic and paralimbic systems. Acta Neurochir (Wien) 1992;118(1-2):40-52. [CrossRef]

Official Journal of Erciyes University Faculty of Medicine

DOI: 10.14744/cpr.2026.34641
J Clin Pract Res 2026;48(2):211–214

Incidental Parasternal Ancient Schwannoma Detected During Breast Cancer Screening

Yasser Ali Kamal[1]

[1]Department of Cardiothoracic Surgery, Faculty of Medicine, Minia University, Al-Minya, Egypt

ABSTRACT

Background: Schwannoma is a rare, slow-growing nerve sheath tumor that is infrequently reported in the anterior chest wall and requires thorough evaluation for accurate identification and appropriate treatment.

Case Report: We describe a case of a 57-year-old woman with an incidentally discovered parasternal ancient schwannoma of the anterior chest wall during breast cancer screening. Contrast-enhanced computed tomography (CT) revealed a well-defined soft tissue mass located in the right third intercostal space. Surgical excision was performed via right anterior thoracotomy. Histopathological examination confirmed the diagnosis of ancient schwannoma. The patient experienced an eventful postoperative recovery, with no recurrence observed during two years of follow-up.

Conclusion: Anterior chest wall schwannomas are rare incidental findings. Accurate imaging and complete surgical excision are essential for diagnosis and management, ensuring favorable outcomes and highlighting the importance of timely recognition of these uncommon tumors.

Keywords: Benign tumor, chest wall mass, intercostal nerve, schwannoma, thoracic surgery.

Cite this article as:
Kamal YA. Incidental Parasternal Ancient Schwannoma Detected During Breast Cancer Screening. J Clin Pract Res 2026;48(2):211–214.

Address for correspondence:
Yasser Ali Kamal.
Department of Cardiothoracic Surgery, Faculty of Medicine, Minia University, Al-Minya, Egypt
Phone: +201015321568
E-mail: yasealikamal@gmail.com

Submitted: 15.12.2026
Accepted: 19.02.2026
Available Online: 03.03.2026

Erciyes University Faculty of Medicine Publications - Available online at www.jcpres.com

INTRODUCTION

Chest wall schwannoma arising from the anterior intercostal nerves is a rare, benign nerve sheath tumor that may present diagnostic challenges due to its non-specific clinical presentation. It typically originates from peripheral nerves and is characterized by slow growth over a prolonged period, often remaining asymptomatic for many years. Diagnosis is often difficult, as schwannomas can masquerade as more common chest wall masses or even breast lesions.[1]

Surgical excision remains the primary treatment approach, with a focus on complete removal to prevent recurrence.[2] Additional complications due to tumor size or nerve involvement can occur in some cases of schwannoma, indicating the need for careful preoperative planning.[3] Although rare, early recognition and treatment are crucial for optimal outcomes. We report a case of a 57-year-old woman with ancient schwannoma of the anterior chest wall, incidentally detected during routine breast cancer screening.

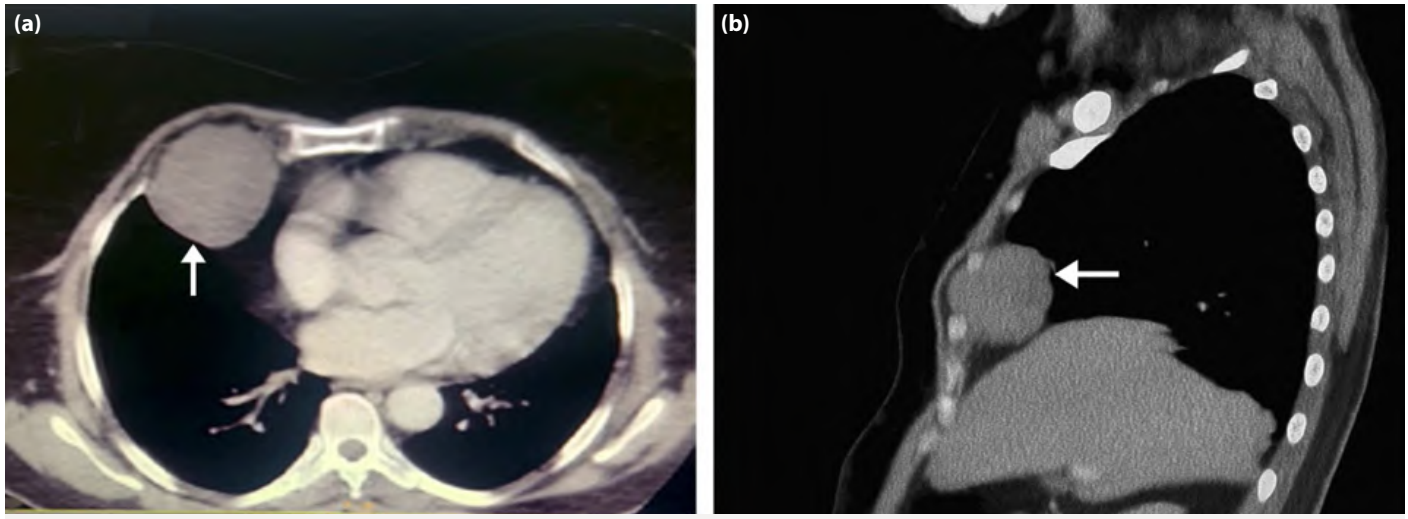

Figure 1. (a) Axial view and **(b)** sagittal views of contrast-enhanced chest computed tomography demonstrating a well-defined, encapsulated mass located in the right third intercostal space, without invasion of adjacent tissues.

CASE REPORT

A 57-year-old woman with an unremarkable medical history underwent routine breast cancer screening. During evaluation, a painless mass was noted on the right anterior chest wall. Ultrasound demonstrated a well-defined hypoechoic mass at the right third costal cartilage measuring 6 × 5 × 5.5 cm. Biopsy findings suggested an inflammatory pseudotumor. Contrast-enhanced computed tomography (CT) revealed a right parasternal soft tissue mass located at the third intercostal space, measuring 5.8 cm in diameter. The lesion elevated the overlying muscles and displaced the lung without invasion (Fig. 1). Given the benign imaging features and absence of symptoms, a right anterior thoracotomy was performed.

The excised mass (Fig. 2a) was encapsulated, measuring 6 × 5.5 cm, soft in consistency, with an additional fibrofatty fragment measuring 4.5 × 3.5 cm. Microscopic examination (Fig. 2b–c) revealed a low-grade spindle cell neoplasm with degenerative changes, consistent with ancient schwannoma. Margins were free of tumor, and S-100 staining was positive (Fig. 2d). The patient had an uneventful postoperative recovery and was discharged on postoperative day 4. At two-year follow-up, there was no evidence of recurrence.

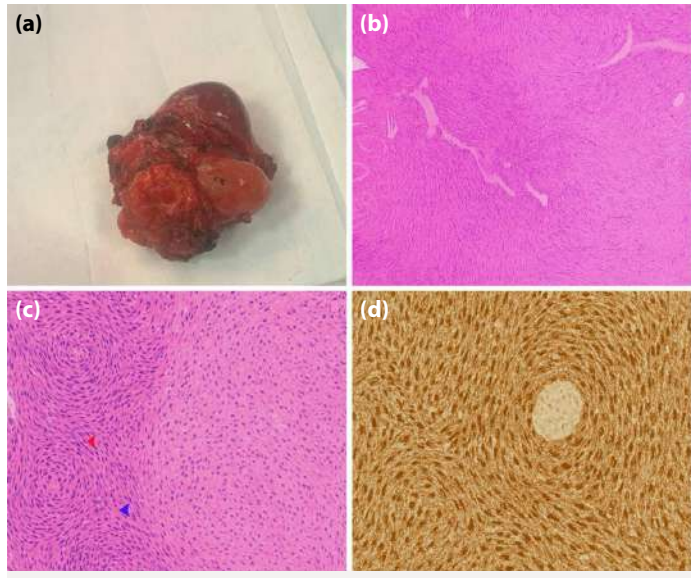

Figure 2. (a) Gross image of the excised mass. **(b)** Low-power microscopic view of the hematoxylin and eosin (H&E)-stained specimen showing a spindle cell lesion with degenerative changes. **(c)** High-power view (×400) demonstrating well-defined hypercellular (Antoni A) and hypocellular (Antoni B) areas, with nuclear palisading (elongated spindle cell nuclei arranged in parallel rows; red arrowhead) and a Verocay body (an acellular eosinophilic zone located between two rows of palisaded nuclei; blue arrowhead). **(d)** Positive immunohistochemical staining for S-100.

DISCUSSION

Ancient schwannoma is a rare nerve sheath tumor that is infrequently reported in the anterior chest wall adjacent to the sternum (Table 1). These tumors may remain asymptomatic for years and are often incidentally detected during evaluation for unrelated conditions.[4] Diagnosis can be challenging because chest wall schwannomas may mimic breast or other soft tissue tumors.[1] In the present case, the tumor was discovered during routine breast cancer screening, and its anterior chest wall location was unusual.

Table 1. Reported cases of ancient schwannomas of the anterior chest wall

Author	Age (years)/Sex	Presentation	Side	Size	Journal
Olcmen et al., 2010[a]	13/M	Chest pain	Right	5 × 6 cm	Pediatr Int
Ceberut et al., 2011[b]	66/M	Mediastinal mass	Left	13 cm (middle mediastinum) and 5 cm (6th costochondral junction)	Case Rep Med
Akgul et al., 2012[c]	33/M	Chest pain	Right	5 × 4.5 × 3.5 cm	Turk Gogus Kalp Damar Cerrahisi Derg
Bhat et al. 2012[d]	34/M	Chest pain	Left	7 × 6 × 3 cm	Nitte Uni J Health Sci
Kale et al., 2015[e]	51/F	Chest pain, cough	Right	14.1 × 9.1 × 8.8 cm	Med J Dr D Y Patil Univ
Krishnamurthy et al., 2015[f]	33/F	Painless mass	Left	9.5 × 8.8 × 5.8 cm	Indian J Surg Oncol
Jain et al., 2016[g]	62/M	Chest wall swelling, pain	Left	9 × 5 × 3 cm	Int J Health Sci Res
Gilbert et al., 2016[h]	53/F	Breathlessness, cough with expectoration	Right	20 × 2 × 15 cm	Lung India
Kongjarern et al., 2017[i]	53/M	Asymptomatic	Bilateral (multifocal)	Right: 5.5 × 4.2 cm, Left: smaller	J Med Cases
Miyawaki et al., 2023[j]	65/F	Chest pain and cough	Left	13 cm	J Cardiothorac Surg
Al Sharqi et al., 2024[k]	44/M	Painless mass	Right	5.1 × 3.9 × 4 cm	Oman Med J
Current case	57/F	Painless mass	Right	6 × 5 × 5.5 cm	J Clin Pract Res

a. Olcmen A, Kara HV, Gunluoğlu MZ, Buyukpinarbasili N, Dince SI. Ancient schwannoma of the chest wall in the pediatric age group: First case in the literature. Pediatr Int 2010;52(2):e65-6. [CrossRef]

b. Ceberut K, Naseri E, Celik A, Muslehiddinoglu A, Ergin I. One-stage combined thoracic ancient schwannomas total removal and coronary artery bypass. Case Rep Med 2011;2011:497960. [CrossRef]

c. Akgul AG, Cobanoglu U, Yurt ZK. An asymptomatic schwannoma originating from an intercostal nerve: A case report. Turk Gogus Kalp Damar Cerrahisi Derg 2012;20(3):662-4. [CrossRef]

d. Bhat SP, Permi HS, Shetty R, Shenoy J, Prasad K, Hegde P. Ancient schwannoma of the chest wall diagnosed by fine needle aspiration cytology- a rare case report. Nitte Uni J Health Sci 2012;2(3):27-29. [CrossRef]

e. Kale SS, Gosavi VS, Jagadale RV. Ancient chest wall schwannoma: A case report with review of literature. Med J Dr D Y Patil Univ 2015;8(4):505-7. [CrossRef]

f. Krishnamurthy A, Raghunandhan GC, Majhi U. Dumbbell Shaped Schwannoma of the Lateral Chest Wall masquandering as a soft tissue sarcoma. Indian J Surg Oncol 2015;6(3):307-10. [CrossRef]

g. Jain A, Wani AS, Dhar R, Sahu S, Ambrish PI. Ancient schwannoma of chest wall-a rare finding. Int J Health Sci Res 2016;6(1):582-4.

h. Gilbert S, Singh D, Kaliappan SM, Mehta SS. Giant solitary ancient schwannoma of the pleura masquerading as bronchopneumonia. Lung India 2016;33(4):447-8. [CrossRef]

i. Kongjarern S, Tajarernmuang P, Wannasopha Y, Wannasai K, Saeteng S. Multifocal Ancient Thoracic Schwannomas: A Case Report and Review of Literature. J Med Cases 2017;8(9):277-9. [CrossRef]

j. Miyawaki M, Karashima T, Abe M, Takumi Y, Hashimoto T, Kamohara R, et al. Giant benign intrathoracic schwannoma: a decade-long progression towards fatality. J Cardiothorac Surg 2023;18(1):328. [CrossRef]

k. Al Sharqi A, Al Aufi N, Al Hanaai M, Al Kitani H, Al Shehhi R, Al Qadhi H, et al. Ancient Schwannoma of the Anterior Chest Wall. Oman Med J 2024:D-24-00466. [CrossRef]

Preoperative diagnosis is difficult due to several factors: 1) non-specific radiologic features, as schwannomas typically appear as well-defined, encapsulated masses resembling other tumors; 2) variable enhancement patterns resulting from necrosis or degenerative changes; and 3) inconclusive biopsy results, since fine-needle or core biopsies may yield low cellularity or degenerative tissue, leading to misinterpretation. Histologically, ancient schwannomas may exhibit atypical features, further complicating preoperative identification.[5] In our case, the diagnosis was established postoperatively through histopathological

examination and S-100 immunohistochemistry, underscoring the importance of integrating radiologic, histopathologic, and immunohistochemical findings.

Complete surgical excision is the optimal treatment and is generally curative when free margins are achieved.[3,6] Although these tumors are typically benign, recurrence can occur, particularly following incomplete excision or in cases of multifocal tumors, necessitating careful surgical planning and long-term follow-up.[7] In our patient, no recurrence was observed at the two-year follow-up. Recurrent lesions may mimic malignant peripheral nerve sheath tumors on imaging,[8] making continued radiologic surveillance essential, particularly for larger or multiple lesions.[6,9,10]

CONCLUSION

Ancient schwannomas of the anterior chest wall are uncommon lesions that may be discovered incidentally. Favorable outcomes can be achieved with appropriate radiologic assessment and complete surgical excision. These tumors should be included in the differential diagnosis of incidental chest wall masses, particularly in asymptomatic patients.

Ethics Committee Approval: This is a single case report, and therefore ethics committee approval was not required in accordance with institutional policies.

Informed Consent: Written informed consent was obtained from the patient.

Conflict of Interest: The author have no conflicts of interest to declare.

Financial Disclosure: The author declared that this study received no financial support.

Use of AI for Writing Assistance: No use of AI-assisted technologies was declared by the authors.

Peer-review: Externally peer-reviewed.

REFERENCES

1. Datta S, Pal A, Maiti M, Boler AK. Rare case of chest wall schwannoma with destruction of rib, masquerading as a breast mass. J Clin Diagn Res 2014;8(6):FD01-2. [CrossRef]
2. Jain A, Wani AS, Dhar R, Sahu S, Ambrish PJ. Ancient schwannoma of chest wall-a rare finding. Int J Health Sci Res 2016;6(1):582-4.
3. Al Sharqi A, Al Aufi N, Al Hanaai M, Al Kitani H, Al Shehhi R, Al Qadhi H, et al. Ancient Schwannoma of the Anterior Chest Wall. Oman Med J 2024:D-24-00466. [CrossRef]
4. Ertekin A, Öcalan K. Detection of incidental schwannoma by traumatic hemothorax. Ulus Travma Acil Cerrahi Derg 2022 Mar;28(3):399-401.
5. Kale SS, Gosavi VS, Jagadale RV. Ancient chest wall schwannoma: A case report with review of literature. Med J DY Patil Univ 2015;8(4):505-7. [CrossRef]
6. Miyawaki M, Karashima T, Abe M, Takumi Y, Hashimoto T, Kamohara R, et al. Giant benign intrathoracic schwannoma: a decade-long progression towards fatality. J Cardiothorac Surg 2023;18(1):328. [CrossRef]
7. Kongjarern S, Tajarernmuang P, Wannasopha Y, Wannasai K, Saeteng S. Multifocal Ancient Thoracic Schwannomas: A Case Report and Review of Literature. J Med Cases 2017;8(9):277-9. [CrossRef]
8. Gilbert S, Singh D, Kaliappan SM, Mehta SS. Giant solitary ancient schwannoma of the pleura masquerading as bronchopneumonia. Lung India 2016;33(4):447-8. [CrossRef]
9. Sun WK, Yang W, Ma CH, Xiao XW, Shi Y, Song Y. Multiple intercostal neurilemmomas in a Chinese woman. J Can Res Ther 2018;14(12):S1220-2. [CrossRef]
10. Morris PD, Chuong B, Meredith G. Giant ancient intercostal schwannoma: a rare cause of chronic cough and progressive dyspnoea. ANZ J Surg 2021;91(11):E734-6. [CrossRef]

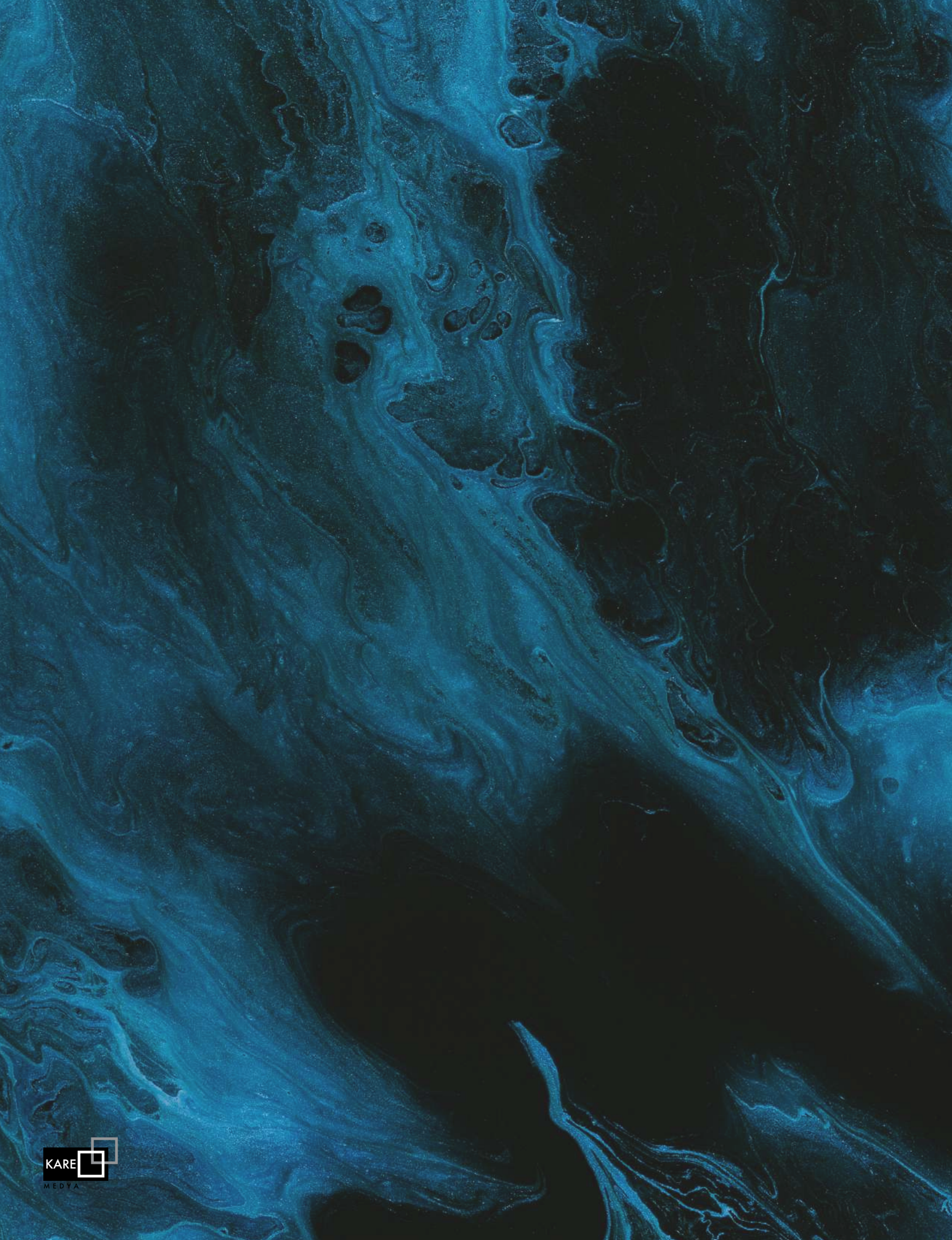
KARE
MEDYA